

**CARBENE AND COORDINATION COMPLEXES OF
GOLD, PALLADIUM, PLATINUM AND MANGANESE
DERIVED FROM N-CONTAINING HETEROCYCLES**

by

MAGGEL DEETLEFS

DISSERTATION

submitted in fulfilment of the requirements for the degree

PHILOSOPHIAE DOCTOR

in

CHEMISTRY

in the

Pectus roburant cultus recti

FACULTY OF SCIENCE

at the

UNIVERSITY OF STELLENBOSCH

PROMOTER: PROF. H. G. RAUBENHEIMER

JULY 2001

ABSTRACT

This study investigated the synthesis of N-containing, heterocyclic precursors in the presence of gold nanoparticles and the subsequent coordination complexes of gold, silver and platinum nanoparticles. In addition, the synthesis of such ligands and their use in the synthesis of gold, silver and platinum nanoparticles catalyzed by gold nanoparticles.

Declaration

I declare that the work presented in this dissertation, except where otherwise stated, is based on my own research carried out in The Department of Chemistry at the University of Stellenbosch, between January 1998 and July 2001.

ABSTRACT

This study comprises the utilisation of N-containing, heterocyclic precursors in the preparation and characterisation of new carbene and coordination complexes of gold, palladium, platinum and manganese. In addition, the syntheses of ionic liquids and their use in the preparation of free diamino(carbenes) and homogeneous catalysis are also reported.

The room temperature ionic liquids, 1-butyl-3-methylimidazolium triflate and 1-butyl-3-methylimidazolium hexafluorophosphate, are deprotonated with alkyllithium reagents to afford the free diamino(carbene), 1-butyl-3-methylimidazol-2-ylidene, which readily displaces thioether ligands from $[\text{Au}(\text{Cl})\text{SMe}_2]$ and $[\text{Au}(\text{Cl})\text{tht}]$, to yield gold(I) carbene complexes. Imidazolium-based ionic liquids also react with the dialkylaurate, $[\text{AuMe}_2]^-$, to afford a free diamino(carbene) as the major product and a small amount of a *bis*(carbene) gold(I) complex.

Metathesis of 3-butyl-4-methylthiazolium bromide with NaAuCl_4 or HAuCl_4 affords the gold(III)-containing thiazolium salt, $[\text{HC}=\text{C}(\text{Me})\text{N}(\text{Bu})=\text{CHS}][\text{AuBrCl}_3]$, which is the first compound of its kind that qualifies as an ionic liquid by melting at *ca.* 80°C. The crystal and molecular structure of this salt exhibits severe positional disorder in both the organic cation and halogold(III) counterion. The complex anions exhibit gold-halogen contacts arranged in a way to produce infinite chains of the anions in the crystal lattice. Hydration of phenylacetylene proceeds with this compound as catalyst in ionic liquids, indicating that gold(III)-based ionic liquids could serve as both solvents and catalysts for organic transformations. Deprotonation of the new compound with a base affords a rather unstable gold(III) amino(thio)carbene complex, $[\text{Cl}_3\text{Au}(\text{CN}(\text{Bu})\text{C}(\text{Me})=\text{CHS})]$.

In contrast to the vast majority of palladium, platinum and manganese carbene complexes that result from azole precursors in which the heteroatom is adjacent to the conjugated carbene carbon, the new di(organo) carbene complexes prepared in this study are unique in that they have been prepared from heterocycles in which the nucleophilic heteroatom is a distant oxygen atom.

In the quinoline-based compounds, 4-chloro-*N*-methylquinolinone and 4-chloro-2-methoxy-*N*-methylquinolinium tetrafluoroborate, electrophilic attack on the distant carbonyl oxygen that effects rare di(organo)carbene complex formation, can be performed both before and after ligand attachment to the metal via initial oxidative addition to palladium(0) or platinum(0), or halide displacement with Na[Mn(CO)₅]. The crystal and molecular structure determination of a palladium(II) carbene complex, [(PPh₃)₂Pd(Cl){CCH=C(OMe)N(Me)C₆H₄}] [BF₄], shows that both the γ nitrogen and oxygen atoms within the conjugated framework play a role in carbene formation and stabilisation. The bond lengths in this compound indicate that the dominant resonance forms have a partly negative charge on the metal and partly positive charges on either the nitrogen or oxygen atom.

Reaction of HAuCl₄ with mono- and bidentate imines in water, furnishes cationic complexes, independent of the employed reagent ratio, whereas similar reactions with NaAuCl₄ only affords neutral imine-AuCl₃ adducts. ¹⁵N NMR measurements provide diagnostic proof for monodentate coordination of gold(III) to the imine donor in bifunctional heterocycles, prepared by reaction with NaAuCl₄, and also indicate that gold(III) preferentially bonds to nitrogen in the five-membered heterocyclic azole rather than to the pyridine nitrogen or soft sulphur atom in an attached ring. This is confirmed by an x-ray crystallographic study of the neutral adduct, [Cl₃Au{N=C(CSCH=CHCH)OCH₂CMe₂}] . Similarly, the cationic gold(III) complexes, [Cl₂Au{N=C(py)NMeCH=CH}][AuCl₄] and [Cl₂Au{N=C(Ph)NMeCH=CH}₂][AuCl₄], respectively contain mono- and bidentate ligand arrangements and the latter represents the first crystallographically-characterised *cis*-diazole complex. In both salts, chlorine-proton interactions probably partly govern the overall assembly in the crystalline phase.

SAMEVATTING

Hierdie studie behels die gebruik van *N*-bevattende, heterosikliese voorloperbindings in die bereiding en karakterisering van nuwe karbeen en koördinasiekomplekse van goud, palladium, platinum en mangaan. Voorts word die sintese van ioniese vloeistowwe en hul gebruik in die bereiding van stabiele diamino(karbene) en in homogene katalise ook gerapporteer.

Die ioniese vloeistowwe, 1-butiel-3-metielimidiasoliumtriflaat en -heksafluorofosfaat, kan met alkiellitiumreagense gedeprotoneer word om 'n stabiele diamino(karbeen) te gee wat gereedlik die tioeter ligande in $[\text{Au}(\text{Cl})\text{SMe}_2]$ en $[\text{Au}(\text{Cl})\text{tht}]$ verplaas om goud(I) karbeenkomplekse te vorm. Ioniese vloeistowwe gebaseer op imidasolium soute, reageer met die dialkielauraat, $[\text{AuMe}_2]^-$, om 'n vry diamino(karbeen) as hoofproduk te gee sowel as 'n *bis*(karbeen)kompleks van goud(I) in lae opbrengs.

Die nuwe goud(III)-bevattende tiasolium sout, $[\text{HC}=\text{C}(\text{Me})\text{N}(\text{Bu})=\text{CHS}][\text{AuBrCl}_3]$, is berei deur metatiese van 3-butiel-4-metieltiasoliumbromied met NaAuCl_4 of HAuCl_4 en word as 'n ioniese vloeistof geklassifiseer aangesien dit laer as 100°C smelt. Die kristalstruktuurbeplanning van dié sout toon ernstige wanorde in beide die organiese kation en die teenioon. Goud-halogen interaksies is waargeneem tussen onafhanklike kompleksanione, wat lei tot aaneenlopende teenioonkettings in die kristal. Die goud(III) sout kataliseer die hidratisie van fenielasetileen in ander ioniese vloeistowwe en toon dat goud(III)-gebaseerde ioniese vloeistowwe as beide oplosmiddels en katalisatore vir organiese reaksies kan optree. Behandeling van die nuwe tiasoliumverbinding met verskeie basise, lewer 'n onstabiele goud(III) amino(tio)karbeenkompleks, $[\text{Cl}_3\text{Au}(\overline{\text{CN}(\text{Bu})\text{C}(\text{Me})=\text{CHS}})]$.

In teenstelling met die meeste karbeenkomplekse van palladium, platinum en mangaan wat berei word uit asooluitgangstowwe waarin die heteroatoom langs die gekoördineerde koolstof voorkom, is die nuwe di(organo)karbeenkomplekse uniek, aangesien hulle berei is vanuit heterosikliese bindings met die nukleofiliese suurstofatoom drie bindingslengtes verwyderd van die gekoördineerde koolstof.

In die kinolien-gebaseerde verbindings, 4-chloro-*N*-metielkinoloon en 4-chloro-2-metoksi-*N*-metielkinolieniumtetrafluoroboraat, kan die elektrofiliese aanval wat tot karbeenvorming lei, voor of na metaalkoördinasie plaasvind deur óf van oksidatiewe addisie met palladium(0) en platinum(0)fosfiene, óf van haliedverplasing met Na[Mn(CO)₅] gebruik te maak. Die kristalstruktuur van so 'n palladium(II) karbeenkomples, $[(PPh_3)_2Pd(Cl)\{CCH=C(OMe)N(Me)C_6H_4\}][BF_4]$, toon dat beide die stikstof- en suurstofatome in die ligand stabiliserend funksioneer. Die bindingslengtes in dié komples toon dat die dominante resonansstrukture 'n gedeeltelike negatiewe lading op die metaal dra en gedeeltelike positiewe lading op die stikstof- of suurstofatoom.

Onafhanklik van die verhoudings waarin reaktante aangewend word, lewer die reaksie van HAuCl₄ met mono- en bidentate imiene in water kationiese goud(III) komplekse, terwyl soortgelyke reaksies met NaAuCl₄ slegs neutrale imien-addukte van AuCl₃ gee. ¹⁵N-KMR-eksperimente voorsien direkte getuienis vir monodentate koördinasie van goud(III) aan die imien-stikstof in die neutrale verbindings en dit blyk ook dat die metaal by voorkeur aan die stikstof van 'n vyflidring eerder as dié in 'n naasliggende piridienring bind. 'n Kristalstruktuurbevestiging van so 'n verbinding, $[Cl_3Au\{N=C(CSCH=CHCH)OCH_2CMe_2\}]$, toon ook dat die sagte metaal eerder aan 'n imien-stikstof as 'n beskikbare, sagter swawelatoom bind. In die kationiese digesubstitueerde goud(III)komplekse, $[Cl_2Au\{N=C(Ph)NMeCH=CH\}_2][AuCl_4]$ en $[Cl_2Au\{N=C(py)NMeCH=CH\}][AuCl_4]$, word onderskeidelik mono- en bidentate rangskikking van die imienligande waargeneem. Laasgenoemde komples is die eerste voorbeeld waarin só 'n *cis*-asool-ligandkonfigurasie gevind word. In beide komplekse, kom chloor-waterstof interaksies voor wat waarskynlik die algehele pakking binne die kristal beïnvloed.

ACKNOWLEDGEMENTS

My sincere gratitude goes out to the following persons and institutions that provided support during the study described in this thesis:

The NRF and the University of Stellenbosch for financial support.

Prof. H. G. Raubenheimer for outstanding leadership, guidance and always having time for discussions.

Prof. K. R. Seddon for giving me the opportunity to work at QUILL in Belfast.

Dr. John Bacsa, Dr. Dave Billing and Matthias Esterhuysen for crystal structure determinations.

Elisna, Johan Greyvenstein and (the late) Mr. Hendrik Spies for NMR measurements.

Dr. S. Cronje for willing advice.

My laboratory colleagues for their optimism.

Tatum and Samantha for their constant interest and encouragement.

My mother and father for their continued support and sacrifice during my studies.

John for always believing in me.

CONTENTS

ABSTRACT	I
SAMEVATTING	III
ACKNOWLEDGEMENTS	V
CONTENTS	VI
ABBREVIATIONS	IX

CHAPTER 1

INTRODUCTION AND AIMS

1.1 General Background	1
1.2 Aims and Objectives	8
References	11

CHAPTER 2

PREPARATION AND CHARACTERISATION OF A FREE DIAMINO(CARBENE) AND CARBENE COMPLEXES OF GOLD(I) UTILISING IONIC LIQUIDS

2.1 Introduction	13
2.2 Results and Discussion	17
2.2.1 Free Carbene Precursor Preparations	17
2.2.2 A Free Imidazolinylidene	19
2.2.3 A Neutral Gold(I) Diamino(carbene) Complex	23
2.2.4 A Cationic Gold(I) Diamino(carbene) Complex	27
2.3 Summary	33
2.4 Experimental	34
References	36

CHAPTER 3**PREPARATION, REACTIONS AND CATALYTIC ACTIVITY OF THIAZOLIUM IONIC LIQUIDS**

3.1	Introduction	38
3.2	Results and Discussion	42
3.2.1	Thiazolium Salt Precursors	44
3.2.2	A Room Temperature Thiazolium Ionic Liquid	46
3.2.3	A Thiazolium Salt Ionic Liquid that contains AuCl_4^- as Counterion	49
3.2.4	A Thiazolyl Dimer	53
3.2.5	A Gold(III) Thiazol-2-ylidene Complex	55
3.2.6	Gold(III) Catalysed Hydration of Phenylacetylene	58
3.2.6.1	Catalysis in Conventional Solvents	58
3.2.6.2	Catalysis in Ionic Liquids	60
3.2.6.3	Hydration of Phenylacetylene in Recycled Ionic Liquid Phases	63
3.2.7	Benzoin Condensation Catalysis	64
3.3	Summary	65
3.4	Experimental	66
	References	71

CHAPTER 4**PREPARATION AND CHARACTERISATION OF PALLADIUM, PLATINUM AND MANGANESE DI(ORGANO)CARBENE COMPLEXES FROM QUINOLINONE AND QUINOLINIUM PRECURSORS**

4.1	Introduction	73
4.2	Results and Discussion	78
4.2.1	Quinolinone and Quinolinium Ligand Precursor Preparations	78
4.2.2	Neutral Quinolin-2-on-4-yl Palladium and Platinum Complexes	81
4.2.3	Cationic Quinolin-4-ylidene Palladium and Platinum Complexes	86
4.2.4	Quinolin-2-on-4-yl and Quinolin-4-ylidene Manganese Complexes	98
4.3	Summary	106
4.4	Experimental	107
	References	111

CHAPTER 5**PREPARATION AND CHARACTERISATION OF GOLD(I) AND GOLD(III)****IMINE COORDINATION COMPLEXES**

5.1	Introduction	114
5.2	Results and Discussion	119
5.2.1	Bicyclic Ligand Precursor Preparations	119
5.2.2	Gold(I) Imine Complexes	123
5.2.3	Neutral Gold(III) Imine Compounds	132
5.2.4	Cationic Gold(III) Imine Complexes	144
5.3	Summary	158
5.4	Experimental	160
	References	166

ABBREVIATIONS

Å	Angstrom (10^{-10} m)
Bu	Butyl
<i>tert</i> -Bu	Tertiary butyl
BuLi	Butyllithium
EI	Electron Ionisation
eV	Electron volt
FAB	Fast Atom Bombardment
HETCOR	Heteronuclear correlation
Hz	Hertz
IR	Infrared
Me	Methyl
MeLi	Methylithium
mmol	millimole
MS	Mass spectrometry
M. p.	Melting point
M. W.	Molecular weight
NMR	Nuclear magnetic resonance
OTf	Triflate
Ph	Phenyl
PPh ₃	Triphenylphosphine
<i>i</i> -Pr	Isopropyl
py	Pyridine
SMe ₂	Dimethylsulphide
thf	Tetrahydrofuran
TON	Turnover number
tht	Tetrahydrothiophene

CHAPTER 5

NMR

br	Broadened
Δ	Difference between two values
δ	Chemical shift (ppm)
d	Doublet
dd	Doublet of doublets
ddd	Doublet of doublets of doublets
ddm	Doublet of doublets of multiplets
dt	Doublet of triplets
J	Coupling constant (Hz)
m	Multiplet
s	Singlet
t	Triplet
td	Triplet of doublets

'You see things that are and wonder "Why?" but I dream things that never were and wonder "Why not?" '

George Benard Shaw

"We never cease to stand like curious children before the great mystery into which we are born"

Albert Einstein

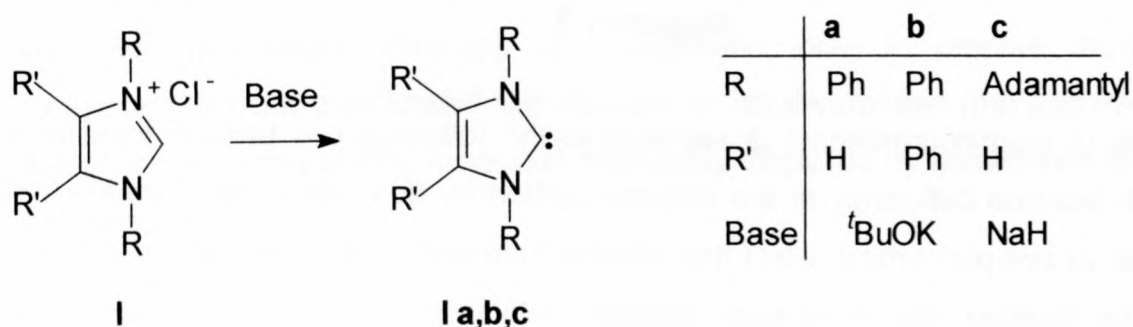
CHAPTER 1

INTRODUCTION AND AIMS

1.1 GENERAL BACKGROUND

Beginning as chemical curiosities, carbenes have evolved into one of the most intensively investigated species in modern research.^[1] Introduced by Fischer and Maassböl into organometallic chemistry in 1964,^[2] the discovery of Group 6 alkoxy(carbene) complexes revolutionised organometallic chemistry and led to a number of applications in synthesis and catalysis.^[3,4,5,6]

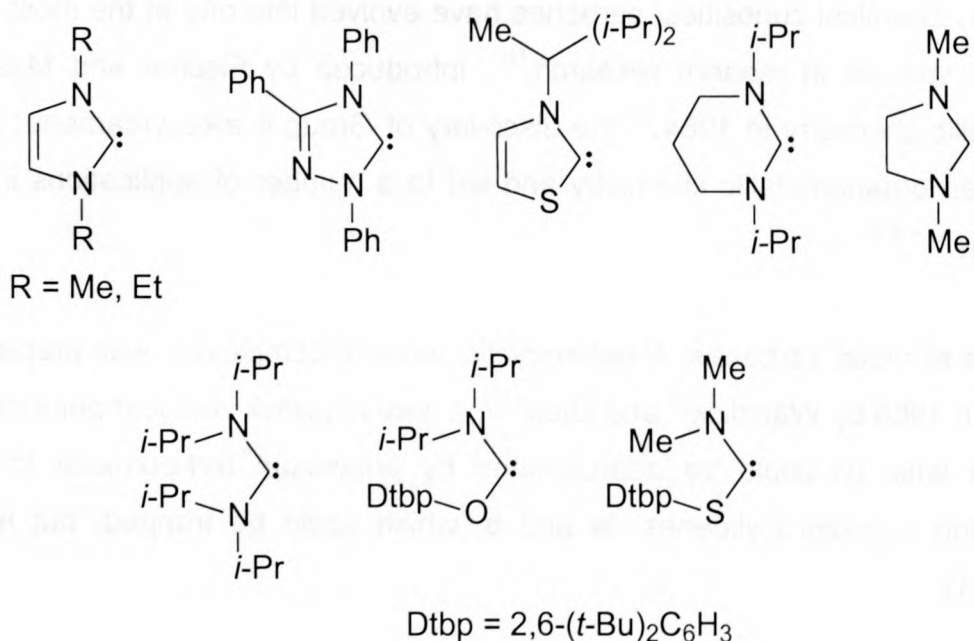
A new class of metal carbenes, *N*-heterocyclic carbene complexes, was prepared shortly afterwards in 1968 by Wanzlick^[7] and Öfele.^[8] It was Wanzlick who first demonstrated that imidazolium salts (**I**) could be deprotonated by potassium *tert*-butoxide to afford the corresponding imidazol-2-ylidenes, **la** and **b**, which could be trapped, but not isolated (Scheme 1.1).



Scheme 1.1

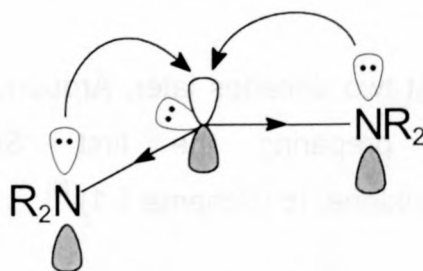
Following this principle, almost two decades later, Arduengo spurred renewed interest in heterocyclic carbenes by preparing the first “*Stable Crystalline Carbene*”, 1,3-*bis*(adamantyl)imidazol-2-ylidene, **lc** (Scheme 1.1).^[9]

Arduengo's landmark discovery led to furious activity in a number of research groups and the isolation of a variety of free, *N*-containing carbenes (Scheme 1.2).^[1] A common feature of these carbenes is the presence of at least one amino group for stabilisation. Indeed, a number of physical and theoretical studies on diamino and related carbenes have shown that their unusual stability mainly results from electronic effects and resonance stabilisation occurs only to a very limited extent.^[10,11] Experimental confirmation of this came in the late 1990's with the isolation of saturated cyclic diamino(carbenes),^[12,13] as well as acyclic diamino-, amino(oxo)-^[14] and amino(thio)carbenes^[15] (Scheme 1.2).



Scheme 1.2

The stability of diamino(carbenes) is ascribed to the following two factors: mesomeric reduction of electron deficiency at the carbene carbon by donation of the nitrogen lone pairs into its vacant $p(\pi)$ orbital, while the carbene lone pair is stabilised by the inductive effect of the flanking electronegative nitrogens inhibiting dimerisation (Scheme 1.3). Monoamino(carbenes), of course, experience these stabilising features to a lesser extent and are generally more difficult to handle.



Scheme 1.3

As a whole, the physical and theoretical data available for *N*-heterocyclic carbenes indicate that C-N bonds have multiple bond character and are best described by resonance forms **A** and **B**, summarised as **C** in Figure 1.1. For amino(oxo)- and amino(thio)carbenes, the O-C and S-C bonds have very little π -character and are best represented by **A**.

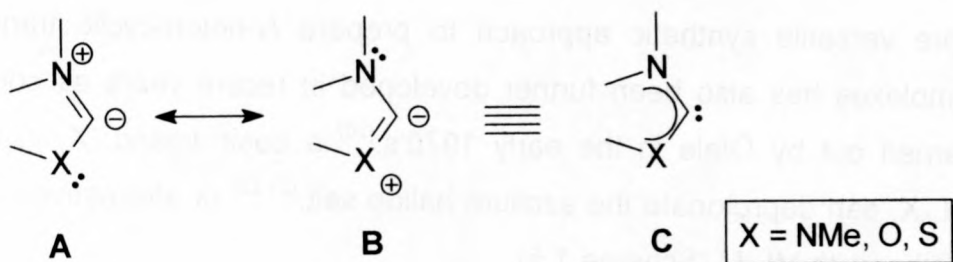
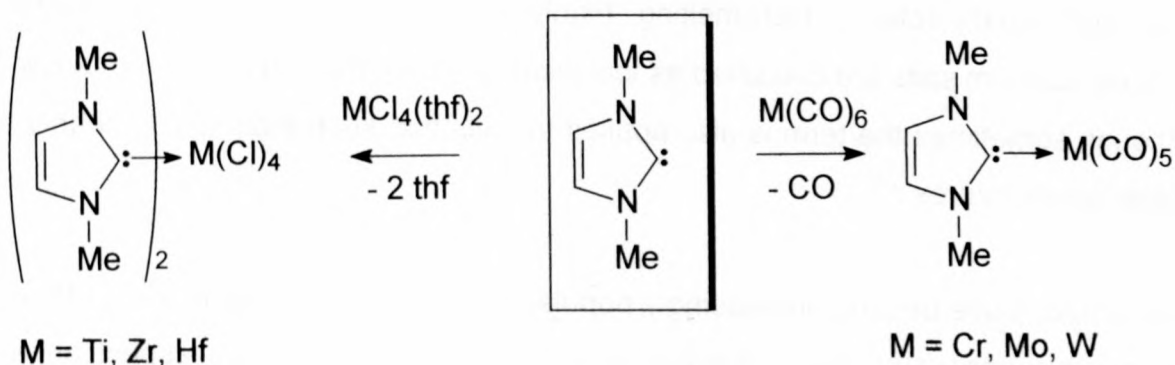


Figure 1.1 *N*-heterocyclic carbene resonance forms

During the decade following the advent of Arduengo-type carbenes, heterocyclic diamino(carbenes) attracted considerable attention in the preparation of transition metal complexes. This is largely because donation from the nitrogens in diamino(carbenes) is such that the carbene carbon may actually become a partial π -donor.^[16,17] These heterocyclic carbenes are thus pure σ -donor ligands, similar to phosphines.

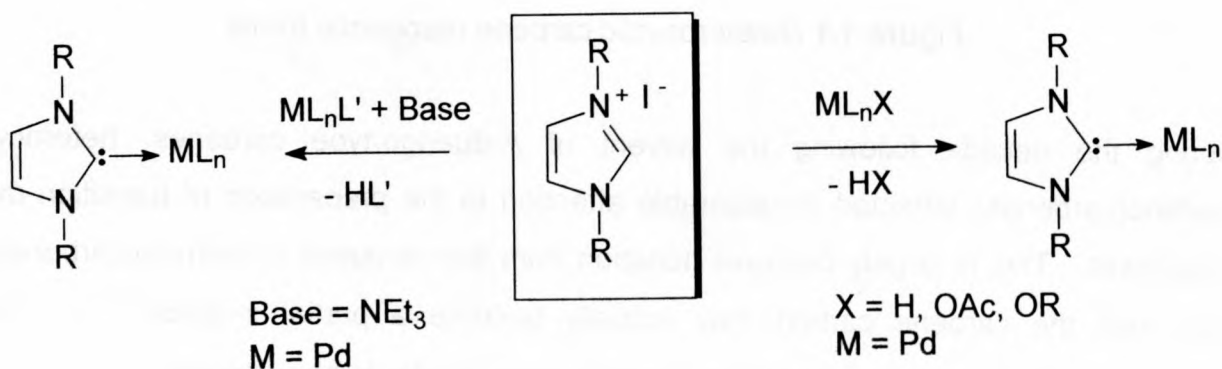
Given their strong σ -donor properties, it is not surprising that ligand substitution reactions with diamino(carbenes) emerged as a synthetic route to prepare transition metal complexes. Weakly coordinated ligands such as tetrahydrofuran (thf) and even generally strongly coordinating carbon monoxide are readily displaced by nucleophilic free carbenes (Scheme 1.4).^[1]



Scheme 1.4

Note that 1,3-dimethylimidazol-2-ylidene forms stable complexes with Group 4 metals,^[18,19] which are incapable of π -backbonding, supporting the current view that diamino(carbenes) bind to transition metals mainly through σ -donation. For this reason, the arrow notation used in Schemes 1.4 and 1.5 are more correct than the standard representation of a metal-carbene bond as $M=C$, although many chemists prefer to use the latter notation.

Another more versatile synthetic approach to prepare *N*-heterocyclic transition metal carbene complexes has also been further developed in recent years as continuation of research carried out by Öfele in the early 1970's.^[20] a basic ligand, X, in the reactant complex, ML_nX , can deprotonate the azolium halide salt,^[21,22] or alternatively, a base can be used together with ML_nL' (Scheme 1.5).



Scheme 1.5

Certain imidazolium salts, similar to those employed as stable carbene precursors in these metal complex preparations, form part of a new class of solvents, ionic liquids, which are attractive alternatives to conventional organic media. Ionic liquids are liquids consisting only of ions. However, they can be distinguished from the classical definition of molten salts that usually refer to high-melting, highly viscous and very corrosive media.^[23] In general, azolium salts are classified as ionic liquids if their melting points are below 100°C , although sometimes the term is also applied to salts that keep their liquid integrity at even higher temperatures.^[24]

Ionic liquids have become increasingly popular in recent years, mainly due to their lack of measurable vapour pressure, thereby promoting the environmental aspect of synthesis and catalysis.^[25] In addition, the physical and chemical properties of ionic liquids can be specifically varied by selection of suitable cations and anions (Figure 1.2), allowing

optimisation of the reaction medium for a specific application. For this reason, ionic liquids have been referred to as “designer solvents” and a number of excellent reviews are available.^[23,24,26]

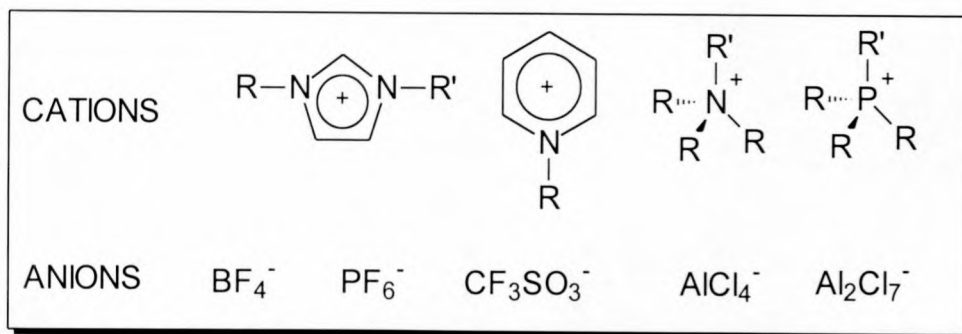
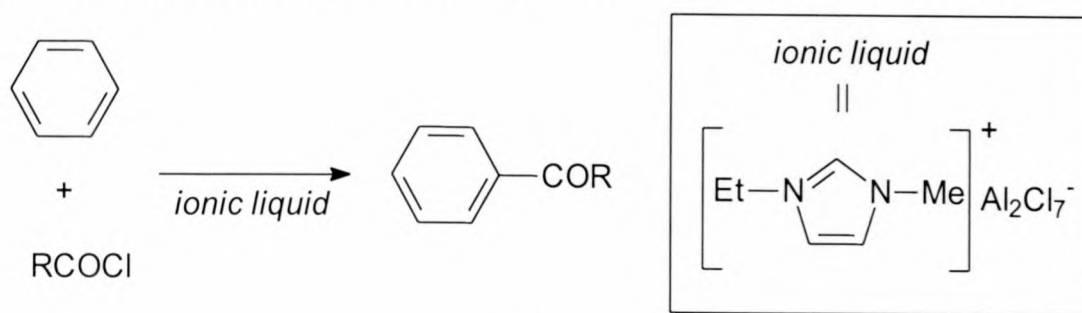


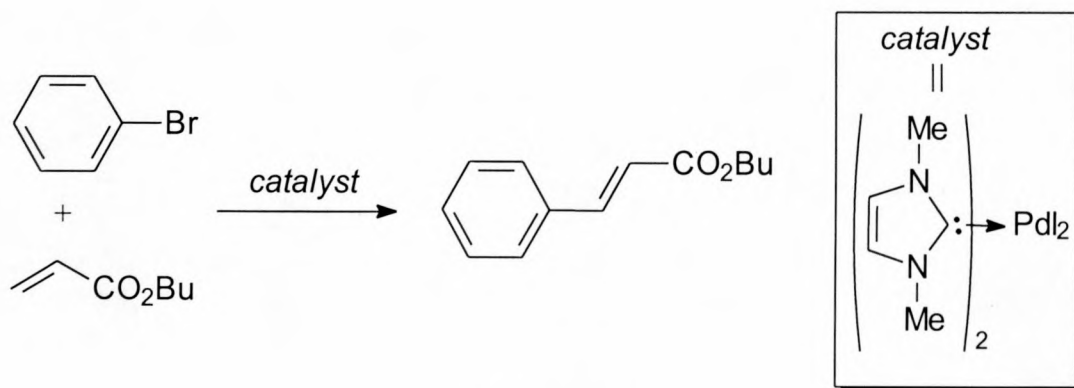
Figure 1.2 Important types of cations and anions for ionic liquids

Although many ionic liquids are known, those based on dialkyl(imidazolium) salts have attracted particular attention since a number of transition metal catalysts have displayed enhanced chemical reactivity in these media.^[27,28] Furthermore, by incorporating metals (Lewis acids) in the counterion, these ionic liquids can function as both solvent and catalyst. Imidazolium chloroaluminate melts, for example, promote Friedel-Crafts acylation (Scheme 1.6).^[29] The catalysis products exhibit poor solubility in the low melting ionic liquid and are, therefore, easily removed from the non-volatile reaction phase.



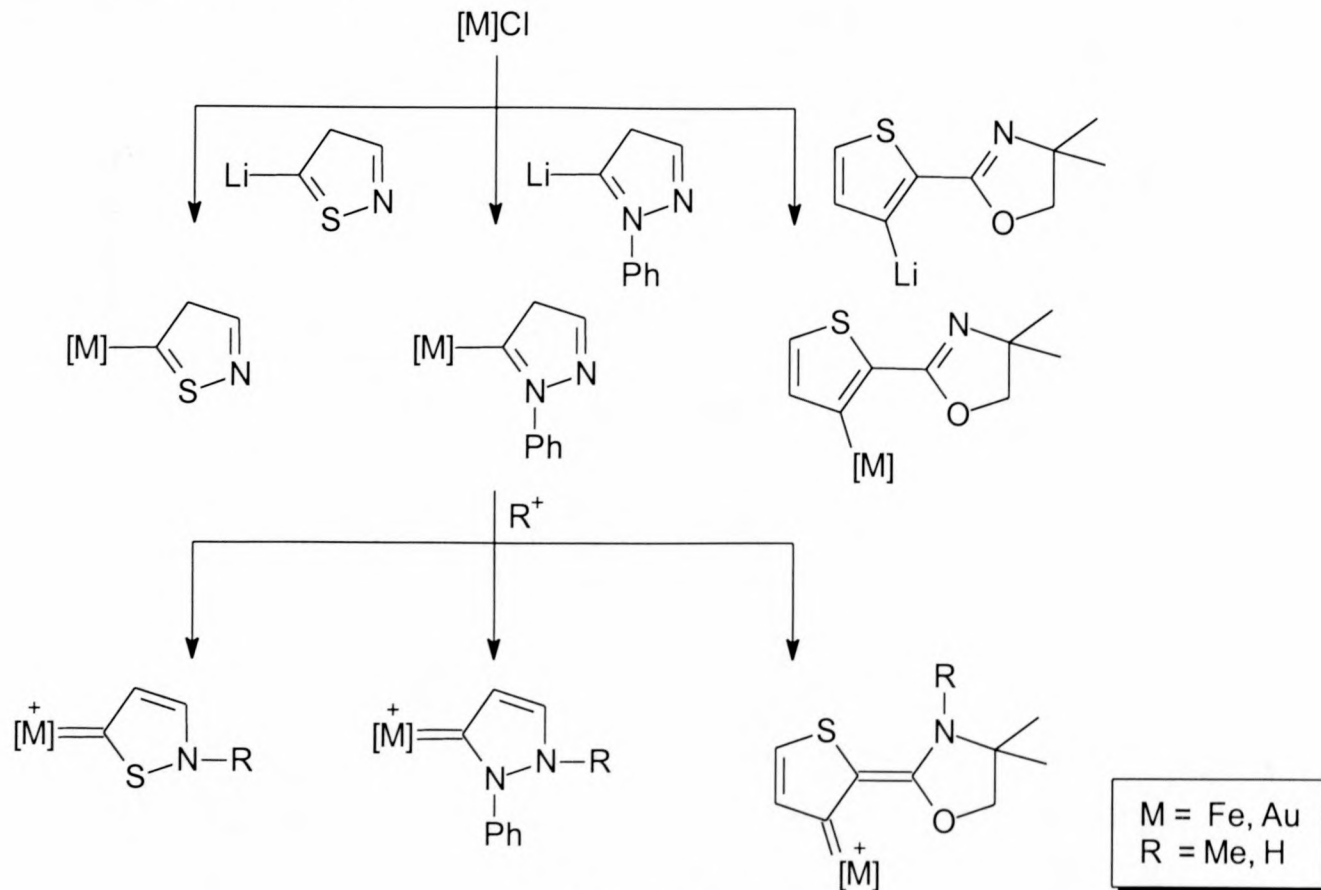
Scheme 1.6

Extensive studies on the Heck reaction in imidazolium-based ionic liquids have also proved especially fruitful. Herrmann was the first to report the excellent catalytic activity of palladium *bis*(imidazol-2-ylidene) complexes for this type of coupling reaction (Scheme 1.7).^[17] Later work in Seddon's group^[30] suggested that these carbene complexes form *in situ* under the experimental conditions of the Heck reaction, and more recently Xiao^[31] isolated such complexes from ionic liquid media, showing for the first time that an ionic liquid can function as both solvent and catalyst precursor.



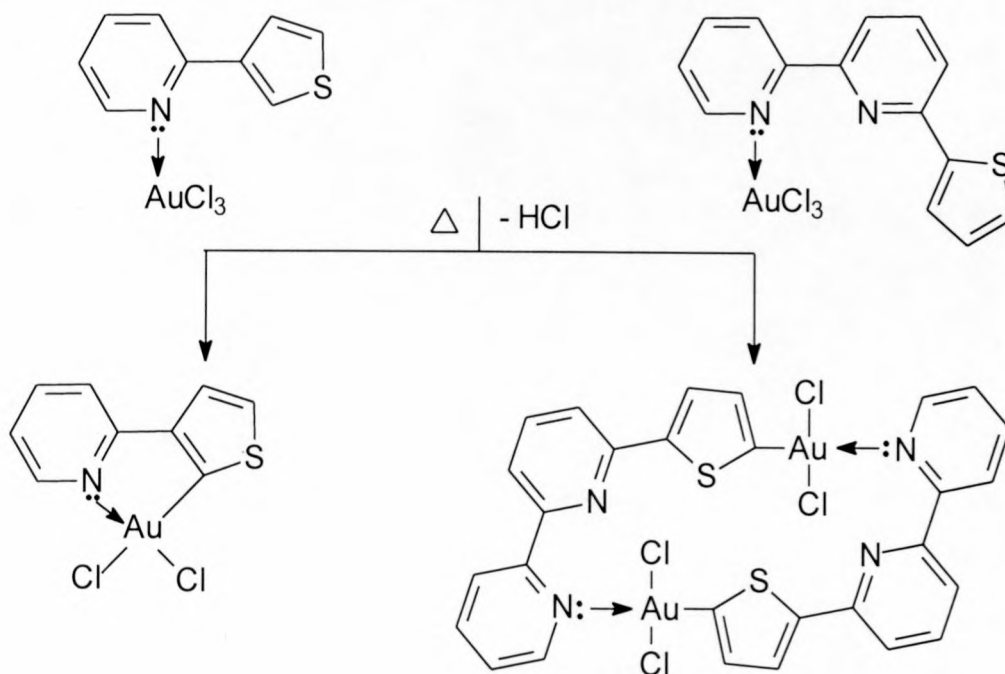
Scheme 1.7

Of the numerous and growing number of heterocyclic carbene complexes that have been characterised, relatively few are known that do not contain at least one heteroatom, usually nitrogen, attached to the carbene carbon and that are not derived from azoles. A variety of procedures are available to prepare these complexes, one of which was developed in our group.^[35] It involves the treatment of suitable metal starting compounds with lithiated azoles prior to protonation or alkylation, which generates the metal-carbene bond. In this way, the first examples of metal carbene complexes that contain a remote nitrogen atom within, or outside the coordinated ring-system, were isolated in our laboratory (Scheme 1.8).



Scheme 1.8

Imine nitrogens are also known as donor atoms towards gold in coordination complexes. This despite the fact that gold is classified as class (b) or soft metal, according to the soft and hard acids and bases (SHAB) principle and is expected to preferentially form bonds with soft, polarisable donor ligands such as carbenes or phosphines. Notwithstanding the SHAB expectation, a large number of compounds with gold-nitrogen bonds is known.^[32,33] In particular, gold(III) imine-bonded compounds have been used in the synthesis of auracycles by thermal elimination of HCl (Scheme 1.9).^[34]



Scheme 1.9

Heterometallacyclic gold(I) compounds (Figure 1.3) were also recently prepared in our laboratory by self-assembly of gold(I)-containing units in which the relative positions of C and N donor atoms determine the number of monomeric units in the product.

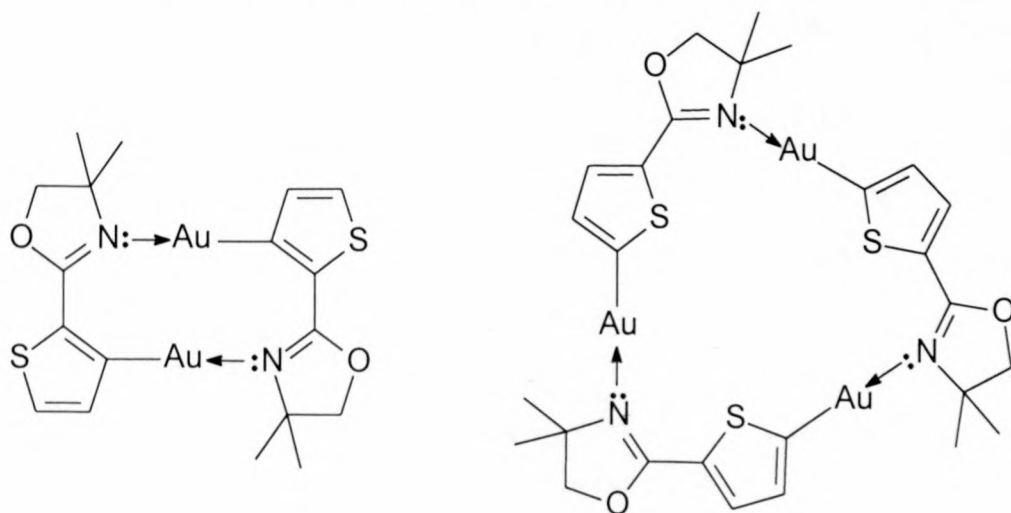
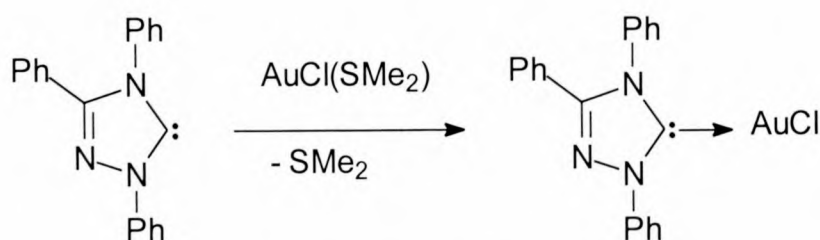


Figure 1.3 Cyclic gold complexes

1.2 AIMS AND OBJECTIVES

Ionic liquids derived from azoles are potential precursors for free carbenes and, therefore, also for carbene complexes. We envisaged the synthesis and characterisation of ionic liquids and their utilisation in the preparation of free carbenes as well as gold(I) carbene complexes. Although a variety of procedures are available to prepare gold(I) carbene complexes,^[35,36] only one report describes ligand substitution as such a method (Scheme 1.10).^[37] The preparation of ionic liquids and their conversion into stable carbenes and gold(I) carbene complexes are described in Chapter 2.



Scheme 1.10

Gold complexes are rarely used in homogeneous catalysis^[38] and in most instances reduction to gold metal signals catalyst deactivation. Ionic liquids have not been utilised as reaction media for gold catalysis, although stabilisation of other catalysts have often been observed in such solvents.

The hydration of phenylacetylene, known to be catalysed by NaAuCl₄,^[39] was now investigated in low melting ionic liquids. In addition, the possibility of incorporating gold in the anion of ionic liquids presented the dual advantage of the compound functioning as both solvent and catalyst. Since imidazolium ionic liquids with AuCl₄⁻ as the anion^[40] have recently been prepared, similar thiazolium compounds were now targeted to examine the catalytic hydration of acetylenes with a gold(III) compound and serving as both solvent and catalyst. Moreover, such thiazolium tetrachloroaurate salts were identified as potential precursors for carbene complex preparation by consecutive deprotonation and coordination. The results of these investigations are presented in Chapter 3.

Moving away from the azoles (compare Scheme 1.8), the question arose whether alternative heterocycles, which contain a distant oxygen atom as nucleophilic target, could also be utilised in preparing carbene complexes. The quinoline-based compounds, 4-

chloro-*N*-methylquinolinone and 4-chloro-2-methoxy-*N*-methylquinolinium tetrafluoroborate (Figure 1.4) qualified. The former should lead to a carbene complex precursor and the latter directly to a carbene complex. The synthesis of transition metal complexes utilising quinoline-based compounds is discussed in Chapter 4.

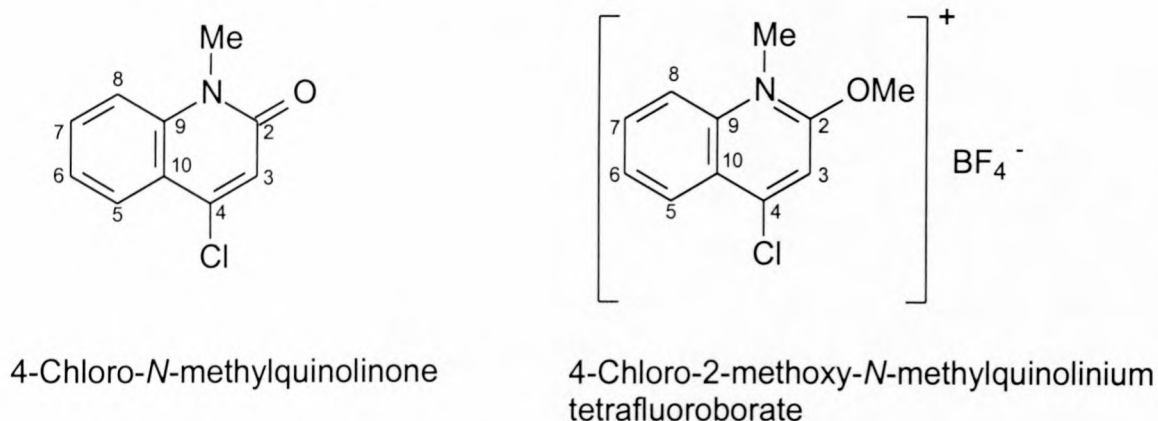
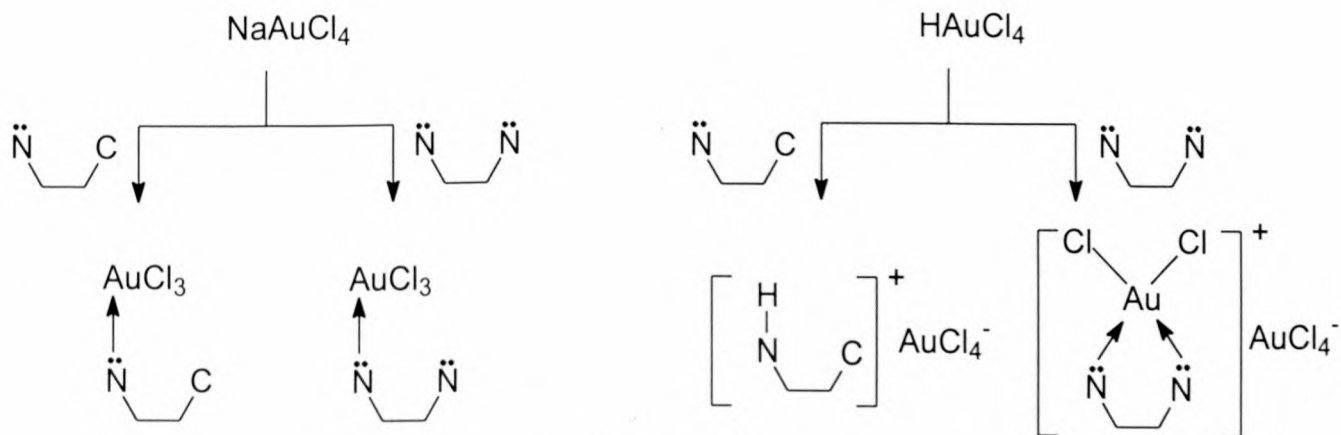


Figure 1.4 Quinoline-based ligand precursors

The growing interest in heterometallacyclic gold compounds (compare Scheme 1.9 and Figure 1.3) prompted the preparation of a series of gold(I) and gold(III) imine coordination compounds to establish the affinity of nitrogen for gold, and to characterise this coordination mode by structural and NMR studies. Although tetrachloroaurate(III) imonium salts are apparently obtained by the reaction of HAuCl_4 with monodentate imines in water, analogous preparation with chelating imines furnishes cationic complexes, independent of the employed reagent ratio and in addition, similar reactions with NaAuCl_4 only affords neutral imine- AuCl_3 adducts (Scheme 1.11).^[32,41] The reason for this difference is not clear and is discussed in Chapter 5.



Scheme 1.11

The nucleophilic nature of nitrogen and its use in the preparation of transition metal carbene and coordination complexes is the main theme of this thesis. The aims and objectives of this work can be summarised as follows:

- to use imidazolium-based ionic liquids for the preparation of free diamino(carbenes) and gold(I) carbene complexes;
- to investigate the catalytic hydration of phenylacetylene with NaAuCl_4 in imidazolium ionic liquids;
- to prepare new ionic liquids with thiazolium as cation and AuCl_4^- as counterion;
- to investigate the catalytic activity of gold(III) thiazolium salts for the hydration of phenylacetylene;
- to prepare gold(III) carbene complexes by deprotonation of gold(III) thiazolium salts;
- to prepare and characterise transition metal carbene complexes from heterocycles other than azoles in which a distant oxygen atom serves as nucleophilic target for carbene stabilisation;
- to utilise nitrogen σ -donors in the preparation of gold(I) and gold(III) imine coordination complexes and establish the affinity of the soft metal for the hard ligands
- to address ambiguities which exist for the preparation of gold(III) imine-coordinated complexes and structurally characterise this coordination mode of ligand to metal attachment.

REFERENCES

- [1] D. Bourissou, O. Guerret, F. P. Gabbaï and G. Bertrand, *Chem. Rev.*, 2000, **100**, 39.
- [2] E. O. Fischer and A. Maassböl, *Angew. Chem.*, 1964, **76**, 645.
- [3] D. L. Cardin, B. Cetinkaya and M. F. Lappert, *Chem. Rev.*, 1972, **72**, 545.
- [4] H. Fischer, in *The Chemistry of the Metal Carbon Bond*, (ed. S. Patai,) Wiley Interscience, New York, 1982, pp. 181.
- [5] K. H. Dötz, H. Fischer, P. Hoffman, F. R. Freissl, U. Schubert and K. Weiss, in *Transition Metal Carbene Complexes*, (ed. P. J. Bieel) Verlag Chemie, Weinheim, 1983, pp. 2.
- [6] W. D. Wulff, in *Comprehensive Organic Synthesis*, (eds. B. M. Trost and I. Fleming), Pergamon Press, New York, 1990, **5**, pp. 1065.
- [7] H. –W. Wanzlick and H. –J. Schönherr, *Angew. Chem.*, 1968, **80**, 154.
- [8] K. Öfele, *J. Organomet. Chem.*, 1968, **12**, 42.
- [9] A. J. Arduengo, R. L. Harlow and M. J. Kline, *J. Am. Chem. Soc.*, 1991, **113**, 361.
- [10] D. A. Dixon and A. J. Arduengo, *J. Phys. Chem.*, 1991, **95**, 4180.
- [11] C. Boehme and G. Frenking, *J. Am. Chem. Soc.*, 1996, **118**, 2039.
- [12] A. J. Arduengo, J. R. Goerlich and W. J. Marshall, *J. Am. Chem. Soc.*, 1995, **117**, 11027.
- [13] R. W. Alder, M. E. Blake, C. Bortolotti, S. Bufali, C. Butts, E. Linehan, J. M. Oliva, A. G. Orpen and M. J. Quayle, *J. Chem. Soc., Chem. Comm.*, 1999, 241.
- [14] R. W. Alder, P. R. Allen, M. M. Murray and A. G. Orpen, *Angew. Chem., Int. Ed. Engl.*, 1996, **35**, 1121.
- [15] R. W. Alder, C. P. Butts and A. G. Orpen, *J. Am. Chem. Soc.*, 1998, **120**, 11526.
- [16] N. Fröhlich, U. Pidun, M. Stahl and G. Frenking, *Organometallics*, 1997, **16**, 442.
- [17] W. A. Herrmann, M. Elison, J. Fischer, C. Köcher and G. R. J. Artus, *Angew. Chem., Int. Ed. Engl.*, 1994, **34**, 2371.
- [18] W. A. Herrmann, K. Öfele, M. Elison, F. E. Kühn and P. W. Roesky, *J. Organomet. Chem.*, 1994, **480**, C7.
- [19] N. Kuhn, T. Kratz, D. Bläser and R. Boese, *Inorg. Chim. Acta*, 1995, **238**, 179.
- [20] K. Öfele and C. G. Kreiter, *Chem. Ber.*, 1972, **105**, 529.
- [21] C. Köcher and W. A. Herrmann, *J. Organomet. Chem.*, 1997, **532**, 261.
- [22] W. A. Herrmann, C. P. Reisinger and M. Spiegler, *J. Organomet. Chem.*, 1998, **557**, 93.

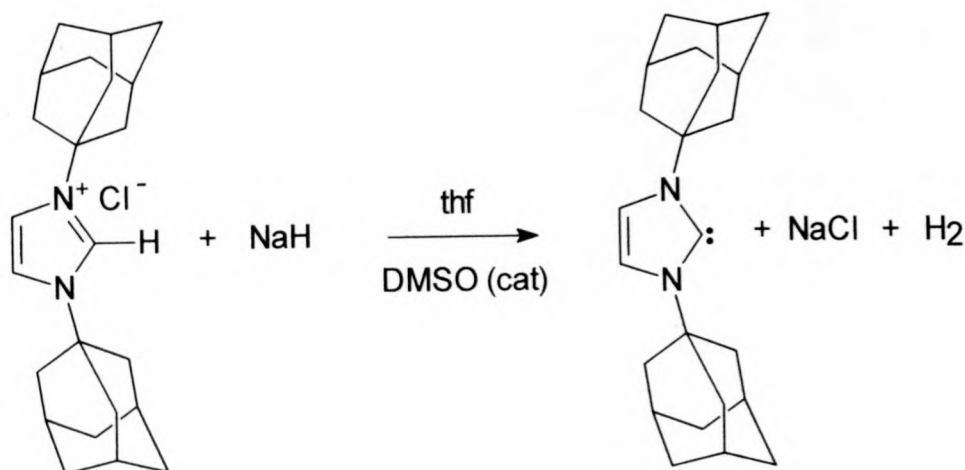
- [23] K. R. Seddon, *J. Chem. Biotechnol.*, 1997, **68**, 351; K. R. Seddon, *Kinet. Catal. Engl. Transl.*, 1996, **37**, 693.
- [24] P. Wasserscheid and W. Keim, *Angew. Chem., Int. Ed. Engl.*, 2000, **39**, 3773.
- [25] M. Freemantle, *Chem. Eng. News*, 1998, **76**, 32.
- [26] T. Welton, *Chem. Rev.*, 1999, **99**, 2071.
- [27] W. A. Herrmann and C. Köcher, *Angew. Chem., Int. Ed. Engl.*, 1997, **36**, 2162.
- [28] A. J. Arduengo and R. Krafczyk, *Chem. Unserer Zeit*, 1998, **32**, 6.
- [29] J. D. Holbrey and K. R. Seddon, *Clean Products and Processes*, 1999, **1**, 223.
- [30] A. J. Carmichael, M. J. Earle, J. D. Holbrey, P. B. McCormac and K. R. Seddon, *Org. Lett.*, 1999, **1**, 997.
- [31] L. Xu, W. Chen and J. Xiao, *Organometallics*, 2000, **19**, 1123.
- [32] R. J. Puddephatt, in *Comprehensive Coordination Chemistry*, (eds. G. Wilkinson, R. D. Gillard and J. A. McCleverty) Pergamon, Oxford, 1987, pp. 862.
- [33] J. Strähle, in *Gold: Progress in Chemistry, Biochemistry and Technology*, (ed. H. Schmidbaur), John Wiley and Sons, New York, 1999, pp. 311.
- [34] E. C. Constable, R. P. G. Henney, P. R. Raithby and L. R. Sousa, *Angew. Chem., Int. Ed. Engl.*, 1991, **30**, 1363.
- [35] H. G. Raubenheimer and S. Cronje, *J. Organomet. Chem.*, 2001, **617 - 618**, 170.
- [36] H. G. Raubenheimer and S. Cronje, in *Gold: Progress in Chemistry, Biochemistry and Technology*, ed. H. Schmidbaur, John Wiley and Sons, New York, 1999, pp. 557.
- [37] J. H. Teles, S. Brode and M. Chabanas, *Angew. Chem., Int. Ed. Engl.*, 1998, **37**, 1415.
- [38] D. Thompson, *Gold Bulletin*, 1999, **32**, 1.
- [39] Y. Fukuda and K. Utimoto, *J. Org. Chem.*, 1991, **56**, 3729.
- [40] M. Hasan, I. V. Kozhevnikov, M. R. H. Siddiqui, A. Steiner and N. Winterton, *Inorg. Chem.*, 1999, **38**, 5637.
- [41] R. J. Puddephatt, *The Chemistry of Gold*, Elsevier, Amsterdam, 1978, pp. 98.

CHAPTER 2

PREPARATION OF A FREE DIAMINO(CARBENE) AND CARBENE COMPLEXES OF GOLD(II) UTILISING IONIC LIQUIDS

2.1 INTRODUCTION

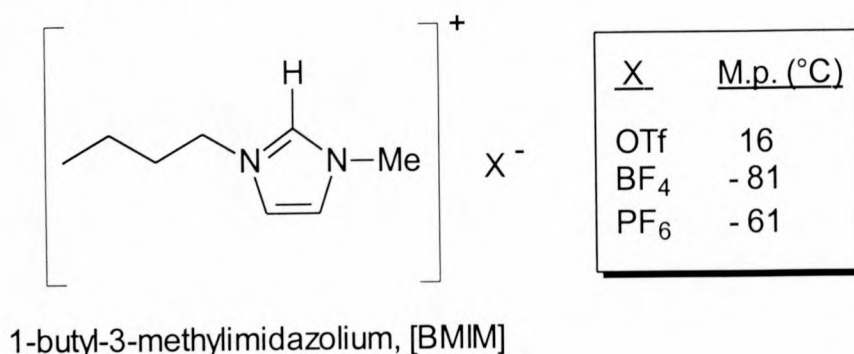
Arduengo achieved the synthesis of the first stable crystalline diamino(carbene) in 1991 by the deprotonation of *bis(adamantyl)imidazolium chloride* with sodium hydride in the presence of a catalytic amount of dimethylsulphoxide (Scheme 2.1).^[1] A number of alternative routes to unsaturated *N*-heterocyclic singlet carbenes have been reported since then,^[2,3] but Arduengo's original procedure remains the method of choice.



Scheme 2.1

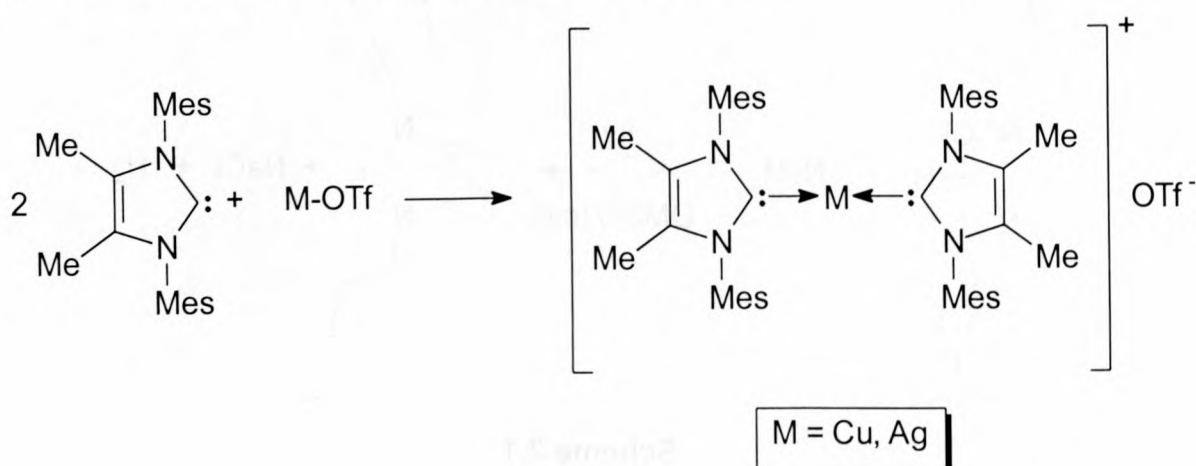
In general, imidazolium salts are classified as ionic liquids if their melting point is below 100°C.^[4] In particular, 1-butyl-3-methylimidazolium, [BMIM], salts with anions such as triflate, [OTf]⁻,^[5] tetrafluoroborate, [BF₄]⁻ and hexafluorophosphate, [PF₆]⁻^[6] are liquid at room temperature (Scheme 2.2). At present, imidazolium halide salts are generally employed as free diamino(carbene) precursors, but in this chapter it is shown that ionic liquids are also available as substrates for free carbene synthesis and the preparation of 1-

butyl-3-methylimidazol-2-ylidene is described. This leads to the possibility of coordinating carbenes *in situ* during catalysis.



Scheme 2.2

The beginnings of gold carbene chemistry date back nearly two decades^[7,8] and until recently these complexes have known very few applications. Although a number of strategies are available for the preparation of gold carbene complexes,^[9] a free *N*-heterocyclic diamino(carbene) was first utilised for this purpose in 1998.^[10] No experimental or characterisation data for the catalytically active *mono*(carbene) compound were, however, provided. Copper(I) and silver(I) diamino(carbene)-adducts have been prepared by the reaction of the metal triflate with 1,3-dimesitylimidazol-2-ylidene (Scheme 2.3),^[11] but no related accounts exist for gold compounds.

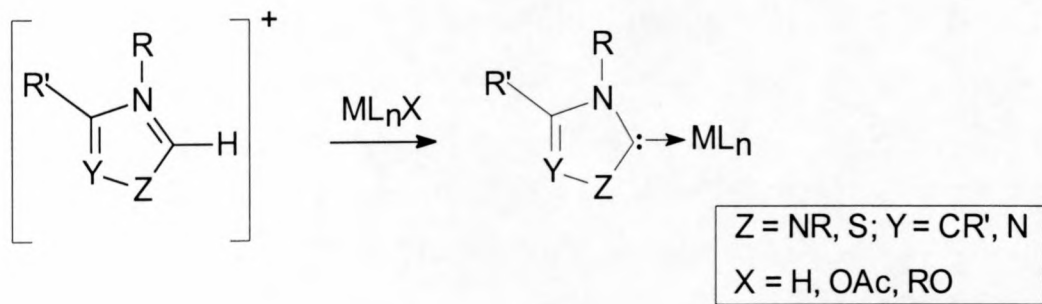


Scheme 2.3

In this chapter, the preparation and characterisation of a gold(I) free carbene adduct utilising a ligand substitution reaction is described.

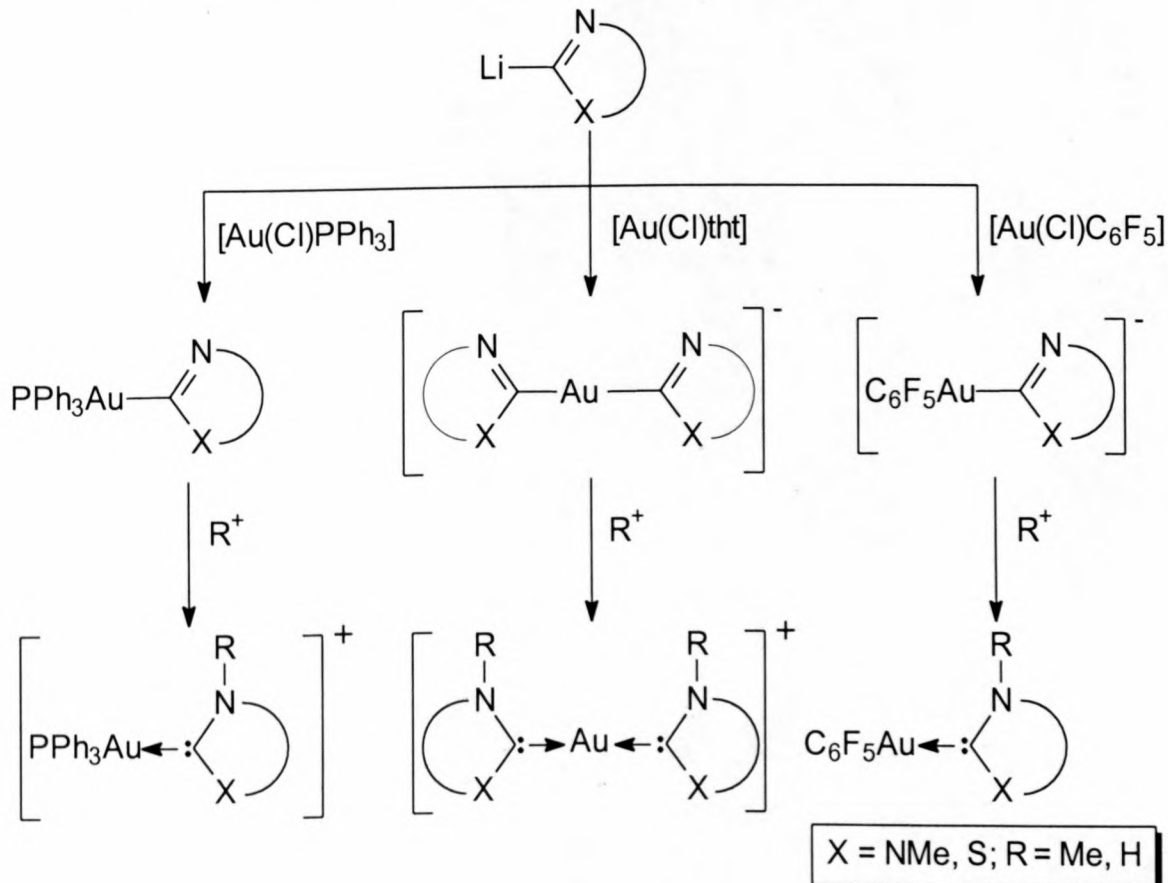
Organometallic fragments, ML_nX , with a sufficiently basic ligand X, such as hydride^[12], alkoxide^[13] or acetate,^[14] deprotonate azolium salts to furnish the corresponding carbene

complexes (Scheme 2.4). This synthetic strategy was recognised by Öfele as early as 1972^[12] and remains a more general method to prepare metal carbene complexes than starting from isolated carbenes. Although this methodology has been successfully applied to prepare a variety of transition metal carbene complexes, no similar reports are available for gold.



Scheme 2.4

In recent years, our research group have been interested in the synthesis of heterocyclic carbene complexes of gold.^[9] A preparative procedure developed for this purpose involves the treatment of halogold compounds with lithiated azoles prior to protonation or alkylation (Scheme 2.5). With the non-halide ligand labile, disubstitutions occur and predominantly *bis*(carbene) complexes are produced.



Scheme 2.5

Free imidazol-2-ylidene carbenes are described as better σ -donors than the best phosphine donors^[15] and should thus be alternatives for such soft donor ligands. Neutral methyl gold(I) phosphine complexes are easily prepared, but, as yet, no analogous methyl gold(I) carbene complexes have been isolated. Dimethylaurate (AuMe_2^-) is prepared by the addition of two molar amounts of methyllithium (MeLi) to $[\text{Au}(\text{Cl})\text{PPh}_3]$ at low temperature. The addition of AuMe_2^- to $[\text{BMIM}][\text{OTf}]$ was envisaged to afford a neutral methyl gold(I) carbene complex by a consecutive deprotonation-coordination mechanism. This approach, however, did not produce the desired result and is discussed in this chapter. In a similar reaction, $[\text{Au}(\text{Cl})\text{tht}]$ was employed as the dimethylaurate precursor, and also gave an unexpected result that is presented here.

The nucleophilicity of the newly prepared free diamino(carbene), 1-butyl-3-methylimidazol-2-ylidene, was investigated by its attempted reaction with AuMe_2^- prepared from $[\text{Au}(\text{Cl})\text{tht}]$ and two molar equivalents of MeLi. Substitution of a methyl ligand from AuMe_2^- could afford a neutral methyl gold(I) carbene complex and the synthetic attempt is described in this chapter.

2.2 RESULTS AND DISCUSSION

2.2.1 Free Carbene Precursor Preparations

A Preparation of [BMIM][OTf] and [BMIM][PF₆]

[BMIM][OTf]^[5] and [BMIM][PF₆]^[6] were prepared according to literature procedures, which involves the metathesis of [BMIM][Cl] with HOTf and HPF₆, respectively. In this way, the ionic liquids were obtained in near quantitative yield.

B Spectroscopic characterisation of [BMIM][OTf] and [BMIM][PF₆]

1. NMR spectroscopy

The ¹H and ¹³C-¹H NMR spectroscopic data of [BMIM][OTf] and [BMIM][PF₆] are given in Table 2.1 to simplify the comparison of chemical shifts in the starting compounds and products in the text.

The ¹³C-¹H NMR spectra of [BMIM][OTf] and [BMIM][PF₆] are very similar, whereas the ¹H NMR spectra display the H² signal respectively at δ 9.12 and 8.58. It is generally accepted that ¹³C-¹H NMR spectra give a better indication of electron density redistribution than ¹H NMR chemical shifts,^[16] since in the former, the paramagnetic components can be ignored when correlating chemical shifts and charge densities.^[17] Charge distribution in the organic cation of the respective ionic liquids should not be affected by the different anions and similar proton shifts are expected.

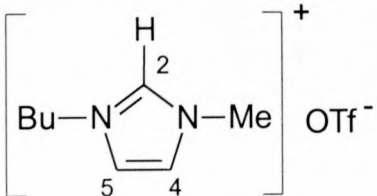
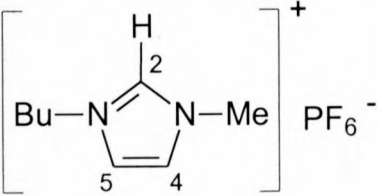
A change in signal positions is often observed when a compound interacts with a range of solvents of varying polarity^[18] - a so-called solvent effect. Since [BMIM][OTf] and [BMIM][PF₆] were dissolved in polar acetone (μ = 2.88D)^[19] and less polar tetrahydrofuran (μ = 1.75D),^[19] respectively, the change in the H² signal position is attributed to a solvent effect.

Long-range coupling (J = <1 Hz) between H² and the H⁴ and H⁵ protons is displayed as a doublet of triplets in both the ionic liquids.

The triflate carbon of [BMIM][OTf] resonates as a quartet due to coupling with fluorine and the observed coupling constant, $^1J(\text{CF}) = 3834 \text{ Hz}$, is similar to literature values.^[16]

Note the position of the C² carbon in [BMIM][OTf] and [BMIM][PF₆] at δ 138.1.

Table 2.1 ^1H and $^{13}\text{C}\{-^1\text{H}\}$ NMR data for [BMIM][OTf] and [BMIM][PF₆]

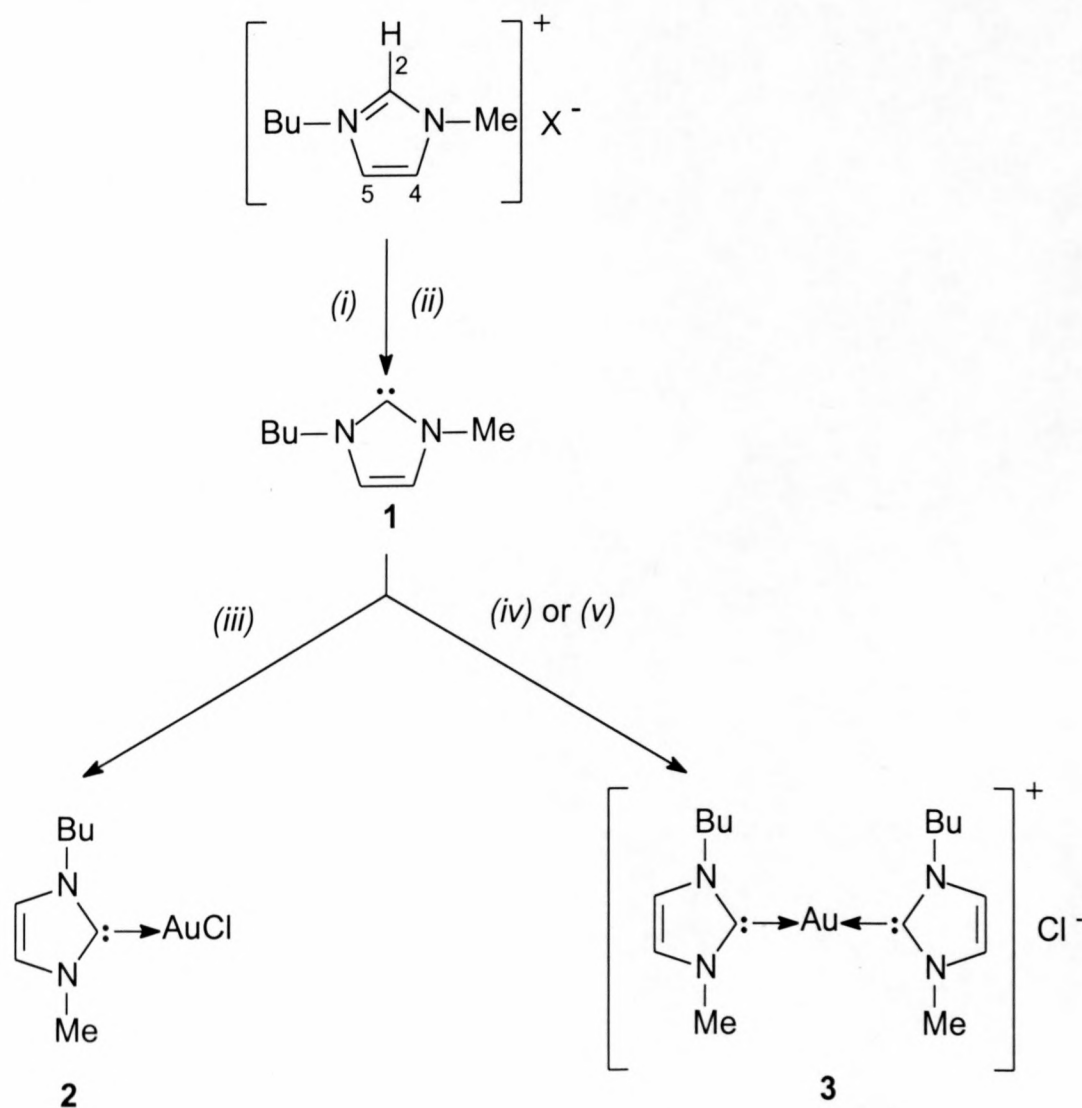
Ionic liquid		
Solvent	d-acetone	d-thf
^1H NMR ^a		
H ²	9.12 (1H, s)	8.58 (1H, s)
H ⁴ and H ⁵	7.79 (2H, dt, J = 18, <1)	7.34 (2H, dt, J = 18, <1)
NMe	4.06 (3H, s)	3.95 (3H, s)
NCH ₂ -	4.38 (2H, t, J = 15)	4.18 (2H, t, J = 15)
NCH ₂ CH ₂ -	1.42 / 1.92 (2H, m)	1.34 / 1.86 (2H, m)
N(CH ₂) ₂ CH ₂ -	1.42 / 1.92 (2H, m)	1.34 / 1.86 (2H, m)
terminal CH ₃	0.95 (3H, t, J = 15)	0.96 (3H, t, J = 15)
^{13}C NMR ^a		
C ²	138.1	138.1
C ⁴ and C ⁵	123.8 / 125.1	122.9 / 124.4
NMe	36.7	36.7
NCH ₂ -	50.2	50.6
NCH ₂ CH ₂ -	32.8	32.3
N(CH ₂) ₂ CH ₂ -	20.0	19.9
terminal CH ₃	13.7	13.5
Other ^a		
CF ₃ SO ₃ ⁻	122.1 (1C, q, J = 3834)	-

^a J in Hz

2.2.2 A Free Imidazolinylidene

A Preparation of $[\text{CN}(\text{Me})\text{CH}=\text{CHN}(\text{Bu})]$, **1**

1-Butyl-3-methylimidazol-2-ylidene, **1**, was obtained according to two synthetic routes. The preparation of carbene **1** utilising MeLi is described under Method 1 and its unexpected free existence in the reaction of [BMIM][OTf] and a MeLi/[Au(Cl)PPh₃] mixture (2:1) is discussed under Method 2.



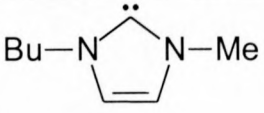
Reagents: (i) MeLi; X = OTf, PF₆ (ii) MeLi:[Au(Cl)PPh₃] (2:1); X = OTf
 (iii) [Au(Cl)tht] or [Au(Cl)SMe₂] (iv) MeLi:[Au(Cl)tht] (2:1)
 (v) [Au(Cl)PPh₃]

Scheme 2.6

Method 1

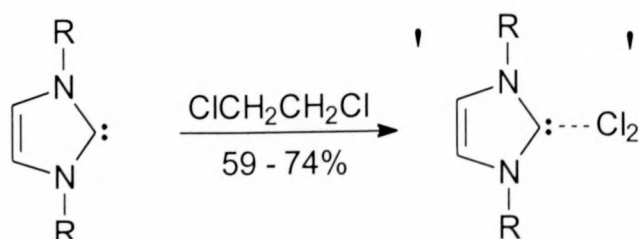
Treatment of [BMIM][OTf] or [BMIM][PF₆] at room temperature with MeLi gave diamino(carbene) **1** in yields of 73% and 85% (Scheme 2.6). Filtration through Celite afforded the pure carbene as a pale yellow, oily compound. The product is unstable in air and readily soluble in diethyl ether, acetone and thf. Analytical and physical data for carbene **1** are reported in Table 2.2.

Table 2.2 Analytical and physical data for free carbene **1**

Carbene	
	1
Colour	Pale yellow
Yield (%)	73 / 85
M.p./ °C	oil
M.W.	138.21
Analysis (%) ^a	
C	69.81 (69.52)
H	10.24 (10.21)
N	20.13 (20.27)

^a Required values given in parentheses

Free imidazolynilidenes react with organohalides to form halide derivatives (Scheme 2.7).



Scheme 2.7

Although the precise structure of the derivatives is not known, these compounds have been used as chlorinating and chloride donor reagents.^[20] Imidazolin-2-ylidenes also react with alkyl halides to simultaneously furnish olefins as well as the corresponding imidazolium salts and the structures of such compounds have been determined.^[21,22] Chlorinated solvents are, therefore, excluded as reaction media for free carbenes.

Method 2

Aiming for the formation of $[\text{Li}(\text{PPh}_3)][\text{AuMe}_2]$, $[\text{Au}(\text{Cl})\text{PPh}_3]$ in thf or diethyl ether at -78°C was mixed with two molar amounts of MeLi.^[23] Treatment of $[\text{BMIM}][\text{OTf}]$ with a solution of the expected aurate was anticipated to furnish a neutral (methyl)gold(I) carbene complex. Repeated attempts, however, predominantly afforded the uncoordinated diamino(carbene), **1**. This result is again discussed in paragraph 2.2.5.

B Spectroscopic characterisation of diamino(carbene) **1**

1. NMR spectroscopy

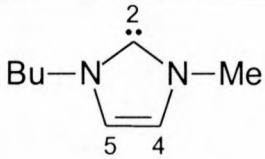
The ^1H and $^{13}\text{C}\{-^1\text{H}\}$ NMR data for carbene **1** are presented in Table 2.3.

Disappearance of the H^2 signal in the proton spectra indicated deprotonation at this position. A small downfield shift of $\Delta\delta$ 0.11 for the H^4 and H^5 protons is evident. The downfield shift of imidazolinylidene ring protons, with respect to those of the imidazolium salt precursors has previously been ascribed to decreased π -delocalisation in the free carbene ring.^[1]

The long-range coupling between the ring protons and the H^2 proton, as observed in $[\text{BMIM}][\text{OTf}]$ and $[\text{BMIM}][\text{PF}_6]$, is of course, no longer visible. Although not generally utilised to verify carbene formation, long-range coupling is clearly absent in the free carbene.

The $^{13}\text{C}\{-^1\text{H}\}$ NMR spectroscopic data for carbene **1** display the carbene signal at δ 210.9, downfield by $\Delta\delta$ 72.8 with respect to C^2 in $[\text{BMIM}][\text{OTf}]$. The chemical shift of the carbene atom is similar to that observed for a range of related imidazol-2-ylidenes that exhibit these signals between δ 205.9 and δ 215.2.^[2,24] The remaining carbon atoms show no significant chemical shift changes.

Table 2.3 NMR spectroscopic data for diamino(carbene) **1**

Carbene 1		
¹ H NMR ^a	H ²	-
	H ⁴ and H ⁵	7.79 (2H, d, J= 18)
	NMe	4.07 (3H, s)
	NCH ₂ -	4.38 (2H, t, J = 15)
	NCH ₂ CH ₂ -	1.39 / 1.92 (2H, m)
	N(CH ₂) ₂ CH ₂ -	1.39 / 1.92 (2H, m)
	terminal CH ₃	0.97 (3H, t, J = 15)
¹³ C NMR	C ²	210.9
	C ⁴ and C ⁵	123.7 / 125.1
	NMe	36.7
	NCH ₂ -	50.3
	NCH ₂ CH ₂ -	32.8
	N(CH ₂) ₂ CH ₂ -	20.0
	Terminal CH ₃	13.7

^a J in Hz

2. Mass spectrometry

The electron ionisation (EI) mass spectral data of carbene **1** are summarised in Table 2.4. The molecular ion of the free carbene is observed at m/z 138 as the base peak and the fragmentation pattern shows the loss of either the methyl or the butyl group.

Table 2.4 Mass spectral data of carbene **1**

m/z	I ^a	Fragment ions
138	100	$[\overline{\text{CN}(\text{Me})\text{CH}=\text{CHN}(\text{Bu})}]^+$
123	11	$[\overline{\text{CNCH}=\text{CHN}(\text{Bu})}]^+$
82	21	$[\overline{\text{CN}(\text{Me})\text{CH}=\text{CHN}}]^+$

^a Intensity relative to the base peak

2.2.3 A Neutral Diamino(carbene) Complex of Gold(I)

A Preparation of $[\text{ClAu}\{\overline{\text{CN}(\text{Me})\text{CH}=\text{CHN}(\text{Bu})}\}], \mathbf{2}$

Free imidazole-derived carbenes are described as better σ -donors than the best phosphine donors^[25] and should readily displace weakly coordinated ligands. The neutral complex, **2**, was prepared by the displacement of thioether ligands in gold(I) precursor compounds and the synthetic procedure is described as Method 3. An attempted preparation of AuMe_2^- by treatment of $[\text{Au}(\text{Cl})\text{tht}]$ with two molar amounts of MeLi , followed by addition to $[\text{BMIM}][\text{OTf}]$, was expected to afford a neutral methyl gold(I) carbene complex. However, as mentioned before, complex **2** was obtained. The procedure is discussed as Method 4.

Method 3

Treatment of a diethyl ether suspension of $[\text{Au}(\text{Cl})\text{SMe}_2]$ or $[\text{Au}(\text{Cl})\text{tht}]$ at -50°C with one molar equivalent of carbene **1** afforded the neutral gold(I) adduct **2** in 35% yield (Scheme 2.6). Filtration through Celite and drying *in vacuo* afforded the product as a white powder. Complex **2** is readily soluble in acetone, thf and dichloromethane and is unstable in air. The product can be stored for extended periods under an inert atmosphere and at low temperature.

Mixed ligand gold(I) compounds regularly exhibit homoleptic rearrangement (Equation 1, in which charges are omitted), but this behavior was not observed for compound **2**.^[9]



Equation 2.1

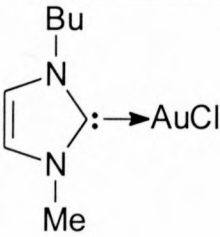
Method 4

The attempted preparation of $[\text{Li}(\text{tht})][\text{AuMe}_2]$ by treatment of $[\text{Au}(\text{Cl})\text{tht}]$ in thf at -78°C with two equivalents of MeLi , followed by addition to one molar equivalent of $[\text{BMIM}][\text{OTf}]$, yielded complex **2**, $[\text{ClAu}\{\overline{\text{CN}(\text{Me})\text{CH}=\text{CHN}(\text{Bu})}\}]$, in 20% yield. Evidenced by both deposition of gold and unreacted $[\text{BMIM}][\text{OTf}]$, it was concluded that the aurate complex,

[Li(tht)][AuMe₂], was not quantitatively formed. The formation of the *mono*(carbene) **2** was ascribed to the reaction of the free carbene **1** with unconverted [Au(Cl)tht] (*vide infra*).

The physical and analytical data for complex **2** are given in Table 2.5.

Table 2.5 Analytical and physical data for complex **2**

Complex 2	
M.p./°C	192 – 193
Colour	Colourless
Yield(%)	20
M.W.	370.64
Analysis(%) ^a	
C	25.88 (25.92)
H	4.01 (3.80)
N	7.43 (7.56)

^a Required values given in parentheses

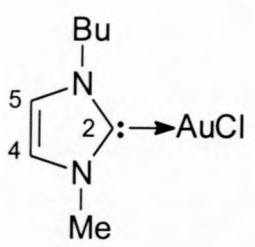
Complex **2** was also obtained as a product of the reaction between a MeLi/[Au(Cl)tht] (2:1) mixture and carbene **1**. The result is discussed in paragraph 2.2.4.

B Spectroscopic characterisation of complex **2**

1. NMR spectroscopy

The ¹H and ¹³C-{¹H} NMR data for complex **2** are presented in Table 2.6.

Table 2.6 Spectroscopic data for complex **2**

Complex 2		
Solvent	d-acetone	
$^1\text{H NMR}^a$	H^2	-
	H^4 and H^5	7.43 (2H, d, $J = 18$)
	NMe	3.86 (3H, s)
	NCH_2-	4.24 (2H, t, $J = 15$)
	NCH_2CH_2-	1.39 / 1.93 (2H, m)
	$\text{N}(\text{CH}_2)_2\text{CH}_2-$	1.39 / 1.93 (2H, m)
	terminal CH_3	0.96 (3H, t, $J = 15$)
$^{13}\text{C NMR}$	C^2	171.5
	C^4 and C^5	123.7 / 125.0
	NMe	37.6
	NCH_2-	50.2
	NCH_2CH_2-	33.8
	$\text{N}(\text{CH}_2)_2\text{CH}_2-$	20.2
	terminal CH_3	13.7

^a J in Hz

Disappearance of the H^2 signal in complex **2** as well as the absence of long-range coupling between the ring protons and H^2 indicated carbene formation. In contrast to Fischer-type carbene complexes, imidazol-2-ylidenes bind to transition metals mainly by σ -donation with π -back-bonding being negligible.^[26] The slight upfield shift noted for H^4 and H^5 at δ 7.43 is therefore surprising, but similar to that observed for a similar neutral cyano carbenegold(I) complex at δ 7.38.^[27] This suggests that complex **2** and the gold(I) cyanide carbene complex share similar π -electron distributions, albeit with one different *N*-alkyl group. The remaining proton chemical shifts of complex **2** were not changed from their positions in the free carbene.

The $^{13}\text{C}\{-^1\text{H}\}$ NMR spectroscopic data for complex **2** display a $\Delta\delta$ 39.4 upfield shift of C^2 with respect to carbene **1**. The carbene carbon in neutral^[28] as well as cationic gold(I) carbene complexes generally resonates δ ca. 180.^[29] The present chemical shift of δ 171.5 and the δ ca. 180 of other gold(I) carbene complexes seems rather low, since the σ -donor character of the carbene ligand is expected to produce a downfield shift of the carbene atom relative to the free carbene carbon position at δ ca. 210. As already mentioned in paragraph 2.2.1, $^{13}\text{C}\{-^1\text{H}\}$ NMR spectra give a better indication of electron density distribution than ^1H NMR spectra. In the presence of large atoms, however, the diamagnetic contribution to shielding increases with increasing atomic number^[30] and although the paramagnetic contribution remains important, the overall shielding decreases and an upfield shift is observed. This "heavy atom effect" probably contributes to the unexpected upfield position of σ -donor carbene carbons coordinated to gold. A similar trend is evident for thiazolylynylidene gold(I) carbene complexes that have their carbene signal at δ ca. 210, with respect to the corresponding free carbene signal, which appears at δ ca. 250.^[31] Heteroatom electronegativity and amine substituent effects undoubtedly also affect the carbene signal position, but in the absence of detailed investigations, no generalisations can be made. The remaining carbon shifts of complex **2** display no significant changes.

2. Mass spectrometry

The EI mass spectral data of complex **2** are summarised in Table 2.7. The molecular ion of the complex is observed at m/z 371. Fragmentation consists of sequential loss of chlorine and gold to give the free carbene fragment ion at m/z 138 as the base peak.

Table 2.7 Mass spectral data of complex **2**

m/z	I^a	Fragment ions
371	13	$[\text{ClAu}\{\text{CN}(\text{Me})\text{CH}=\text{CHN}(\text{Bu})\}]^+$
335	20	$[\text{Au}\{\text{CN}(\text{Me})\text{CH}=\text{CHN}(\text{Bu})\}]^+$
138	100	$[\text{CN}(\text{Me})\text{CH}=\text{CHN}(\text{Bu})]^+$

^a Intensity relative to the base peak

2.2.4 A Cationic Gold(I) Diamino(carbene) Complex

A Preparation of $[\text{Au}\{\text{CN}(\text{Me})\text{CH}=\text{CHN}(\text{Bu})\}_2]\text{Cl}$, **3**

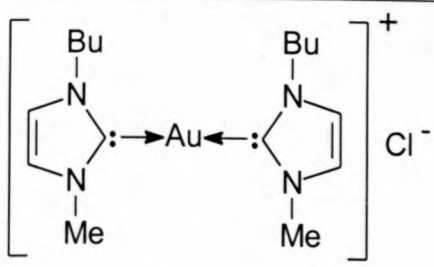
A substitution reaction between diamino(carbene) **1** and a $\text{MeLi}/[\text{Au}(\text{Cl})\text{tht}]$ (2:1) mixture was expected to afford a neutral gold(I) carbene complex. The addition of carbene **1** to such a mixture, however, afforded a cationic gold(I) (*bis*)carbene complex and the procedure is mentioned in Method 5.

Since free diamino(carbenes) have superior σ -donor character compared to phosphine ligands,^[25] an equimolar substitution of PPh_3 from $[\text{Au}(\text{Cl})\text{PPh}_3]$ by carbene **1**, was predicted to afford a neutral (chloro)gold(I) carbene complex. A cationic *bis*(carbene), complex **3**, unexpectedly formed in this reaction, as described under Method 6.

As mentioned previously, reaction of a 2:1, $\text{MeLi}:[\text{Au}(\text{Cl})\text{PPh}_3]$ mixture with $[\text{BMIM}][\text{OTf}]$, did not afford the anticipated neutral methyl gold(I) carbene complex (see Method 7). Carbene **1** formed predominantly, and small amounts of a cationic carbene complex were also detected.

The physical data for complex **3** are given in Table 2.8. An analytically pure sample of the *bis*(carbene) complex could not be isolated according to any of these procedures and elemental analyses were not performed.

Table 2.8 Analytical and physical data for complex **3**

Complex 3	
M.p./°C	212 – 225, Decomposition without melting
Colour	White
Yield(%)	20 ^a , 22 ^b , 26 ^c
M.W.	508.85

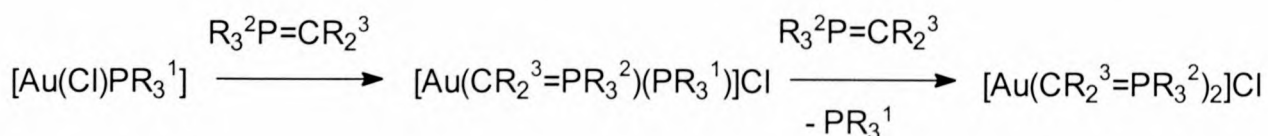
^aMethod 5; ^bMethod 6; ^cMethod 7

Method 5

Addition of carbene **1** to a thf solution at -78°C , containing two molar amounts of MeLi and one molar amount of $[\text{Au}(\text{Cl})\text{tht}]$, afforded predominantly the *bis*(carbene) complex **3**, as well as a low concentration of the *mono*(carbene) compound, **2** (Scheme 2.6). As determined by ^1H NMR, the neutral and cationic complexes were present in a ratio of 1:6. The product mixture is a white powder and is readily soluble in thf, acetone and dichloromethane and can be stored under an inert atmosphere at low temperature for extended periods of time.

Formation of the *mono*(carbene) **2** was again ascribed to the reaction of carbene **1** and unconverted $[\text{Au}(\text{Cl})\text{tht}]$ (paragraph 2.2.3).

The formation of complex **3** is reminiscent of a reaction between ylides of the type $\text{R}_2^3\text{C}=\text{PR}_3^2$ and halogold(I) phosphine compounds.^[32] A *mono*(ylide) species forms initially and converts into a *bis*(ylide) gold(I) complex with an excess of the ligand (Equation 2.2).



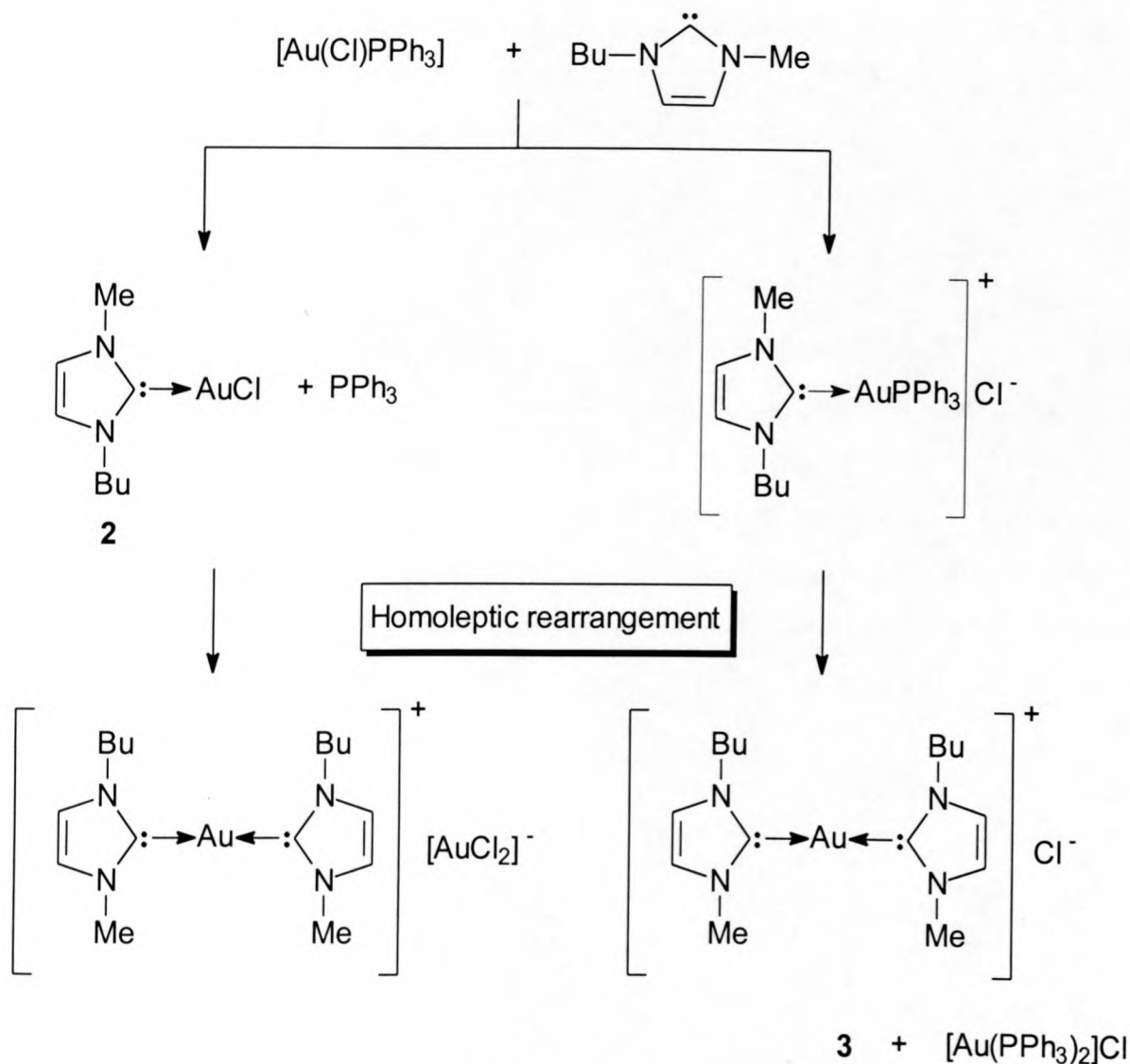
Equation 2.2

In the current reaction, diamino(carbene) **1** is present in excess, since some $[\text{Au}(\text{Cl})\text{tht}]$ decomposes upon treatment with MeLi. Furthermore, the *trans* influence of free imidazol-2-ylidene carbenes is greater than that of PPh_3 ^[28] and labilises the Au-Cl bond. The required excess of carbene **1** is evidenced by the exclusive formation of complex **2**, by stoichiometric reaction of carbene **1** with either $[\text{Au}(\text{Cl})\text{tht}]$ or $[\text{Au}(\text{Cl})\text{SMe}_2]$ (paragraph 2.2.3). Homoleptic rearrangement of complex **2** occurs to furnish complex **3**, with AuCl_2^- as counterion.

Method 6

Stoichiometric addition of $[\text{Au}(\text{Cl})\text{PPh}_3]$ in a 1:1 ratio to a tetrahydrofuran (thf) solution of carbene **1** at room temperature, furnished mainly the cationic *bis*(carbene) complex, **3** and an unidentified phosphine-containing product (Scheme 2.6). The product mixture is a

white powder that readily dissolves in polar organic solvents and is stable at low temperature under an inert atmosphere.



Scheme 2.8

Three possible pathways could account for the result obtained (Scheme 2.8 - pathways 1 and 2; Equation 2.2 – pathway 3): (a) ligand substitution of PPh_3 by carbene **1** to furnish the adduct **2**, followed by rapid homoleptic rearrangement to give complex **3**, but with AuCl_2^- as counterion; (b) ligand displacement of chloride by carbene **1** to afford a cationic complex, followed by rapid homoleptic rearrangement to give complex **3** and $[\text{Au}(\text{PPh}_3)_2]\text{Cl}$; (c) sequential substitution (compare Equation 2.2) as a result of the addition of $[\text{Au}(\text{Cl})\text{PPh}_3]$ to a local excess of carbene **1**, where half of the original $[\text{Au}(\text{Cl})\text{PPh}_3]$ remains unreacted. The first pathway is not feasible since solutions of complex **2** did not exhibit homoleptic rearrangement and no free PPh_3 was present in the reaction mixture. The third pathway is also unlikely since the product mixture contained very little unreacted

[Au(Cl)PPh₃]. The second pathway is the most convincing and is supported by a previous report from our group.^[33] A rapid rearrangement of a cationic triphenylphosphine gold(I) isothiazolylynylidene complex was suggested to afford the corresponding *bis*(carbene) complex. Transient electrophilic carbenes are known to react with Lewis bases, such as PPh₃, to give ylides.^[34] The additional phosphine-containing product was not characterised, but the possibility of ylide formation was excluded by the nucleophilic character of both carbene **1** and PPh₃.

Method 7

Aiming for [Li(PPh₃)]AuMe₂, one equivalent of [Au(Cl)PPh₃] in thf or diethyl ether at -78°C was added to two molar amounts of MeLi.^[35] The expected aurate solution was filtered at -78°C directly into a thf solution of [BMIM][OTf]. Cold filtration through an adapted filtration apparatus removed excess PPh₃. Treatment of [BMIM][OTf] with a solution of the aurate was expected to furnish a neutral methyl gold(I) complex by a sequential deprotonation-coordination mechanism, as mentioned before. Carbene **1**, however, formed predominantly as well as a 7% yield of complex **3** (Scheme 2.6).

Formation of the *bis*(carbene) complex was attributed to the reaction of unconverted [Au(Cl)PPh₃] and carbene **1** as in the MeLi/[Au(Cl)tht] (2:1) mixture (see Method 3, Equation 2.2).

B Spectroscopic characterisation of complex **3**

1. NMR spectroscopy

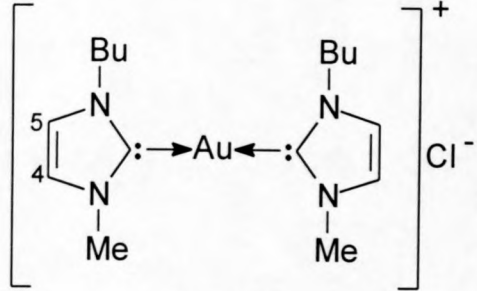
The ¹H and ¹³C-¹H NMR data for complex **3** are summarised in Table 2.9.

Disappearance of the H² signal and the absence of long-range coupling indicated carbene formation. Due to the positive charge on the *bis*(carbene) complex, the remaining proton resonances are all shifted downfield with respect to the neutral complex **2**.

The ¹³C-¹H NMR spectroscopic data for complex **3** similarly display a Δδ 13.8 downfield shift for C² with respect to the coordinated carbon in compound **2**. The resonance of the carbene atom at δ 185.3 is comparable with the chemical shift observed for an analogous

gold(I) *bis*(imidazol-2-ylidene) complex (δ 185.7).^[27] The remaining signals show insignificant changes.

Table 2.9 ^1H and $^{13}\text{C}\{-^1\text{H}\}$ NMR data for complex **3**

Complex 3		
Solvent		d-acetone
^1H NMR ^a	H ²	-
	H ⁴ and H ⁵	7.57 (4H, d, J = 15)
	NMe	4.01 (6H, s)
	NCH ₂ -	4.36 (4H, t, J = 15)
	NCH ₂ CH ₂ -	1.41 (4H, m) / 1.94 (4H, m)
	N(CH ₂) ₂ CH ₂ -	1.41 (4H, m) / 1.94 (4H, m)
	terminal CH ₃	0.97 (6H, t, J = 15)
^{13}C NMR	C ²	185.3
	C ⁴ and C ⁵	123.8 / 125.2
	NMe	38.4
	NCH ₂ -	51.6
	NCH ₂ CH ₂ -	34.5
	N(CH ₂) ₂ CH ₂ -	20.4
	terminal CH ₃	13.9
^{31}P NMR	[Au(Cl)PPh ₃]	31.2
	[Au(PPh ₃) ₂]Cl	23.8 (br)
	PPh ₃	-2.7

^a J in Hz

The ^1H NMR spectra of the product mixture obtained according to Method 6 includes triphenylphosphine signals that overlay the H⁴ and H⁵ signals. Nonetheless, the absence of the H² resonance, as well as identical ^{13}C -signals in the individual spectra, confirmed the composition of the product. The $^{31}\text{P}\{-^1\text{H}\}$ NMR spectra displayed signals attributed

respectively to $[\text{Au}(\text{PPh}_3)_2]\text{Cl}$ and $[\text{Au}(\text{Cl})\text{PPh}_3]$ at δ 27.8 and δ 33.1. The corresponding triphenylphosphine $^{13}\text{C}\{-^1\text{H}\}$ resonances are not given.

The product mixture obtained by Method 7 showed a $^{31}\text{P}\{-^1\text{H}\}$ signal for PPh_3 at δ -2.7 and indicated that excess PPh_3 was not completely removed by cold filtration.

2. Mass spectrometry

The EI mass spectral data of complex **3** is summarised in Table 2.10.

The molecular ion of the *bis*(carbene) complex is not observed but the cationic fragment appears at m/z 473. The fragmentation pattern shows sequential loss of one free carbene fragment followed by gold to give the molecular ion of the free carbene at m/z 138 as the base peak.

Table 2.10 Mass spectral data for complex **3**

m/z	I^a	Fragment ions
473	35	$[\text{Au}\{\overline{\text{CN}(\text{Me})\text{CH}=\text{CHN}(\text{Bu})}\}_2]^+$
335	20	$[\text{Au}\{\overline{\text{CN}(\text{Me})\text{CH}=\text{CHN}(\text{Bu})}\}]^+$
138	100	$[\overline{\text{CN}(\text{Me})\text{CH}=\text{CHN}(\text{Bu})}]^+$

^a Intensity relative to the base peak

2.3 SUMMARY

Free carbene formation by the deprotonation of azolium salts has long been known. Now, imidazolium salts classified as room temperature ionic liquids, have been utilised as diamino(carbene) precursors. An alkyllithium reagent, as opposed to the more generally employed alkali metal hydrides or alkoxides, was employed as a base. The isolated free carbene exhibited similar stability to previously reported singlet diamino(carbenes).

The prepared nucleophilic diamino(carbene) easily substituted thioether ligands and a gold(I) carbene-adduct was successfully prepared and characterised in an equimolar ligand substitution reaction. The gold(I) *mono*(carbene) complex did not exhibit homoleptic rearrangement. The $^{13}\text{C}\{-^1\text{H}\}$ NMR spectra displayed the coordinated carbene signal of the diamino(carbene) at a more downfield position than that of the corresponding gold(I)carbene adduct, and was ascribed, in part, to the “heavy atom effect”.

A *bis*(carbene) gold(I) complex was prepared by a reaction reminiscent to that observed for ylides. Reaction of the nucleophilic free carbene resulted in disubstitution of two different ligands in the gold(I) precursor compound. The $^{13}\text{C}\{-^1\text{H}\}$ NMR spectra showed the carbene atom downfield and, therefore, less shielded than in the corresponding neutral *mono*(carbene) complex.

Unfortunately, we could not successfully utilise $[\text{Me}_2\text{Au}]^-$ as a base and then $[\text{MeAu}]$ as an acid to form $\text{MeAu}(\text{carbene})$ complexes.

The preliminary experiments described in this chapter, show that room temperature imidazolium-based ionic liquids are available as gold(I) carbene complex precursors. However, further work is necessary to develop cleaner synthetic routes to these carbene complexes and furthermore, to ascertain whether these complexes can be generated *in situ* in ionic liquids.

2.4 EXPERIMENTAL

2.4.1 Materials

The gold compounds $[\text{Au}(\text{Cl})\text{PPh}_3]$,^[36] $[\text{Au}(\text{Cl})\text{tht}]$, $[\text{Au}(\text{Cl})\text{Me}_2\text{S}]$ ^[37] as well as the ionic liquids $[\text{BMIM}][\text{OTf}]$ ^[5] and $[\text{BMIM}][\text{PF}_6]$ ^[6] were prepared according to literature procedures. Tetrahydrofuran, hexane, toluene and diethyl ether were distilled under nitrogen from sodium diphenylketyl and dichloromethane from CaH_2 .

1-Methylimidazole, *n*-butyllithium (1.6 M in hexane), methyllithium (1.4 M in hexane) were obtained from Aldrich and triethylamine was purchased from Merck.

2.4.2 Physical Methods

All reactions involving organometallic and free carbene reagents were performed under an atmosphere of argon using standard vacuum-line and Schlenk-techniques. Melting points were determined on a standardised Buchi 535 apparatus. Electron impact mass spectra were recorded on a Finnigan Matt 8200 instrument at ca. 70eV (1.12×10^{-17} J) and NMR spectra on a Varian 300 FT spectrometer.

2.4.3 Preparations

2.4.3.1 Preparation of $[\text{CN}(\text{Me})\text{CH}=\text{CHN}(\text{Bu})]$, **1**

Method 1

The ionic liquids, $[\text{BMIM}][\text{OTf}]$ (577 mg, 2 mmol) and $[\text{BMIM}][\text{PF}_6]$ (506 mg, 2 mmol) were treated with MeLi ($1.40 \text{ mol}\cdot\text{dm}^{-3}$, 1.4 cm^{-3} , 2 mmol) at room temperature. The mixture was stirred for 15 minutes, 15 cm^{-3} diethyl ether added, the reaction mixture filtered through Celite and the solvent removed.

Method 2

The preparation of $[\text{Li}(\text{PPh}_3)][\text{AuMe}_2]$ was attempted by treatment of $[\text{Au}(\text{Cl})\text{PPh}_3]$ (494 mg, 1 mmol) in thf or diethyl ether at -78°C with MeLi ($1.40 \text{ mol}\cdot\text{dm}^{-3}$, 1.4 cm^{-3} , 2 mmol). This

solution was filtered at -78°C , through an adapted filtration apparatus, into [BMIM][OTf] (288 mg, 1 mmol) dissolved in thf or diethyl ether at -78°C . The reaction mixture was stirred for 30 minutes, warmed to room temperature and the solvent removed.

2.4.3.2 Preparation of $[\{\text{ClAu}[\overline{\text{CN}(\text{Me})\text{CH}=\text{CHN}(\text{Bu})}]\}]_2$, **2**

Method 3

1-Butyl-3-methylimidazol-2-ylidene (**1**) (371 mg, 1 mmol) dissolved in thf was added to $[\text{Au}(\text{Cl})\text{SMe}_2]$ (295 mg, 1 mmol) or $[\text{Au}(\text{Cl})\text{tht}]$ (321 mg, 1 mmol) in thf at -50°C . The reaction mixture was stirred for 30 minutes, warmed to room temperature, filtered through Celite and the solvent removed.

Method 4

$[\text{Au}(\text{Cl})\text{tht}]$ (321 mg, 1 mmol) in thf at -78°C was treated with MeLi ($1.40 \text{ mol}\cdot\text{dm}^{-3}$, 1.4 cm^3 , 2 mmol) and stirred for 20 minutes. [BMIM][OTf] (288 mg, 1 mmol) dissolved in thf was added, the reaction mixture stirred for 30 minutes and warmed to room temperature. The mixture was filtered through Celite and the solvent removed.

2.4.3.3 Preparation of $[\text{Au}\{\overline{\text{CN}(\text{Me})\text{CH}=\text{CHN}(\text{Bu})}\}_2]\text{Cl}$, **3**

Method 5

$[\text{Au}(\text{Cl})\text{tht}]$ (321 mg, 1 mmol) dissolved in thf at -78°C was treated with MeLi ($1.40 \text{ mol}\cdot\text{dm}^{-3}$, 1.4 cm^3 , 2 mmol), stirred for 20 minutes and 1-butyl-3-methylimidazol-2-ylidene (**1**) (371 mg, 1 mmol) dissolved in thf added. The reaction mixture was stirred for 30 minutes, warmed to room temperature and the solvent removed.

Method 6

The preparation of $[\text{Li}(\text{PPh}_3)][\text{AuMe}_2]$ was attempted by treatment of $[\text{Au}(\text{Cl})\text{PPh}_3]$ (494 mg, 1 mmol) with MeLi ($1.40 \text{ mol}\cdot\text{dm}^{-3}$, 1.4 cm^3 , 2 mmol). The resulting suspension was filtered at -78°C , through an adapted filtration apparatus, into 1-butyl-3-methylimidazol-2-ylidene (**1**) (371 mg, 1 mmol) dissolved in thf or diethyl ether. The reaction mixture was stirred for 30 minutes, warmed to room temperature and the solvent removed.

Method 7

The preparation was performed as for Method 6, but with [BMIM][OTf] (288 mg, 1 mmol).

REFERENCES

- [1] A. J. Arduengo, R. L. Harlow and M. J. Kline, *J. Am. Chem. Soc.*, 1991, **113**, 361.
- [2] N. Kuhn and T. Kratz, *Synthesis*, 1993, 561.
- [3] D. Enders, K. Breuer, G. Raabe, J. Runsink, J. H. Teles, J. P. Melder, K. Ebel and S. Brode, *Angew. Chem., Int. Ed. Engl.*, 1995, **34**, 1021.
- [4] K. R. Seddon, *J. Chem. Biotechnol.*, 1997, **68**, 351; K. R. Seddon, *Kinet. Catal. Engl. Transl.*, 1996, **37**, 693.
- [5] P. Bonhôte, A. -P. Dias, N. Papegeorgiou, N. Kalyanasundaram and M. Grätzel, *Inorg. Chem.*, 1996, **35**, 1168.
- [6] P. A. Z. Suarez, J. E. L. Dullius, S. Einloft, R. F. de Souza and J. du Pont, *Polyhedron*, 1996, **15**, 1217.
- [7] J. E. Parks and A. L. Balch, *J. Organomet. Chem.*, 1973, **57**, C103.
- [8] J. A. McCleverty and M. M. M. Da Mota, *J. Chem. Soc., Dalton Trans.*, 1973, 2571.
- [9] H. G. Raubenheimer and S. Cronje, in *Gold: Progress in Chemistry, Biochemistry and Technology*, (ed. H. Schmidbaur), John Wiley and Sons, New York, 1999, pp. 557.
- [10] J. H. Teles, S. Brode and M. Chabanas, *Angew. Chem., Int. Ed. Engl.*, 1998, **37**, 1415.
- [11] A. J. Arduengo, H. V. R. Dias, J. C. Calabrese and F. Davidson, *Organometallics*, 1993, **12**, 3405.
- [12] K. Öfele and C. G. Kreiter, *Chem. Ber.*, 1972, **105**, 529.
- [13] C. Köcher and W. A. Herrmann, *J. Organomet. Chem.*, 1997, **532**, 261.
- [14] W. A. Herrmann, C. P. Reisinger and M. Spiegler, *J. Organomet. Chem.*, 1998, **557**, 93.
- [15] J. Huang, E. D. Stevens, S. P. Nolan and J. L. Peterson, *J. Am. Chem. Soc.*, 1999, **121**, 2674.
- [16] J. B. Stothers, *Carbon-13 NMR Spectroscopy*, Academic Press, New York, 1972.
- [17] R. F. Frenske, in *Organometallic Compounds; Synthesis, Structure and Theory*, (ed. B. L. Shapiro), Texas A & M University Press, Texas, 1983, pp. 305.
- [18] H. Friebolin, *Basic One- and Two-dimensional NMR Spectroscopy*, Wiley-VCH, Weinheim, 1998, pp. 51.
- [19] E. Pretsch, T. Clerc, J. Seibl, W. Simon, *Spectral Data for Structure Determination of Organic Compounds*, (eds., W. Frensius, J. F. K. Huber, E. Pungor, G. A. Rechnitz, W. Simon and T. S. West), Springer-Verlag, Berlin, 1989.

- [20] N. Kuhn, J. Fahl, R. Fawzi, C. Maichle-Mossmer and M. Steinmann, *Z. Naturforsch.*, 1998, **53b**, 720.
- [21] A. J. Arduengo, F. Davidson, H. V. R. Dias, J. R. Goerlich, D. Khasnis, W. J. Marshall and T. K. Prakasha, *J. Am. Chem. Soc.*, 1997, **119**, 12742.
- [22] A. J. Arduengo, M. Tamm and J. C. Calabrese, *J. Am. Chem. Soc.*, 1994, **116**, 3625.
- [23] A. Tamaki and J. K. Kochi, *J. Organomet. Chem.*, 1973, **51**, C39.
- [24] A. J. Arduengo, H. V. R. Dias, R. L. Harlow and M. Kline, *J. Am. Chem. Soc.*, 1992, **114**, 5530.
- [25] J. Huang, E. D. Stevens, S. P. Nolan and J. L. Peterson, *J. Am. Chem. Soc.*, 1999, **121**, 2674.
- [26] J. C. Green, R. G. Scurr, P. L. Arnold and F. G. N. Cloke, *J. Chem. Soc., Chem. Commun.*, 1997, 1963.
- [27] H. G. Raubenheimer, L. Lindeque and S. Cronje, *J. Organomet. Chem.*, 1996, **511**, 177.
- [28] H. M. J. Wang, C. Y. L. Chen and I. J. B. Lin, *Organometallics*, 1999, **18**, 1216.
- [29] H. G. Raubenheimer and S. Cronje, *J. Organomet. Chem.*, 2001, **617 - 618**, 170.
- [30] F. W. Wehrli and T. Wirthlin, *Interpretation of Carbon-13 NMR Spectra*, Heyden, London, 1978, pp. 310.
- [31] D. Bourissou, O. Guerret, F. P. Gabbaï and G. Bertrand, *Chem. Rev.*, 2000, **100**, 39.
- [32] R. J. Puddephatt in *Comprehensive Organometallic Chemistry*, (eds., G. Wilkinson, F. G. A. Stone and E. W. Abel), Pergamon Press, Oxford, 1985, Vol. 2, pp. 765.
- [33] H. G. Raubenheimer, M. Desmet and G. J. Kruger, *J. Chem. Soc., Dalton Trans.*, 1995, 2067.
- [34] D. A. Dixon in, *Ylides and Imines of Phosphorus*, Wiley, New York, 1993, pp. 115.
- [35] A. Tamaki and J. K. Kochi, *J. Organomet. Chem.*, 1973, **51**, C39.
- [36] A. Hass, J. Helmbrecht and U. Niemann in *Handbuch der Präparativen Anorganischen Chemie*, Third, Ferdinand Enke, Stuttgart, 1974, pp. 1014.
- [37] P. C. Rây and D. C. Chen, *J. Indian Chem. Soc.*, 1930, 67.

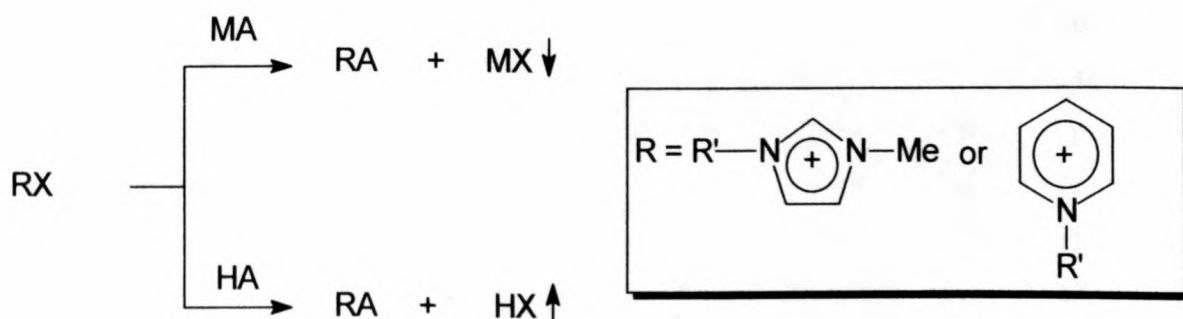
CHAPTER 3

PREPARATION, REACTIONS AND CATALYTIC ACTIVITY OF THIAZOLIUM IONIC LIQUIDS

3.1 INTRODUCTION

Thiazolium salts have recently attracted attention and broadened the structural diversity of cations used in ionic liquid synthesis.^[1] *N*-alkyl(thiazolium) ionic liquids share the same low symmetry features and synthetic methodology as their imidazolium counterparts, but a major disadvantage is the high cost of the thiazolium cation precursor. Investigations of the physical properties of these novel solvents are currently limited.

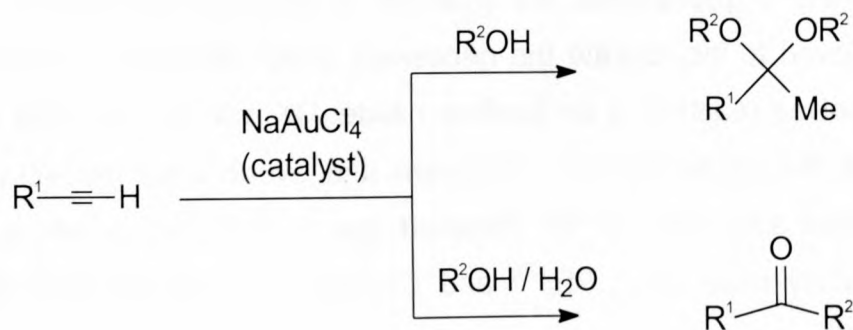
Although a variety of procedures are available to prepare ionic liquids,^[2] metathesis is generally employed to incorporate the necessary bulky counterion. The final step in the preparation involves reaction of an azolium halide, RX, with a metal salt or acid to afford the ionic liquid, RA (Scheme 3.1). Filtration and evaporation respectively remove the precipitated metal salt, MX, or the liberated gas, HX. Ionic liquids prepared by this procedure typically have BF_4^- , PF_6^- ^[3] and CF_3SO_3^- ^[4] as counterions, although anionic transition metal complexes can also be used.



Scheme 3.1

In this chapter, the utilisation of metathesis to prepare two new thiazolium ionic liquids is described. Although low melting point imidazolium ionic liquids incorporating gold in the anion have recently become accessible,^[5,6] we have prepared the first example of a gold(III) thiazolium salt that qualifies as an ionic liquid, according to the characteristics set down by Seddon.^[7] Crystals of the gold thiazolium compound suitable for X-ray crystallographic studies were obtained and the molecular structure determined. By a second metathesis, the new room temperature ionic liquid, 3-butyl-4-methylthiazolium triflate, was prepared and spectroscopically characterised.

The use of gold complexes in homogeneous catalysis is rare and available examples are summarised elsewhere.^[8] At present the most encouraging achievement for catalytically active gold(I) compounds is the addition of alcohols to alkynes to afford acetals.^[9] Of particular interest in this catalysis report, is the observation that a gold(I) diaminocarbene complex can promote the addition reaction. An earlier report shows that NaAuCl_4 also functions as a catalyst for the addition^[10] but that hydration products are obtained when wet alcohols are used (Equation 3.1).

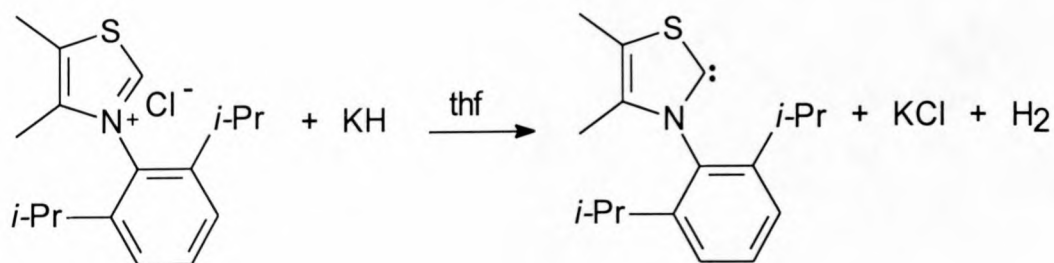


Equation 3.1

The catalytic hydration of phenylacetylene with a new gold(III) thiazolium salt was investigated and the results are presented in this chapter. The relatively high melting point of this ionic liquid unfortunately made it unsuitable as a solvent for the hydration reaction and catalyst decomposition was observed. Catalysis with gold compounds in imidazolium ionic liquids has not been reported until now. The catalytic activity of the new gold(III) thiazolium salt as well as NaAuCl_4 was tested in the ionic solvents well as in a conventional solvent and the results are compared.

Although simple *N*-alkyl substituted imidazolinylienes are stable monomers, the same is not true for free thiazole-derived carbenes. Amino(thio)carbenes experience less electronic and geometric stabilisation than their diamino counterparts due to the sulphur atom in the ring that disrupts the stable ring geometry present in imidazol-2-ylidenes. The sulphur is larger than nitrogen and $p\pi$ - $p\pi$ interaction with the carbene center is much less.^[11,12]

Utilising a combination of the required steric and geometric requirements, Arduengo isolated the first stable amino(thio)carbene, 3-(2,6-diisopropylphenyl)thiazol-2-ylidene, in 1997 (Scheme 3.2).^[13] The bulky amine group is believed to kinetically stabilise the amino(thio)carbene and thereby prevent dimerisation.

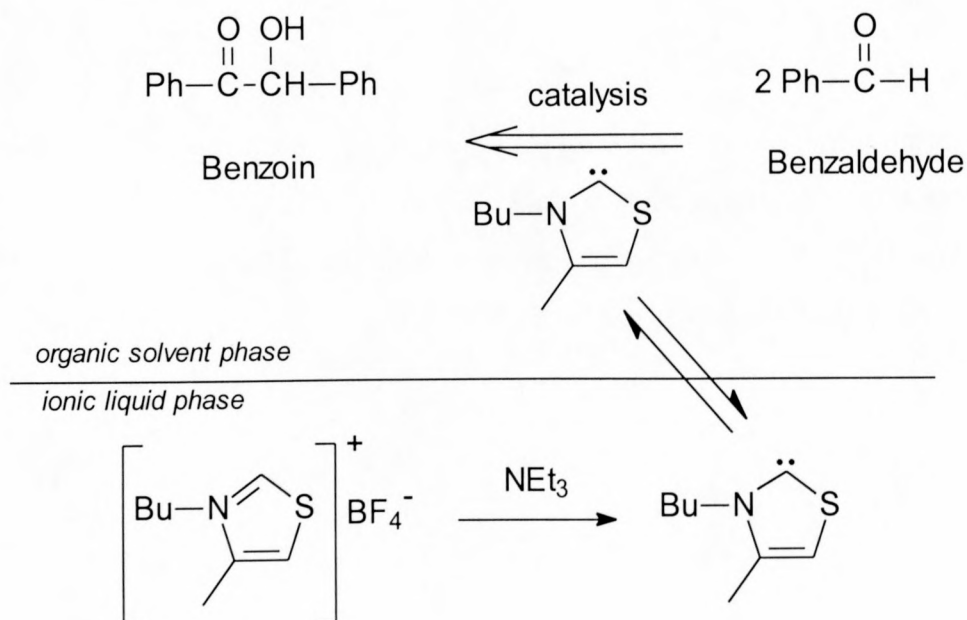


Scheme 3.2

Analogous amino(thio)carbenes with small *N*-Me substituents have been observed at low temperatures, but do not enjoy the necessary kinetic and electronic stabilisation to exist as monomers at room temperature. We confirmed the latter result, even with a much larger substituent. Treatment of the newly prepared 3-butyl-4-methylthiazolium triflate, as well as its tetrafluoroborate counterpart with a variety of bases, gave the corresponding dimeric product. The alkene proved to be unstable in solution but sufficient spectroscopic data were obtained to confirm the structural assignment.

Upon addition of a catalytic amount of base, imidazolium and triazolium salts, with BF_4^- and OTf^- counterions, are known to promote the benzoin condensation reaction.^[14] Using the same procedure, 3-butyl-4-methylthiazolium tetrafluoroborate has recently been found to catalyse the reaction (Scheme 3.3).^[15] Treatment of the azolium salts with a base presumably generates a free carbene that promotes C-C bond formation. Since amino(thio)carbenes need bulky amine groups to prevent dimer formation, catalysis at room temperature by a free carbene as in Scheme 3.3 seems doubtful. In the current

preliminary experiment, we established that 3-butyl-4-methylthiazolium triflate promotes the condensation reaction only to a very limited extent upon addition of a catalytic amount of NEt_3 .

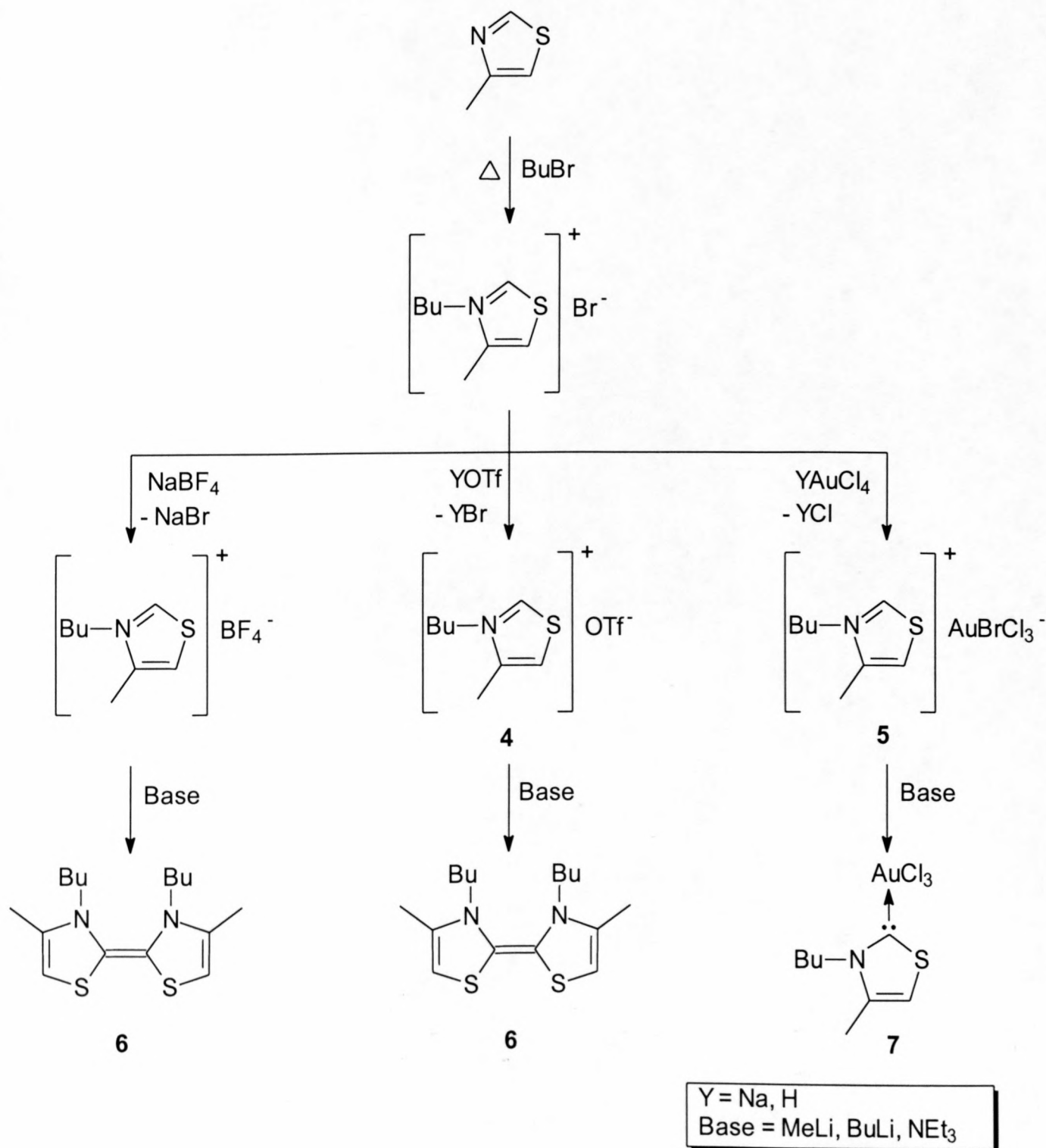


Scheme 3.3

Finally, the new gold(III) thiazolium salt was successfully converted into the corresponding carbene complex by treatment with a base and the preparation is also discussed in this chapter.

3.2 RESULTS AND DISCUSSION

The preparation of the new compounds, **4**, **5**, **6** and **7**, described in this chapter are shown schematically below (Scheme 3.4). Their physical data appear in Table 3.1.



Scheme 3.4

Table 3.1 Analytical and physical data for compounds **4**, **5**, **6** and **7**

Compound				
Colour	Colourless	Deep red	Dark orange	Orange
Yield (%)	92/ 83 ^a	82/ 79 ^b	15/ 12 ^c	15
M.p./ °C	- 10	80 – 82	150 - 151	115 - 117 ^d
M.W.	305.34	495.05	310.53	458.60

^a Prepared from HOTf and NaOTf, respectively^b Prepared from HAuCl₄ and NaAuCl₄, respectively^c Prepared from [BMTz][OTf] and [BMTz][BF₄], respectively^d Decomposition without melting

3.2.1 Thiazolium Salt Precursors

A Preparation of $[\text{HC}=\text{C}(\text{Me})\text{N}(\text{Bu})=\text{CHS}][\text{Br}]$ and $[\text{HC}=\text{C}(\text{Me})\text{N}(\text{Bu})=\text{CHS}][\text{BF}_4]$

3-Butyl-4-methylthiazolium bromide, $[\text{BMTz}][\text{Br}]$, was prepared according to a literature procedure by refluxing an equimolar mixture of 4-methylthiazole and 1-bromobutane.^[15] $[\text{BMTz}][\text{BF}_4]$ has previously been prepared by metathesis with NaBF_4 , but no spectroscopic data are available.^[15] The tetrafluoroborate ionic liquid was synthesised by treatment with NaBF_4 and NMR spectroscopic data obtained.

B Spectroscopic characterisation of $[\text{HC}=\text{C}(\text{Me})\text{N}(\text{Bu})=\text{CHS}][\text{Br}]$ and $[\text{HC}=\text{C}(\text{Me})\text{N}(\text{Bu})=\text{CHS}][\text{BF}_4]$

1. NMR spectroscopy

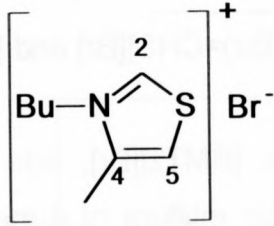
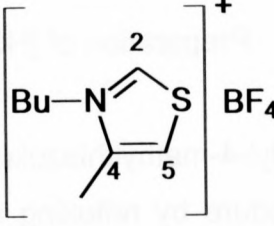
The ^1H NMR and $^{13}\text{C}\{-^1\text{H}\}$ NMR spectroscopic data of $[\text{BMTz}][\text{Br}]$ and $[\text{BMTz}][\text{BF}_4]$ are summarised in Table 3.2.

^1H NMR spectra of $[\text{BMTz}][\text{Br}]$ and $[\text{BMTz}][\text{BF}_4]$ are very similar except for the H^2 resonance. As discussed in paragraph 2.2.3, different anions are not expected to affect electron redistribution within the thiazolium ring and the different shift observed for H^2 in the respective spectra is therefore surprising and cannot be readily explained in terms of charge density and electron distribution.

Proton spectra of the respective ionic liquids display the terminal Me as well as the N-CH_2 -signals as triplets and the coupling constant of 15 Hz is similar to the value observed in imidazolium ionic liquid spectra.^[4]

The $^{13}\text{C}\{-^1\text{H}\}$ NMR data of $[\text{BMTz}][\text{Br}]$ and $[\text{BMTz}][\text{BF}_4]$ display insignificant differences and together with the ^1H NMR data, shows that the electron distribution within the framework of the respective compounds are comparable.^[16,17]

Table 3.2 NMR spectroscopic data for [BMTz][Br] and [BMTz][BF₄]

Ionic liquid		
Abbreviation	[BMTz][Br]	[BMTz][BF ₄]
Solvent	CD ₂ Cl ₂	CD ₂ Cl ₂
¹H NMR^a	H ² 11.49 (1H, s) H ⁵ 7.87 (1H, s) 4-Me 2.62 (3H, s) NCH ₂ - 4.72 (2H, t, J = 15) NCH ₂ CH ₂ - 1.49 (2H, m) / 1.88 (2H, m) N(CH ₂) ₂ CH ₂ - 1.49 (2H, m) / 1.88 (2H, m) terminal CH ₃ 1.02 (3H, t, J = 15)	10.17 (1H, s) 7.96 (1H, s) 2.63 (3H, s) 4.61 (2H, t, J = 15) 1.47 (2H, m) / 1.94 (2H, m) 1.47 (2H, m) / 1.94 (2H, m) 1.01 (3H, t, J = 15)
¹³C NMR	C ² 161.8 C ⁴ 154.7 C ⁵ 122.3 4-Me 20.0 NCH ₂ - 54.5 NCH ₂ CH ₂ - 32.6 N(CH ₂) ₂ CH ₂ - 13.9 terminal CH ₃ 13.7	160.2 156.7 122.8 19.9 52.4 32.3 13.8 13.7

^a J in Hz

3.2.2 A Room Temperature Thiazolium Ionic Liquid

A Preparation of $[\text{HC}=\text{C}(\text{Me})\text{N}(\text{Bu})=\text{CHS}][\text{OTf}]$, **4**

The reaction of [BMTz][Br] with a 5% excess of HOTf or NaOTf in water at 0°C followed by extraction with dichloromethane and repeated washing of the organic phase with ice water, gave ionic liquid **4** in 85 – 93% yield (Scheme 3.4).

The product is a viscous, colourless liquid that is miscible with thf, acetone and dichloromethane, but immiscible with toluene and hexane. The analytical and physical data (Table 3.1) indicate the low melting point (-10°C) of the salt that qualifies it as a room temperature ionic liquid.

B Spectroscopic characterisation of compound **4**

1. NMR spectroscopy

The ^1H and $^{13}\text{C}\{-^1\text{H}\}$ NMR data for ionic liquid **4** are summarised in Table 3.3.

^1H NMR spectra of ionic liquid **4** exhibits an upfield shift of H^2 of $\Delta\delta$ 1.09 with respect to the corresponding signal of [BMTz][Br]. As before, the change cannot be readily explained in terms of charge distribution within the respective organic cations.

The $^{13}\text{C}\{-^1\text{H}\}$ NMR spectra of ionic liquid **4**, [BMTz][Br] and [BMIM][BF₄] are very similar. For the same reasons as discussed in paragraph 3.2.1, the similar data indicate that electronic distributions in the three compounds are comparable.

The triflate carbon of ionic liquid **4** is observed as a quartet due to fluorine coupling.

Table 3.3 Spectroscopic data for compounds **4**, **5**, **6** and **7** in CD₂Cl₂

Compound				
¹ H NMR ^a	<p>4</p> <p>10.40 (1H, s)</p> <p>7.86 (1H, s)</p> <p>2.62 (3H, s)</p> <p>4.48 (2H, t, J = 15)</p> <p>1.45 / 1.93 (2H, m)</p> <p>1.45 / 1.93 (2H, m)</p> <p>1.00 (3H, t, J = 15)</p>	<p>5</p> <p>9.85 (1H, s)</p> <p>7.83 (1H, s)</p> <p>2.68 (3H, s)</p> <p>4.50 (2H, t, J = 15)</p> <p>1.52 / 2.01 (2H, m)</p> <p>1.52 / 2.01 (2H, m)</p> <p>1.05 (3H, t, J = 15)</p>	<p>6</p> <p>6.71 (2H, s)</p> <p>2.05 (6H, s)</p> <p>3.76 (4H, t, J = 15)</p> <p>1.41 / 1.88 (4H, m)</p> <p>1.41 / 1.88 (4H, m)</p> <p>0.95 (6H, t, J = 15)</p>	<p>7</p> <p>-</p> <p>7.45 (1H, s)</p> <p>2.48 (3H, s)</p> <p>4.49 (2H, t, J = 15)</p> <p>1.51 / 1.94 (2H, m)</p> <p>1.51 / 1.94 (2H, m)</p> <p>0.92 (3H, t, J = 15)</p>
¹³ C NMR	<p>159.2</p> <p>147.1</p> <p>122.4</p> <p>20.0</p> <p>54.0</p> <p>32.1</p> <p>13.8</p> <p>13.6</p>	<p>158.3</p> <p>147.7</p> <p>122.8</p> <p>20.2</p> <p>54.0</p> <p>32.3</p> <p>14.4</p> <p>13.8</p>	<p>121.9</p> <p>Not observed</p> <p>106.5</p> <p>20.7</p> <p>49.6</p> <p>32.4</p> <p>13.8</p> <p>13.7</p>	<p>173.3</p> <p>145.3</p> <p>119.5</p> <p>20.6</p> <p>55.9</p> <p>33.4</p> <p>14.4</p> <p>14.0</p>

^a J in Hz

2. Mass spectrometry

The fast atom bombardment (FAB) mass spectral data for ionic liquid **4** are summarised in Table 3.4.

The molecular ion is observed at m/z 305 and the fragmentation pattern shows the loss of triflate to give a signal for the organic cation as the base peak at m/z 156. Signals attributed to the loss of either methyl or butyl groups are also evident.

Table 3.4 Mass spectral data of ionic liquid **4**

m/z	I^a	Fragment ions
305	36	$\overbrace{[\text{HC}=\text{C}(\text{Me})\text{N}(\text{Bu})=\text{CHS}]^+}^{\text{triflate}} [\text{OTf}]^+$
156	100	$[\text{HC}=\text{C}(\text{Me})\text{N}(\text{Bu})=\text{CHS}]^+$
141	62	$[\text{HC}=\text{CN}(\text{Bu})=\text{CHS}]^+$
99	45	$[\text{HC}=\text{C}(\text{Me})\text{N}=\text{CHS}]^+$

^a Intensity relative to the base peak

3.2.3 A Thiazolium Salt Ionic Liquid that contains AuCl_4^- as Counterion

A Preparation of $[\text{HC}=\text{C}(\text{Me})\text{N}(\text{Bu})=\text{CHS}][\text{AuBrCl}_3]$, **5**

Addition of HAuCl_4 or NaAuCl_4 to one molar equivalent of $[\text{BMTz}][\text{Br}]$ dissolved in methanol, gave $[\text{BMTz}][\text{AuBrCl}_3]$, **5**, in 79 – 82% yield (Scheme 3.4). Formation of the mixed anion is due to the substitution of chlorine by the softer bromine ion present in the reaction mixture. Crystallisation by vapour diffusion utilising dichloromethane and hexane, afforded deep red crystals of compound **5** that were suitable for X-ray crystallographic studies.

Azolium salts qualify as ionic liquids if their melting point is below 100°C .^[2] The physical and analytical data for compound **5** are given in Table 3.1 and indicate the relatively low melting point (80 - 82°C) of the gold(III) salt that qualifies it as an ionic liquid. The thiazolium triflate salt is readily soluble in thf, acetone and dichloromethane and is stable in air.

B Spectroscopic characterisation of compound **5**

1. NMR spectroscopy

The ^1H and $^{13}\text{C}\{-^1\text{H}\}$ NMR data for ionic liquid **5** are summarised in Table 3.3.

The proton spectrum of ionic liquid **5** again exhibits the inexplicable upfield position of the H^2 signal ($\Delta\delta$ 1.64) with respect to the corresponding signal in $[\text{BMTz}][\text{Br}]$. The remaining signals display insignificant changes. The $^{13}\text{C}\{-^1\text{H}\}$ NMR spectra of ionic liquid **5** and $[\text{BMTz}][\text{Br}]$ are very similar.

2. Mass spectrometry

The molecular ion of the ionic liquid was not observed in FAB- or EI-mass spectra, but the thiazolium cation signal is observed at m/z 156 as the base peak. The remaining signals could not be unambiguously assigned.

C Crystal and molecular structure of compound 5

The molecular structure of compound 5 and the employed numbering scheme are shown in Figure 3.1. Packing in the unit cell, showing weak Au...halide interionic interactions, is displayed in Figure 3.2 and selected bond lengths and angles are given in Table 3.5.

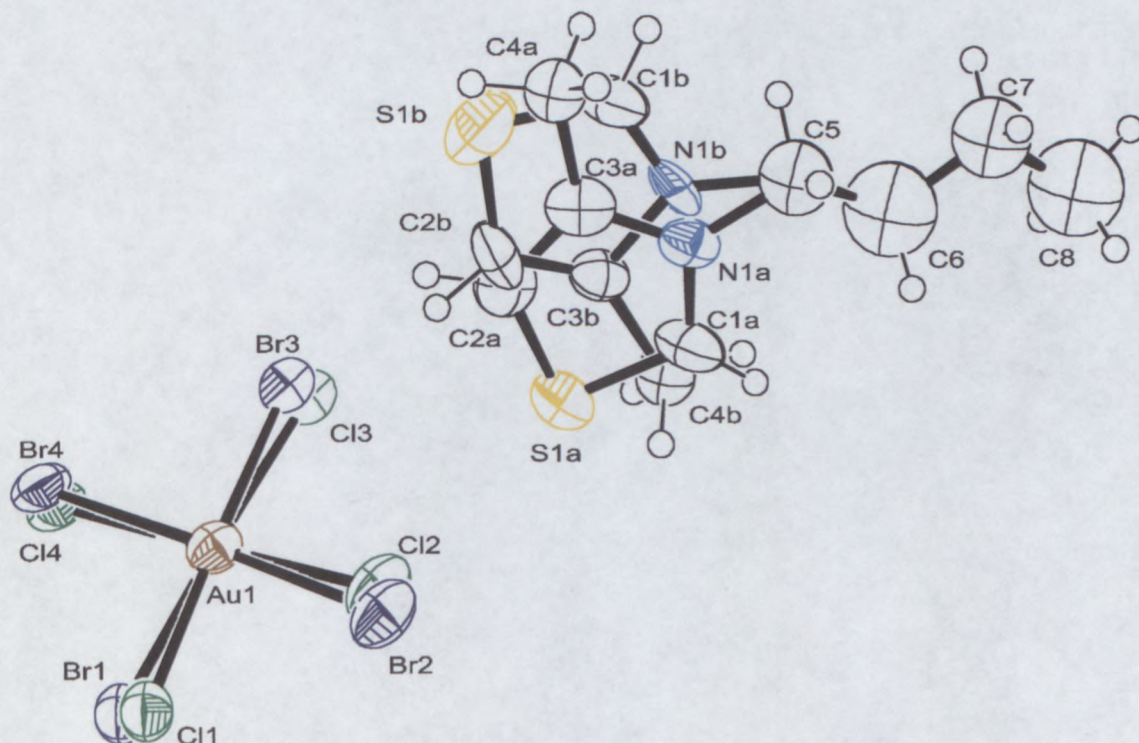


Figure 3.1 Crystal structure of 4 showing disordered atom positions and numbering scheme

Complex 5 crystallizes in the monoclinic space group $P2_1/n$ as dark red crystals and consists of a 3-butyl-4-methylthiazolium cation with AuBrCl_3^- as counterion (Figure 3.1). The Au...Au separations exclude any metal-metal interactions. Both the cation and the square planar anion exhibit disorder. The AuBrCl_3^- anion exhibits positional disorder of the halogen atoms. The occupancy of the bromine atom is distributed over positions 1 - 4 with site occupancies of 0.30, 0.16, 0.42, 0.12, respectively.

The disorder in the thiazolium ring of the cation was modelled as a disordered pair of rings lying across each other at an angle of approximately 174° (angle between least square planes through disordered rings) in a 59%(a) to 41%(b) percentage ratio. The *N*-butyl chain in compound 5 exhibits dynamic disorder, which could not be modelled successfully. The chain, however, lies roughly in the plane of the thiazolium ring, unlike the *N*-butyl chain in the structure of $[\text{BMIM}][\text{AuCl}_4]$ which is nearly perpendicular to the ring plane.^[6] In

[BMIM][AuCl₄], two crystallographically independent AuCl₄⁻ anions are arranged perpendicularly to each other in infinite anionic chains of alternating corner-to-face AuCl₄⁻ units. In the present structure, the anions are arranged with a halide ··· Au ··· halide angle of 108° (mean) also producing infinite anion chains but in a zigzag pattern as every AuBrCl₃⁻ unit contributes one interacting halide atom (Figure 3.2). The gold-halide distance between the anions of **5** is ca. 3.57 Å (mean value for Br and Cl), which is longer than the gold-chlorine separation of 3.45 Å in [BMIM][AuCl₄].

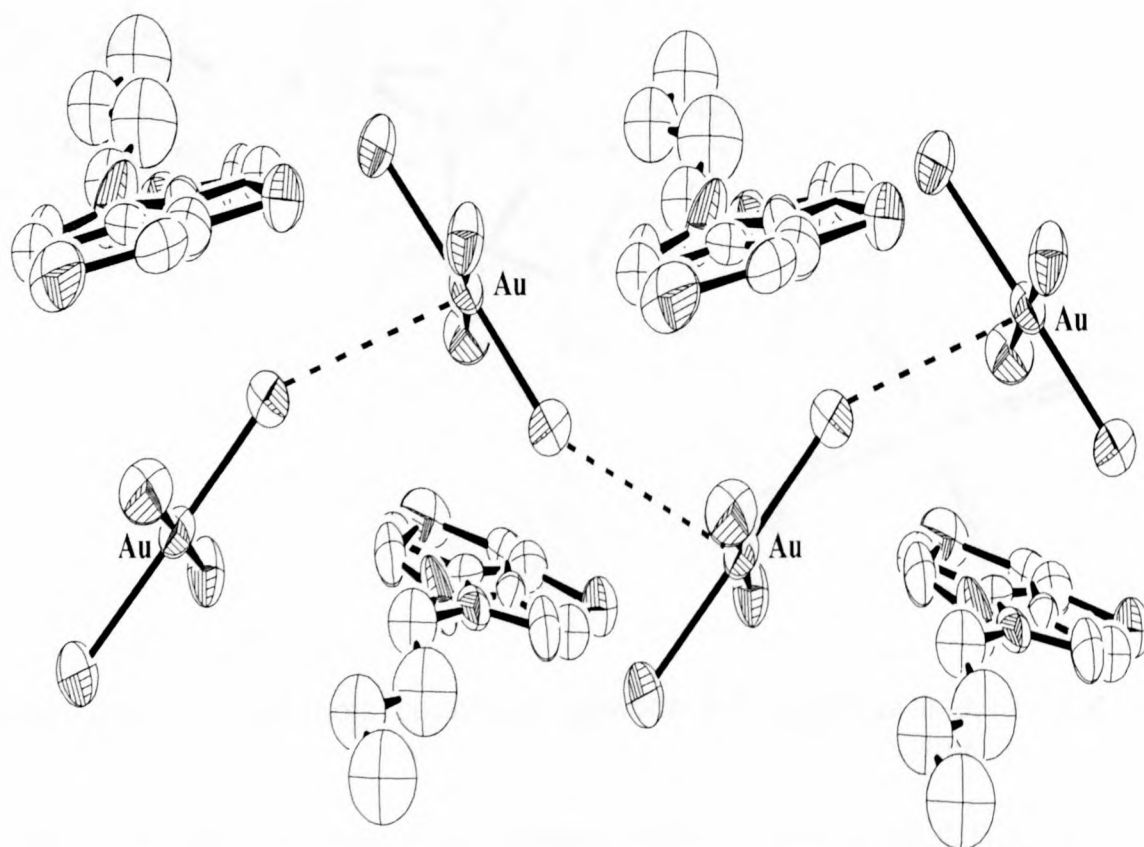


Figure 3.2 Packing diagram of **4**, viewed along the *a*-axis, showing Au-halide interaction (hydrogen atoms and 2nd disordered halide position omitted for clarity).

The closest reliable cationic-anionic contacts involve thiazolium C-bound hydrogens and halogen atoms (H2a-Br1 = 2.73 Å). Although closer CH···halide contacts of 2.53 Å are observed between H4b and Br4, they have to be disregarded, as H4b is a methyl proton in an unreliable calculated position. The interpretation of CH···halide interactions in **4** should be treated with extreme caution as none of the positions of the hydrogen atoms could be determined directly from the Fourier synthesis. Furthermore, the thiazolium rings to which the calculated hydrogens are connected are disordered and could only be refined with both rigid body and planarity restraints. Their positions are thus not reliable and can

certainly not be employed in accurately describing interionic Coulomb interactions. In addition, the fact that such a high degree of disorder with little preference for specific conformations, exists suggests that the aforementioned Coulombic interactions probably play a negligible role in stabilizing the crystalline phase of **5**. It is more likely that the observed Au-halide interactions could direct the orientation of the ions and perhaps govern the overall assembly in the crystalline phase.

Table 3.5 Selected bond lengths (Å) and angles(°) for complex **5**^a

Au1 – Cl1	2.26(3)	Au1 – Br1	2.39(3)
Au1 – Cl2	2.27(2)	Au1 – Br2	2.41(4)
Au1 – Cl3	2.39(3)	Au1 – Br3	2.37(15)
Au1 – Cl4	2.26(9)	Au1 – Br4	2.48(3)
C1a – N1a	1.32(2)	C5 – N1a	1.48(2)
C1b – N1b	1.38(4)	C5 – N1b	1.43(2)
C1a – S1a	1.67(2)		
C1b – S1b	1.56(3)		
Cl1 – Au1 – Cl2	87.3(7)	Cl1 – Au1 – Br2	81.7(13)
Cl1 – Au – Cl3	170.9(7)	Cl1 – Au – Br3	178.1(6)
Cl1 – Au1 – Cl4	93.0(6)	Cl1 – Au1 – Br4	95.5(11)
Cl3 – Au1 – Cl4	95.1(6)	Cl3 – Au1 – Br4	92.9(11)
S1a – C1a- N1a	113.4(19)		
S1b – C1b- N1b	116.0(2)		

^a e.s.d.s. in parentheses

3.2.4 A Thiazolyl Dimer

A Preparation of $[\text{HC}=\text{C}(\text{Me})\text{N}(\text{Bu})\text{CS}]_2$, **6**

Treatment of $[\text{BMTz}][\text{OTf}]$ or $[\text{BMTz}][\text{BF}_4]$ in thf at -78°C with one molar equivalent of MeLi, BuLi or NEt_3 gave dimer **6** in low yield (Scheme 3.4). After filtration through Celite, the product was obtained as a dark orange powder.

The dimer is soluble in thf and acetone, but is unstable in solution and shows limited stability at low temperature under an inert atmosphere. The physical and analytical data for the dimer are presented in Table 3.1.

B Spectroscopic characterisation of compound **6**

1. NMR spectroscopy

The ^1H and $^{13}\text{C}\{-^1\text{H}\}$ NMR data for dimer **6** are given in Table 3.3.

Due to the instability of compound **6** in solution, decomposition products were present in the NMR spectra. Nevertheless, adequate evidence indicating dimer formation was observed.

Broad signals are observed in the ^1H NMR spectra and most likely indicate interconversion between *syn*- and *anti*-isomers of the dimer. Disappearance of the H^2 signal as well as the upfield shift of the remaining proton signals with respect to the starting compounds, indicated dimer formation. Such an upfield shift corresponds with a decrease in positive charge.

The $^{13}\text{C}\{-^1\text{H}\}$ NMR spectroscopic data for compound **6** show an upfield shift of C^2 ($\Delta\delta$ ca. 38) and C^5 ($\Delta\delta$ ca. 16) with respect to the corresponding signals of $[\text{BMTz}][\text{OTf}]$ and $[\text{BMTz}][\text{BF}_4]$. Comparable shift changes for C^2 and C^5 in an analogous 3-methylthiazol-2-ylidene dimer ($\Delta\delta$ ca. 40 and 14)^[13] indicate that carbon shielding is better in the dimer than in the cationic precursor. The quaternary C^4 carbon was not observed.

2. Mass spectrometry

The EI mass spectral data of compound **6** are summarised in Table 3.7.

The molecular ion of the dimer is observed as a weak signal at m/z 310 and a signal at m/z 295 shows loss of the methyl group. Ionised 4-methylthiazole is present as the base peak at m/z 99. A signal at m/z 156 is attributed to the monomeric carbene, but the remaining signals could not be unambiguously assigned.

Table 3.7 Mass spectral data of compound **6**

m/z	I^a	Fragment ions
310	< 1	$[\overbrace{\text{HC}=\text{C}(\text{Me})\text{N}(\text{Bu})\text{CS}}]_2^+$
295	9	$[\overbrace{\text{HC}=\text{CN}(\text{Bu})\text{CS}}]_2^+$
155	63	$[\overbrace{\text{HC}=\text{C}(\text{Me})\text{N}(\text{Bu})\text{CS}}]^+$
99	100	$[\overbrace{\text{HC}=\text{C}(\text{Me})\text{NCS}}]^+$

^a Intensity relative to the base peak

3.2.5 A Gold(III) Thiazol-2-ylidene Carbene Complex

A Preparation of $[\text{Cl}_3\text{Au}(\text{HC}=\text{C}(\text{Me})\text{N}(\text{Bu})\text{CS})]$, **7**

Dissolution of $[\text{BMTz}][\text{AuBrCl}_3]$ in thf, cooling to -78°C and treatment with MeLi, BuLi or NEt_3 , yielded carbene complex **7** as an orange powder after filtration through Celite (Scheme 3.4). The isolation of complex **7** shows that 3-butyl-4-methylthiazol-2-ylidene substitutes only bromide in the mixed anion of complex **5**. This result is somewhat unexpected, because Br^- is softer than Cl^- . Since only compound **7** was isolated by crystallisation, the bromo analogue could have remained in the mother liquor.

Complex **7** is readily soluble in thf, acetone and dichloromethane, but is sparingly soluble in hexane, pentane and toluene. The orange complex cannot be handled in air and shows limited stability under an inert atmosphere at low temperature as well as in solution. The analytical and physical data for complex **7** is given in Table 3.2.

B Spectroscopic characterisation of complex **7**

1. NMR spectroscopy

The ^1H and $^{13}\text{C}\{-^1\text{H}\}$ NMR data for complex **7** are summarised in Table 3.3.

Absence of the H^2 signal in ^1H NMR spectra of complex **7** indicated deprotonation in this position. The H^5 signal experiences more shielding than the H^5 signal in $[\text{BMTz}][\text{AuBrCl}_3]$ and shifts upfield ($\Delta\delta$ 0.38).

The most prominent feature of the $^{13}\text{C}\{-^1\text{H}\}$ NMR spectra is the significant upfield shift of C^2 ($\Delta\delta$ 52) with respect to the corresponding signal in the precursor. The C^2 signal at δ 173.3 is comparable to a chemical shift of a related halogold(III) thiazolinylidene complex.^{18]}

Free thiazol-2-ylidene carbenes have their carbene signals at δ ca. 250, which is substantially downfield from the carbene signal of imidazol-2-ylidenes at δ ca. 210.^[19] This has been suggested to be due to the limited π -character of S-C bonds in thiazolyl rings^[20]

that reduce hyperconjugative stabilisation of cyclic amino(thio)carbenes, with respect to their diamino analogues (compare Scheme 1.3).^[13,21] The carbene atom of amino(thio)carbenes is consequently less shielded than in its diamino analogues and resonates at a more downfield position. By analogy, gold amino(thio)carbene complexes should have their carbene resonance more downfield than their diamino analogues. This appears to be true when carbene carbon chemical shifts in gold(III) thiazol-2-ylidene and gold(III) imidazol-2-ylidenes are compared. The carbene signal of complex **7** at δ 173.3 and at δ 167.8 for a related halogold(III) thiazolinyliidene complex,^[18] is nearly an order of magnitude larger, in both cases, than downfield chemical shifts of δ 154.5 and δ 160.6 observed for two gold(III) imidazol-2-ylidene compounds.^[18] Moreover, this is despite the former compounds being cationic *bis*(carbene) complexes and thus experiencing additional deshielding due to the positive charge on the complexes.

2. Mass spectrometry

The FAB mass spectral data for complex **7** are summarised in Table 3.8.

The molecular ion of the neutral complex appears as a strong signal at m/z 459. The $[M]^+$, $[M+2]^+$, $[M+4]^+$ and $[M+6]^+$ isotope lines due to the presence of Cl_3 in the molecular ion are clearly visible and shown in Figure 3.3. The fragmentation pattern shows the consecutive loss of the three chlorines followed by gold, to give the free carbene peak at m/z 154.

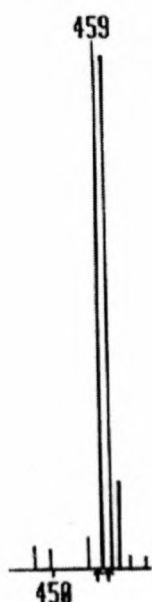
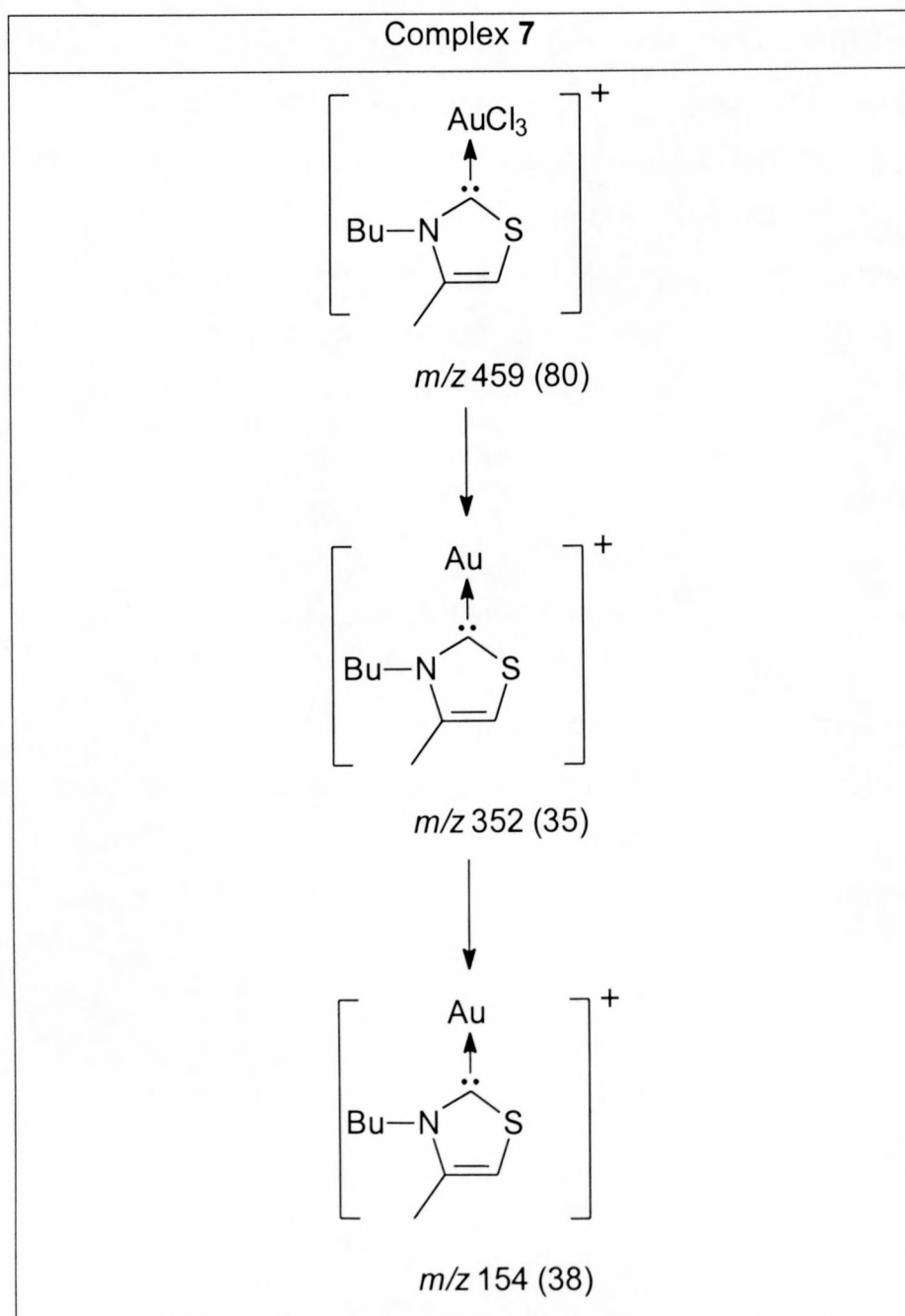


Figure 3.3 $[M]^+$ peak of complex **7** showing isotope lines for $\{Cl_3\}$

EI-mass spectra did not exhibit a signal for the molecular ion, but displayed the same fragmentation pattern as the FAB spectra.

Table 3.8 Mass-spectral data of compound **7^a**



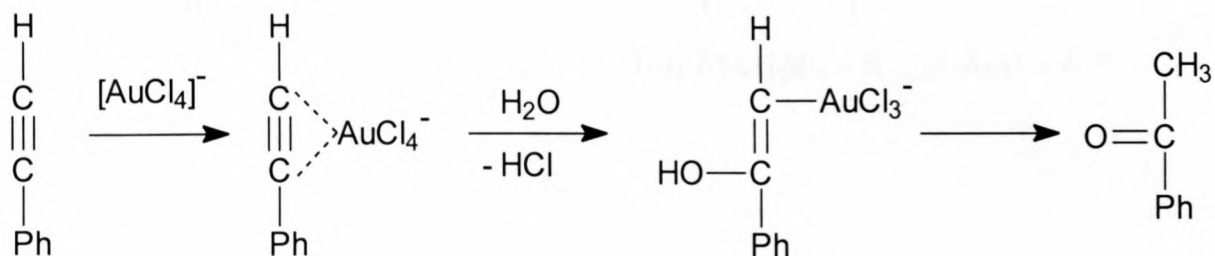
^a Relative intensities in parentheses

3.2.6 Gold(III) Catalysed Hydration of Phenylacetylene

Preliminary results are presented here and the employed catalysis terminology is described in the experimental section of this chapter.

3.2.6.1 Catalysis in Conventional Solvents

The hydration of phenylacetylene in refluxing aqueous methanol with NaAuCl_4 as catalyst has been reported by Utimoto and co-workers,^[10] where the addition of water to an alkyne affords the Markovnikov product (Equation 3.2). In the current investigation, the addition reaction was performed in methanol with NaAuCl_4 and the new ionic compound, $[\text{BMTz}][\text{AuBrCl}_3]$ (2.4 mol%), as catalyst precursors. The reaction time was 24 hours at temperatures of 30, 40 and 60°C.



Equation 3.2

The hydration reaction is temperature dependent and the best conversions were obtained at 30°C for both catalyst precursors in methanol. A histogram using the mean of the conversion values given in Table 3.9, appears in Figure 3.4.

The activities of the gold complexes were similar at the chosen temperatures but a decrease in the total yield of acetophenone (65%) was obtained compared to the previous study by Utimoto (91%). Nevertheless, employing extended reaction times in conjunction with milder temperatures, decreased the catalyst deactivation rate and thereby increased phenylacetylene conversion.

Acetophenone formation ceased after 24 hours (as determined by GC-MS) and the deposition of gold, indicating catalyst decomposition, became visible.

Table 3.9 Catalysis values for the hydration of phenylacetylene in methanol

Temperature (°C)	Conversion/ Total Yield (%) ^a		TON		Activity (h ⁻¹)	
	A	B	A	B	A	B
30	65	60	27	25	1.1	1.0
	63	61	26	25	1.1	1.0
	64	59	27	25	1.1	1.0
40	42	40	18	17	0.8	0.7
	41	41	17	17	0.7	0.7
	40	39	17	16	0.7	0.7
60	16	12	7	5	0.3	0.2
	17	13	7	5	0.3	0.2
	15	11	6	5	0.3	0.2

^a A = NaAuCl₄; B = [BMTz][AuBrCl₃]

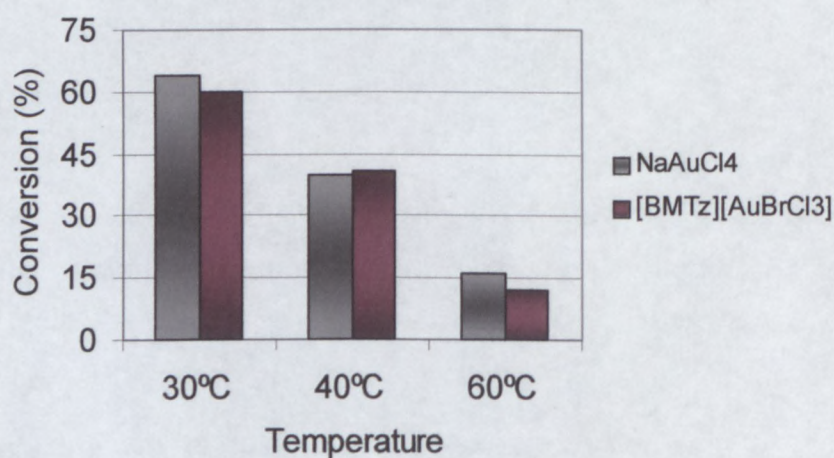


Figure 3.4 Dependence of conversion on reaction temperature

3.2.6.2 Catalysis in Ionic Liquids

Catalytic hydration of phenylacetylene with two molar equivalents of wet methanol also proceeded with the individual catalysts in a biphasic mixture of the respective ionic liquids and toluene. Catalyst dissolution in the ionic liquid, introduction of phenylacetylene and methanol and heating to 30, 40 and 60°C, respectively, afforded acetophenone in various yields. Histograms using the mean of the conversion values given in Table 3.10, appear in Figures 3.5 and 3.6.

The introduction of toluene eliminated the need for a final product extraction procedure. Blank reactions were performed in the ionic liquids and showed no conversion of phenylacetylene. The two catalysts showed limited solubility in toluene and the yield of acetophenone was much lower than in the corresponding reactions in the ionic liquids. Conversions, TON's and activities followed the order $[\text{BMIM}][\text{OTf}] > [\text{BMIM}][\text{PF}_6] \approx [\text{BMIM}][\text{BF}_4]$ and deposition of gold metal was again evident. In $[\text{BMIM}][\text{BF}_4]$ and $[\text{BMIM}][\text{PF}_6]$, the yield of acetophenone was the same as in methanol, whereas the reaction in $[\text{BMIM}][\text{OTf}]$ gave a slight increase (ca. 10%).

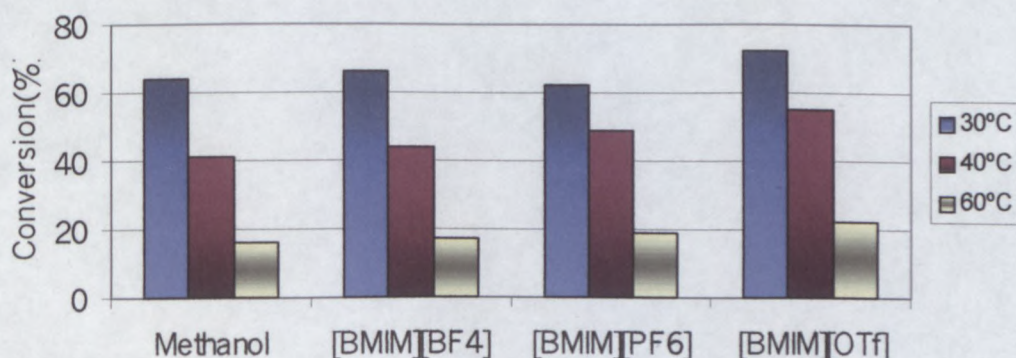


Figure 3.5 Conversion comparisons for NaAuCl₄

Performing the reaction at the melting point of $[\text{BMTz}][\text{AuBrCl}_3]$ (80°C) gave significantly lower yields of acetophenone (ca. 10%). Nevertheless, catalysis of the hydration reaction by $[\text{BMTz}][\text{AuBrCl}_3]$ indicates that gold(III)-containing ionic liquids could serve as both solvents and catalysts for organic transformations, but that further work is necessary.

Table 3.10 Catalysis values for the hydration of phenylacetylene in ionic liquids^a

Temperature (°C)	[BMIM][BF ₄]			[BMIM][PF ₆]			[BMIM][OTf]													
	Conversion /Total Yield (%)	TON	Activity (h ⁻¹)	Conversion /Total Yield (%)	TON	Activity (h ⁻¹)	Conversion /Total Yield (%)	TON	Activity (h ⁻¹)											
	A	B	A	B	A	B	A	B	A	B										
30	68	66	28	28	1.2	1.2	65	64	28	27	1.2	1.1	75	74	31	31	31	31	1.3	1.3
	66	65	28	27	1.2	1.1	60	63	25	26	1.0	1.1	70	72	29	30	30	30	1.2	1.3
	65	66	27	28	1.1	1.2	61	63	25	26	1.0	1.1	72	74	30	31	31	31	1.3	1.3
40	45	43	19	18	0.8	0.8	49	50	20	21	0.8	0.9	55	56	23	23	23	23	1	1
	45	43	19	18	0.8	0.8	48	51	20	21	0.8	0.9	54	56	23	23	23	23	1	1
	43	43	18	18	0.8	0.8	50	47	21	20	0.9	0.9	55	54	23	23	23	23	1	1
60	18	19	8	8	0.3	0.3	21	20	9	8	0.4	0.3	23	22	10	9	9	9	0.4	0.4
	16	17	7	7	0.3	0.3	19	21	8	9	0.3	0.4	23	22	10	9	9	9	0.4	0.4
	16	19	7	8	0.3	0.3	18	17	8	7	0.3	0.3	22	22	9	9	9	9	0.4	0.4

^a A = NaAuCl₄; B = [BMTz][AuBrCl₃]

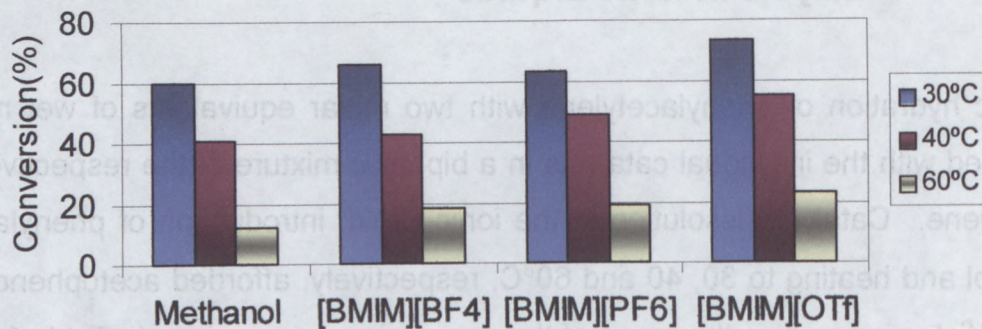


Figure 3.6 Conversion comparisons for [BMTz][AuBrCl₃]

The introduction of the reaction procedure. Blank reactions were performed in the ionic liquids and showed no conversion of phenylacetylene. The two catalysts showed limited solubility in toluene and the yield of acetophenone was much lower than in the corresponding reactions in the ionic liquids. Conversions, TON's and activities followed the order [BMIM][OTf] > [BMIM][PF₆] > [BMIM][BF₄] and deposition of gold metal was again evident in [BMIM][BF₄] and [BMIM][PF₆], the yield of acetophenone was the same as in methanol, whereas the reaction in [BMIM][OTf] gave a slight increase (ca. 10%).



Figure 3.5 Conversion comparisons for NaAuCl₄

Performing the reaction at the melting point of [BMTz][AuBrCl₃] (80°C) gave significantly lower yields of acetophenone (ca. 10%). Nevertheless, catalysts of the hydration reaction by [BMTz][AuBrCl₃] indicates that gold(III)-containing ionic liquids could serve as both solvents and catalysts for organic transformations, but that further work is necessary.

3.2.6.3 Hydration of Phenylacetylene in Recycled Ionic Liquid Phases

One of the reported advantages of utilising ionic liquids as opposed to conventional solvents is their capacity to be re-cycled.^[7] The potential re-use of catalysts within the ionic liquid phase could then also be an advantage. Filtering off deposited gold, repeated washing of the ionic liquid phase with toluene and drying *in vacuo*, removed deposited gold metal and traces of acetophenone present from the original hydration reactions. Fresh phenylacetylene and methanol were introduced and the reactions repeated. The conversion values obtained for the hydration reaction in recycled ionic liquid phases are given in Table 3.11.

At the three temperatures, the conversions were now 50% lower, but nevertheless, indicates the potential to re-use catalyst-containing ionic liquids. The conversion of phenylacetylene showed a similar dependency on the ionic liquids as before, with the best yields obtained in [BMIM][OTf], but activities and TON's could not be determined since the amount of catalyst present in the ionic liquids was unknown.

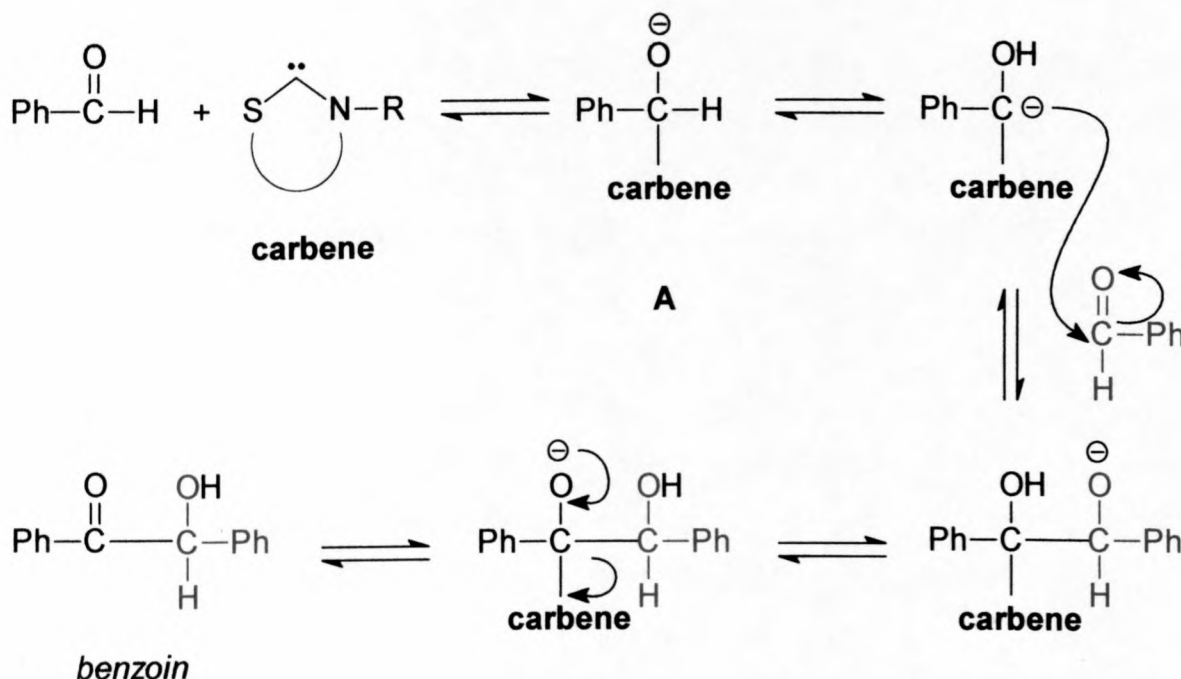
Table 3.11 Conversion % of acetophenone in recycled ionic liquids^a

	[BMIM][BF ₄]		[BMIM][PF ₆]		[BMIM][OTf]	
Temperature (°C)	Conversion/ Total Yield (%)		Conversion/ Total Yield (%)		Conversion/ Total Yield (%)	
	A	B	A	B	A	B
30°C	28	27	30	28	34	30
	31	29	33	30	32	32
	33	32	33	26	32	29
40°C	20	17	20	22	21	19
	20	18	22	20	20	18
	23	22	23	18	24	21
60°C	8	11	10	9	11	12
	8	9	13	13	10	8
	10	7	15	9	13	9

^a A = NaAuCl₄; B = [BMTz][AuBrCl₃]

3.2.7 Benzoin Condensation Catalysis

Free amino(thio)carbenes have been reported to promote the benzoin condensation reaction after *in situ* generation from an ionic liquid and a base (Equation 3.3).^[1] The nucleophilic carbene presumably generates an adduct, **A**, which rearranges to **B**, which after reaction with a second mole of benzaldehyde and carbene ejection, affords benzoin as product.



Scheme 3.5

Addition of NEt₃ (2 mol%) to ionic liquid **4**, followed by introduction of benzaldehyde and stirring for 7 days, afforded a maximum yield of only 15% benzoin. This is significantly less than the findings of a previous study utilising [BMTz][BF₄] where 80% conversion to benzoin is obtained after 7 days. This result indicates the important role played by the side chain and counterion in the ionic liquid and merits further detailed investigation.

3.3 SUMMARY

Thiazolium cations are alternatives to imidazolium units in ionic liquids. 3-Butyl-4-methylthiazolium triflate was prepared by metathesis and has a low melting point of -10°C . Treatment of the new room temperature ionic liquid with a variety of bases resulted in dimerisation of free amino(thio)carbene, but the dimer could not be isolated in pure form. Although free thiazolinylienes have been reported to promote the benzoin condensation reaction, addition of triethylamine to the new ionic liquid produced benzoin in low yield.

A number of procedures are available for preparing ionic liquids containing a metal in the counterion. By again employing metathesis as synthetic procedure, we have isolated and crystallographically characterised the first gold(III) thiazolium salt that qualifies as an ionic liquid. Treatment of the new gold(III) thiazolium salt with a variety of bases furnished the corresponding carbene complex.

NaAuCl_4 has previously been used as a catalyst for the hydration of phenylacetylene. The catalytic activity of NaAuCl_4 and the new gold(III) thiazolium salt were utilised for the hydration reaction in imidazolium ionic liquids as well as in an organic solvent. The two types of gold(III) compounds displayed similar activities but a decrease in the previously reported yield of acetophenone was obtained.

Performing the catalytic reaction at the melting point of the gold(III) thiazolium salt (80°C) showed limited conversion of phenylacetylene, once again due to catalyst decomposition. Nevertheless, catalysis of the hydration reaction by $[\text{BMTz}][\text{AuBrCl}_3]$ indicates that gold(III)-based ionic liquids could serve as both solvents and catalysts for organic transformations, but that further work is necessary to increase catalyst stability and, therefore, also catalytic activity. The catalyst-containing ionic liquid phases were recycled and then used for a second catalytic run. Significantly lower yields of acetophenone were obtained.

3.4 EXPERIMENTAL

3.4.1 Materials

The ionic liquids [BMIM][OTf]^[4], [BMIM][PF₆] and [BMIM][BF₄]^[3] were prepared according to literature methods. The thiazolium based ionic liquids, [BMTz][Br] and [BMTz][BF₄], were prepared by applying the procedures for [BMIM][Cl]^[22] and [BMIM][BF₄]. Tetrahydrofuran, hexane, toluene and diethyl ether were distilled under nitrogen from sodium diphenylketyl and dichloromethane from CaH₂. Methanol was distilled from magnesium methanolate and stored over 3Å molecular sieves.

3.4.2 Physical Methods

The same experimental conditions as in Section 2.4.2 apply.

Fast atom bombardment mass spectra were recorded on a VGA70-70E mass spectrometer at 70 eV with xenon as bombardment gas and *m*-nitrobenzylalcohol as matrix.

3.4.3 Preparations

3.4.3.1 Preparation of $\overline{\text{HC}=\text{C}(\text{Me})\text{N}(\text{Bu})=\text{CHS}}$ [OTf], **4**

Halide displacement procedure

3-Butyl-4-methylthiazolium bromide (4.23 g, 17.9 mmol) was dissolved in water (25 cm³), cooled to 0°C and CF₃SO₃H (2.8 g, 1.7 cm³, 18.8 mmol) added dropwise over 30 minutes. The reaction mixture was stirred for 72 hours and extracted with dichloromethane (100 cm³). The organic phase was washed with ice water until the washings were neutral. The organic phase was dried over MgSO₄, which was then filtered off, the solvent removed *in vacuo* and the ionic liquid dried under high vacuum (1mmHg) at 60°C for 48 hours.

Halide exchange procedure

3-Butyl-4-methylthiazolium bromide (4.23 g, 17.9 mmol) was dissolved in water (25 cm³), cooled to 0°C and CF₃SO₃Na (3.2 g, 18.8 mmol) added in solid form. The reaction mixture was stirred for 72 hours and worked up as described under the halide displacement procedure.

3.4.3.2 Preparation of $\overline{[\text{HC}=\text{C}(\text{Me})\text{N}(\text{Bu})=\text{CHS}]}\text{[AuBrCl}_3\text{]}$, **5**

Halide displacement procedure

3-Butyl-4-methylthiazolium bromide (605 mg, 2.56 mmol) was dissolved in methanol (10 cm³) and HAuCl₄ (1 g, 2.56 mmol) dissolved in methanol (10 cm³) added dropwise over 10 minutes. The reaction mixture was stirred for 2 hours, the methanol removed *in vacuo* and the ionic liquid dried under high vacuum (1 mmHg) at 30°C for 24 hours.

Halide exchange procedure

3-Butyl-4-methylthiazolium bromide (525 mg, 2.22 mmol) was dissolved in methanol (10 cm³) and NaAuCl₄ (963 mg, 2.22 mmol) dissolved in methanol (10 cm³) added dropwise over 10 minutes. The reaction mixture is stirred for 2 hours and the methanol removed *in vacuo*. The product was redissolved in dichloromethane, the precipitated NaCl filtered off and the ionic liquid dried under high vacuum (1 mmHg) at 30°C for 24 hours.

3.4.3.3 Preparation of $\overline{[\text{HC}=\text{C}(\text{Me})\text{N}(\text{Bu})=\text{CS}]_2}$, **6**

3-Butyl-4-methylthiazolium tetrafluoroborate (243 mg, 1 mmol) or triflate (305 mg, 1 mmol) was dissolved in thf (15 cm³) and cooled to -78°C. MeLi (1.40 mol.dm⁻³, 0.7 cm⁻³, 1 mmol), BuLi (1.60 mol.dm⁻³, 0.6 cm⁻³, 1 mmol) or NEt₃ (101 mg, 1 mmol) was added and the reaction mixture stirred for 2 hours with gradual warming to room temperature. The reaction residue was filtered through Celite and the solvent removed.

3.4.3.4 Preparation of $\overline{[\text{Cl}_3\text{Au}(\text{HC}=\text{C}(\text{Me})\text{N}(\text{Bu})\text{CS})]}$, **7**

3-Butyl-4-methylthiazolium tetrachloroaurate (495 mg, 1 mmol) was dissolved in thf (15 cm³) and cooled to -78°C. MeLi (1.40 mol.dm⁻³, 0.7 cm⁻³, 1 mmol), BuLi (1.60 mol.dm⁻³, 0.6 cm⁻³, 1 mmol) or NEt₃ (101 mg, 1 mmol) was added and stirring was continued for 2 hours

with gradual warming to room temperature. The reaction residue was filtered through Celite and the solvent removed.

3.4.3.5 Crystallography for complex 5

M. Esterhuysen solved the crystal and molecular structure of complex 5. The crystal data as well as collection and refinement details for complex 5 are given in Table 3.12. All other crystallographic information is available from M. Esterhuysen, Chemistry Department, P/Bag X1, Matieland, Stellenbosch, 7602, RSA.

X-ray diffraction data were collected on an Enraf-Nonius Kappa CCD diffractometer at 150(2)K using graphite monochromated Mo- K_{α} radiation ($\lambda = 0.71073\text{\AA}$)^[23] and corrected for Lorentz and absorption effects using the Scalepack package.^[24] Structure solution and refinement was carried out using the program SHELX-97.^[25] ORTEP-3 for Windows was used to generate the figures at 50% probability level.^[26] The structure was solved by direct methods and completed by full-matrix least-squares refinement against F^2 . All non-hydrogen atoms were refined anisotropically, except those in the *N*-butyl chain (C5, C6, C7, C8), which exhibited dynamic disorder. Equal bond length restraints with an effective standard deviation of 0.02\AA were applied to the $C_{sp^3}-C_{sp^3}$ bonded carbon atoms in the *N*-butyl chain in order to obtain sensible bond lengths. The disorder in the thiazolium ring was resolved by identifying disordered atom pairs for the components of the ring from the difference Fourier map and restraining the sum of their common site occupancy factors to 1. Rigid body and planarity restraints were applied to the disordered ring pair after which the atoms involved were allowed anisotropic motion. Final refined occupation factors gave a disordered ring ratio of 0.59(a):0.41(b). The positional disorder found for the bromine atom in the AuBrCl_3^- anion was dealt with as follows: The halide positions around the gold atom were each split into a chlorine and bromine atom with the sum of their respective site occupancy factors independently restrained to 1. Refinement of these halide positions yielded a total site occupancy of exactly 1 for the bromine atom over all 4 halide positions in the ratio 0.30 : 0.16 : 0.42 : 0.12 for halide positions 1,2,3 and 4 respectively, thus crystallographically confirming the AuBrCl_3^- empirical formula for the anion. Hydrogen positions were calculated with C-H distances of 0.98\AA (methyl C-H) and 0.95\AA (methylene C-H) and assigned isotropic displacement parameters 1.5 (methyl H) and 1.2 (methylene H) times the equivalent isotropic displacement parameters of their parent atoms.

Table 3.12 Crystal data, collection and refinement details for complex **5**

Formula	C ₈ H ₁₄ AuBrCl ₃ NS
Formula weight	539.41
Crystal system, space group	Monoclinic, P2 ₁ /n
Radiation, T/ °C	Mo-K α (0.71073Å), -123(2)
a, b, c/ Å	8.2241(3), 9.6725(3), 18.5555(8)
α , β , γ / °	90, 93.6050(10), 90
Z	4
U/ Å ³	1473.12(9)
Crystal size	0.13 x 0.20 x 0.20 mm ³
Calculated density (D _c) g/cm ⁻³	2.232
Absorption coefficient (μ)	13.356 mm ⁻¹
Absorption correction method	Empirical (Scalepack)
T _{min}	0.1753
T _{max}	0.2756
F(000)	1000
Diffractometer	Enraf Nonius KappaCCD
Scan type	ϕ and ω to fill an Ewald sphere
Scan range, θ /°	2.38 \leq θ \leq 27.52
<i>hkl</i> ranges	-10 \leq <i>h</i> \leq 9, -12 \leq <i>k</i> \leq 11, -24 \leq <i>l</i> \leq 17
Reflections collected/ unique	7160 / 2603 [R(int) = 0.0328]
Data / restraints / parameters	3357 / 32 / 178
Refinement method	Full-matrix least-squares on F ²
Final R indices [<i>l</i> > 2 σ (<i>l</i>)]	R ₁ = 0.0446, wR ₂ = 0.0978
R indices (all data)	R ₁ = 0.0639, wR ₂ = 0.1054
Weighting scheme	Calculated w = 1/[σ^2 (Fo ²) + [(0.0290) ² + 13.1169P] where P = (Fo ² + 2Fc ²)/3
Goodness of fit on F ²	1.061
Largest peak, deepest hole	1.56 e ⁻ / Å ³ , -1.73 e ⁻ / Å ³ (0.72 Å from Au)
Maximum shift/esd	0.001

3.4.4 Catalysis

3.4.4.1 Terminology

$$\text{Conversion / Total Yield (\%)} = \frac{\text{mol of product}}{n \text{ mol of monomer}} \times 100$$

$$\text{Turnover number (TON)} = \frac{\text{mol of converted monomer}}{\text{mol of catalyst}}$$

$$\text{Activity} = \frac{\text{TON}}{t} \quad (t = \text{hours})$$

3.4.4.2 Catalysis in methanol

To NaAuCl₄ (87 mg, 0.24 mmol) or [BMTz][AuCl₄] (119 mg, 0.24 mmol) dissolved in methanol (15 cm³) in a glass bomb, was added phenylacetylene (1 g, 0.93 cm³, 10 mmol). The bomb was sealed and heated to 30°C, 40°C or 60°C for 24 hours. The vessel was allowed to cool to room temperature, the reaction mixture filtered and the excess methanol removed *in vacuo*.

3.4.4.3 Catalysis in ionic liquids

NaAuCl₄ (87 mg, 0.24 mmol) or [BMTz][AuCl₄] (119 mg, 0.24 mmol) was dissolved in [BMIM][BF₄], [BMIM][PF₆] or [BMIM][OTf] (10 cm³) and layered with toluene (10 cm³) in a glass bomb. Phenylacetylene (1 g, 0.93 cm³, 10 mmol) and methanol (160 mg, 5 mmol) was added, the bomb sealed and heated to 30°C, 40°C or 60°C for 24 hours. The vessel was allowed to cool to room temperature, the toluene layer decanted off and the excess toluene removed *in vacuo*.

3.4.4.4 Recycling of ionic liquid phases

After the initial reaction, the ionic liquid was filtered (porosity 4), washed repeatedly with toluene (3 x 10 cm³) and dried under high vacuum (3 mmHg) for 24 hours at room temperature. The reaction was then executed as described in paragraph 3.3.4.3.

REFERENCES

- [1] J. H. Davis Jr., K. J. Forrester and T. Merrigan, *Tetrahedron Lett.*, 1998, **39**, 8955.
- [2] P. Wasserscheid and W. Keim, *Angew. Chem., Int. Ed. Engl.*, 2000, **39**, 3773.
- [3] P. A. Z. Suarez, J. E. L. Dullius, S. Einloft, R. F. de Souza and J. du Pont, *Polyhedron*, 1996, **15**, 1217.
- [4] P. Bonhôte, A. -P. Dias, N. Papegeorgiou, N. Kalyanasundaram and M. Grätzel, *Inorg. Chem.*, 1996, **35**, 1168.
- [5] E. R. Schreiter, J. E. Stevens, M. F. Ortwerth and R. G. Freeman, *Inorg. Chem.*, 1999, **38**, 3935.
- [6] M. Hasan, I. V. Kozhevnikov, M. R. H. Siddiqui, A. Steiner and N. Winterton, *Inorg. Chem.*, 1999, **38**, 5637.
- [7] K. R. Seddon, *J. Chem. Biotechnol.*, 1997, **68**, 351; K. R. Seddon, *Kinet. Catal. Engl. Transl.*, 1996, **37**, 693.
- [8] D. Thompson, *Gold Bulletin*, 1999, **32**, 1.
- [9] J. H. Teles, S. Brode and M. Chabanas, *Angew. Chem., Int. Ed. Engl.*, 1998, **37**, 1415.
- [10] Y. Fukuda and K. Utimoto, *J. Org. Chem.*, 1991, **56**, 3729.
- [11] D. A. Dixon and A. J. Arduengo, *J. Phys. Chem.*, 1991, **95**, 4180.
- [12] C. Boehme and G. Frenking, *J. Am. Chem. Soc.*, 1996, **118**, 2039.
- [13] A. J. Arduengo, J. R. Goerlich and W. J. Marshall, *Liebigs Ann. Recueil*, 1997, 365.
- [14] J. H. Teles, J. P. Melder, K. Ebel, R. Schneider, E. Gehrler, W. Harder, S. Bröde, D. Enders, K. Breuer and G. Raabe, *Helv. Chim. Acta*, 1996, **79**, 61.
- [15] J. H. Davis and K. J. Forrester, *Tetrahedron Lett.*, 1999, **40**, 1621.
- [16] R. F. Frenske in, *Organometallic Compounds; Synthesis, Structure and Theory*, (ed. B. L. Shapiro), Texas A & M University Press, Texas, 1983, p. 305.
- [17] J. B. Stothers, *Carbon-13 NMR Spectroscopy*, Academic Press, New York, 1972.
- [18] H. G. Raubenheimer, P. J. Olivier, L. Lindeque, M. Desmet, J. Hrušak and G. J. Kruger, *J. Organomet. Chem.*, 1997, **544**, 91.
- [19] D. Bourissou, O. Guerret, F. P. Gabbaï and G. Bertrand, *Chem. Rev.*, 2000, **100**, 39.
- [20] J. Kapp, C. Schade, A. M. El-Nahasa and P. v. R. Schleyer, *Angew. Chem., Int. Ed. Engl.*, 1996, **35**, 2236.
- [21] A. J. Arduengo, D. A. Dixon, K. K. Kumashiro, C. Lee, W. P. Power and K. W. Zilm, *J. Am. Chem. Soc.*, 1994, **116**, 6361.

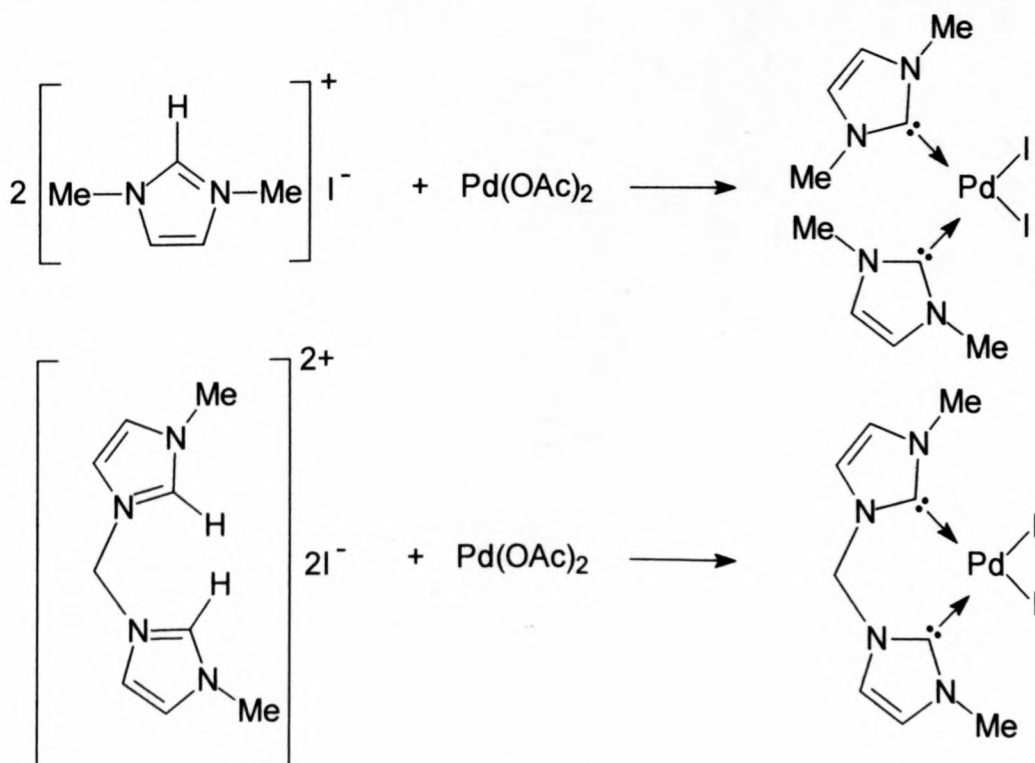
- [22] J. S. Wilkes, J. A. Levisky, R. A. Wilson and C. L. Hussey, *Inorg. Chem.*, 1982, **21**, 1263.
- [23] Nonius, COLLECT., Nonius BV, Delft, The Netherlands, 1999.
- [24] Z. Otwinowski, W. Minor, *Methods Enzymol.*, 1997, **276**, 307.
- [25] G.M. Sheldrick, SHELX-97 – *Program for Crystal Structure Analysis*, Institut für Anorganische Chemie der Universität Göttingen, Tammanstrasse 4, D-3400 Göttingen, Germany, 1998.
- [26] L.J. Farrugia, *J. Appl. Cryst.*, 1997, **30**, 565.

CHAPTER 4

PREPARATION AND CHARACTERISATION OF PALLADIUM, PLATINUM AND MANGANESE DI(ORGANO)CARBENE COMPLEXES FROM QUINOLINONE AND QUINOLINIUM PRECURSORS

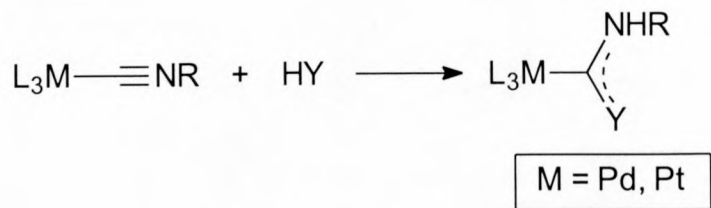
4.1 INTRODUCTION

A large number of heterocyclic palladium and platinum carbene complexes have been prepared over the past forty years and many excellent review articles are available.^[1,2] One of the most exciting recent developments comes from the laboratory of Herrmann.^[3] Deprotonation of an imidazolium salt with palladium acetate affords extremely stable *bis(carbene)* complexes (Scheme 4.1) that homogeneously catalyse the Heck reaction. Even more recently, it was experimentally established that analogous palladium carbene complexes are generated *in situ* with an ionic liquid functioning as both carbene substrate and solvent^[4] (compare also Chapters 1 and 3).



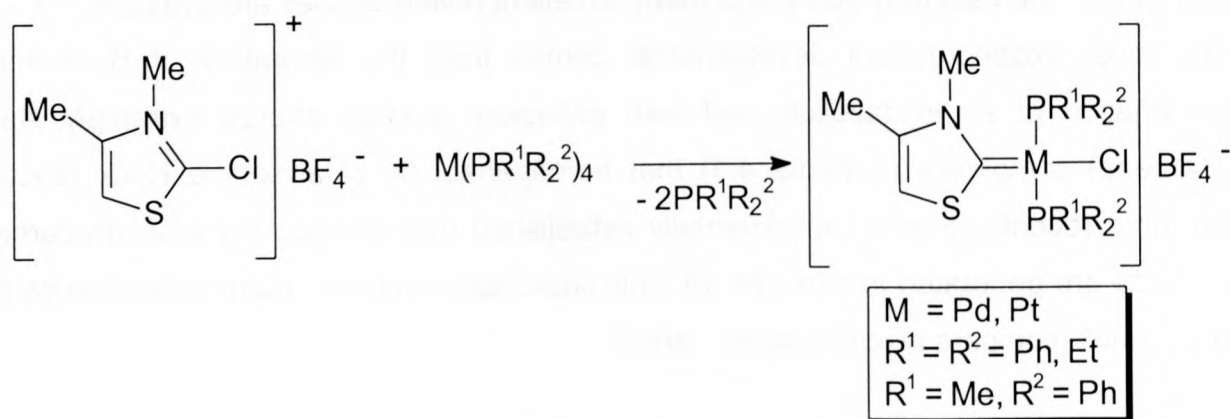
Scheme 4.1

Early research established a convenient synthesis of palladium and platinum carbene complexes that involves the addition of protonic reagents to divalent Pd and Pt isocyanide compounds (Equation 4.1).^[5] This method remains widely used to prepare group 10 carbene compounds.



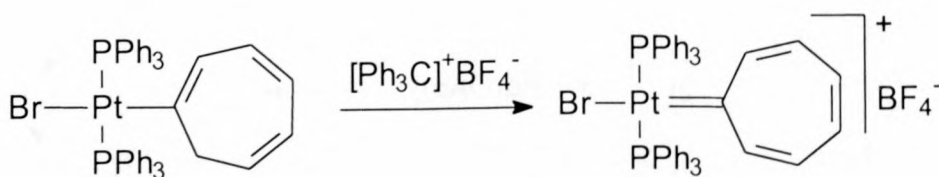
Equation 4.1.

Using another approach, Stone prepared α -methylated amino(thio)carbene complexes by oxidatively adding 2-chloro-3,4-dimethylthiazolium tetrafluoroborate to platinum(0) or palladium(0) phosphines (Equation 4.2).^[6]



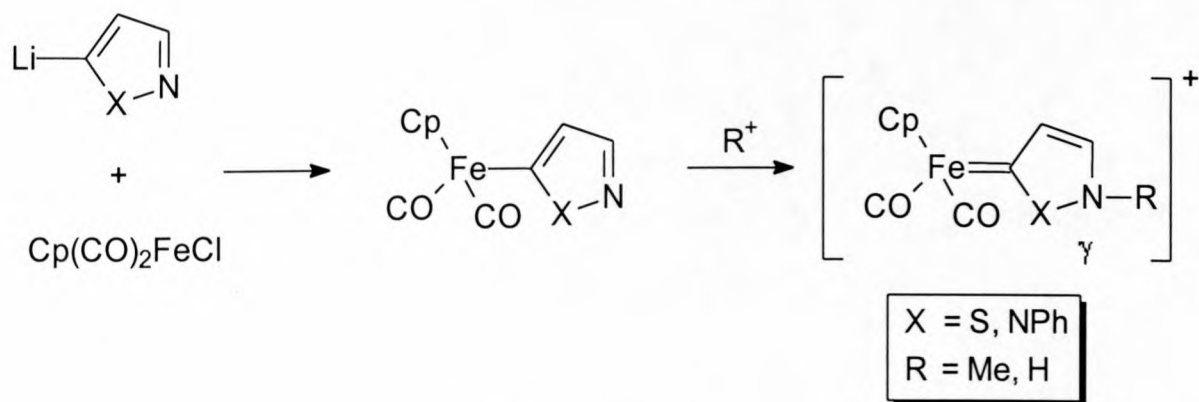
Equation 4.2

As is typical for most Fischer- and Öfele-Lappert-type carbene complexes,^[7] the vast majority of the known group 10 family contain at least one heteroatom attached to the carbene carbon. Only one exception has been crystallographically characterised and is prepared by deprotonation of a neutral precursor complex (Equation 4.3).^[8]

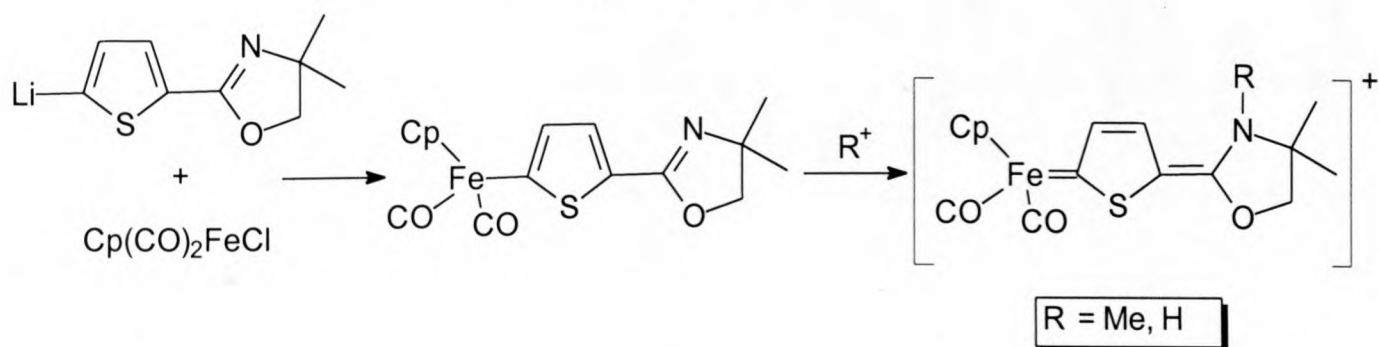


Equation 4.3

A variety of neutral and cationic transition metal carbene complexes have been prepared in our laboratory in recent years^[9] by employing a consecutive deprotonation-transmetallation-protonation/alkylation approach. The preparation involves transmetallation of a suitable metal starting compound with a lithiated azole to form an azolyl precursor complex, followed by protonation or alkylation of the nitrogen atom to yield the corresponding carbene complex.^[10,11,12] In this way, novel amino(thio)-, (amino)organo- and (organo)thiocarbene (Equation 4.4) complexes of iron have been prepared. In the latter examples, the nucleophilic nitrogen atom of the isothiazolyl and pyrazolyl precursor compounds is situated γ to the metal bonded carbon and not α , as in most comparable transformations.^[13] In a further development (Equation 4.5), 5-thienyl compounds with the nitrogen atom outside the coordinated ring system and separated from the coordinated carbon by several bonds were prepared.^[14]



Equation 4.4

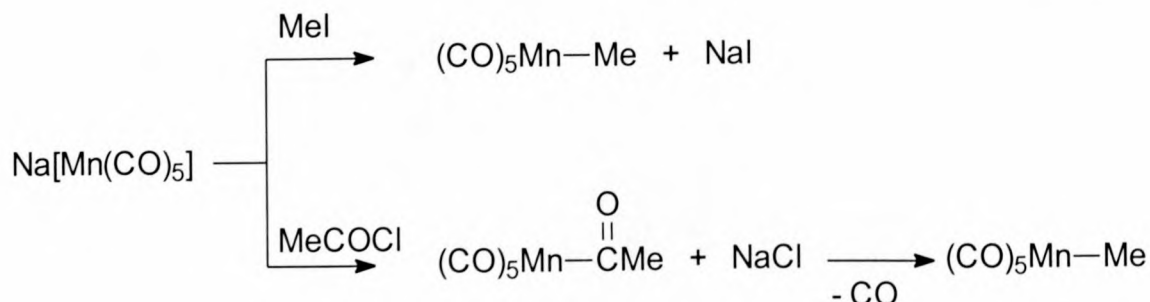


Equation 4.5

Moving away from the azoles to alternative heterocycles, the question of whether carbene preparation can also be utilised with a distant oxygen atom serving as nucleophilic target, was now addressed for the first time in preparing a series of palladium and platinum carbene compounds via initial oxidative-addition. As will be explained, the electrophilic attack on the oxygen atom was performed both before and after ligand attachment to the

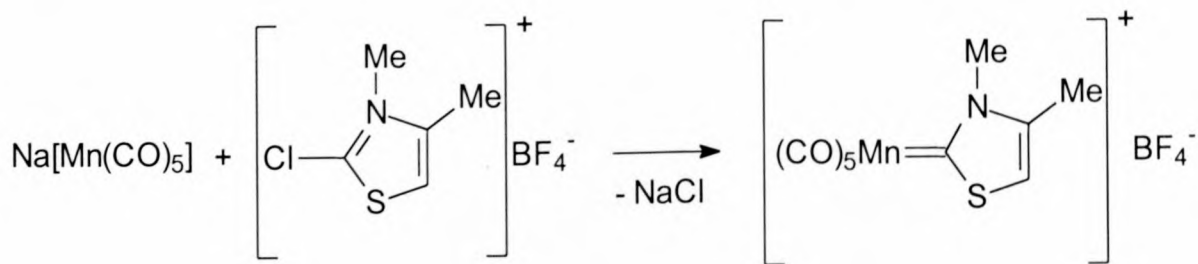
metal. 4-Chlor-2-methoxy-*N*-methylquinolinium tetrafluoroborate and 4-chlor-*N*-methylquinolinone, were the respective reagents of choice. In these compounds, the nucleophilic carbonyl oxygen in the precursor and product is separated from the coordinating carbon by three bonds. A single crystal structure determination confirmed the connectivities within the palladium carbene complex.

The synthesis of manganese carbene and coordination complexes enjoys a rich history that is comprehensively documented elsewhere.^[15] As early as 1957, Closson and co-workers prepared the first manganese compounds with a metal-C σ -bond.^[16] Reaction of sodium pentacarbonylmanganate, Na[Mn(CO)₅], with an alkyl- or acylhalide forms a Mn-C bond by halide displacement (Equation 4.6). Subsequent decarbonylation of the acylmanganese complexes affords alkyl(pentacarbonyl)manganese compounds.^[17] At present, Closson's original procedure remains the method of choice to prepare alkylmanganese compounds.



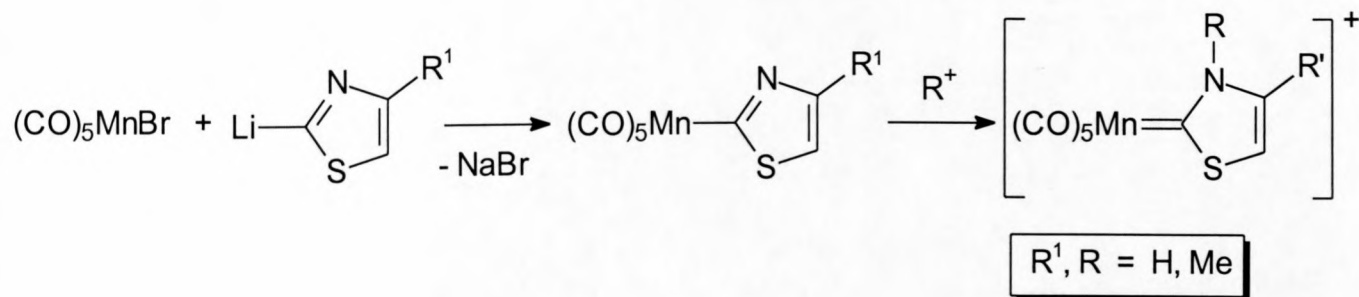
Equation 4.6

Stone reported the first "one-pot" synthesis of cationic manganese amino(thio)carbene complexes utilising halide displacement.^[18,19] Reaction of Na[Mn(CO)₅] with 2-chloro-3,4-dimethylthiazolium tetrafluoroborate gives the corresponding carbene complexes with a nitrogen atom adjacent to the carbene carbon (Equation 4.7).



Equation 4.7

Similar Öfele-Lappert-type manganese complexes have recently been prepared in our laboratory by employing a transmetallation synthetic approach.^[20] Neutral manganese thiazolyl precursor products are converted into the corresponding cationic carbene complexes by methylation or protonation (Equation 4.8).



Equation 4.8

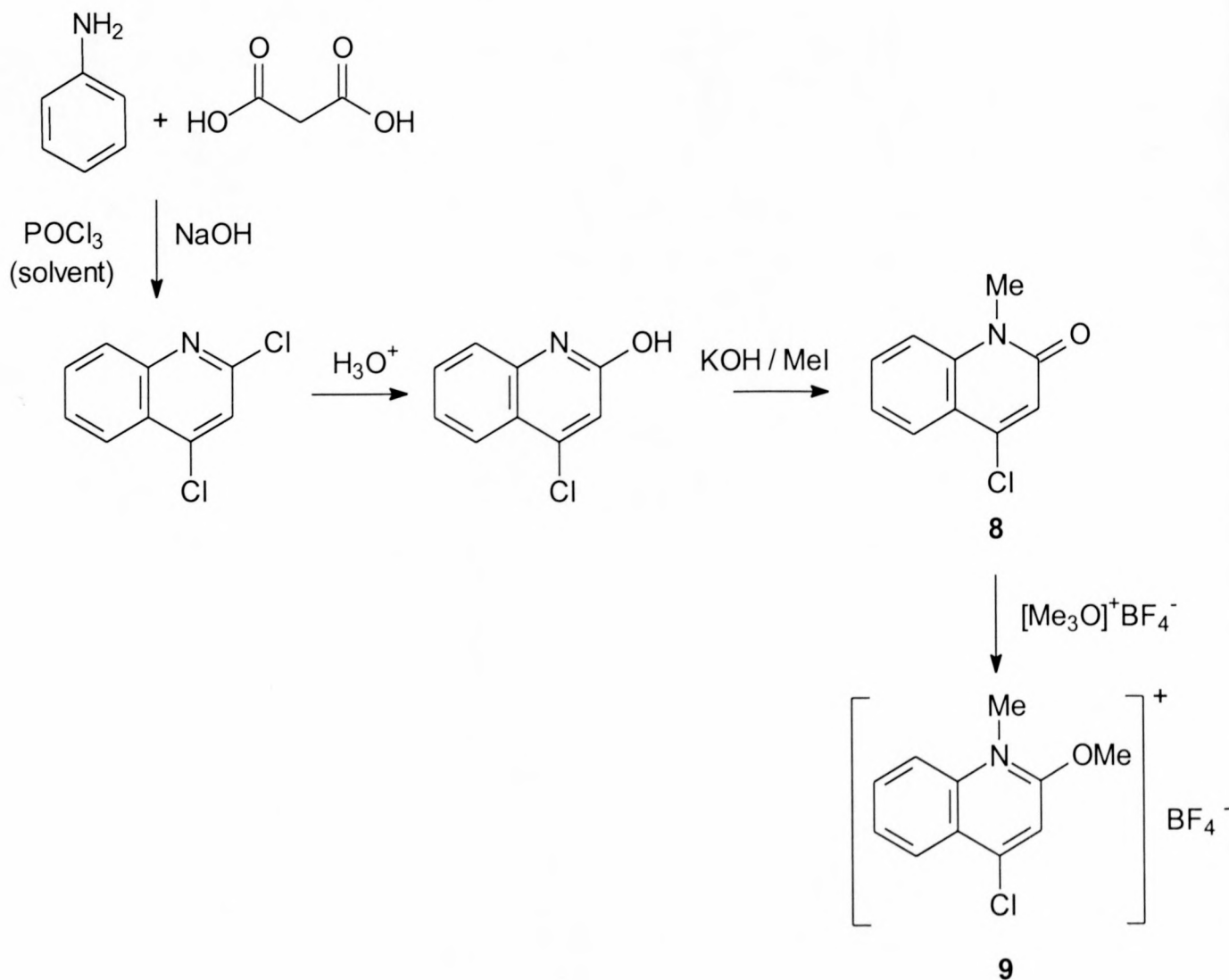
In this chapter, results of the investigation towards the synthesis of manganese carbene compounds based on Stone's "one-pot" route, but by employing neutral quinolinone and cationic quinolium precursors as alternatives to azoles, are reported. New coordination compounds and carbene complexes of manganese were envisaged and, once again, a far-removed oxygen atom served as electrophilic target for carbene formation.

4.2 RESULTS AND DISCUSSION

4.2.1 Quinolinone and Quinolinium Ligand Precursor Preparations

A Preparation of $\overbrace{\text{C}(\text{Cl})=\text{CHC}(=\text{O})\text{N}(\text{Me})\text{C}_6\text{H}_4}$, **8** and $\overbrace{[\text{C}(\text{Cl})=\text{CHC}(\text{OMe})\text{N}(\text{Me})\text{C}_6\text{H}_4]}\text{[BF}_4\text{]}$, **9**.

Existing literature procedures were followed or slightly modified to prepare the necessary ligand precursors **8** and **9** (Scheme 4.2).



Scheme 4.2

Addition of aniline to a POCl₃ solution of malonic acid and subsequent treatment with NaOH afforded 2,4-dichloroquinoline^[21] that was selectively hydrolysed in the 2-position to furnish 2-hydroxy-4-chloroquinoline.^[22] Treatment of 2-hydroxy-4-chloroquinoline with KOH in the presence of iodomethane afforded 4-chloro-*N*-methylquinolinone, **8**.^[22]

The new ion pair, 4-chloro-2-methoxy-*N*-methylquinolinium tetrafluoroborate, **9**, was prepared according to a literature method for the synthesis of 1,3-dimethylimidazolium tetrafluoroborate.^[23] Addition of Meerwein's salt, [Me₃O]⁺BF₄⁻, to compound **8** yielded the ligand precursor, **9**, in an overall yield of 15%. Both compounds **8** and **9** are white powders that readily dissolve in polar organic solvents, but show limited solubility in non-polar solvents.

B Spectroscopic characterisation of compounds **8** and **9**.

1. NMR spectroscopy

NMR spectroscopic data and the numbering scheme employed for compounds **8** and **9** are presented in Table 4.1.

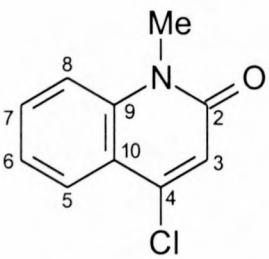
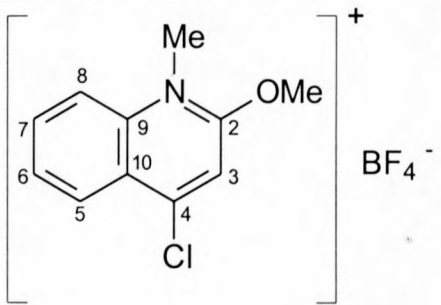
Due to the deshielding effect of the positive charge, the ¹H NMR spectrum of the ligand precursor, **9**, displays a downfield shift of the signals relative to those of compound **8**. The methoxy group of **9** resonates at δ 4.60 and the respective NMe signals of compounds **8** and **9** appear at δ 3.70 and 4.37.

¹³C-¹H NMR assignments for both ligand precursors are based on HETCOR experiments.

The deshielding effect of the positive charge on compound **9** is again evident in a general downfield shift of signals with respect to those of compound **8**. The C³ carbon of the latter compound, however, shows a small upfield shift of Δδ 10, possibly due to the positive inductive effect of the neighbouring methoxy group.

Note that alkylation of **8** produces a compound in which the cationic charge is probably again located on a nitrogen atom. Therefore, a nitrogen rather than oxygen could once again play the important role in eventual coordinated carbene stabilisation.

Table 4.1 ^1H and ^{13}C - $\{^1\text{H}\}$ NMR data of compounds **8** and **9**

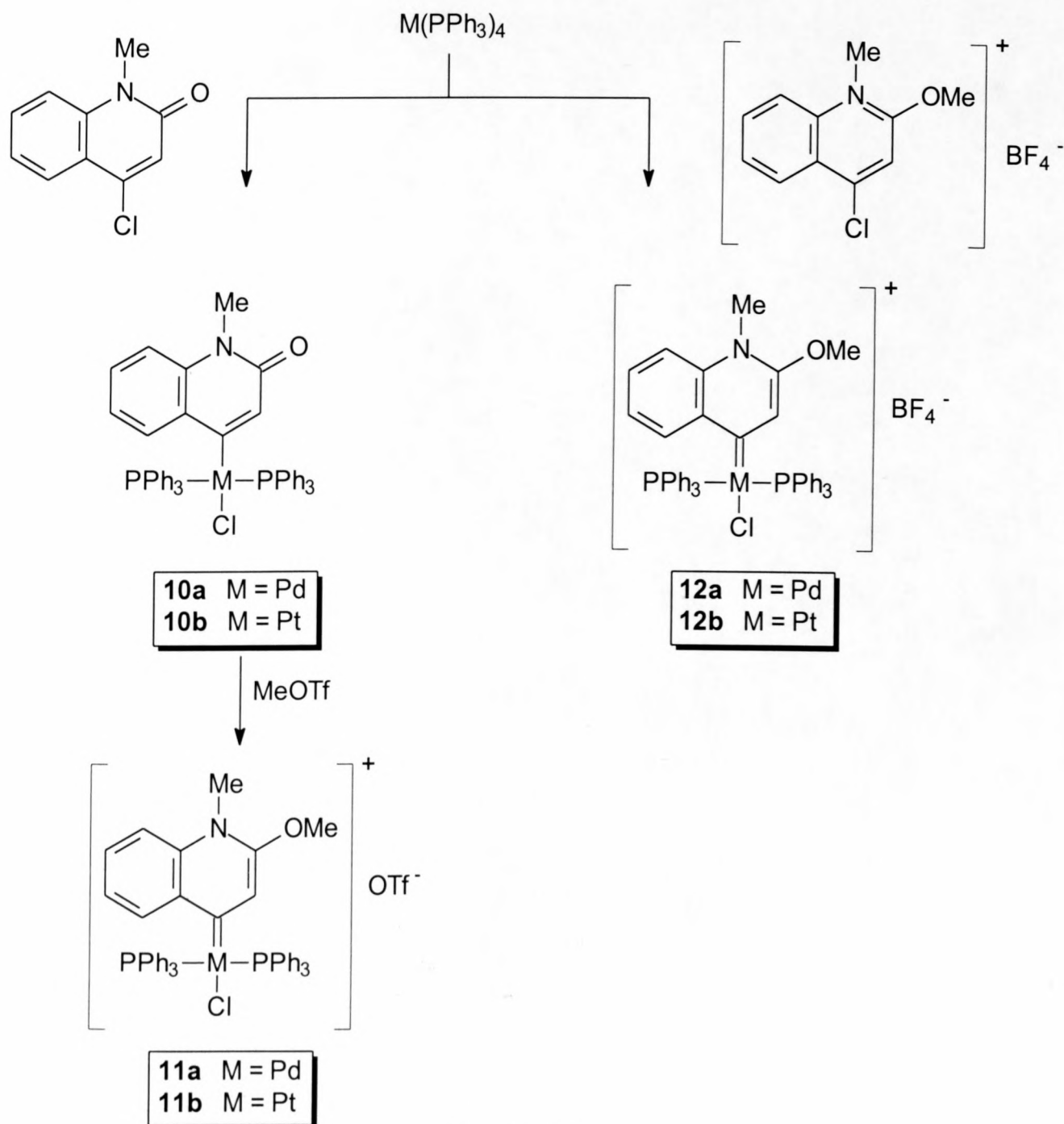
Compound			
Solvent		CD_2Cl_2	CD_2Cl_2
^1H NMR ^a	NMe	3.70 (3H, s)	4.37 (3H, s)
	OMe	-	4.65 (3H, s)
	H ³	6.88 (1H, s)	8.28 (1H, s)
	H ⁵	8.00	8.52
		(1H, dd, $J_{56,57} = 8.1, 4.1$)	(1H, ddd, $J_{56,57,58} = 8.3, 1.5, 0.6$)
	H ⁶	7.31	8.00
		(1H, ddd, $J_{56,67,68} = 8.1, 7.2, 1.0$)	(1H, ddd, $J_{56,67,68} = 8.3, 7.1, 1.0$)
	H ⁷	7.64	8.28
	(1H, ddd, $J_{78,67,57} = 8.6, 7.2, 1.5$)	(1H, ddd, $J_{78,67,57} = 8.9, 7.1, 1.5$)	
	H ⁸	7.38	8.46
		(1H, dd, $J_{78,68} = 8.6, 4.0$)	(1H, ddd, $J_{78,68,58} = 8.9, 1.0, 0.6$)
^{13}C NMR	NMe	29.5	35.1
	OMe	-	61.7
	C ²	161.0	162.7
	C ³	121.0	111.3
	C ⁴	144.3	154.3
	C ⁵	126.2	127.4
	C ⁶	122.6	129.4
	C ⁷	131.9	137.1
	C ⁸	114.4	119.4
	C ⁹	139.7	139.3
C ¹⁰	119.2	123.4	

^a J in Hz

4.2.2 Neutral Quinolin-2-on-4-yl Palladium and Platinum Complexes

A Preparation of $[(PPh_3)_2Pd(Cl)\{C=CHC(=O)N(Me)C_6H_4\}]$, **10a** and $[(PPh_3)_2Pt(Cl)\{C=CHC(=O)N(Me)C_6H_4\}]$, **10b**.

The preparation of neutral complexes **10a** and **10b**, as well as other cationic complexes isolated in the current investigation, are illustrated in Scheme 4.3.

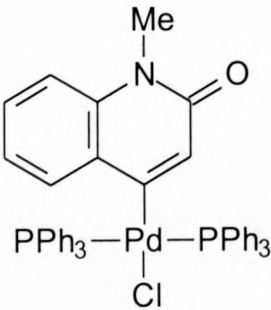
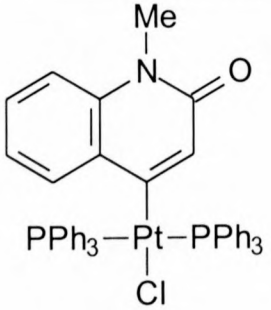


Scheme 4.3

Refluxing a benzene solution of halide **8** with an equimolar amount of Pd(PPh₃)₄ or Pt(PPh₃)₄, followed by filtration of the reaction mixture through Celite and *in vacuo* solvent removal, gave complexes **10a** and **10b** as pale yellow, crystalline compounds. The progress of the reaction was followed by thin layer chromatography (tlc) in a thf/hexane (1:1) eluant (R_f = 0.72).

The complexes are stable in air for short periods of time and dissolve in polar organic solvents. The analytical and physical data for complexes **10a** and **10b** are presented in Table 4.2.

Table 4.2 Analytical and physical data for complexes **10a** and **10b**

Complex	 <p style="text-align: center;">10a</p>	 <p style="text-align: center;">10b</p>
Colour	Pale yellow	Pale yellow
Yield (%)	72	69
M.p./ °C	161	195
M.W.	824.63	913.29
Analysis (%) ^a		
C	67.41	60.51
	(67.00)	(60.49)
H	4.68	4.10
	(4.64)	(4.19)
N	1.66	1.48
	(1.69)	(1.53)

^a Required values given in parentheses

B Spectroscopic characterisation of complexes 10a and 10b.**1. NMR spectroscopy**

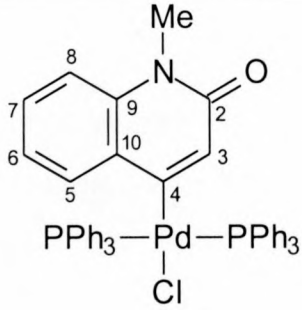
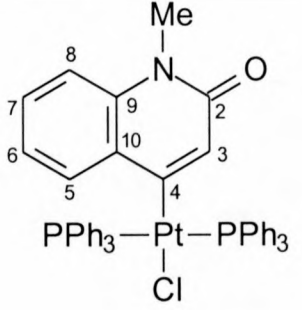
The ^1H NMR spectra of complexes **10a** and **10b** (Table 4.3) are very similar. All the signals appear upfield with respect to the corresponding values of compound **8**, except H^5 that displays a small downfield shift of $\Delta\delta$ ca. 0.3. Palladium and platinum $\text{MCl}(\text{PR}_3)_2$ groups have been described as “strong electron donors to aromatic rings in both inductive and resonance modes”^[24] and the upfield position of the complex signals are attributed to this effect.

The $^{13}\text{C}\{-^1\text{H}\}$ NMR data of complexes **10a** and **10b** are also very similar, indicating that electron distribution within the individual ligand frameworks is comparable. The C^4 resonance of complexes **10a** and **10b** respectively appears at δ 176.0 and δ 178.4, representing a downfield shift of $\Delta\delta$ ca. 34 from the corresponding signal in compound **8**. This chemical shift change is of the same order of magnitude reported for analogous palladium and platinum compounds, $\Delta\delta$ ca. 30, in which a metal-carbene bond is formed.^[25] The C^4 signal of complex **10b** appears as a doublet due to coupling with ^{195}Pt and the coupling constant, $^1\text{J}(\text{Pt-C})$ 35 Hz, is similar to the value observed for a platinum *tetrakis*(thiazolinylidene) complex, $^1\text{J}(\text{Pt-C})$ 37 Hz.^[26] These coupling constants, however, are somewhat smaller than those observed for other Pt-C σ -bonds (50 – 100 Hz).^[27]

The PPh_3 phenyl carbons of complex **10a** couple with the neighbouring phosphorus atoms and resonate as doublets. The corresponding signals of complex **10b** are multiplets due to additional coupling with the ^{195}Pt nucleus.

A single resonance observed in the $^{31}\text{P}\{-^1\text{H}\}$ NMR spectrum of complex **10a** indicates the presence of equivalent phosphorus atoms. Complex **10b** shows a doublet of doublets due to coupling between ^{195}Pt and the adjacent phosphorus nuclei. The observed coupling pattern is typical for platinum compounds with *trans* phosphine ligands although $^1\text{J}(\text{Pt-P})$ 575 Hz is somewhat smaller than previously reported values of up to 800 Hz in higher resolution spectra.^[27]

Table 4.3 ^1H , ^{13}C - $\{^1\text{H}\}$ and ^{31}P NMR data of complexes **10a** and **10b**

Complex	 <p style="text-align: center;">10a</p>	 <p style="text-align: center;">10b</p>
Solvent	CD ₂ Cl ₂	CD ₂ Cl ₂
^1H NMR ^a	NMe 3.13 (3H, s) H ³ 6.30 (1H, t, $J_{\text{HP}} = 1.7$) H ⁵ 8.30 (1H, dd, $J_{56,67} = 7.8, 1.6$) H ⁶ 6.86 (1H, ddd, $J_{56,67,68} = 7.8, 7.3, 1.1$) H ⁷ 7.16 (1H, ddd, $J_{56,67,68} = 8.5, 7.3, 1.6$) H ⁸ 6.68 (1H, m) PPh ₃ 7.19 – 7.92 (30H, 3 x m)	3.21 (3H, s) 6.38 (1H, t, $J_{\text{HP}} = 1.8$) 8.35 (1H, dd, $J_{56,67} = 7.9, 1.7$) 6.96 (1H, ddd, $J_{56,67,68} = 7.8, 7.4, 1.2$) 7.25 (1H, ddd, $J_{56,67,68} = 8.5, 7.5, 1.7$) 6.72 (1H, m) 7.21 – 7.95 (30H, 3 x m)
^{13}C NMR ^a	NMe 28.7 C ² 156.5 C ³ 121.5 C ⁴ 176.0 (br) C ⁵ 127.9 C ⁶ 123.6 C ⁷ 132.1 C ⁸ 114.1 C ⁹ 139.7 C ¹⁰ 119.7 C _{ortho} 133.1 (d, $J = 6.3$) C _{para} 129.7 (d, $J = 0.9$) C _{meta} 128.2 (d, $J = 5.0$) C _{ipso} 127.9 (d, $J = 24.5$)	29.3 157.4 121.9 178.4 (d, $J_{\text{PtC}} = 35$) 128.2 124.6 131.7 115.2 140.1 120.7 134.2 (m, $J = 6.1$) 130.3 (m, $J = 1.0$) 126.7 (m, $J = 4.8$) 128.6 (m, $J = 25.1$)
^{31}P NMR ^a	PPh ₃ 22.5	21.1 (dd, $J_{\text{PtP}} = 575$)

^a J in Hz

2. Mass spectrometry

The EI mass spectral data of complexes **10a** and **10b** are summarised in Table 4.4.

The molecular ions of complexes **10a** and **10b** are observed as weak intensity signals at m/z 824 and 913. Fragmentation patterns for the complexes are similar and consists of sequential loss of chlorine, two PPh₃ ligands and the metal atom to give the molecular ion of the ligand as the base peak at m/z 158. Fragment ions of the MCl(PPh₃)₂ moieties at m/z 666 (Pd) and m/z 755 (Pt), as well as the respective metal ion peaks at m/z 106 and 195, are also observed in the spectra.

Table 4.4 Mass spectral data for complexes **10a** and **10b**

Complex 10a		Complex 10b		Fragment ions
m/z	I ^a	m/z	I ^a	
824	< 5	913	< 5	$[(PPh_3)_2M(Cl)\{C=CHC(=O)N(Me)C_6H_4\}]^+$
789	21	878	15	$[(PPh_3)_2M\{C=CHC(=O)N(Me)C_6H_4\}]^+$
666	32	755	29	$[(PPh_3)_2M(Cl)]^+$
527	19	616	25	$[(PPh_3)M\{C=CHC(=O)N(Me)C_6H_4\}]^+$
-	-	465	22	$[(PPh)M\{C=CHC(=O)N(Me)C_6H_4\}]^+$
265	61	353	47	$[M\{C=CHC(=O)N(Me)C_6H_4\}]^+$
158	100	158	100	$[C=CHC(=O)N(Me)C_6H_4]^+$
106	20	195	31	$[M]^+$

^a Intensity relative to the base peak

4.2.3 Cationic Quinolin-4-ylidene Palladium and Platinum Complexes

A Preparation of $[(PPh_3)_2Pd(Cl)\{\overbrace{CCH=C(OMe)N(Me)C_6H_4}\}] [OTf]$, **11a**,
 $[(PPh_3)_2Pt(Cl)\{\overbrace{CCH=C(OMe)N(Me)C_6H_4}\}] [OTf]$, **11b**,
 $[(PPh_3)_2Pd(Cl)\{\overbrace{CCH=C(OMe)N(Me)C_6H_4}\}] [BF_4]$, **12a** and
 $[(PPh_3)_2Pt(Cl)\{\overbrace{CCH=C(OMe)N(Me)C_6H_4}\}] [BF_4]$, **12b**.

Methylation of complexes **10a** and **10b** with MeOTf in thf at $-60^\circ C$, furnished the corresponding cationic di(organo)carbene complexes, **11a** and **11b** (Scheme 4.3). Filtration through Celite and recrystallisation from dichloromethane gave the products as colourless, crystalline compounds.

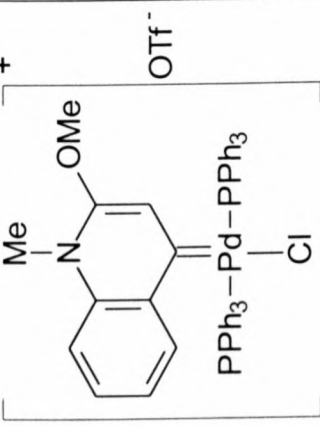
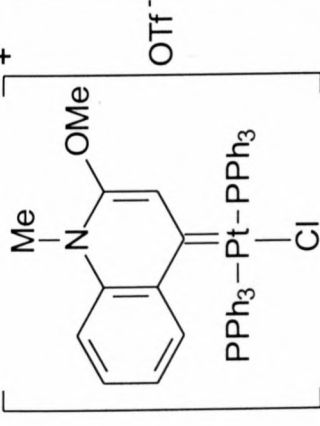
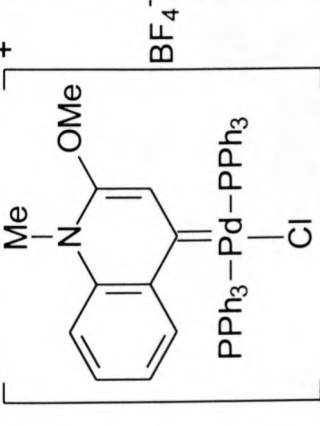
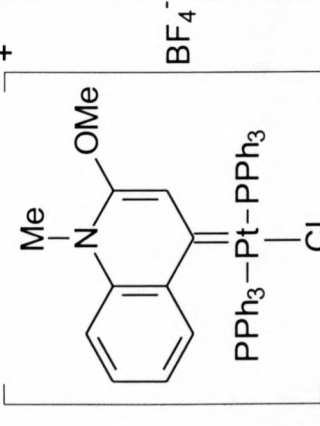
The same cationic complexes, albeit with different counterions, **12a** and **12b**, were prepared by adding cation **9** oxidatively to *tetrakis*(triphenylphosphine)palladium(0) or platinum(0). Refluxing an equimolar benzene mixture of the cationic precursor, **9** and the chosen metal(0) starting compound, followed by filtration through Celite and *in vacuo* solvent removal, afforded the products as colourless, crystalline compounds (Scheme 4.3).

All the complexes described here represent the first examples of group 10 carbene complexes prepared from precursor compounds in which the nucleophilic heteroatom is a γ -oxygen.

Layering a dichloromethane solution of complex **12a** with hexane and cooling to $-20^\circ C$ yielded single crystals that were suitable for X-ray crystallographic studies.

Complexes **11a**, **11b**, **12a** and **12b** decompose in air but are stable for extended periods of time under an inert atmosphere. The physical and analytical data for the complexes are presented in Table 4.5.

Table 4.5 Analytical and physical data for complexes **11a**, **11b**, **12a** and **12b**

Complex	 11a	 11b	 12a	 12b
Colour	Colourless	Colourless	Colourless	Colourless
Yield (%)	43	40	95	90
M.p./ °C	189	225	171	221
M.W.	988.74	1077.4	926.47	1015.13
Analysis (%) ^a				
C	58.22 (58.31)	53.42 (53.51)	60.62 (60.93)	55.13 (55.61)
H	4.00 (4.18)	3.80 (3.84)	4.40 (4.46)	4.00 (4.07)
N	1.41 (1.42)	1.26 (1.30)	1.48 (1.51)	1.36 (1.38)

^a Required values given in parentheses

B Spectroscopic characterisation of complexes **11a**, **11b**, **12a** and **12b**.

1. NMR spectroscopy

The ^1H NMR data for complexes are summarised in Table 4.6 and the $^{13}\text{C}\{-^1\text{H}\}$ NMR data in Table 4.7.

The positive charge on complexes **11a** and **11b** deshields the protons that resonate at higher field strength than the corresponding signals of the neutral precursors, **10a** and **10b**.

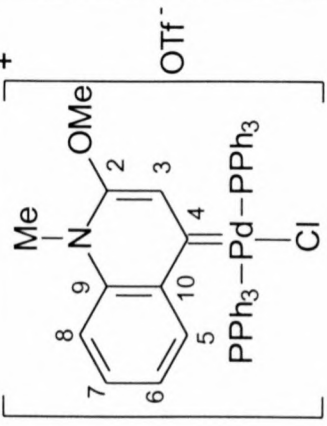
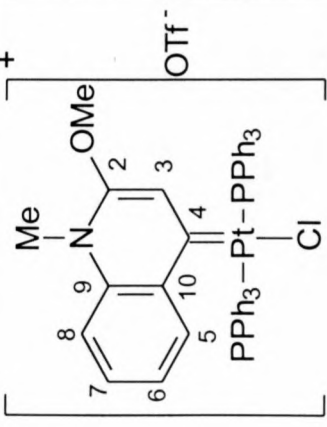
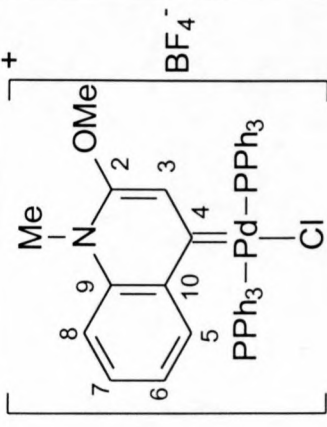
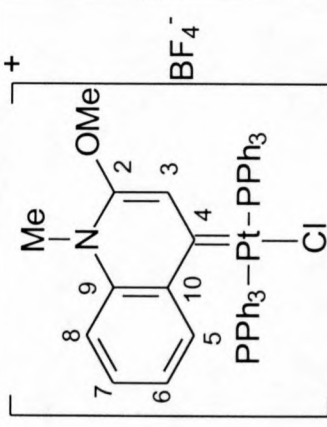
The ^1H NMR spectra of complexes **12a** and **12b** are similar to those of their triflate analogues and exhibit very small upfield shifts of the resonances relative to those of compound **9**. The H^3 proton exhibits the largest change, $\Delta\delta$ ca. 1.5.

The OMe resonances of complexes **11a** and **11b** respectively appear at δ 4.11 and 3.94, indicating methylation of the carbonyl group of the precursor. The analogous signals of complexes **12a** and **12b** resonate at comparable chemical shifts, δ 3.86 and 4.24.

The PPh_3 protons of complexes **11a**, **11b**, **12a** and **12b** resonate as broad multiplets between ca. δ 7.1 and 7.9, due to $^3\text{J}(\text{H-P})$ coupling. The H^8 signals of complexes **11a** and **12b**, as well as the H^6 signals of complexes **11b** and **12a**, fall under these multiplets.

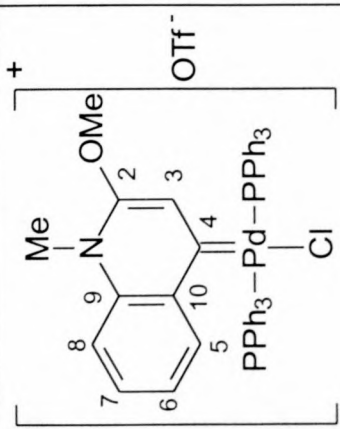
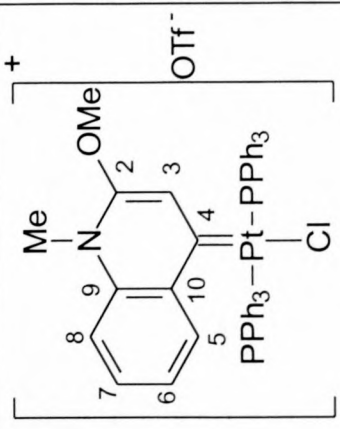
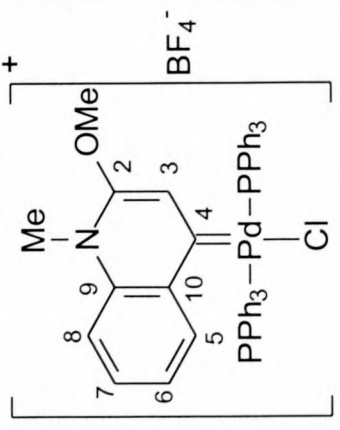
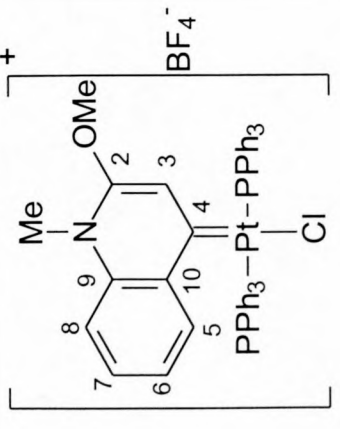
Complexes **11a**, **11b**, **12a** and **12b** have their respective carbene signals at δ 208.1, 202.4, 207.8 and 201.8, which is similar to previously reported chemical shifts of *trans* palladium and platinum diaminocarbene complexes.^[25] The carbene carbon of [*trans*-Pd(PBu₃)Cl₂{CN(Me)CH₂CH₂N(Me)}], for example, resonates at δ 200.5 and that of the platinum analogue at δ 196.5.

Table 4.6 ^1H NMR data of complexes **11a**, **11b**, **12a** and **12b**^a

Complex				
Solvent	CD_2Cl_2	CD_2Cl_2	CD_2Cl_2	CD_2Cl_2
NMe	3.69 (3H, s)	3.71 (3H, s)	3.68 (3H, s)	3.78 (3H, s)
OMe	4.11 (3H, s)	3.94 (3H, s)	3.86 (3H, s)	4.24 (3H, s)
H^3	6.87 (1H, s)	6.82 (1H, s)	6.79 (1H, s)	6.83 (1H, s)
H^5	8.92 (1H, dd, J = 7.8, 1.3)	9.00 (1H, dd, J = 7.8, 1.2)	8.87 (1H, dd, J = 7.7, 1.3)	9.21 (1H, dd, J = 7.9, 1.4)
H^6	7.84 (1H, ddd, J = 7.7, 7.0, 1.1)	Not observed	Not observed	7.78 (1H, ddd, J = 7.7, 7.0, 1.0)
H^7	7.88 (1H, ddd, J = 8.5, 7.5, 1.7)	7.96 (1H, ddd, J = 8.5, 7.5, 1.7)	7.80 (1H, ddd, J = 8.5, 7.3, 1.6)	7.93 (1H, ddd, J = 8.5, 7.5, 1.7)
H^8	Not observed	7.63 (1H, m)	7.54 (1H, m)	Not observed
PPh_3	7.19 – 7.92 (30H, 3 x m)	7.11 – 7.87 (30H, 3 x m)	7.19 – 7.94 (30H, 3 x m)	7.12 – 7.89 (30H, 3 x m)

^a J in Hz

Table 4.7 $^{13}\text{C}\{-^1\text{H}\}$ NMR data of complexes **11a**, **11b**, **12a** and **12b**^a

Complex	11a 	11b 	12a 	12b 
NMe	33.2	32.9	32.7	32.5
OMe	61.1	59.2	59.6	59.7
C ²	155.3	157.1	154.6	157.2
C ³	115.2	114.5	114.9	115.0
C ⁴	208.1	202.4 (d, J _{PtC} = 75)	207.8	201.8 (d, J _{PtC} = 73)
C ⁵	130.4	129.3	129.7	129.5
C ⁶ ; C ⁷	130.6; 135.0	130.5; 133.9	130.3; 134.9	130.4; 134.5
C ⁸	116.7	117.3	117.0	116.9
C ⁹ ; C ¹⁰	135.8; 127.2	136.7; 126.7	135.7; 127.0	136.6; 126.6
C _{ortho}	135.1	135.9; 133.0	135.0	136.1; 132.3
C _{para}	(J = 6.3); 132.5	(J = 6.1; 0.9)	(J = 6.1); 131.7	(J = 6.4; 1.1)
C _{meta} ; C _{ipso}	129.1; 130.1 (J = 5.0; 25.0)	128.6; 130.3 (J = 5.1; 26.2)	129.0; 129.8 (J = 4.9; 24.5)	128.8; 129.9 (J = 5.1; 26.2)
P(Ph ₃) ₂	27.8	26.4 (dd, J _{PtP} = 600)	27.9	26.6 (dd, J _{PtP} = 625)

^a J in Hz

The $^{13}\text{C}\{-^1\text{H}\}$ NMR spectra of complexes **11b** and **12b** exhibit the C^4 carbon as a doublet due to coupling with ^{195}Pt . The respective platinum-carbon coupling constants of 75 and 73 Hz are larger than the 35 Hz of complex **10b**.

Carbon-phosphorus coupling of the PPh_3 groups produces similar coupling patterns and constants to those observed for complexes **10a** and **10b** (paragraph 4.2.2).

The positive charges on complexes **11a** and **11b** causes the ^{31}P -atoms to resonate downfield ($\Delta\delta$ ca. 5) from those of complexes **10a** and **10b**. A doublet of doublets is observed in the ^{31}P NMR spectra of complexes **11b** and **12b** due to coupling between the phosphorous nuclei and ^{195}Pt .

2. Mass spectrometry

The FAB mass spectral data for complexes **11a**, **11b**, **12a** and **12b** are summarised in Table 4.8.

The molecular ions of complexes **11a**, **11b**, **12a** and **12b** are not observed in their individual mass spectra, but all the cationic fragments are visible as peaks of weak intensity.

Signals for the respective $\text{MCl}(\text{PPh}_3)_2$ fragment ions are observed for complexes **11a**, **11b**, **12a** and **12b** at m/z 666 (Pd) and m/z 755 (Pt).

The fragmentation patterns of the four complexes are remarkably similar and consist of sequential loss of chlorine and two PPh_3 groups to indicate formation of $[\text{M}\{\text{CCH}=\text{C}(\text{OMe})\text{N}(\text{Me})\text{C}_6\text{H}_4\}]^+$ and PPh_3^+ .

Fragments at m/z 554 and m/z 477 for complex **12b** indicate consecutive ejection of two phenyl groups from $[(\text{PPh}_3)\text{M}\{\text{CCH}=\text{C}(\text{OMe})\text{N}(\text{Me})\text{C}_6\text{H}_4\}]^+$.

Table 4.8 Mass spectral data for complexes **11a**, **11b**, **12a** and **12b**

Complex 11a		Complex 11b		Complex 12a		Complex 12b		Fragment ions
m/z	I ^a	m/z	I ^a	m/z	I ^a	m/z	I ^a	
783	5	871	9	840	11	928	3	$[(\text{PPH}_3)_2\text{M}(\text{Cl})\{\text{CCH}=\text{C}(\text{OMe})\text{N}(\text{Me})\text{C}_6\text{H}_4\}]^+$
747	27	836	35	804	29	893	40	$[(\text{PPH}_3)_2\text{M}\{\text{CCH}=\text{C}(\text{OMe})\text{N}(\text{Me})\text{C}_6\text{H}_4\}]^+$
666	41	755	55	666	64	755	46	$[(\text{PPH}_3)_2\text{M}(\text{Cl})]^+$
485	56	493	63	542	49	631	52	$[(\text{PPH}_3)\text{M}\{\text{CCH}=\text{C}(\text{OMe})\text{N}(\text{Me})\text{C}_6\text{H}_4\}]^+$
408	15	-	-	-	-	554	12	$[(\text{PPH}_2)\text{M}\{\text{CCH}=\text{C}(\text{OMe})\text{N}(\text{Me})\text{C}_6\text{H}_4\}]^+$
-	-	339	19	-	-	477	15	$[(\text{PPh})\text{M}\{\text{CCH}=\text{C}(\text{OMe})\text{N}(\text{Me})\text{C}_6\text{H}_4\}]^+$
262	18	262	28	262	31	262	23	$[\text{PPh}_3]^+$
223	39	231	22	280	25	368	28	$[\text{M}\{\text{CCH}=\text{C}(\text{OMe})\text{N}(\text{Me})\text{C}_6\text{H}_4\}]^+$
77	51	77	48	77	39	77	41	$[\text{Ph}]^+$

^a Relative intensities

C Crystal and molecular structure of complex **12a**.

The employed numbering scheme and molecular structure of complex **12a** in which the counterion and solvent molecules are omitted for clarity are shown in Figure 4.1. Unit cell packing is displayed in Figure 4.4 and includes the disordered anion and solvent molecules. Selected bond lengths and angles are presented in Table 4.9.

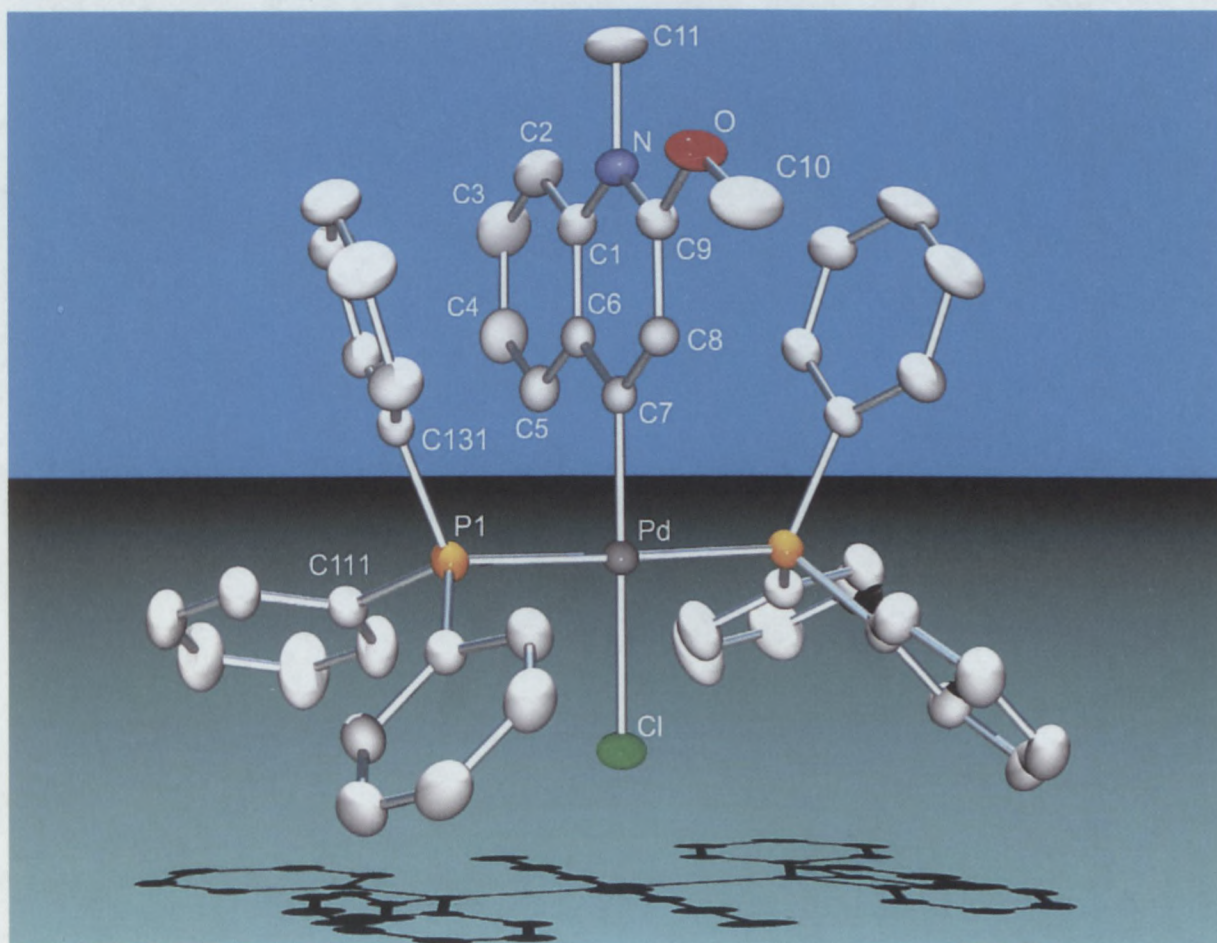


Figure 4.1 Molecular structure of complex **12a** (hydrogen atoms omitted for clarity).

Colourless crystals of complex **12a** crystallise in the orthorhombic space group $Pbcm$ and consist of a chloro-(2-methoxy-*N*-methylquinolin-4-yl)*bis*(triphenylphosphine)palladium(II) cation with tetrafluoroborate as counterion (Figure 4.1).

In the complex cation, the palladium centre is in a square planar environment with the two PPh_3 ligands occupying mutually *trans* positions. The Cl and C7 atoms are located 0.005 Å, 0.006 Å respectively below and the metal, 0.012 Å above the least squares plane through Pd, P1, P1a, Cl and C7. A dihedral angle of 89.29° positions the ligand and mean

coordination plane at right angles. This orthogonal arrangement is observed for most palladium(II) carbene complexes except where chelation constraints occur.^[2]

A search of the Cambridge Structural Database revealed that four cationic platinum(II) carbene complexes that contain a halide ligand and have their two phosphine ligands *trans*, have been structurally characterised, but that only one palladium(II) analogue is known.^[28] Of these structures, only compound **E** (as mentioned previously) lacks a nucleophilic heteroatom attached to the carbene carbon (Figure 4.2).

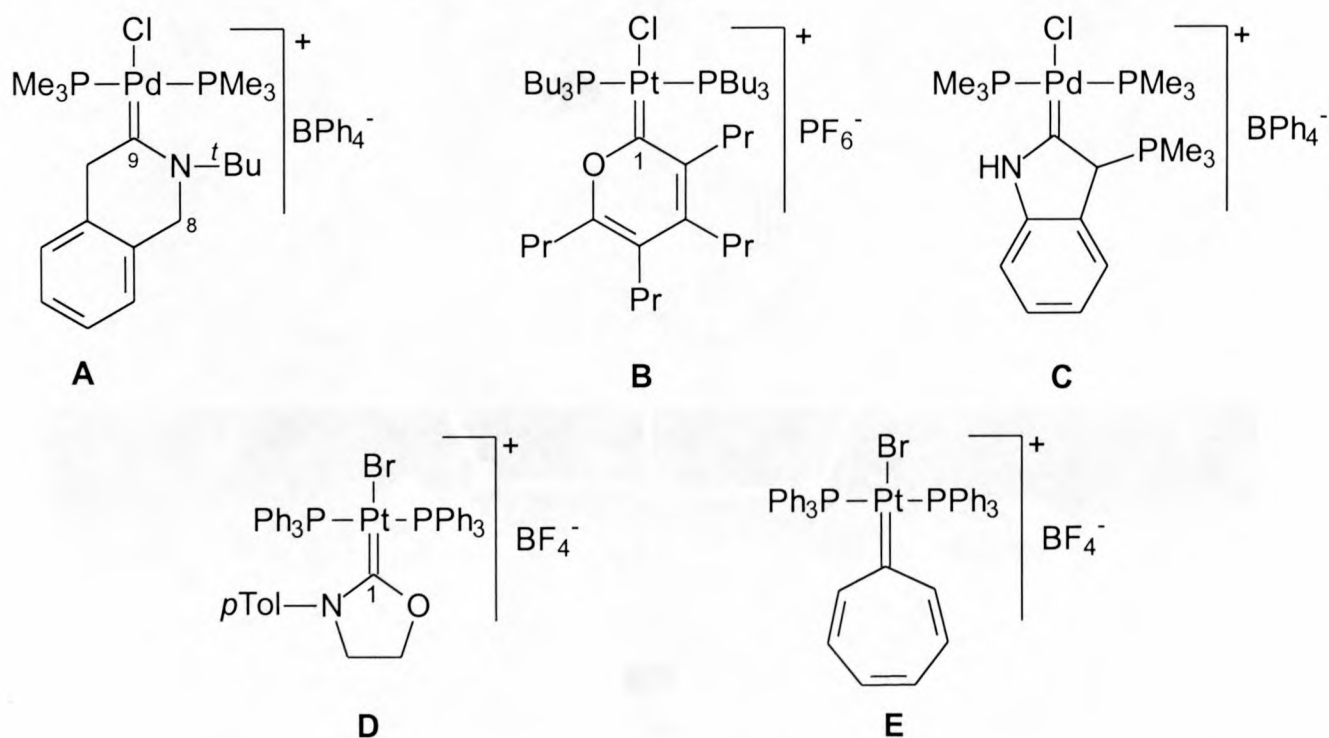


Figure 4.2 Cationic group 10 carbene complexes previously structurally characterised

Palladium-carbene bond lengths are generally shorter than other palladium-C(sp²) bonds^[29] due to synergic ligand σ -contributions and metal π -back bonding and the Pd-C_(carbene) bond length in complex **12a**, 1.987(3) Å, falls within the 1.91 – 2.10 Å range observed for a variety of palladium(II) carbene complexes.^[2]

In the present structure, the O-C9 bond length (1.320(4) Å) is shorter than the O-C_(carbene) distance (1.370(2) Å) of complex **B**^[30] but is comparable to the analogous bond length in complex **D** (1.330(1) Å) as well as the *ca.* 1.33 Å values found in the alkoxy(carbene) complexes, *cis*-[Cl₂Pt{C(OEt)NHPPh}]⁺^[31] and *trans*-[Pt{(PMe₂Ph)₂{C(OMe)Me}Me}]⁺.^[32] Both the N-C bonds in complex **12a**, N-C9 (1.348(4) Å) and N-C1 (1.386(5) Å), are significantly longer than the N-C_(carbene) bond distances found in complexes **A** (1.308(33) Å)^[33] and **D**

(1.300(1) Å),^[34] as well values observed in the range 1.25 – 1.29 Å for other heterocyclic group 10 carbenes, in which the carbene carbon is stabilised only by an adjacent nitrogen atom.^[2] All the C-C bond lengths in complex 12a (see Table 4.9) exhibit bond distances that are typical for conjugated aromatic rings *viz.* 1.37 – 1.42 Å.^[35] From the above, it follows that all of the resonance forms, **F**, **G** and **H**, in Figure 4.3 are important and can be summarised as structure **I**. As far as we know, complex **12a** represents the first example where both a distant nitrogen and oxygen atom contribute to the stabilisation of a heterocyclic carbene complex.

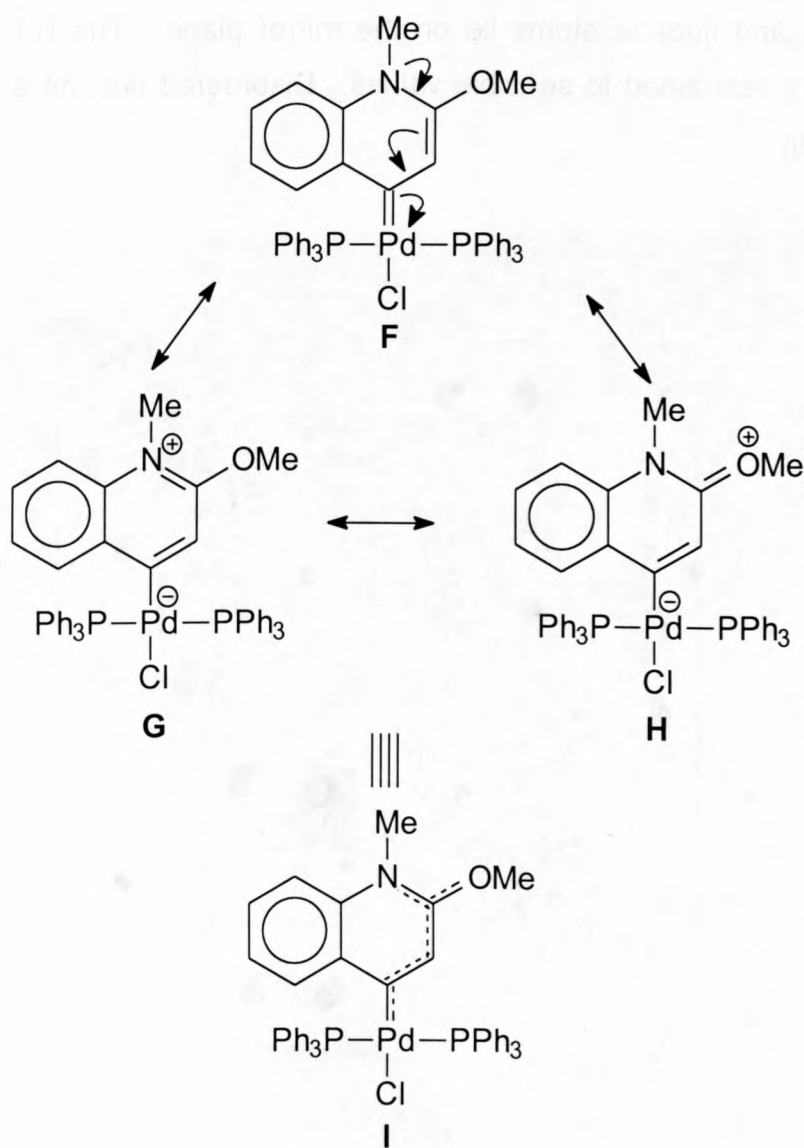


Figure 4.3 Resonance forms of complex **12a**

Because of a crystallographic mirror plane through each cation/anion pair in the plane of the aromatic ligand, eight symmetry-equivalent asymmetric units make up the four complex **12a** molecules in the unit cell, and a solvent molecule accompanies each complex molecule. Packing in the unit cell shows that the dichloromethane molecules occupy the large spaces

caused by the size discrepancy between the bulky cation and small anion (Figure 4.4). In the solvent molecule, the chlorine atoms exhibit disorder over two positions with the site occupancy restrained to 1.

Although the boron atom (blue) and one fluorine atom (pink) of the BF_4^- anion do not exhibit positional disorder, the remaining three fluorines are distributed across several positions in a circular, planar path across the molecular mirror plane. The sum of the site occupancy of the disordered fluorine atoms in the asymmetric unit was restrained to 1.5, as the non-disordered boron and fluorine atoms lie on the mirror plane. The B-F bond lengths and F-B-F angles were restrained to sensible values. Disordered fluorine atoms could only be refined isotropically.

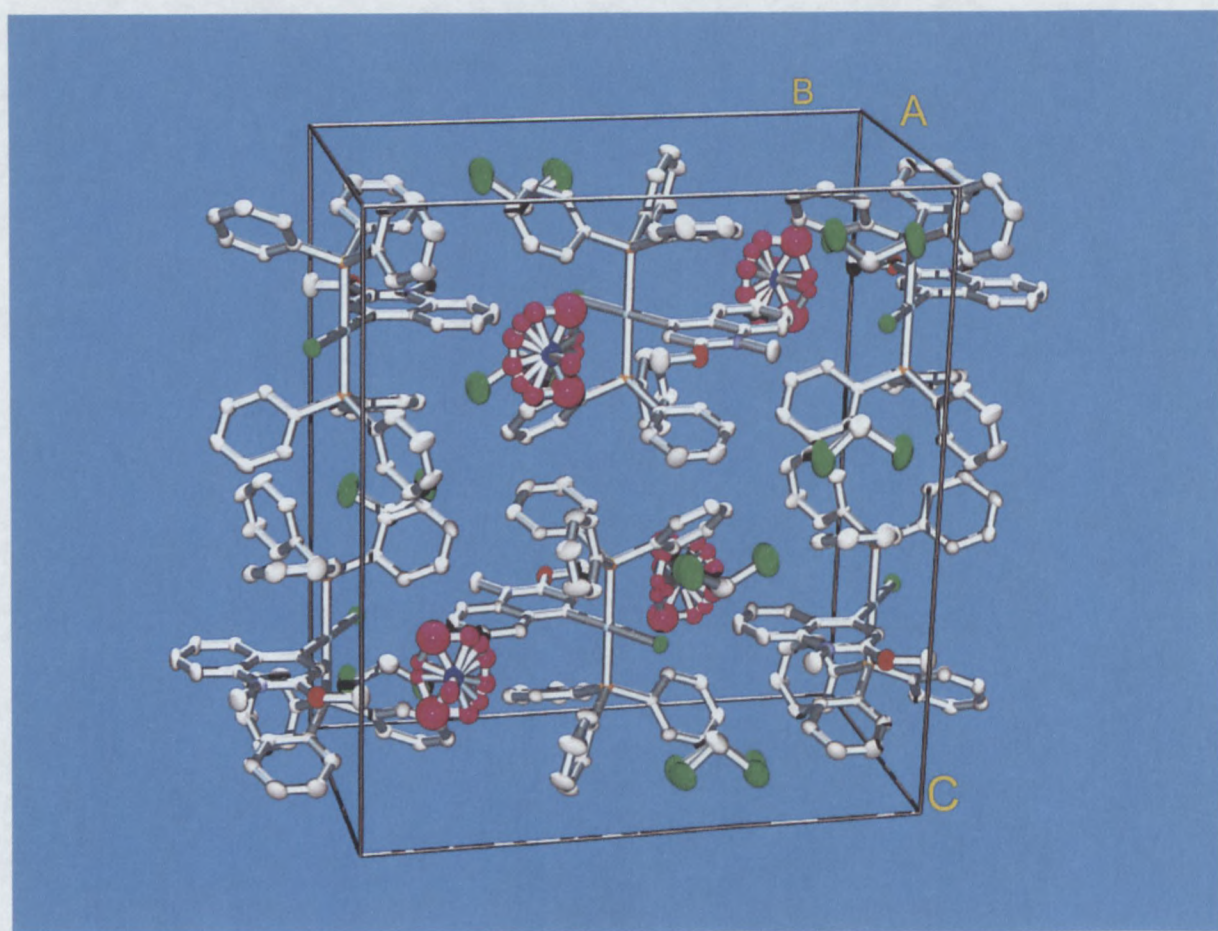
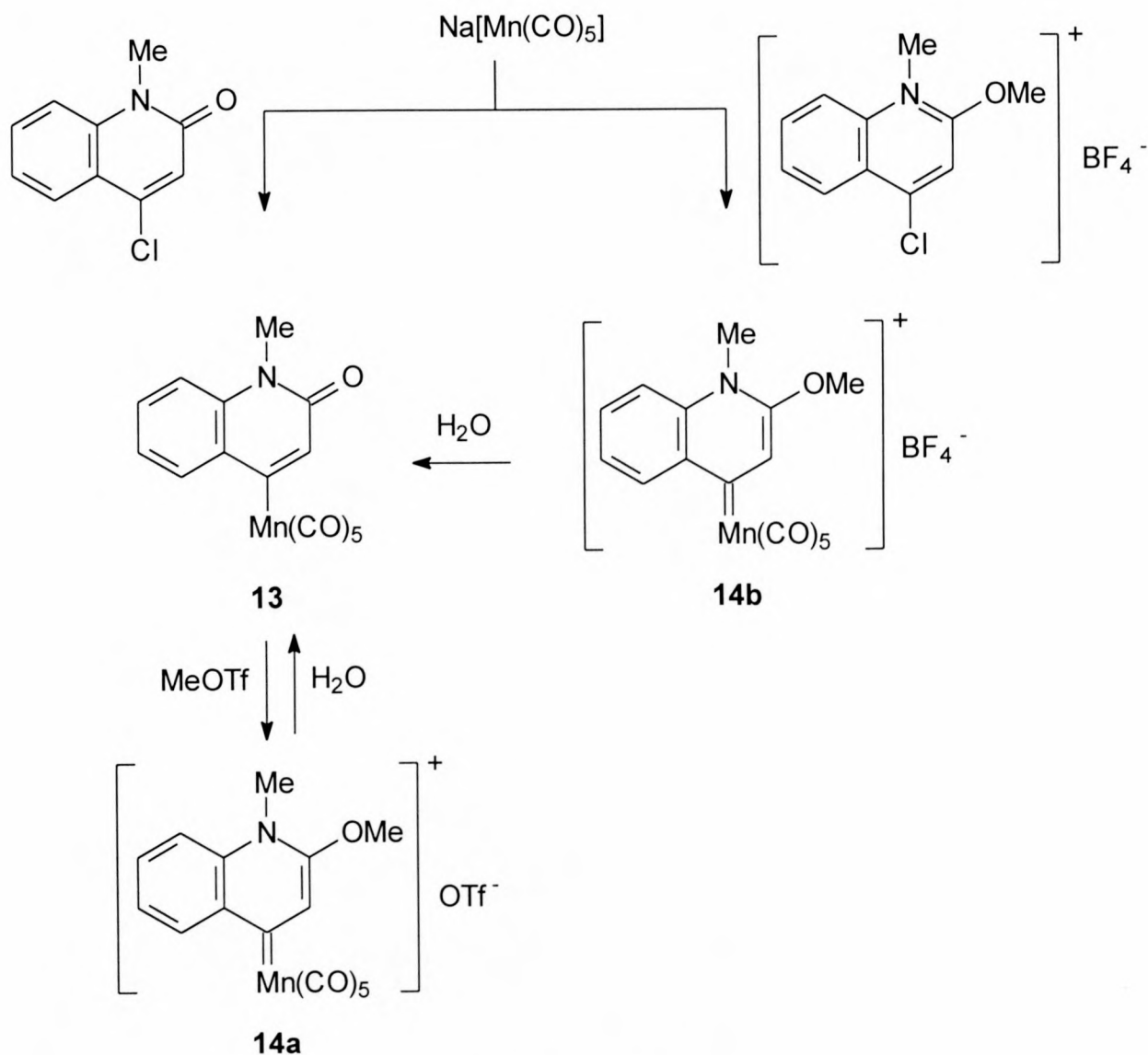


Figure 4.4 Unit cell packing of complex **12a** showing disordered BF_4^- anions (boron, fluorine and chlorine atoms are respectively depicted as blue, pink and green ellipsoids at 50% probability level).

4.2.4 Quinolin-2-on-4-yl and Quinolin-4-ylidene Manganese Complexes

- A Preparation of $[(\text{CO})_5\text{Mn}\{\text{C}=\text{CHC}(\text{O})\text{N}(\text{Me})\text{C}_6\text{H}_4\}]$, **13**,
 $[(\text{CO})_5\text{Mn}\{\text{CCH}=\text{C}(\text{OMe})\text{N}(\text{Me})\text{C}_6\text{H}_4\}][\text{OTf}]$, **14a** and
 $[(\text{CO})_5\text{Mn}\{\text{CCH}=\text{C}(\text{OMe})\text{N}(\text{Me})\text{C}_6\text{H}_4\}][\text{BF}_4]$, **14b**.

The same “one-pot” procedure originally used by Stone to prepare manganese (amino)thiocarbene complexes (compare Equation 4.7)^[18,19] was employed to prepare the new complexes **13** and **14b** (Scheme 4.4). Alkylation of complex **13** affords the complex cation of **14b**, but now with a different counterion (**14a**).



Scheme 4.4

Addition of Na[Mn(CO)₅] to a thf solution of compound **8**, followed by filtration of the reaction mixture and *in vacuo* solvent evaporation, afforded complex **13** as a pale yellow powder. In the same way, addition of compound **9** to a thf solution of Na[Mn(CO)₅] furnished complex **14b** as a colourless, crystalline product (Scheme 4.4).

Carbene complex **14a** was obtained by halide abstraction of compound **8** with Na[Mn(CO)₅] in thf, followed by O-alkylation with MeOTf at -20°C. The reaction residue was extracted with CH₂Cl₂ and subsequently filtered through Celite to remove deposited NaCl. *In vacuo* solvent evaporation afforded the cationic product as a colourless crystalline compound (Scheme 4.4).

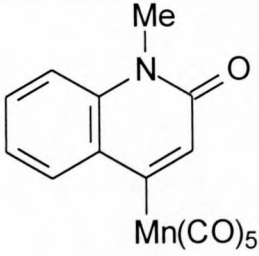
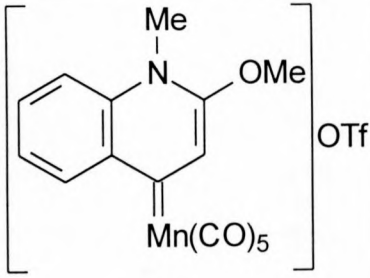
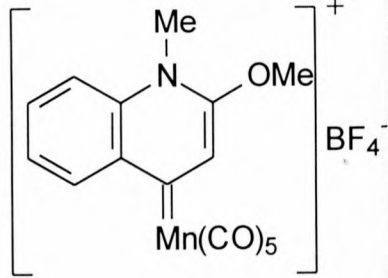
It is interesting that complexes **14a** and **14b** hydrolyse in the presence of moisture to form their neutral precursor, complex **13**.

Similarly to complexes **11a**, **11b**, **12a** and **14b** discussed before, complexes **14a** and **14b** represent the first examples of a class of manganese di(organo)carbene complexes formed and stabilised by alkylation of a γ -oxygen atom.

Complexes **13**, **14a** and **14b** are readily soluble in polar organic solvents but display limited solubility in non-polar solvents such as hexane and toluene. The complexes can be stored for indefinite periods under a dry, inert atmosphere.

The physical and analytical data for complexes **13**, **14a** and **14b** are reported in Table 4.10.

Table 4.10 Analytical and physical data for complexes **13**, **14a** and **14b**

Complex			
	13	14a	14b
Colour	Pale yellow	White	White
Yield (%)	65	59	55
M.p./ °C	226	278	291
M.W.	353.16	517.27	455.00
Analysis (%) ^a			
C	49.92 (51.02)	39.02 (39.47)	42.12 (42.23)
H	2.24 (2.28)	2.10 (2.14)	2.40 (2.44)
N	3.95 (3.97)	2.65 (2.70)	3.00 (3.08)

^a Required values given in parentheses

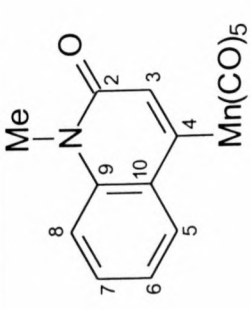
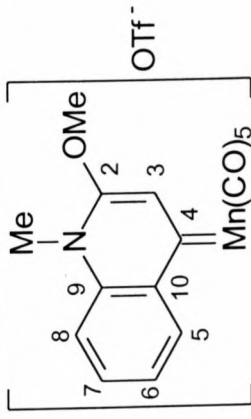
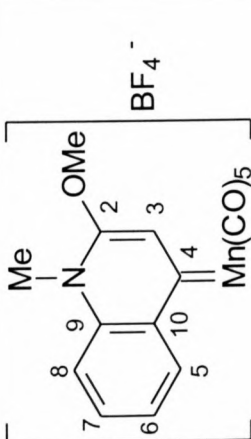
B Spectroscopic characterisation of complexes **13**, **14a** and **14b**.

1. NMR spectroscopy

The ¹H NMR data for complexes **13**, **14a** and **14b** are summarised in Table 4.11 and the ¹³C-¹H NMR data in Table 4.12. ¹³C-¹H NMR assignments of the resonances were based on HETCOR experiments.

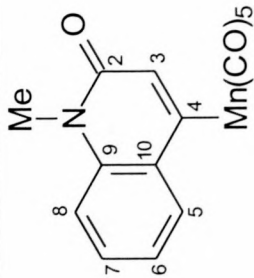
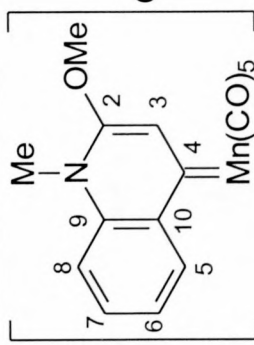
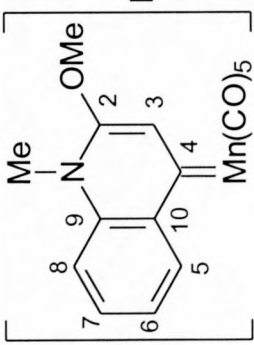
The ¹H NMR data of complex **13** and compounds **8** are very similar, indicating that the electron distribution within the compound is essentially identical.

Table 4.11 ^1H NMR data of complexes **13**, **14a** and **14b**

Complex			
Solvent	CDCl_3	d-acetone	d-acetone
^1H NMR ^a			
NMe	3.74 (3H, s)	4.31 (3H, s)	4.27 (3H, s)
OMe	-	4.63 (3H, s)	4.58 (3H, s)
H ³	7.26 (1H, br s)	8.38 (1H, s)	8.35 (1H, s)
H ⁵	7.82	8.72	8.68
H ⁶	(1H, dm, J = 8.4)	(1H, ddm, J ₅₇ = 1.2)	(1H, ddm, J ₅₇ = 1.2)
H ⁷	7.32 (1H, m)	8.01	7.92
H ⁸	7.58	(1H, ddd, J _{56, 67, 68} = 8.1, 7.2, 0.9)	(1H, ddd, J _{56, 67, 68} = 8.1, 7.2, 0.9)
	(1H, ddd, J _{78, 67, 57} = 8.7, 7.2, 1.2)	8.15	8.10
	7.43 (1H, m)	(1H, ddd, J _{78, 67, 57} = 8.7, 7.2, 1.2)	(1H, ddd, J _{78, 67, 57} = 8.7, 7.2, 1.2)
		8.38 (1H, dm)	8.32 (1H, dm)

^a J in Hz

Table 4.12 $^{13}\text{C}\{-^1\text{H}\}$ NMR data of complexes **13**, **14a** and **14b**

Complex			
Solvent	CDCl_3	d-acetone	d-acetone
^{13}C NMR	29.5	34.6	33.9
NMe	-	61.1	60.4
OMe	-	153.6	153.7
C^2	158.2	125.8	125.6
C^3	141.1	226.2	226.5
C^4	167.6 (br)	137.6	136.7
C^5	134.3	128.1	127.4
C^6	121.5	135.1	134.7
C^7	129.9	120.2	119.5
C^8	115.3	136.5	135.8
C^9	130.8	137.3	136.1
C^{10}	139.4	203.3 (cis), 212.6 (trans)	202.1 (cis), 211.3 (trans)
CO	209.6(cis), 210.9 (trans)		

In the $^{13}\text{C}\{-^1\text{H}\}$ NMR spectrum of complex **13**, only the C^3 , C^4 and C^{10} chemical shifts exhibit significant downfield changes, $\Delta\delta$ ca. 20, with respect to the corresponding signals of compound **8**. This again suggests that electron distribution of the former and latter compounds are similar, except at C^3 , C^4 and C^{10} where the local charge density is probably reduced by the π -acid containing a $\text{Mn}(\text{CO})_5$ unit. The coordinated carbon of thiazolyl(pentacarbonyl)manganese complexes generally resonates at δ ca. 270^[20] and the C^4 signal of complex **13** at δ 167.6 seems rather low. Nevertheless, IR and MS data confirmed the structural assignment of the compound.

^1H NMR spectra of complex **13** dissolved in CDCl_3 gave better resolution than those recorded in deuterated acetone, which are not reported here.

Methylation of the carbonyl group in complex **13** is indicated by a methoxy resonance at δ 4.63 in the spectrum of complex **14a**. The corresponding chemical shift of complex **14b** is found at δ 4.58.

The C^4 resonances in complexes **14a** and **14b** appear at δ 226.2 and 226.5 and is shifted significantly downfield from the corresponding signals of the precursors, complex **13** and compound **9**. The large changes in chemical shifts ($\Delta\delta$ 72.2 for the tetrafluoroborate complex and $\Delta\delta$ 58.6 for the triflate complex) are certainly indicative of carbene formation, although carbene carbons of manganese complexes were previously found as high as δ 330 - 360.^[36,37,38]

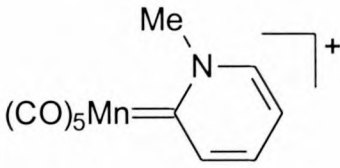
2. Infrared spectroscopy

Infrared data for complexes **13**, **14a**, **14b**, $(\text{CO})_5\text{MnC}_6\text{H}_5$,^[36] and (N-methylpyridin-2-yl)pentacarbonylmanganese^[23] appear in Table 4.13.

The $\nu(\text{CO})$ stretching bands of complexes **14a** and **14b** occur at slightly higher wavenumbers than in complex **13**. In terms of $\sigma_{\text{donor}}/\pi_{\text{acceptor}}$ ratios, this suggests that the CO-bond orders are slightly lower in the neutral complex than in the cationic derivatives. Shifts to higher frequencies have formerly been observed upon transformation of neutral thiazolyls into carbene complexes.^[20]

The carbonyl ligand stretching frequencies in complexes **14a** and **14b** appear at very similar energies to those of a previously reported cationic manganese *N*-methylpyridin-2-yl carbene complex,^[23] indicating that the respective carbene ligands experience the same electron withdrawing effect from the different metal carbonyl units. The same is true for $\nu(\text{CO})$ in complex **13** and the known compared $(\text{CO})_5\text{MnC}_6\text{H}_5$.^[36]

Table 4.13 IR data for complexes **13**, **14a** and **14b**^a. $(\text{CO})_5\text{MnC}_6\text{H}_5$ and $[(\text{CO})_5\text{Mn}\{\overline{\text{C}_4\text{H}_4\text{N}(\text{Me})\}]^+$ are included for comparison.

Complex	$\nu(\text{CO}) / \text{cm}^{-1}$		
	$A_1^{(1)}$	E	$A_1^{(2)}$
13	2120(m)	2024(vs)	2007(s,sh)
$(\text{CO})_5\text{MnC}_6\text{H}_5$	2114(m)	2013(vs)	1997(w)
14a	2129(m)	2036(vs)	2078(w)
14b	2130(m)	2036(vs)	2079(w)
 $(\text{CO})_5\text{Mn}=\text{C}_6\text{H}_4\text{N}(\text{Me})^+$	2138(m)	2032(vs)	2078(w)

^a Recorded in CH_2Cl_2

3. Mass spectrometry

The EI mass spectral data of complexes **13**, **14a** and **14b** are summarised in Table 4.14.

The mass spectrum of complex **13** displays a peak for the molecular ion at m/z 353. The fragmentation pattern consists of the loss of three carbonyl groups, followed by the remaining two CO's and Mn to give a signal for the ionised ligand at m/z 157. A peak for Ph^+ is observed at m/z 77.

Mass spectral data of complexes **14a** and **14b** have no peaks for the respective molecular ions, although a weak signal for the cationic metal-carbene complex is present. The fragmentation patterns of the complexes are quite similar and show initial loss of two carbonyl ligands from the cationic component. Thereafter, complex **14b** exhibits further loss of one CO, followed by the remaining two, to give a signal for

$[\text{Mn}\{\overline{\text{CCH}=\text{C}(\text{OMe})\text{N}(\text{Me})\text{C}_6\text{H}_4}\}]^+$ at m/z 228. The same peak is observed in the mass spectrum of complex **14a**, but results from direct ejection of three carbonyl groups. Both complexes exhibit signals for the cationic ligand fragment at m/z 177 after loss of the manganese nucleus. Finally, Ph^+ is responsible for the base peak at m/z 77.

Table 4.14 Mass spectral data for complexes **13**, **14a** and **14b**

Complex 13				Fragment ions
m/z	I^a			
353	< 10			$[(\text{CO})_5\text{Mn}\{\overline{\text{C}=\text{CHC}(\text{O})\text{N}(\text{Me})\text{C}_6\text{H}_4}\}]^+$
269	21			$[(\text{CO})_2\text{Mn}\{\overline{\text{C}=\text{CHC}(\text{O})\text{N}(\text{Me})\text{C}_6\text{H}_4}\}]^+$
213	23			$[\text{Mn}\{\overline{\text{C}=\text{CHC}(\text{O})\text{N}(\text{Me})\text{C}_6\text{H}_4}\}]^+$
159	42			$[\overline{\text{C}=\text{CHC}(\text{O})\text{N}(\text{Me})\text{C}_6\text{H}_4}]^+$
77	100			$[\text{Ph}]^+$
Complex 14a		Complex 14b		Fragment ions
m/z	I^a	m/z	I^a	
368	< 10	368	< 10	$[(\text{CO})_5\text{Mn}\{\overline{\text{CCH}=\text{C}(\text{OMe})\text{N}(\text{Me})\text{C}_6\text{H}_4}\}]^+$
312	25	312	31	$[(\text{CO})_3\text{Mn}\{\overline{\text{CCH}=\text{C}(\text{OMe})\text{N}(\text{Me})\text{C}_6\text{H}_4}\}]^+$
-	-	284	22	$[(\text{CO})_2\text{Mn}\{\overline{\text{CCH}=\text{C}(\text{OMe})\text{N}(\text{Me})\text{C}_6\text{H}_4}\}]^+$
228	23	228	19	$[\text{Mn}\{\overline{\text{CCH}=\text{C}(\text{OMe})\text{N}(\text{Me})\text{C}_6\text{H}_4}\}]^+$
173	59	173	52	$[\overline{\text{CCH}=\text{C}(\text{OMe})\text{N}(\text{Me})\text{C}_6\text{H}_4}]^+$
77	100	77	100	$[\text{Ph}]^+$

^a Intensity relative to the base peak

4.3 SUMMARY

The question of whether carbene complex formation would still occur with a distant oxygen atom serving as nucleophilic target for carbene stabilisation was addressed and answered in this study by the preparation of palladium(II), platinum(II) and manganese(I) carbene complexes from quinoline-based precursor compounds.

Two carbene complexes of palladium and platinum(II) were prepared by oxidative addition of neutral quinolinone and cationic quinolium precursor compounds to suitable metal(0) starting materials and alkylation of the former product. A crystal and molecular structure determination of the palladium(II) quinolin-2-on-4-yl complex indicated that extensive delocalisation occurs within the conjugated ligand framework and, therefore, that no dominant resonance structure is present. This new compound represents the first example of a carbene complex in which both the nitrogen and oxygen atoms play a role in carbene formation and stabilisation.

Similar to group 10 carbene complexes, the majority of manganese carbene complexes have a nitrogen atom attached to the coordinated carbon. By utilising halide displacement with $\text{Na}[\text{Mn}(\text{CO})_5]$ as synthetic procedure, new carbene and carbene-precursor complexes of manganese were prepared from neutral quinolinone and cationic quinolium halides. Alkylation of the former readily leads to carbene formation.

4.4 EXPERIMENTAL

4.4.1 Materials

2,4-Dichloroquinoline, 2-hydroxy-4-chloroquinoline, 4-chloro-N-methylquinolinone, **8**,^[22] [4-chloro-2-methoxy-N-methylquinolinium]BF₄, **9**,^[23] Pd(PPh₃)₄ and Pt(PPh₃)₄^[39] were prepared according to literature procedures. Decacarbonyldimanganese was purchased from Aldrich.

Tetrahydrofuran, hexane, benzene and diethyl ether were distilled under nitrogen from sodium diphenylketyl and dichloromethane from CaH₂.

4.4.2 Physical Methods

The same experimental conditions apply as in Section 2.4.2 and Section 3.4.2. Infrared spectra in CH₂Cl₂ were recorded on a Perkin Elmer 1600 Series FTIR apparatus.

4.4.3 Preparations

4.4.3.1 Preparation of [(PPh₃)₂Pd(Cl)]{C=CHC(=O)N(Me)C₆H₄}, **10a** and [(PPh₃)₂Pt(Cl)]{C=CHC(=O)N(Me)C₆H₄}, **10b**.

A mixture of Pd(PPh₃)₄ (1.15 g, 1 mmol) or Pt(PPh₃)₄ (1.24 g, 1 mmol) and halide **8** (194 mg, 1 mmol) were suspended in benzene (25 cm³) and refluxed at 60°C for 3h. During this time, formation of a white precipitate was observed. After cooling to room temperature, the reaction mixture was filtered through Celite to remove PPh₃, followed by *in vacuo* solvent removal.

4.4.3.2 Preparation of [(PPh₃)₂Pd(Cl)]{CCH=C(OMe)N(Me)C₆H₄}[OTf], **11a** and [(PPh₃)₂Pt(Cl)]{CCH=C(OMe)N(Me)C₆H₄}[OTf], **11b**.

Complex **10a** (412 mg, 0.5 mmol) or complex **10b** (457 mg, 0.5 mmol) was dissolved in thf (15 cm³) and cooled to -60°C. CF₃SO₃CH₃ (99 mg, 0.6 mmol) in thf (10 cm³) was added

drop-wise over 10 minutes and stirring continued for 1 h. The reaction mixture was warmed to room temperature and stirring continued at -60°C for 1 h. The thf was evaporated under vacuum and the residue repeatedly washed with diethyl ether ($6 \times 3 \text{ cm}^3$) to remove any unreacted $\text{CF}_3\text{SO}_3\text{CH}_3$. The white products were dried overnight under high vacuum at room temperature (1 mmHg).

4.4.3.3 Preparation of $\left[(\text{PPh}_3)_2\text{Pd}(\text{Cl})\left\{ \overline{\text{CCH}=\text{C}(\text{OMe})\text{N}(\text{Me})\text{C}_6\text{H}_4} \right\} \right] [\text{BF}_4]$, **12a** and $\left[(\text{PPh}_3)_2\text{Pt}(\text{Cl})\left\{ \overline{\text{CCH}=\text{C}(\text{OMe})\text{N}(\text{Me})\text{C}_6\text{H}_4} \right\} \right] [\text{BF}_4]$, **12b**.

The reaction and work-up was performed as in paragraph 4.4.3.1, with the same amounts of $\text{Pd}(\text{PPh}_3)_4$ and $\text{Pt}(\text{PPh}_3)_4$, but with halide **9** (295.5 mg, 1 mmol) as the organic substrate.

4.4.3.4 Preparation of $\left[(\text{CO})_5\text{Mn}\left\{ \overline{\text{C}=\text{CHC}(\text{O})\text{N}(\text{Me})\text{C}_6\text{H}_4} \right\} \right]$, **13**

$\text{Na}[\text{Mn}(\text{CO})_5]$ was prepared by reaction of $\text{Mn}_2(\text{CO})_{10}$ and Na as follows: Sodium metal (55 mg, 2.4 mmol) was added in small pieces, in 5 min intervals, to Hg (1 cm^3). The amalgam was allowed to cool to room temperature and $\text{Mn}_2(\text{CO})_{10}$ (371 mg, 0.95 mmol), dissolved in thf (15 cm^3) added drop-wise to the Na/Hg amalgam and the mixture stirred for 2.5 h.

The $\text{Na}[\text{Mn}(\text{CO})_5]$ suspension was allowed to settle for 15 min and filtered through Celite directly into a Schlenk flask containing halide **8** (271 mg, 1.14 mmol) in solid form. The addition procedure resulted in a red suspension. After stirring overnight, the suspension was filtered (por. 4) and the solid on the filter dried *in vacuo*. The crude product on the filter was then extracted with CH_2Cl_2 ($3 \times 5 \text{ cm}^3$). Recrystallisation from CH_2Cl_2 (ca. 5 cm^3) and cooling to -20°C gave the pure product.

4.4.3.5 Preparation of $\left[(\text{CO})_5\text{Mn}\left\{ \overline{\text{CCH}=\text{C}(\text{OMe})\text{N}(\text{Me})\text{C}_6\text{H}_4} \right\} \right] [\text{OTf}]$, **14a**

Complex **13** (353 mg, 1 mmol) was dissolved in thf (10 cm^3) and cooled to -20°C . $\text{CF}_3\text{SO}_3\text{CH}_3$ (172 mg, 1.05 mmol) in thf (5 cm^3) was added drop-wise over 15 min, the cooling bath removed and stirring continued for 3 h. The thf was evaporated and the resulting off-white residue repeatedly washed with diethyl ether ($5 \times 3 \text{ cm}^3$) to remove unreacted $\text{CF}_3\text{SO}_3\text{CH}_3$.

4.4.3.6 Preparation of $[(\text{CO})_5\text{Mn}\{\overline{\text{CCH}=\text{C}(\text{OMe})\text{N}(\text{Me})\text{C}_6\text{H}_4}\}][\text{BF}_4]$, **14b**

The preparation and work-up was performed as in paragraph 4.4.3.4, but with halide **9** (337 mg, 1.14 mmol) as organic substrate.

4.4.3.7 Crystallography for complex **12a**

M. W. Esterhuysen solved the crystal and molecular structure of complex **12a**. The crystal data as well as collection and refinement details for complex **12a** are given in Table 4.15. All other crystallographic information is available from M. W. Esterhuysen, Chemistry Department, Private Bag X1, Matieland, 7602, RSA.

X-ray diffraction data were collected on an Enraf-Nonius Kappa CCD diffractometer at 150(2)K using graphite monochromated Mo- K_α radiation ($\lambda = 0.71073\text{\AA}$)^[40] and corrected for absorption effects using the Platon package.^[41] Structure solution and refinement was carried out using the program SHELX-97.^[42] ORTEP-3 for Windows was used to generate the figures at 50% probability level.^[43]

The structure was solved by interpretation of a Patterson synthesis that yielded the position of the palladium atom. The remaining non-hydrogen atoms were found by difference Fourier, refined by Full-matrix least squares against F^2 and, except for the disordered F-atoms in the disordered BF_4 anion, were allowed anisotropic thermal motion. Although it was possible to locate most of the H-atoms from the difference Fourier map, all H-atoms were placed in idealised positions with their isotropic displacement parameters fixed at 1.2 times (aromatic H-atoms), and 1.5 times (methyl H-atoms), the equivalent isotropic displacement parameters of their parent atoms.

Table 4.15 Crystal data, collection and refinement details for complex **12a**

Formula	C ₄₉ H ₄₁ BCl ₅ F ₅ NOPdP ₂
Formula weight	1111.23
Crystal system, space group	Orthorhombic, Pbcm
Radiation, T/ °C	Mo-K α (0.71073Å), -175(2)
a, b, c/ Å	10.973(1), 20.051(1), 22.590(1)
α , β , γ / °	90, 90, 90
Z	4
U/ Å ³	4971.0(6)
Crystal size	0.31 x 0.24 x 0.28 mm ³
Calculated density D _c /g cm ⁻³	1.485
Absorption coefficient (μ)	0.762 mm ⁻¹
Absorption correction method	Semi-empirical (Platon)
F(000)	2244
Diffractometer	Enraf Nonius KappaCCD
Scan type	ϕ and ω to fill an Ewald sphere
Scan range, θ /°	1.80 \leq θ \leq 30.53
<i>hkl</i> ranges	-15 \leq <i>h</i> \leq 15, -28 \leq <i>k</i> \leq 27, -32 \leq <i>l</i> \leq 32
Reflections collected/ unique	76307 / 7774 [R(int) = 0.043]
Data / restraints / parameters	7774 / 10 / 342
Refinement method	Full-matrix least-squares on F ²
Final R indices [I > 2 σ (I)]	R ₁ = 0.0455, wR ₂ = 0.1250
R indices (all data)	R ₁ = 0.0695, wR ₂ = 0.1447
Weighting scheme	Calculated w = 1/[σ^2 (F _o ²) + [(0.0802P) ² + 4.7802P] where P = (F _o ² + 2F _c ²)/3
Goodness of fit on F ²	1.055
Largest peak, deepest hole	1.42 e ⁻ / Å ³ (0.62Å from F3a), -0.89 e ⁻ / Å ³ (1.60Å from H122)
Maximum shift/esd	0.001

REFERENCES

- [1] K. H. Dötz, H. Fischer, P. Hoffman, F. R. Freissl, U. Schubert and K. Weiss, in *Transition Metal Carbene Complexes*, Verlag Chemie, Weinheim, (ed. P. J. Biehl) 1983; S. A. Cotton, *Chemistry of Precious Metals*, Blackie Academic and Professional, London, 1997, and references therein.
- [2] K. R. Dixon and A. C. Dixon, in *Comprehensive Organometallic Chemistry II*, Vol. 9, (eds., E. W. Abel, F. G. A. Stone and G. Wilkinson) Elsevier, Oxford, 1995.
- [3] W. A. Herrmann, M. Elison, J. Fischer, C. Köcher and G. R. J. Artus, *Angew. Chem., Int. Ed. Engl.*, 1994, **34**, 2371.
- [4] L. Xu, W. Chen and J. Xiao, *Organometallics*, 2000, **19**, 1123.
- [5] P. M. Maitlis, P. Espinet and M. J. H. Russel, in *Comprehensive Organometallic Chemistry I*, (eds., E. W. Abel, F. G. A. Stone and G. Wilkinson) Elsevier, Oxford, 1978.
- [6] P. J. Fraser, W. R. Roper and F. G. A. Stone, *J. Chem. Soc., Dalton Trans.*, 1974, 102.
- [7] H. Fischer, in *The Chemistry of the Metal Carbon Bond*, (ed. S. Patai) Wiley Interscience, New York, 1982.
- [8] Z. Lu, W. M. Jones and J. D. Scott, *Organometallics*, 1993, **12**, 1344.
- [9] H. G. Raubenheimer and S. Cronje, *J. Organomet. Chem.*, 2001, **617 – 618**, 170.
- [10] H. G. Raubenheimer, M. Desmet and G. J. Kruger, *J. Chem. Soc., Dalton Trans.*, 1995, 2067.
- [11] M. Desmet, *Ph D Thesis*, Rand Afrikaans University, 1996, p. 6.
- [12] M. Desmet, H. G. Raubenheimer and G. J. Kruger, *Organometallics*, 1997, **16**, 3324.
- [13] H. G. Raubenheimer and M. Desmet, *J. Chem. Res. (S)*, 1995, 30.
- [14] J. G. Toerien, M. Desmet, G. J. Kruger and H. G. Raubenheimer, *J. Organomet. Chem.*, 1994, **479**, C12.
- [15] T. C. Flood, in *Comprehensive Organometallic Chemistry II*, (ed. C. P. Casey), Elsevier, Oxford, 1995.
- [16] R. D. Closson, J. Kozikowski and T. H. Coffield, *J. Org. Chem.*, 1957, **22**, 598.
- [17] P. L. Motz, D. J. Sheeran and M. Orchin, *J. Organomet. Chem.*, 1990, **383**, 202.
- [18] F. G. A. Stone, M. Green, J. R. Moss and I. W. Nowell, *J. Chem. Soc., Chem. Comm.*, 1972, 1339.
- [19] F. G. A. Stone, D. H. Bowen, M. Green, D. M. Grove and J. R. Moss, *J. Chem. Soc., Chem. Comm.*, 1974, 1189.

- [20] H. G. Raubenheimer, A. Neveling, S. Cronje and D. G. Billing, *Polyhedron*, 2001, **20**, 1089.
- [21] V. R. Shah, J. L. Bose and R. C. Shah, *J. Chem. Soc., Perkin Trans.*, 1993, **1**, 2747.
- [22] R. J. Rowlett and R. E. Lutz, *J. Am. Chem. Soc.*, 1946, **68**, 1288.
- [23] P. J. Fraser, W. R. Roper and F. G. A. Stone, *J. Chem. Soc., Dalton Trans.*, 1974, 760.
- [24] G. W. Parshall, *J. Am. Chem. Soc.*, 1966, **88**, 704; 1974, **96**, 2360.
- [25] B. E. Mann and B. F. Taylor, in *¹³C NMR Data for Organometallic Compounds* (eds. P. M. Maitlis, F. G. A. Stone and R. West), Academic Press, London, 1981.
- [26] W. E. van Zyl, *M. Sc. Dissertation*, Rand Afrikaans University, 1992.
- [27] J. A. Iggo, *NMR Spectroscopy in Inorganic Chemistry*, Oxford University Press, Oxford, 1999.
- [28] F. H. Allen and O. Kennard, *Chem. Des. Autom. News*, 1993, **8**, 31.
- [29] A. J. Canty in, *Comprehensive Organometallic Chemistry II*, (eds., E. W. Abel, F. G. A. Stone and G. Wilkinson) Elsevier, Oxford, 1995.
- [30] L. Garlaschelli, M. C. Malatesta, S. Panzeri, A. Albinati and F. Ganazzoli, *Organometallics*, 1987, **6**, 63.
- [31] E. M. Badley, K. W. Muir and G. A. Sim, *J. Chem. Soc., Dalton Trans.*, 1976, 1930.
- [32] R. F. Stepaniak and N. C. Payne, *J. Organomet. Chem.*, 1973, **57**, 213.
- [33] J. Cámpora, C. Graiff, P. Palma, E. Carmona and A. Tiripicchio, *Inorg. Chim. Acta*, 1998, **269**, 191.
- [34] R. A. Michelin, L. Zanatto, D. Braga, P. Sabatino and R. J. Angelici, *Inorg. Chem.*, 1988, **27**, 85.
- [35] F. H. Allen, O. Kennard, D. G. Watson, L. Brammer, A. G. Orpen and R. Taylor, *Perkin Trans. II*, 1987, S1 – S19.
- [36] F. R. Kriessl, P. Strückler and E. W. Meineke, *Chem. Ber.*, 1997, **110**, 3040.
- [37] E. O. Fischer and G. Besl, *J. Organomet. Chem.*, 1978, **157**, C33.
- [38] S. Fontana, U. Schubert and E. O. Fischer, *J. Organomet. Chem.*, 1978, **146**, 39.
- [39] A. J. Mukhedkar, M. Green and F. G. A. Stone, *J. Chem. Soc. (A)*, 1969, 3023.
- [40] A. L. Spek, *Acta Crystallogr. (A)*, 1990, **46**, C34.
- [41] Z. Otwinowski, W. Minor, *Methods Enzymol.*, 1997, **276** 307.
- [42] G.M. Sheldrick, SHELX-97 – *Program for Crystal Structure Analysis*, Institut für Anorganische Chemie der Universität Göttingen, Tammanstrasse 4, D-3400, Germany, 1998.

[43] L.J. Farrugia, *J. Appl. Cryst.*, 1997, **30**, 565.

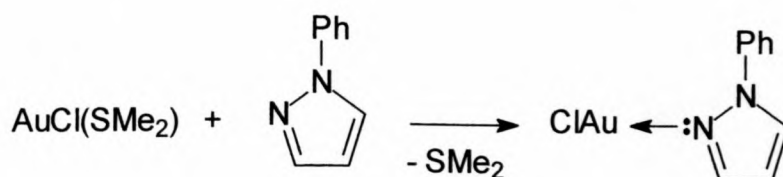
CHAPTER 5

PREPARATION AND CHARACTERISATION OF GOLD(I) AND GOLD(III) IMINE COORDINATION COMPLEXES

5.1 INTRODUCTION

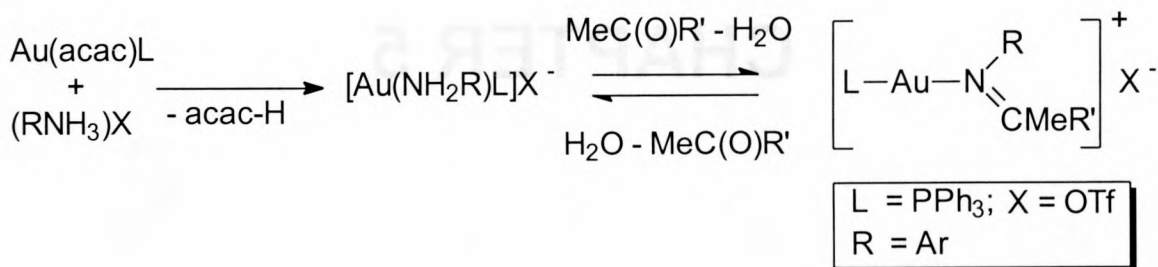
According to the soft and hard acid and base (SHAB) principle,^[1] gold is classified as a soft metal and although some disagreement exists in the literature regarding the relative softness of gold(I) and gold(III),^[2,3] the intrinsic softness of the metal is undisputed.

A large number of compounds with gold-nitrogen bonds is known despite this classification, which predicts only a moderate affinity for gold towards bond formation with nitrogen.^[4,5] In particular, a variety of gold-imine coordination compounds have been prepared from cyclic ketimines.^[6] The reaction of $\text{AuCl}(\text{SMe}_2)$ with pyrazole, for example, affords mononuclear N-coordinated complexes^[7] and Equation 5.1 runs contrary to the expected order in terms of SHAB rules, which is: R_2S : (soft) $>$ $>\text{C}=\text{S}$: $>$ $>\text{C}=\text{N}$: (borderline) $>$ R_2NH (hard).^[1]



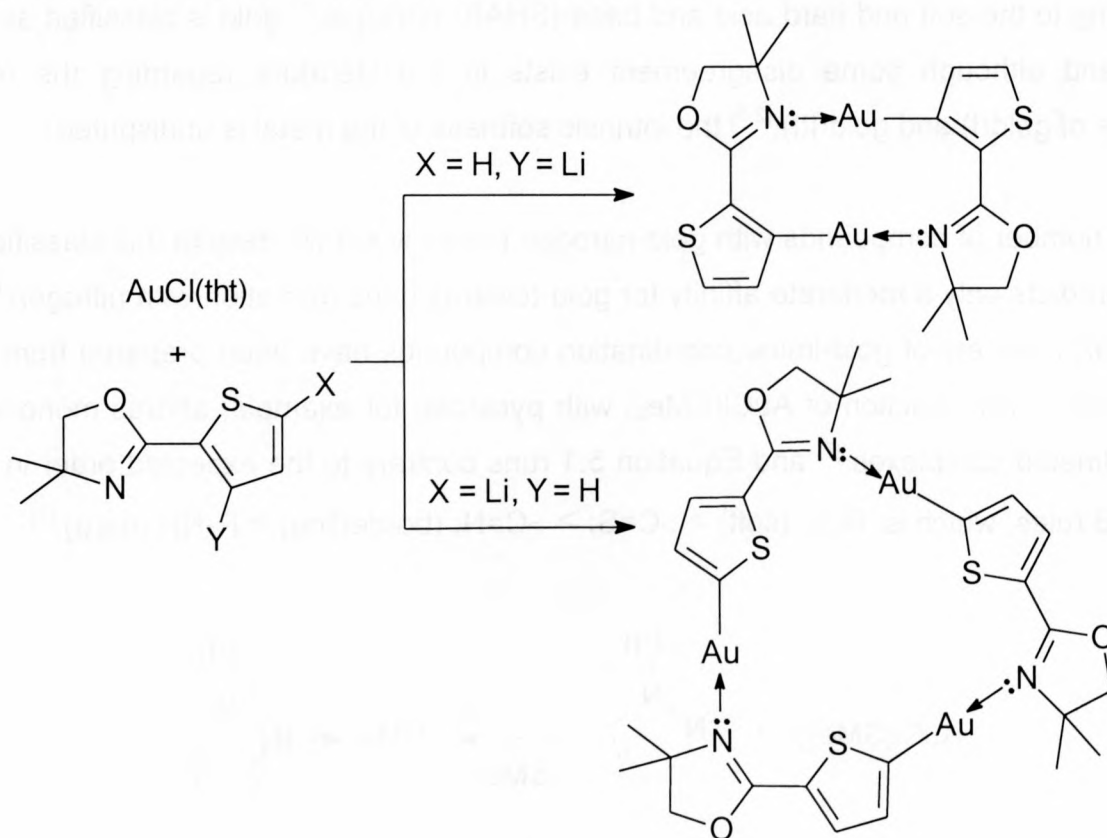
Equation 5.1

An interesting recent addition comes from the laboratory of Vicente,^[8] who describes the synthesis and structure of gold(I) complexes with acyclic imino ligands, prepared by the reaction of $[\text{Au}(\text{acac})\text{L}]$ with ammonium salts via amine(phosphine)gold compounds in ketone solution (Equation 5.2).



Equation 5.2

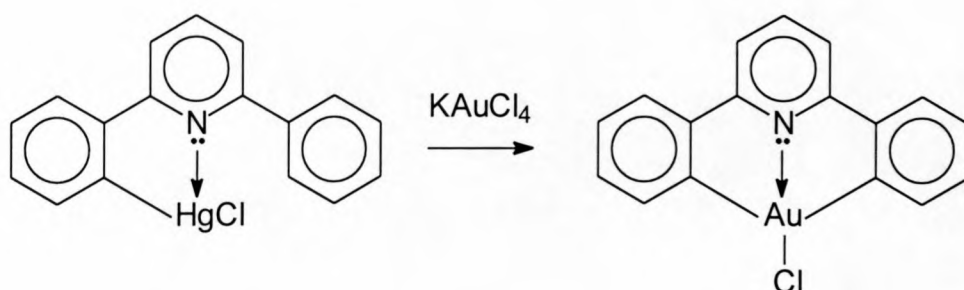
Fascinating heterometallacyclic gold(I) compounds were recently isolated in our laboratory by self-assembly of gold-containing units.^[9] The preparation involves selective deprotonation of a bicyclic, imine-containing ligand followed by transmetalation with AuCl(tht) (Scheme 5.1). Depending on the relative positions of the carbon and nitrogen donor atoms, dimers or trimers of the thienylgold(I) units are formed.



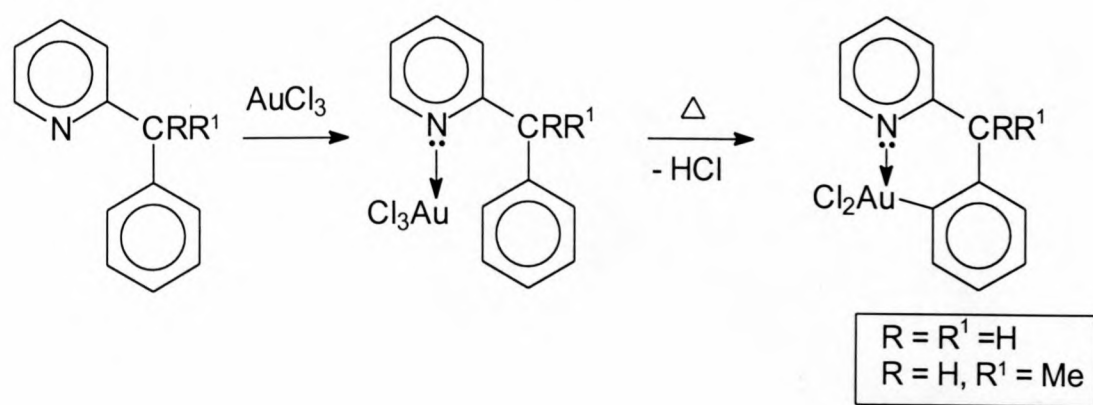
Scheme 5.1

In the present study, attempts to promote self-assembly with different heterocyclic gold(I) units were unsuccessful. However, a parallel series of reactions are described in which gold displays a larger affinity for imine donor groups than for thioethers.

Gold(III) coordination complexes with mono- and bidentate imine ligands have been well-studied^[10] and a large number of review articles are available.^[4,5,6,11] Current interest in gold(III) imine synthesis focuses on the preparation of cycloaurated complexes, which are less common than cyclometallates of isoelectronic metals such as platinum(II) and palladium(II).^[12,13] Cycloaurates are available via two synthetic pathways, one using transmetalation with organomercury(II) compounds (Equation 5.3)^[14,15] and the other employing direct C-H bond activation with AuCl₃ (Equation 5.4).^[16]



Equation 5.3

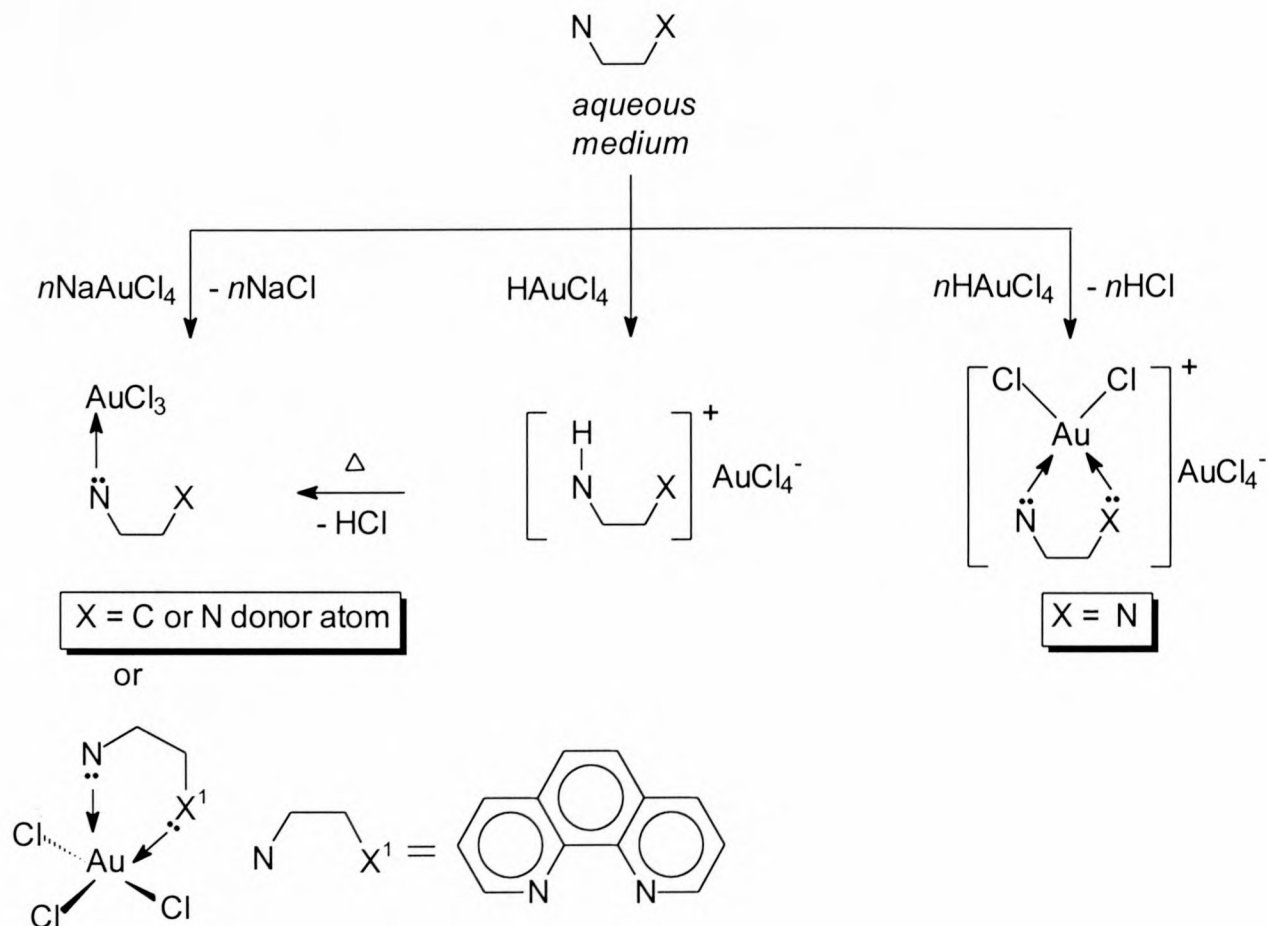


Equation 5.4

The precursors utilised in cycloauration reactions are generally prepared by equimolar reaction of a monodentate imine with NaAuCl₄^[17,18] in aqueous medium (Scheme 5.2). Analogous reactions with HAuCl₄ yield tetrachloroaurate(III) imine salts,^[19] which are converted into the corresponding AuCl₃ adducts upon heating.

Neutral AuCl₃ adducts exhibit the typical square planar coordination of gold(III) with monodentate and rigid bidentate ligands, but with non-rigid bidentate ligands such as phenanthroline, interesting five-coordinate complexes with distorted square pyramidal arrangements have been obtained.^[6]

In this chapter, the preparation of neutral AuCl_3 adducts by reaction of NaAuCl_4 with a series of imines in aqueous medium, is described. The molecular structure of one compound was determined and showed that although a soft sulphur atom is available, square planar coordination of gold(III) occurs at nitrogen.



Scheme 5.2

Although tetrachloroaurate(III) immonium salts have previously been prepared by the reaction of $\text{H[AuCl}_4]$ with monodentate imines in water, analogous preparation with chelating imines furnishes cationic complexes, independent of the employed reagent ratio (Scheme 5.2).^[19] Note that these cationic gold compounds are not obtained in similar procedures utilising NaAuCl_4 , even when an excess of the metal salt is employed.

The reason for this difference is not clear, since in the former and latter reactions, chelate effects are anticipated to favour the formation of similar cationic products, regardless of the metal starting compounds and whether the hydrogens of $\text{H[AuCl}_4]$ are involved or not.

Another unusual observation is that although mono- and bidentate imines should both be readily protonated by HAuCl_4 , only monodentate immonium salts with tetrachloroaurate(III) as anion have been isolated.^[18] This despite the fact that HCl is liberated in the preparation of disubstituted cationic compounds and being capable of producing the conjugate acid of the bidentate imine.

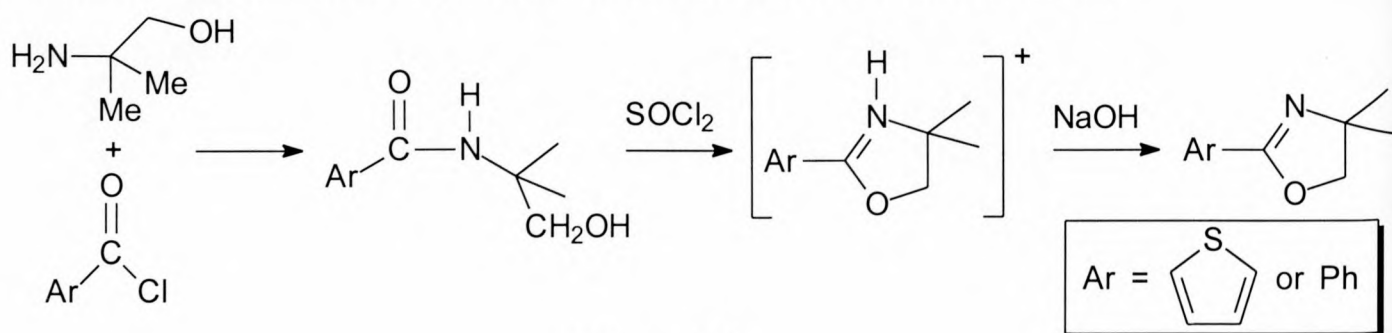
In this chapter, the preparation of a series of cationic coordination compounds, by reaction of mono- or bidentate bicyclic imine ligands with HAuCl_4 in water, is described. All of these carry AuCl_4^- as anion. Two of these compounds were characterised by single crystal X-ray diffraction methods, and respectively exhibited mono- and bidentate coordination of the imine ligands. The *cis*-imine configuration in the former structure, represents only the second example of such an arrangement for gold(III) and the first that contains N-donor atoms. This product also suggests that cationic coordination compounds can be prepared from acidic tetrachloroauric acid and monodentate imines.

5.2 RESULTS AND DISCUSSION

5.2.1 Bicyclic Ligand Precursor Preparations

A1 Preparation of $[N=C(Ph)OCH_2CMe_2]$ and $[N=C(CSCH=CHCH)OCH_2CMe_2]$

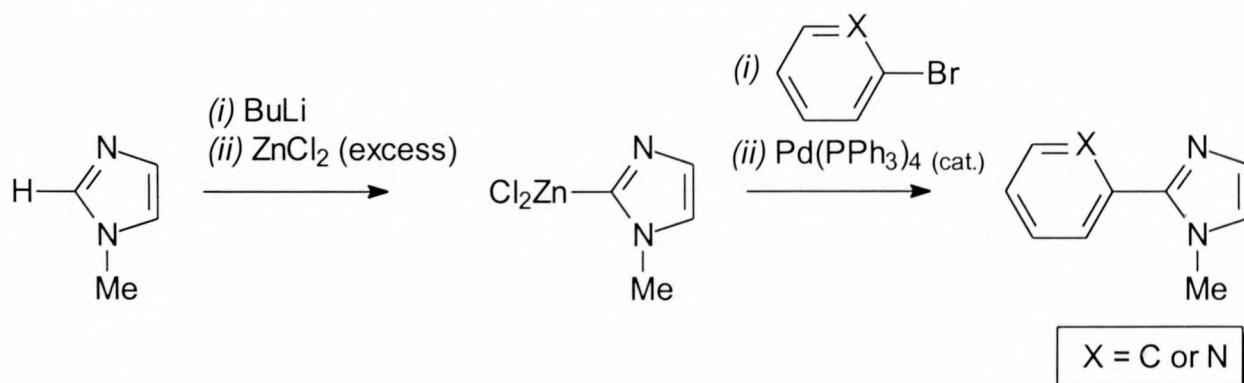
Meyer's general approach to oxazoline formation was followed for the synthesis of 4,4-dimethyl-2-(2'-thienyl)oxazole and 4,4-dimethyl-2-(phenyl)oxazole (Scheme 5.3).^[20] It involves the addition of 2-amino-2-methylpropan-1-ol to 2-thiophene- or benzenecarboxylchloride to form an amide. Successive treatment of the amide with thionyl chloride and a base effects ring closure and the formation of the oxazoline ring.



Scheme 5.3

A2 Preparation of $[N=C(Ph)NMeCH=CH]$ and $[N=C(py)NMeCH=CH]$.

The heterocycles, 1-methyl-2-(2'-pyridinyl)imidazole and 1-methyl-2-(phenyl)imidazole, were prepared utilising a literature, palladium-catalysed, cross-coupling procedure.^[21] Transmetalation of 1-methylimidazol-2-yl lithium with an excess of anhydrous zinc chloride and subsequent addition of bromobenzene or 2-bromopyridine and a catalytic amount of Pd(PPh₃)₄, afforded the bicyclic products as colourless crystalline compounds after purification by column chromatography (Scheme 5.4).



Scheme 5.4

B Spectroscopic characterisation of $[\overline{\text{N}=\text{C}(\text{Ph})\text{OCH}_2\text{CMe}_2}]$, $[\overline{\text{N}=\text{C}(\text{Ph})\text{NMeCH}=\text{CH}}]$, $[\overline{\text{N}=\text{C}(\text{CSCH}=\text{CHCH})\text{OCH}_2\text{CMe}_2}]$ and $[\overline{\text{N}=\text{C}(\text{py})\text{NMeCH}=\text{CH}}]$.

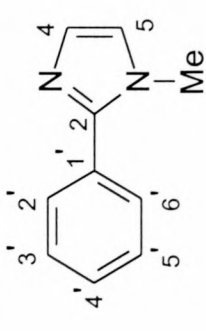
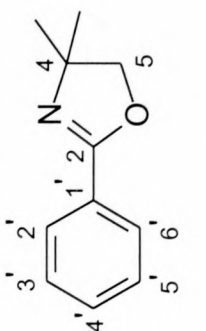
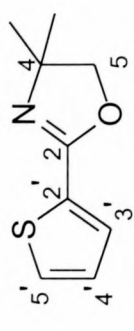
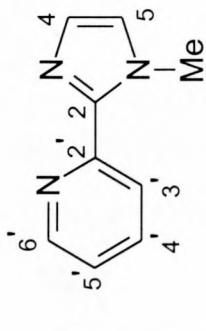
1. NMR spectroscopy

The ^1H NMR data of the ligands appear in Table 5.1, and the $^{13}\text{C}\{-^1\text{H}\}$ as well as the ^{15}N NMR data in Table 5.2. The ^1H and $^{13}\text{C}\{-^1\text{H}\}$ NMR data of 4,4-dimethyl-2-(2'-thienyl)oxazole,^[20] 4,4-dimethyl-2-(phenyl)oxazole^[22,23] and 1-methyl-2-(2'-pyridinyl)imidazole^[21] are in agreement with literature values. The $^{13}\text{C}\{-^1\text{H}\}$ NMR assignments were based on HETCOR experiments.

The ^1H NMR spectra of 1-methyl-2-(phenyl)imidazole and 4,4-dimethyl-2-(phenyl)oxazole show comparable chemical shifts and similar intricate coupling patterns for the phenyl protons. The $^{13}\text{C}\{-^1\text{H}\}$ NMR data of the former and latter compounds display comparable chemical shifts for the phenyl carbons. The NMe, H⁴ and H⁵ protons of 1-methyl-2-(2'-pyridinyl)imidazole respectively resonate at δ 4.16, 7.20 and 7.05. These chemical shifts are similar to those of 1-methyl-2-(phenyl)imidazole at δ 4.13, 7.17 and 7.02, respectively. The $^{13}\text{C}\{-^1\text{H}\}$ NMR data of the phenyl(imidazole) ligand show a C² resonance at δ 153.5 and the corresponding signal of the pyridine derivative appears at a comparable field strength of δ 152.8.

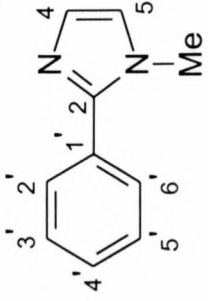
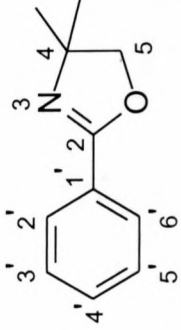
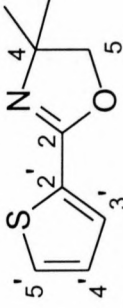
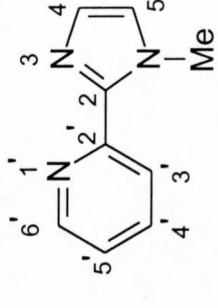
The extreme sensitivity and low natural abundance (0.3%)^[24] of the ^{15}N nucleus places limitations on experimental applications of ^{15}N NMR. The stability of a compound in solution is an important prerequisite to allow sufficient time for acquisition, but becomes less so if the compound displays good solubility. Although all the bicyclic compounds utilised in the present study are stable in solution, only solutions of 4,4-dimethyl-2-(phenyl)oxazole and 1-methyl-2-(2'-pyridinyl)imidazole were sufficiently concentrated for ^{15}N NMR studies, utilising nitromethane as external standard. The ^{15}N NMR data of 1-methylimidazole, not represented here, was recorded in CD_2Cl_2 and exhibited similar chemical shifts for its nitrogens as 1-methyl-2-(phenyl)imidazole. The N-Me and imine nitrogen of 1-methylimidazole respectively resonate at δ -219.5 and δ -116.2 and the comparable signals of 1-methyl-2-(phenyl)imidazole appear at δ -220.3 and -114.4. The pyridine-nitrogen atom is less shielded than the imine nitrogen of the imidazole ring, evidenced by its resonance at δ -74.9. The ^{15}N spectrum of 4,4-dimethyl-2-(phenyl)oxazole has a single resonance for its imine nitrogen at δ -133.6.

Table 5.1 ^1H NMR data of the bicyclic compounds in d-acetone

Compound				
^1H NMR ^a	4.13 (3H, s)	-	-	4.16 (3H, s)
NMe	-	1.33 (6H, s)	1.31 (6H, s)	-
CMe ₂	-	4.15 (2H, s)	4.13 (2H, s)	-
CH ₂	-	-	-	-
H ⁴	7.17 (1H, s)	-	-	7.20 (1H, s)
H ⁵	7.02 (1H, s)	-	-	7.05 (1H, s)
H ^{2'}	7.90 (1H, d, J = 9)	7.97 (1H, d, J = 9)	-	-
H ^{3'}	7.65 (1H, m)	7.51 (1H, m)	7.60 (1H, dd, J = 6, 3)	7.34 (1H, dd, J = 6, 6)
H ^{4'}	7.65 (1H, m)	7.51 (1H, m)	7.17 (1H, dd, J = 6, 6)	7.88 (1H, dd, J = 6, 6)
H ^{5'}	7.65 (1H, m)	7.51 (1H, m)	7.69 (1H, dd, J = 6, 3)	8.23 (1H, dd, J = 6, 3)
H ^{6'}	7.90 (1H, d, J = 9)	7.97 (1H, d, J = 9)	-	8.60 (1H, dd, J = 6, 3)

^a J in Hz

Table 5.2 ^{13}C - $\{^1\text{H}\}$ NMR data of the bicyclic compounds in d-acetone

Compound				
^{13}C NMR	34.9	-	-	36.7
NMe	-	28.2	27.2	-
CMe ₂	-	161.3	158.1	152.8
C ²	153.5	68.4	68.3	123.9
C ⁴	124.1	79.1	78.2	123.5
C ⁵	124.7	133.4	-	-
C ^{1'}	132.8	128.2	133.1	149.6
C ^{2'}	129.3	127.8	128.3	124.1
C ^{3'}	129.4	130.2	130.8	124.6
C ^{4'}	129.6	127.8	131.0	137.8
C ^{5'}	129.4	128.2	-	146.7
C ^{6'}	129.3	-133.6	-	-114.4
^{15}N NMR	-	-	-	-74.9
N ³	-	-	-	-220.3
N ^{1'}	-	-	-	-
NMe	-	-	-	-

5.2.2 Gold(I) Imine Complexes

A Preparation of $[\text{ClAu}\{\text{N}=\text{C}(\text{Ph})\text{NMeCH}=\text{CH}\}]$, **15**, $[\text{ClAu}\{\text{N}=\text{C}(\text{Ph})\text{OCH}_2\text{CMe}_2\}]$, **16**, $[\text{ClAu}\{\text{N}=\text{C}(\text{CSCH}=\text{CHCH})\text{OCH}_2\text{CMe}_2\}]$, **17**, $[\text{ClAu}\{\text{N}=\text{C}(\text{py})\text{NMeCH}=\text{CH}\}]$, **18** and $[\text{Cl}_2\text{Au}_2\{\text{N}=\text{C}(\text{py})\text{NMeCH}=\text{CH}\}]$, **18a**

Complexes **15**, **16**, **17** and **18** were prepared by the addition of a diethyl ether solution of the individual heterocyclic compounds to an equimolar suspension of $\text{AuCl}(\text{SMe}_2)$ or $\text{AuCl}(\text{tht})$ in the same solvent (Scheme 5.4). Filtration of the reaction mixture through anhydrous magnesium sulphate and solvent evaporation under vacuum afforded the neutral compounds as white powders. Unreacted heterocycles were removed by repeated washing of the reaction residue with hexane or pentane.

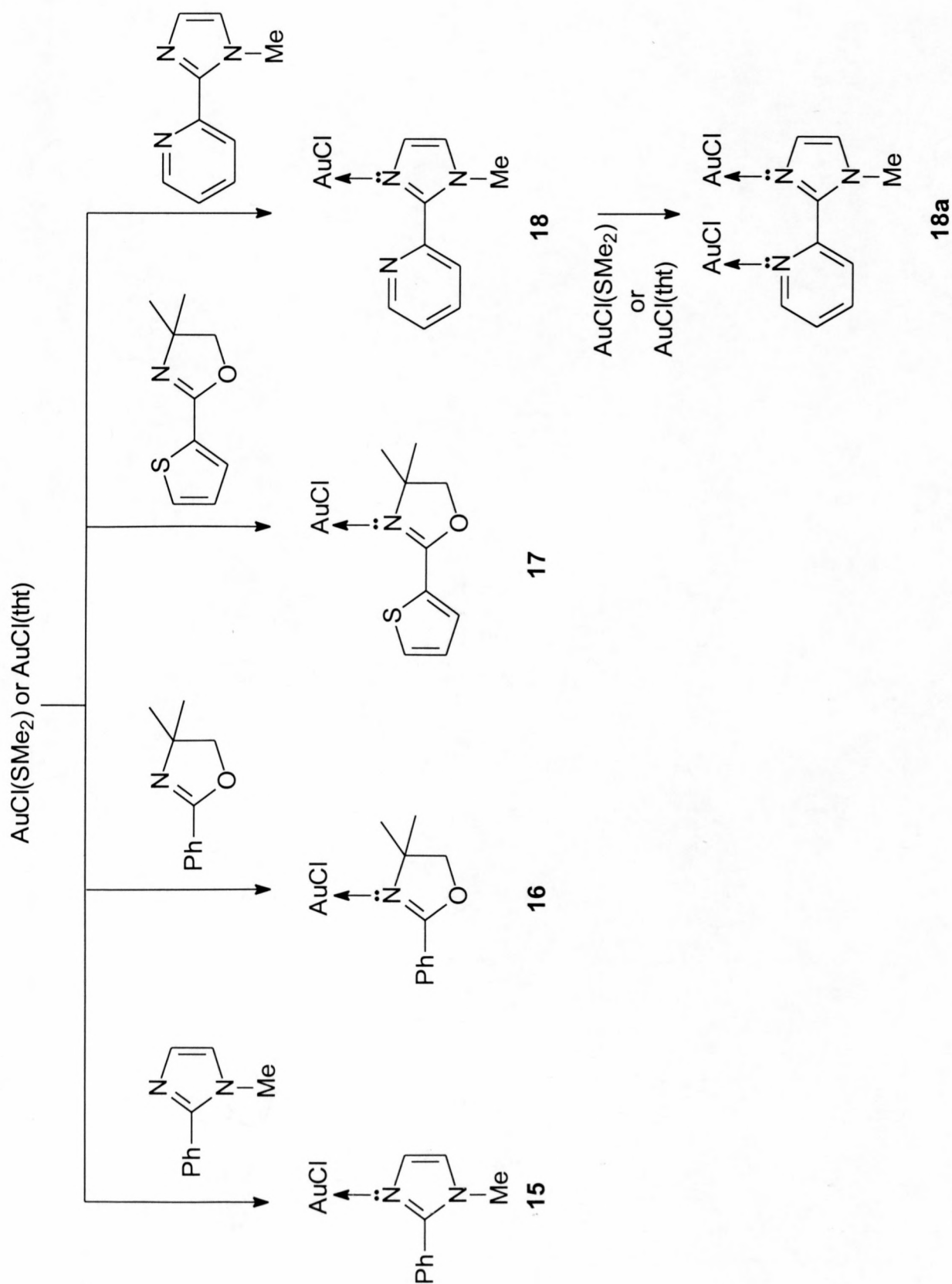
The best yields were obtained by performing the substitution at -20°C although the reaction also proceeds at room temperature.

Complex **18a** was prepared by equimolar addition of $\text{AuCl}(\text{SMe}_2)$ or $\text{AuCl}(\text{tht})$ to a diethyl ether suspension of complex **18** at -20°C (Scheme 5.4). The reaction mixture was then filtered through Celite and the solvent removed *in vacuo*.

Even after repeated crystallisation attempts, the disubstituted complex could not be isolated in pure form and always consisted of a mixture of **18** and complex **18a** in a ratio of ca. 1:2. Nevertheless, NMR and mass spectral data confirmed the presence of two Au-Cl moieties in complex **18a**.

Complexes **15**, **16**, **17**, **18** and **18a** decompose in air and are readily soluble in diethyl ether, dichloromethane and thf. The compounds can be stored for limited periods under an inert atmosphere at low temperature. Gradual decomposition and gold deposition, is evidenced by the appearance of a purple colour.

The analytical and physical data for complexes **15**, **16**, **17** and **18** are presented in Table 5.3.



Scheme 5.4

Table 5.3 Analytical and physical data for complexes **15**, **16**, **17** and **18**

Complex	15	16	17	18
Colour	White	White	White	White
Yield (%)	35	21	57	52
M.p./ °C	163	175	186	196
M.W.	390.63	407.65	413.68	391.61
Analysis (%) ^a				
C	30.68 (30.75)	31.86 (32.41)	25.91 (26.13)	27.42 (27.60)
H	2.61 (2.58)	3.20 (3.21)	2.72 (2.68)	2.16 (2.32)
N	7.24 (7.17)	3.51 (3.44)	3.29 (3.39)	10.55 (10.73)

^a Required values given in parentheses

B Spectroscopic characterisation of complexes **15**, **16**, **17**, **18** and **18a**

1. NMR spectroscopy

The ^1H NMR data of complexes **15**, **16**, **17**, **18** and **18a** are summarised in Table 5.4 and the $^{13}\text{C}\{-^1\text{H}\}$ NMR data in Table 5.5.

Electron density donation by the imine ligands to the metal nucleus in complexes **15**, **16**, **17** and **18** causes the ring protons to resonate downfield relative to the corresponding signals of the free ligands.

The largest chemical shift changes upon coordination are observed in the ^1H NMR spectrum of complex **17**, which exhibits a $\Delta\delta$ 0.49 downfield shift for the CH_2 signal. The $\text{H}^{5'}$ resonance, however, appears only $\Delta\delta$ 0.08 downfield from the corresponding signal of 4,4-dimethyl-2-(2'-thienyl)oxazole. Furthermore, the $^{13}\text{C}\{-^1\text{H}\}$ NMR spectrum of complex **17** exhibits a much larger $\Delta\delta$ 10.1 downfield shift for C^4 than the $\Delta\delta$ 0.7 change observed for $\text{C}^{5'}$. Together with the ^1H NMR data, this suggests that coordination occurs at nitrogen and not sulphur in complex **17**.

The $^{13}\text{C}\{-^1\text{H}\}$ NMR data of complexes **15**, **16**, **17** and **18** exhibit a general downfield shift of the ring carbon signals from the corresponding signals in the individual free ligands. This is in line with σ -donation to the coordinated gold atom by the imine nitrogens of the bicyclic compounds.

Strong deshielding of the $\text{H}^{6'}$ proton adjacent to the pyridine nitrogen, which is observed when chlorine^[25] or a halogold(III)^[16] group is in the proximity of the pyridine ring, is not observed and thus not consistent with coordination of gold at the pyridine nitrogen of complex **18**. The H^4 signal of complex **18** exhibits a larger downfield shift ($\Delta\delta$ 0.38) than $\text{H}^{6'}$ ($\Delta\delta$ 0.14) relative to the free ligand signals. Furthermore, the C^4 resonance appears $\Delta\delta$ 5.3 downfield whereas the $\text{C}^{6'}$ signal moves $\Delta\delta$ 3.2 upfield. These chemical shift changes imply that less electron density is present at position 4 than at position 6' in complex **18**, which in turn suggests that coordination occurs at the imine-nitrogen of the imidazole ring.

Table 5.4 ^1H NMR data of complexes **15**, **16**, **17**, **18** and **18a** in d-acetone

Complex	15	16	17	18	18a
^1H NMR ^a	4.20 (3H, s)	-	-	3.99 (3H, s)	3.80 (3H, s)
NMe	-	1.61 (6H, s)	1.65 (6H, s)	-	-
CMe ₂	-	4.67 (2H, s)	4.62 (2H, s)	-	-
CH ₂	-	-	-	7.58 (1H, s)	7.50 (1H, s)
H ⁴	7.22 (1H, s)	-	-	7.33 (1H, s)	7.21 (1H, s)
H ⁵	7.10 (1H, s)	-	-	-	-
H ^{2'}	8.01 (1H, d, J = 9)	8.52 (1H, d, J = 9)	-	-	-
H ^{3'}	7.78	7.65	7.85	7.60	7.67
	(1H, m)	(1H, dd, J = 6, 6)	(1H, dd, J = 6, 3)	(1H, dd, J = 6, 3)	(1H, dd, J = 6, 3)
H ^{4'}	7.78	7.80	7.34	8.06	8.03
	(1H, m)	(1H, td, J = 12, 6))	(1H, dd, J = 6, 6)	(1H, t, J = 6)	(1H, t, J = 6)
H ^{5'}	7.78 (1H, m)	7.65 (1H, d, J = 6, 6)	7.77 (1H, dd, J = 6, 3)	8.40 (1H, t, J = 6)	8.31 (1H, t, J = 6)
H ^{6'}	8.01	8.52	-	8.78	8.62
	(1H, d, J = 9)	(1H, d, J = 9)	-	(1H, dd, J = 6, 3)	(1H, dd, J = 6, 3)

^a J in Hz

Table 5.5 $^{13}\text{C}\{-^1\text{H}\}$ NMR data of complexes **15**, **16**, **17**, **18** and **18a** in d-acetone

Complex	15	16	17	18	18a
^{13}C NMR	35.1	-	-	36.0	35.5
NMe	-	28.6	27.7	-	-
CMe ₂	156.3	163.5	160.3	149.7	147.9
C ²	126.3	70.5	78.4	129.2	128.3
C ⁴	126.9	81.1	80.3	127.9	125.4
C ⁵	133.1	126.4	-	-	-
C ^{1'}	130.4	130.4	134.6	148.7	146.8
C ^{2'}	131.2	129.9	129.8	123.7	122.5
C ^{3'}	134.6	135.1	131.7	123.2	124.6
C ^{4'}	132.4	129.5	132.5	137.4	137.1
C ^{5'}	130.9	130.9	-	143.3	142.1
C ^{6'}					

The NMR data of complex **18a** show small upfield shifts for ^1H ($\Delta\delta$ 0.1 – 0.4) and ^{13}C ($\Delta\delta$ 1 – 3) relative to the corresponding signals of complex **18**. This is surprising, since an opposite chemical shift change is expected if both the nitrogen atoms provide electron density to the gold(I) atoms. Nevertheless, the small chemical shift changes imply that the mono- and disubstituted compounds have similar electron density distributions.

Unfortunately, the relatively low thermodynamic stability and low solubility of the gold(I) compounds precluded recording of their $^{15}\text{N}\{-^1\text{H}\}$ NMR spectra. Clear evidence for the coordination position of gold(I) in these complexes is, therefore, still needed.

2. *Mass spectrometry*

The fragmentation patterns of complexes **15** and **16** are presented in Table 5.6, while those of complexes **17** and **18** appear in Table 5.7.

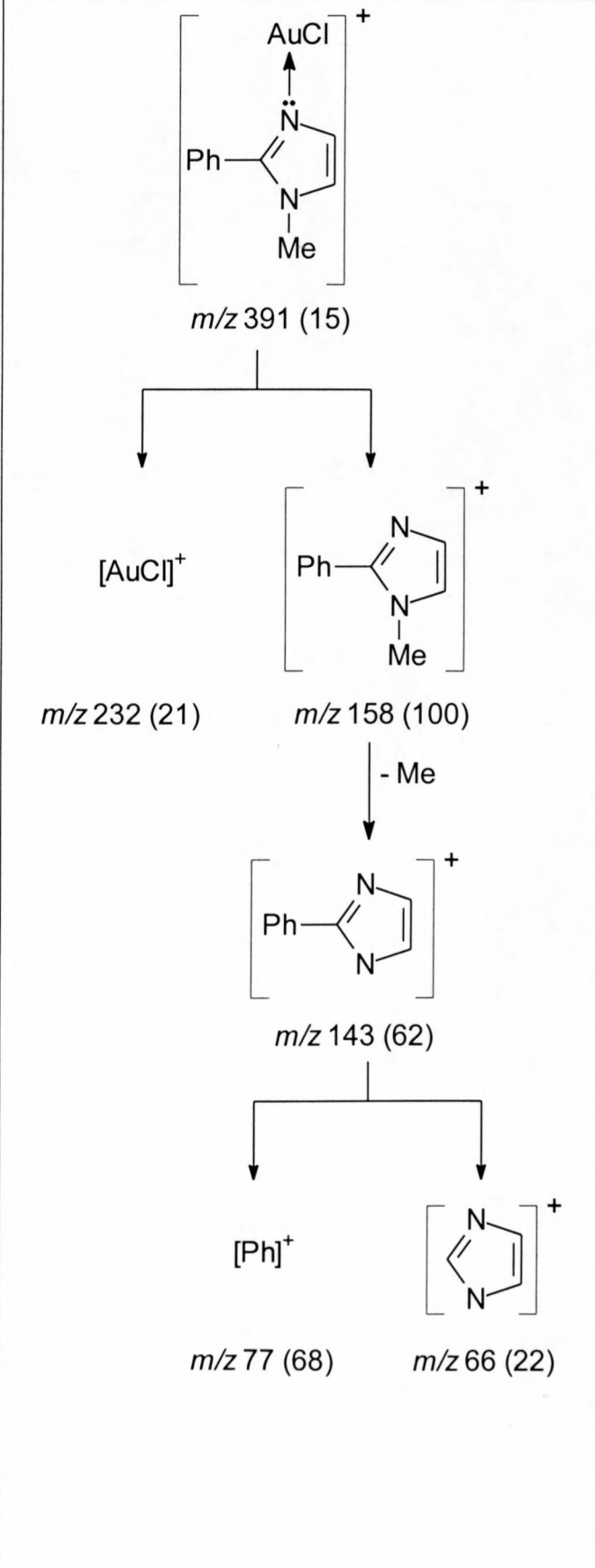
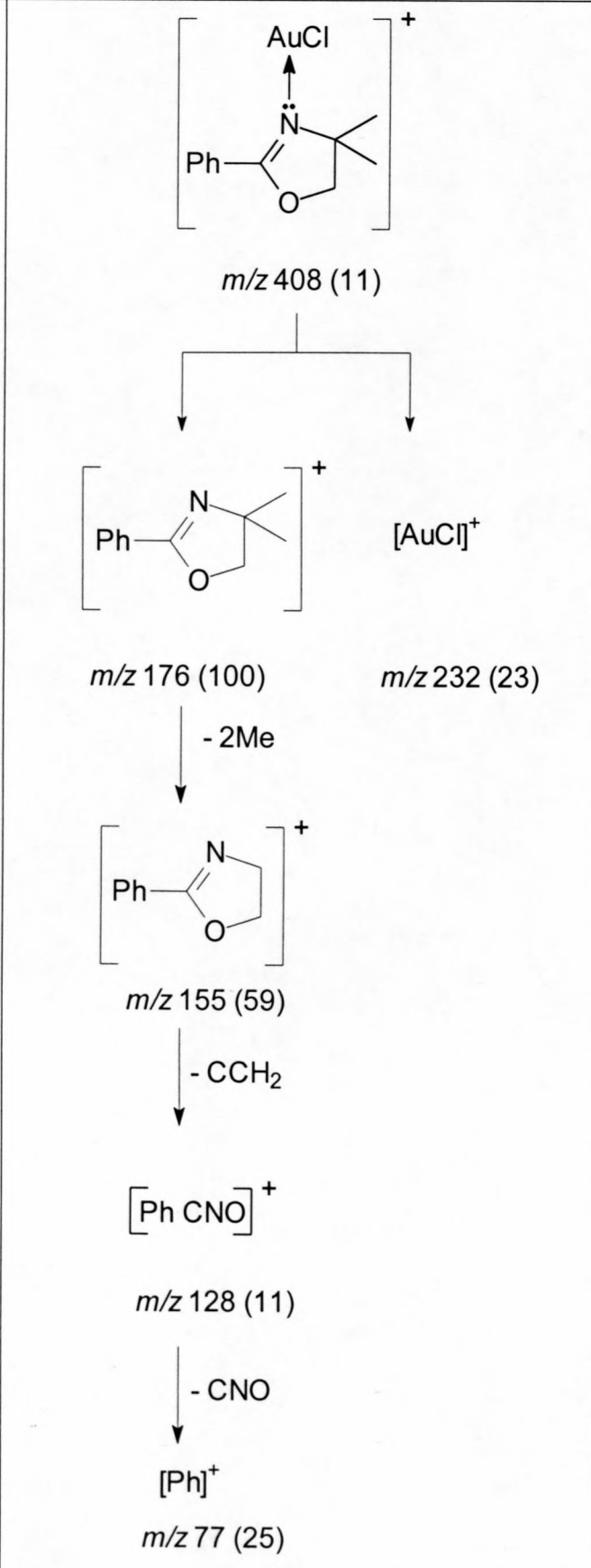
The molecular ion of complexes **15**, **16**, **17** and **18** were observed in EI mass-spectra at m/z 391, 408, 414 and 392, respectively.

The fragmentation pattern of the complexes are quite similar and consists of AuCl loss to give the molecular ion of the respective free ligands as the base peak at m/z 158, 176, 181 and 159. The AuCl peak appears as a weak intensity signal at m/z 232.

The mass spectrum data of complex **18a** display the molecular ion at m/z 624. Since the complex was obtained as a mixture with complex **18**, the subsequent fragment masses could not be unambiguously assigned to the disubstituted complex.

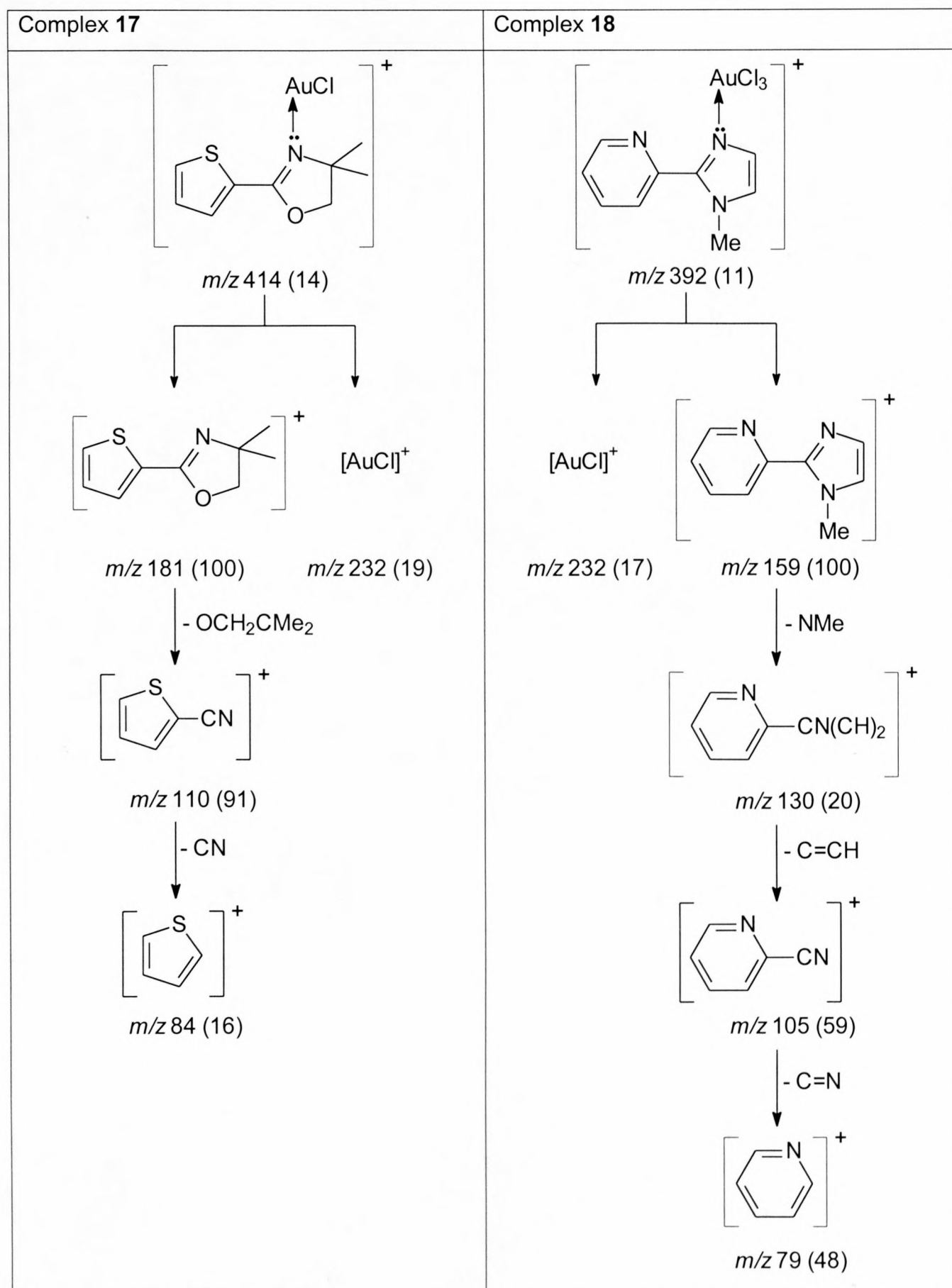
Fragmentation of the ligands after loss of AuCl is as illustrated in Tables 5.6 and Table 5.7. These patterns are similar to those observed in mass spectra of the free ligands, which are not presented here.

Table 5.6 Fragmentation patterns of complexes **15** and **16**^a

Complex 15	Complex 16
 <p> m/z 391 (15) </p> <p> $[AuCl]^+$ m/z 232 (21) </p> <p> m/z 158 (100) </p> <p> $- Me$ </p> <p> m/z 143 (62) </p> <p> $[Ph]^+$ m/z 77 (68) </p> <p> m/z 66 (22) </p>	 <p> m/z 408 (11) </p> <p> $[AuCl]^+$ m/z 232 (23) </p> <p> m/z 176 (100) </p> <p> $- 2Me$ </p> <p> m/z 155 (59) </p> <p> $- CCH_2$ </p> <p> $[Ph\ CNO]^+$ m/z 128 (11) </p> <p> $- CNO$ </p> <p> $[Ph]^+$ m/z 77 (25) </p>

^a Relative intensities in parentheses

Table 5.7 Fragmentation patterns of complexes **17** and **18**^a



^a Relative intensities in parentheses

5.2.3 Neutral Gold(III) Imine Compounds

A Preparation of $[\text{Cl}_3\text{Au}\{\text{N}=\text{C}(\text{Ph})\text{NMeCH}=\text{CH}\}]$, **19**, $[\text{Cl}_3\text{Au}\{\text{N}=\text{C}(\text{Ph})\text{OCH}_2\text{CMe}_2\}]$, **20**, $[\text{Cl}_3\text{Au}\{\text{N}=\text{C}(\text{CSCH}=\text{CHCH})\text{OCH}_2\text{CMe}_2\}]$, **21** and $[\text{Cl}_3\text{Au}\{\text{N}=\text{C}(\text{py})\text{NMeCH}=\text{CH}\}]$, **22**

The neutral gold(III) coordination complexes were prepared by modifying an existing literature procedure which involves addition of an acetonitrile solution of the imine-containing ligand to one molar amount of NaAuCl_4 in water (Scheme 5.5).^[17]

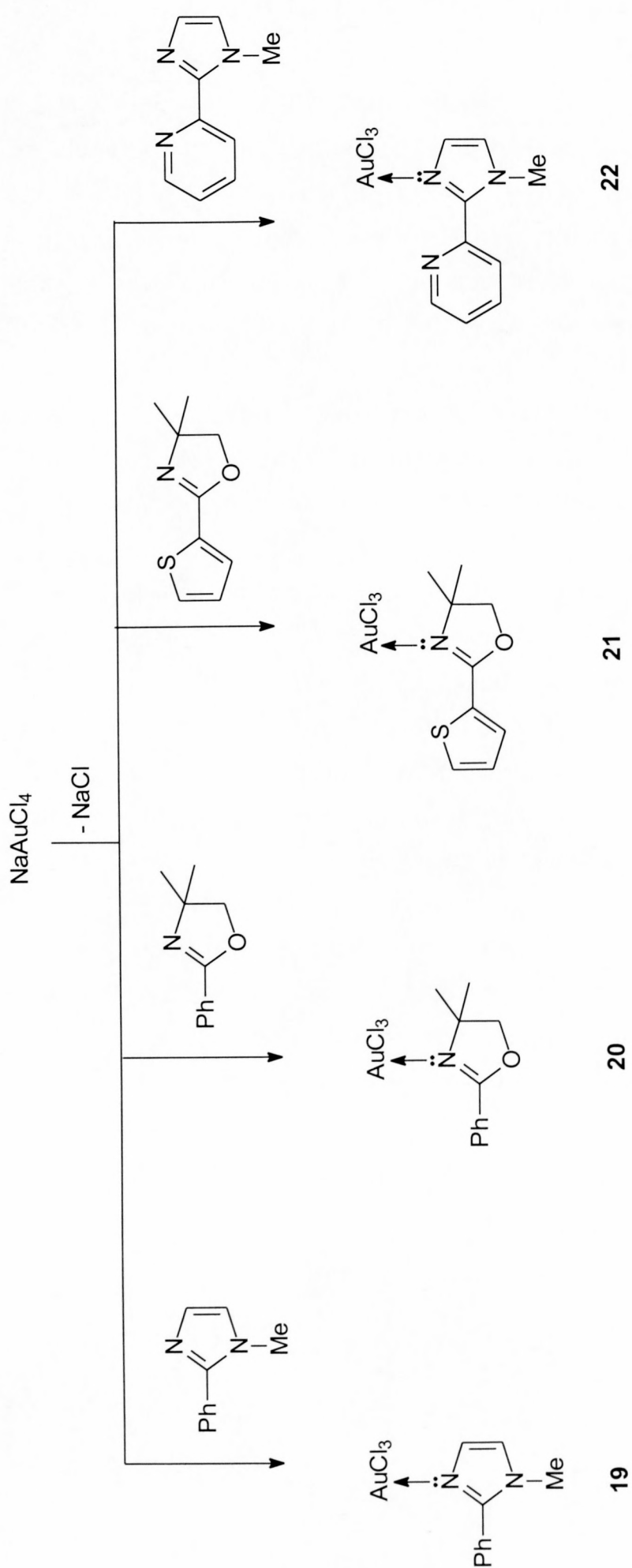
In contrast to the literature procedure, the complexes in the current investigation did not precipitate from the mixed solvent. Extraction with dichloromethane was necessary to remove complexes **19**, **20**, **21** and **22** from the mixed solvent reaction medium.

The organic phase was dried over MgSO_4 , filtered and the complexes crystallised by concentration and cooling of the chlorinated solvent to -20°C . The neutral products were isolated as bright orange, crystalline compounds.

The imine-organo complexes deliquesce but do not decompose in air and were stored under dry conditions. They readily dissolve in dichloromethane, acetone and thf but exhibit limited solubility in non-polar organic solvents.

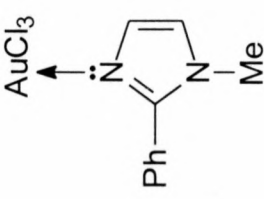
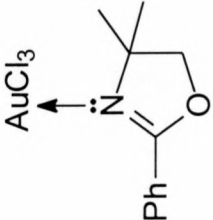
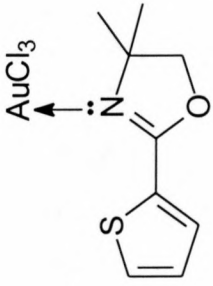
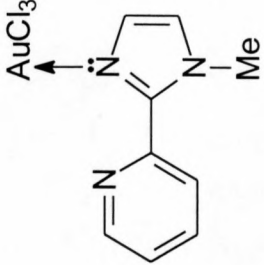
Single crystals of complex **21**, suitable for X-ray crystallographic studies, were obtained by vapour diffusion of hexane into a concentrated dichloromethane solution of the compound. The crystals were isolated by decantation of the mother liquor using Schlenk techniques, and stored under an inert atmosphere to avoid water absorption.

The analytical and physical data of complexes **19**, **20**, **21** and **22** are presented in Table 5.8.



Scheme 5.5

Table 5.8 Analytical and physical data for complexes **19**, **20**, **21** and **22**

Complex	19	20	21	22
				
Colour	Bright Orange	Bright Orange	Bright Orange	Bright Orange
Yield (%)	75	74	78	73
M.p./ °C	195	170	164	233
M.W.	461.53	478.56	484.59	462.52
Analysis (%) ^a				
C	26.12 (26.02)	28.01 (27.61)	22.22 (22.31)	23.41 (23.37)
H	2.10 (2.18)	2.81 (2.74)	2.18 (2.29)	1.88 (1.96)
N	6.21 (6.07)	2.74 (2.93)	2.86 (2.89)	9.21 (9.08)

B Spectroscopic characterisation of complexes **19**, **20**, **21** and **22**

1. NMR spectroscopy

The ^1H NMR data of complexes **19**, **20**, **21** and **22** are presented in Table 5.9 and the ^{13}C - $\{^1\text{H}\}$ NMR as well as the ^{15}N NMR data in Table 5.10.

The ^1H and ^{13}C - $\{^1\text{H}\}$ NMR spectra of complexes **19**, **20**, **21** and **22** show a downfield shift of the proton and carbon signals relative to the individual free ligand signals as well as the corresponding Au(I) compounds, **15**, **16**, **17** and **18**. Chemical shift changes, $\Delta\delta$, of the Au(III) complexes with respect to the ligands are between 0.22 and 1.09, whereas changes of between 0.07 and 0.5 were found with respect to the Au(I) compounds. Stronger deshielding of complexes **19**, **20**, **21** and **22** by gold in a higher oxidation state is expected.

As discussed for the NMR spectra of complex **17** (paragraph 5.2.2), ^1H and ^{13}C - $\{^1\text{H}\}$ NMR shift differences provide indirect evidence for the coordination position of the gold nucleus when a number of possibilities are available. However, in the absence of additional evidence, it is difficult to make confident structural assignments. The molecular structure of complex **21** as determined by X-ray diffraction provides such unequivocal proof by showing exclusive coordination of Au(III) at the imine nitrogen of the oxazole ring (*vide infra*).

In the current investigation, only complexes **20** and **22** displayed the necessary stability and solubility to enable the recording of ^{15}N NMR data and thereby obtain diagnostic proof for the gold(III)-imine coordination site. The N^3 of free 4,4-dimethyl-2-(2'-thienyl)oxazole resonates at δ -133.6 and coordination at this position is evidenced by the resonance appearing at δ -90.5 in the ^{15}N spectrum of complex **20**.

A similar change was observed for complex **22** in which the chemical shift for N^3 in the imidazole ring moves from δ -114.4 in the free ligand to δ -82.2 in the coordinated product. The imidazole NMe and N^1 (-pyridine) signals display much smaller differences of $\Delta\delta$ 17.7 and 8.2, indicating that coordination did occur at N^3 .

Table 5.9 ^1H NMR data of complexes **19**, **20**, **21**, and **22** in d-acetone

Complex	19	20	21	22
^1H NMR ^a	4.35 (3H, s)	-	-	4.72 (3H, s)
NMe	-	1.81 (6H, s)	1.78 (6H, s)	-
CMe ₂	-	4.90 (2H, s)	4.84 (2H, s)	-
CH ₂	-	-	-	8.29 (1H, s)
H ⁴	7.73 (1H, s)	-	-	8.03 (1H, s)
H ⁵	7.56 (1H, s)	-	-	-
H ^{2'}	8.32 (1H, d, J = 6)	8.35 (1H, d, J = 6)	-	-
H ^{3'}	7.87 (1H, td, J = 9, 6)	7.79 (1H, td, J = 9, 6)	8.37 (1H, m)	8.39 (1H, dd, J = 9, 6)
H ^{4'}	7.96 (1H, m)	7.90 (1H, m)	7.50 (1H, t, J = 6, 6)	8.96 (1H, m)
H ^{5'}	7.87 (1H, td, J = 9, 6)	7.79 (1H, td, J = 9, 6)	8.37 (1H, m)	8.96 (1H, m)
H ^{6'}	8.32 (1H, d, J = 6)	8.35 (1H, d, J = 6)	-	9.73 (1H, dd, J = 9, 6)

^a J in Hz

Table 5.10 ^{13}C -{ ^1H } and ^{15}N NMR data of complexes **19**, **20**, **21**, and **22** in d-acetone

Complex	19	20	21	22
^{13}C NMR	35.6	-	-	36.1
NMe	-	28.8	28.2	-
CMe ₂	-	166.1	149.0	152.8
C ²	159.0	72.3	72.2	126.0
C ⁴	129.9	83.3	82.6	123.5
C ⁵	130.3	126.6	-	-
C ^{1'}	129.2	130.8	135.2	146.7
C ^{2'}	131.7	130.6	130.4	126.2
C ^{3'}	132.2	136.2	138.9	129.2
C ^{4'}	135.1	130.6	132.2	137.8
C ^{5'}	132.2	131.3	-	149.6
C ^{6'}	131.7	-90.6	-	-82.2
^{15}N NMR	-	-	-	-66.7
N ³	-	-	-	-202.6
N ^{1'}	-	-	-	-
NMe	-	-	-	-

Recent work in our laboratory has shown that N-coordination of 4-methylthiazole to Au(C₆F₅) effects a downfield shift of ca. 60 ppm.^[26]

2. Mass spectrometry

The FAB mass spectral data of complexes **19**, **20** and **21** are summarised in Table 5.11 and the fragmentation pattern of complex **22** is presented in Table 5.12.

The molecular ions of complexes **19**, **20** and **21** are observed in the individual mass-spectra at *m/z* 462, 479 and 485.

Strong intensity signals for the respective ligands are visible at *m/z* 158, 176 and 181.

The fragmentation pattern of complex **19** indicates the loss of two chlorine atoms to give a peak for [ClAu{N=C(Ph)MeCH=CH}]⁺ at *m/z* 392, followed by the loss of AuCl to give the ligand peak at *m/z* 158. The ionised phenyl unit is also present.

Fragmentation of complexes **20** and **21** both consist of the initial loss of chlorine. Thereafter, complex **21** ejects the remaining two halogen atoms to give a weak intensity signal for [Au{N=C(CSCH=CHCH)OCH₂CMe₂}]⁺ at *m/z* 378, whereas in complex **20**, AuCl₂ is ejected to give the ligand peak at *m/z* 176.

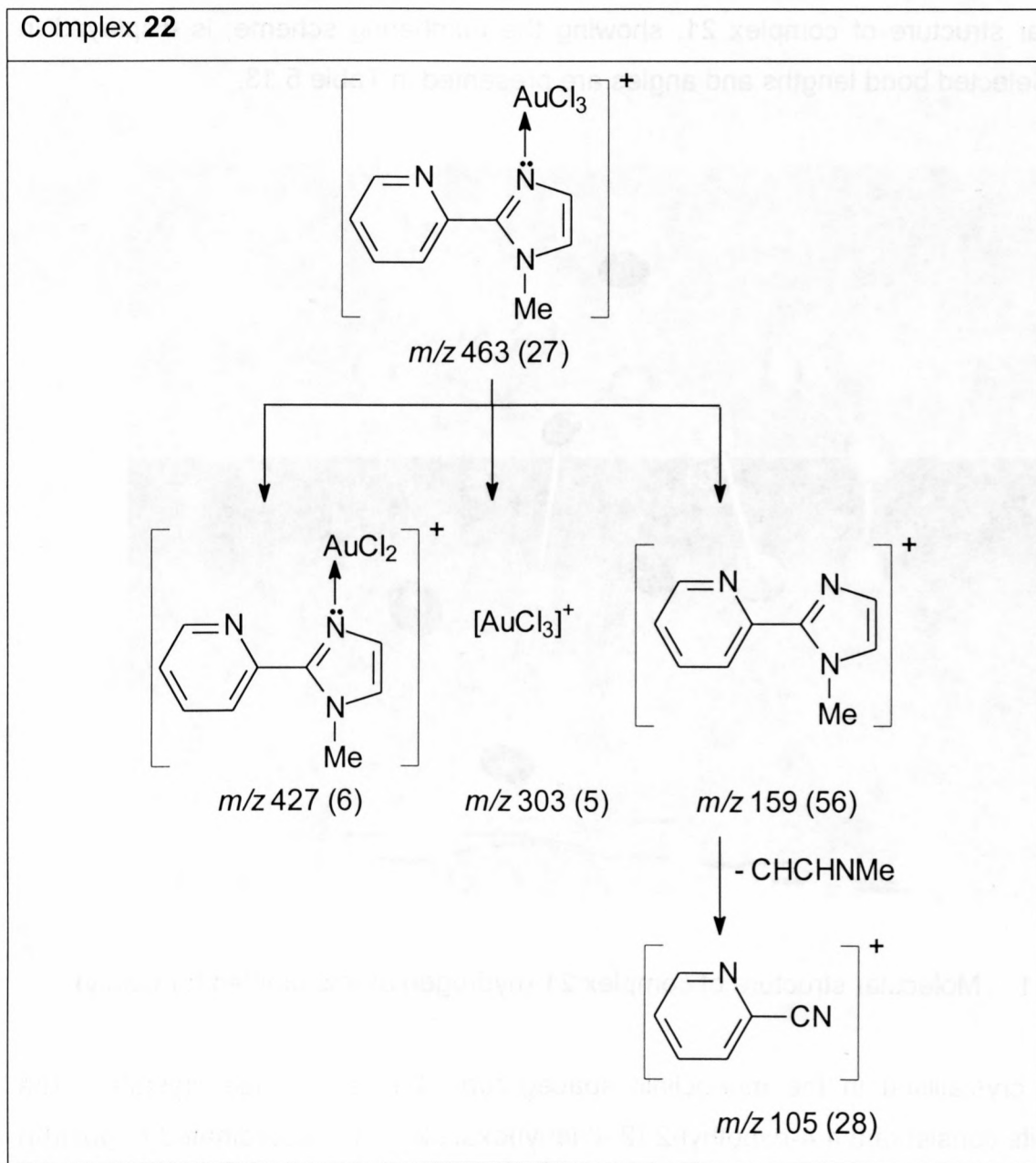
The FAB mass spectrum of complex **22** exhibits the molecular ion at *m/z* 463. The fragmentation pattern consists of the loss of either chlorine or AuCl₃ to give the free ligand peak at *m/z* 159 and low intensity peaks for AuCl₃⁺ at *m/z* 303 and [Cl₂Au{N=C(py)NMeCH=CH}]⁺ at *m/z* 427.

Table 5.11 Mass spectral data for complexes **19**, **20** and **21**

Complex 19		Fragment ions
<i>m/z</i>	<i>I</i> ^a	
462	59	$[\text{Cl}_3\text{Au}\{\text{N}=\text{C}(\text{Ph})\text{NMeCH}=\text{CH}\}]^+$
392	44	$[\text{ClAu}\{\text{N}=\text{C}(\text{Ph})\text{NMeCH}=\text{CH}\}]^+$
158	83	$[\text{N}=\text{C}(\text{Ph})\text{NMeCH}=\text{CH}]^+$
77	100	$[\text{Ph}]^+$
Complex 20		
479	77	$[\text{Cl}_3\text{Au}\{\text{N}=\text{C}(\text{Ph})\text{OCH}_2\text{CMe}_2\}]^+$
443	8	$[\text{Cl}_2\text{Au}\{\text{N}=\text{C}(\text{Ph})\text{OCH}_2\text{CMe}_2\}]^+$
176	100	$[\text{N}=\text{C}(\text{Ph})\text{OCH}_2\text{CMe}_2]^+$
105	91	$[\text{PhCO}]^+$
Complex 21		
485	58	$[\text{Cl}_3\text{Au}\{\text{N}=\text{C}(\text{CSCH}=\text{CHCH})\text{OCH}_2\text{CMe}_2\}]^+$
449	9	$[\text{Cl}_2\text{Au}\{\text{N}=\text{C}(\text{CSCH}=\text{CHCH})\text{OCH}_2\text{CMe}_2\}]^+$
378	16	$[\text{Au}\{\text{N}=\text{C}(\text{CSCH}=\text{CHCH})\text{OCH}_2\text{CMe}_2\}]^+$
181	100	$[\text{N}=\text{C}(\text{CSCH}=\text{CHCH})\text{OCH}_2\text{CMe}_2]^+$

^a Intensity relative to the base peak

Table 5.12 Mass spectral data for complex **22**^a



C Crystal and molecular structure of complex **21**

The molecular structure of complex **21**, showing the numbering scheme, is displayed in Figure 5.1. Selected bond lengths and angles are presented in Table 5.13.

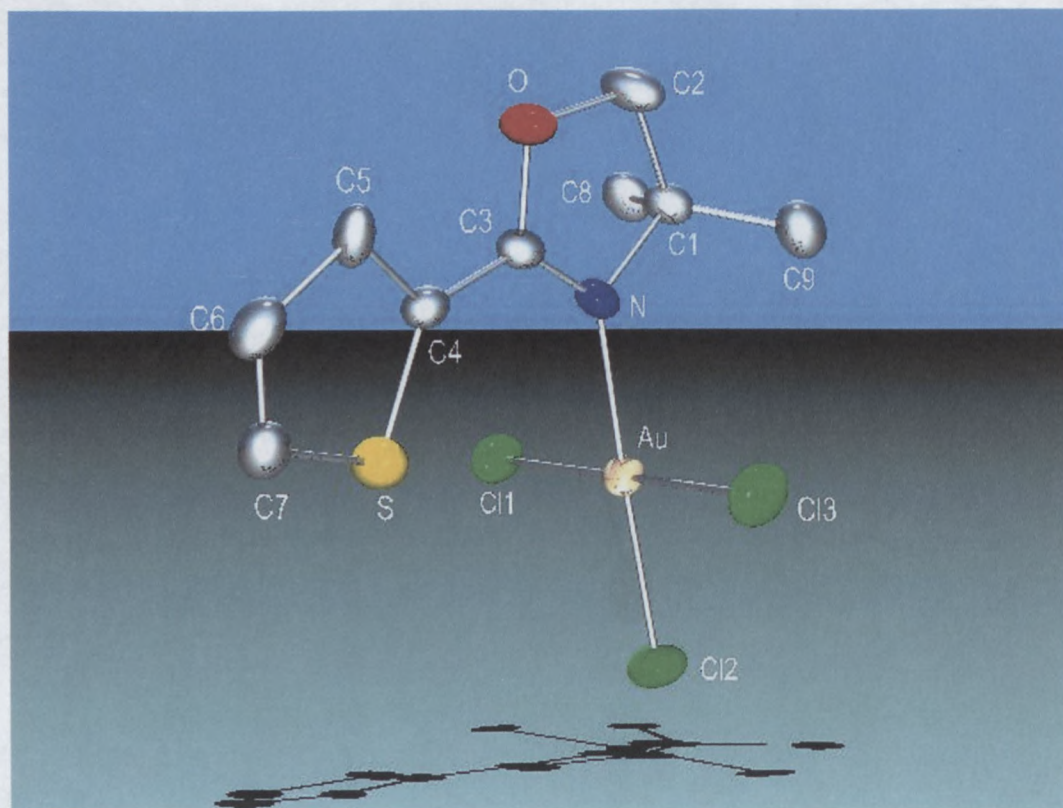


Figure 5.1 Molecular structure of complex **21** (hydrogen atoms omitted for clarity).

Complex **21** crystallised in the monoclinic spacegroup $P2_1/c$ as orange crystals. The molecular units consist of a 4,4-dimethyl-2-(2'-thienyl)oxazole ligand coordinated to gold(III) chloride at the imine nitrogen of the five-membered ring.

Coordination around the gold atom is essentially planar and maximum deviations from the mean square plane composed of Au-Cl1-Cl2-Cl3-N are -0.046 \AA (Cl1) and $+0.049 \text{ \AA}$ (N). The essentially linear N-Au-Cl2 ($177.48(14)^\circ$) and Cl1-Au-Cl3 ($177.65(6)^\circ$) bond angles are similar. The gold-chlorine distances are normal for gold(III) complexes.^[6,27]

A search of the Cambridge Structural Database revealed that a similar pyridine-AuCl₃ adduct has been structurally characterised.^[18] In this complex, the Au-N bond length of

1.993(7) Å is comparable to the Au-N distance of 2.028(4) Å in complex **21**, and, both these values are typical for sp² Au-N bonds.^[19]

A dihedral angle of 87.56° positions the thienyl ring plane through C4-C5-C6-C7-S (deviation from the best plane, 0.005 Å) and the coordination plane through Au-Cl(1)-Cl(2)-Cl(3)-N (deviation from the best plane, 0.041 Å) at right angles to each other. Slight buckling of the oxazole ring occurs due to the sp³ C1 and C2 carbons, which lie 0.071 and 0.078 Å below the least squares plane formed by N-C1-C2-O-C3. A torsion angle of 9.02°, defined by the dihedral angle between the thienyl and oxazole ring planes, separates the five-membered rings.

The packing of the complex shows 4 molecules per unit cell and Au··Au distances therein lie above the upper limit of 3.2 Å for aurophilic interactions.^[28] Intermolecular separations between alternate thienyl rings of 3.9 Å excludes the possibility of π-π interactions, which can occur at values of up to 3.8 Å, but are most favourable at 3.4 Å.^[29] Contacts between chlorine and Au atoms, as observed in the structure of a pyridine-AuCl₃ adduct, are absent in the crystal lattice of complex **21**.

Table 5.13 Selected bond lengths (Å) and angles(°) for complex **21**^a

Au – N	2.028(4)	S – C4	1.719(6)
Au – Cl2	2.2672(15)	N – C3	1.293(7)
Au – Cl1	2.2719(14)	N – C1	1.510(7)
Au – Cl3	2.2821(15)	O – C3	1.334(7)
S – C7	1.687(7)	O – C2	1.446(8)
N – Au – Cl2	177.48(14)	Cl1 – Au – Cl3	177.65(6)
N – Au – Cl1	89.56(15)	C3 – N – Au	127.2(4)
N – Au – Cl3	89.93(14)	C1 – N – Au	122.3(4)
Cl2 – Au – Cl1	90.15(6)	C1 – N – C3	110.5(5)
Cl2 – Au – Cl3	90.46(6)	N – C1 – C8	110.2(5)

^a e.s.d.s. in parentheses

5.2.4 Cationic Gold(III) Imine Complexes

A Preparation of $[\text{Cl}_2\text{Au}\{\text{N}=\text{C}(\text{Ph})\text{NMeCH}=\text{CH}\}_2][\text{AuCl}_4]$, **19a**,
 $[\text{Cl}_2\text{Au}\{\text{N}=\text{C}(\text{Ph})\text{OCH}_2\text{CMe}_2\}_2][\text{AuCl}_4]$, **20a**,
 $[\text{Cl}_2\text{Au}\{\text{N}=\text{C}(\text{CSCH}=\text{CHCH})\text{OCH}_2\text{CMe}_2\}_2][\text{AuCl}_4]$, **21a** and
 $[\text{Cl}_2\text{Au}\{\text{N}=\text{C}(\text{py})\text{NMeCH}=\text{CH}\}][\text{AuCl}_4]$, **22a**.

Complexes **19a**, **20a**, **21a** and **22a** were prepared utilising the same literature procedure employed to prepare complexes **19**, **20**, **21** and **22**,^[17] but by replacing NaAuCl_4 with HAuCl_4 .

Addition of an acetonitrile solution of the respective bicyclic imines to an aqueous solution containing one molar amount of HAuCl_4 (Scheme 5.6), afforded the cationic complexes as yellow precipitates. The products were purified by recrystallisation from dichloromethane.

Note that although the preparations were performed in equimolar ratios, only disubstituted products with AuCl_4^- as counterion were obtained. Unreacted HAuCl_4 was effectively removed by recrystallisation of the products.

Layering a dichloromethane solution of complex **19a** with hexane, yielded single crystals that were suitable for X-ray crystallographic investigation. Single crystals of complex **22a** were obtained by allowing a saturated dichloromethane solution of the compound to slowly warm from -20°C to room temperature.

Complexes **19a**, **20a**, **21a** and **22a** are stable in the presence of air and moisture, readily dissolve in dichloromethane, acetone and thf but exhibit limited solubility in non-polar organic solvents.

The analytical and physical data of complexes **19**, **20**, **21** and **22** are presented in Table 5.8.

Stacking of the molecules in the unit cell, as viewed along the *a*-axis, shows a twofold screw-axis extending through the thienyl rings. This symmetry feature positions the alternate thienyl rings in the unit cell at 180° (Figure 5.2).

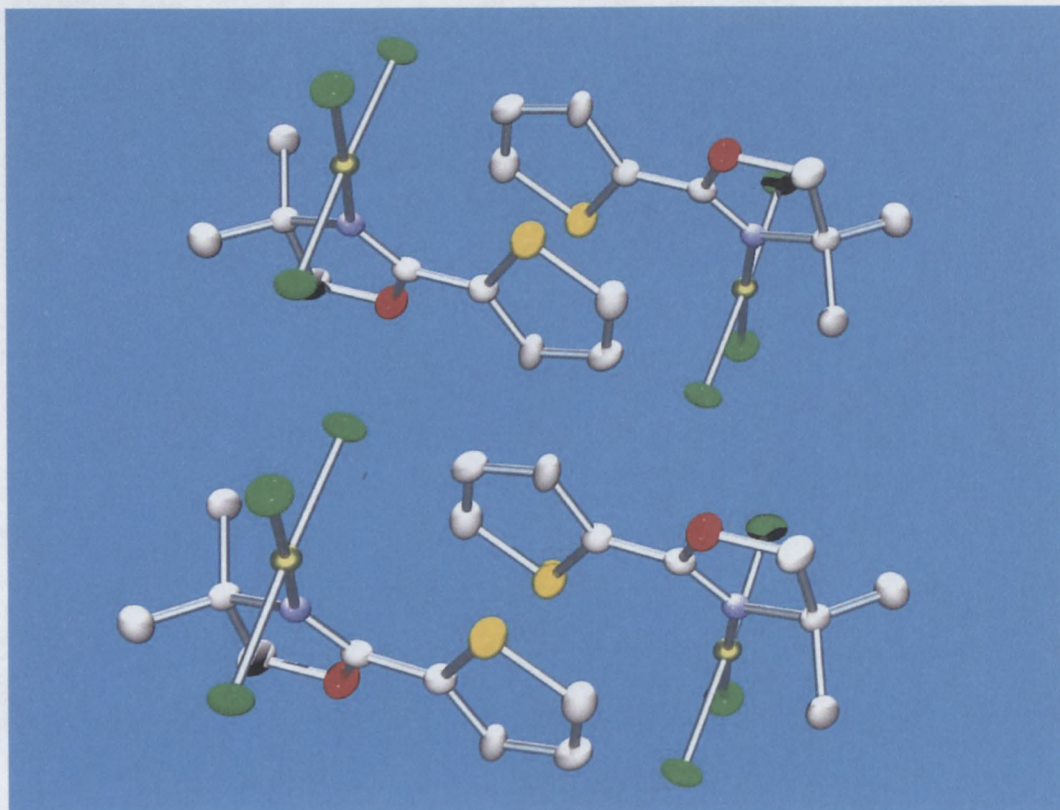
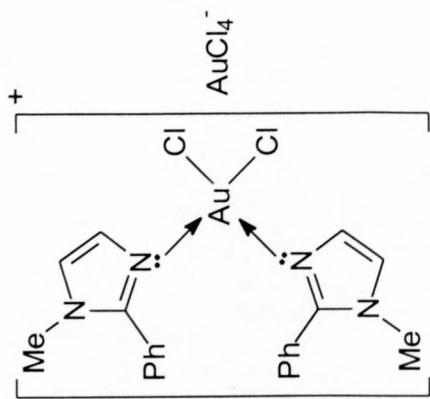
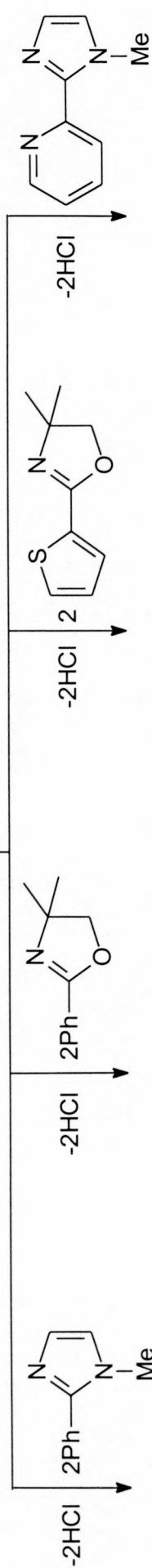
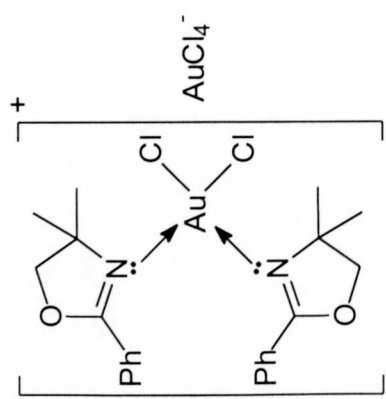


Figure 5.2 Packing diagram of complex **21**, as viewed along the *a*-axis, showing a twofold screw axis extending through the thienyl rings.

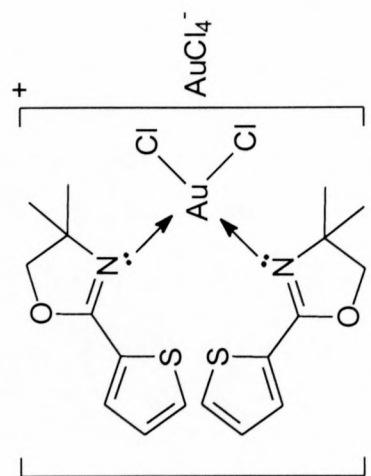
2HAuCl₄



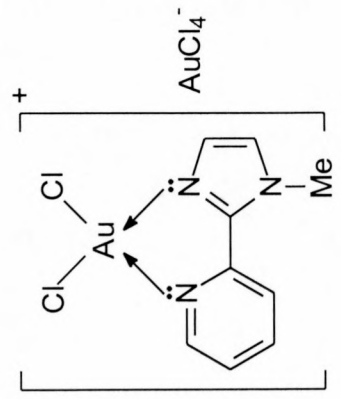
19a



20a



21a



22a

Scheme 5.6

Table 5.14 Analytical and physical data for complexes **19a**, **20a**, **21a** and **22a**

Complex	19a	20a	21a	22a
Colour	Yellow	Yellow	Yellow	Yellow
Yield (%)	34	36	38	41
M.p./ °C	201	222	108	234
M.W.	923.06	957.11	969.17	765.85
Analysis (%) ^a				
C	26.34 (26.02)	28.01 (27.61)	22.26 (22.31)	14.33 (14.11)
H	2.10 (2.18)	2.68 (2.74)	2.22 (2.29)	1.21 (1.18)
N	6.11 (6.07)	2.85 (2.93)	2.81 (2.89)	5.62 (5.49)

^a Required values given in parentheses

B Spectroscopic characterisation of complexes **19a**, **20a**, **21a** and **22a**

1. NMR spectroscopy

The ^1H NMR data of complexes **19a**, **20a**, **21a** and **22a** are summarised in Table 5.14 and the $^{13}\text{C}\{-^1\text{H}\}$ data appear in Table 5.15. The numbering scheme employed for the phenyl ring in complexes **19** and **20** also applies for complexes **19a** and **20a**.

The molecular structure of complex **19a** (*vide infra*) showed that two 1-methyl-2-(phenyl)imidazole ligands are *cis* nitrogen-coordinated to gold(III). This places the proton and carbon nuclei of the two ligands in chemically and magnetically equivalent environments and consequently, the ^1H and ^{13}C signals resonate at matching field positions. The solid state structures of complexes **20a** and **21a** were not determined, but FAB MS data indicated the presence of two bicyclic ligands in the cationic fragment of the complexes. The ^1H and $^{13}\text{C}\{-^1\text{H}\}$ NMR spectra of the respective complexes display only one set of signals for the two coordinated ligands. Furthermore, similar chemical shift changes to those observed for complex **19a** indicated similar ligand arrangements in the two complexes.

The ^1H and $^{13}\text{C}\{-^1\text{H}\}$ NMR data of complexes **19a**, **20a**, **21a** and **22a** show small, unexpected upfield shifts of the resonances with respect to the corresponding signals of complexes **19**, **20**, **21** and **22**, despite the positive charge on the new complex ions. Although these ^1H and $^{13}\text{C}\{-^1\text{H}\}$ NMR chemical shift changes do not exceed $\Delta\delta$ 0.75 and 5, respectively, the upfield shifts are unmistakable. This means that less negative charge is effectively transferred to the metal by each ligand than in the gold trihalides.

Due to the concentration and other requirements for ^{15}N NMR measurements (see paragraph 5.2.3), only the ^{15}N spectrum of complex **20a** could be recorded.

A single resonance observed at δ -103.4 for complex **20a** indicates the presence of equivalent nitrogen atoms and that they are more shielded than the nitrogen of complex **20**, which resonates at δ -90.6. This is in agreement with the upfield positions observed for the ^1H and ^{13}C signals in the cationic complexes.

Table 5.14 ^1H NMR data of complexes **19a**, **20a**, **21a** and **22a** in d-acetone

Complex				
^1H NMR ^a	19a	20a	21a	22a
NMe	3.94 (6H, s)	-	-	4.62 (3H, s)
CMe ₂	-	1.81 (12H, s)	1.42 (12H, s)	-
CH ₂	-	5.15 (4H, s)	4.24 (4H, s)	-
H ⁴	7.55 (2H, s)	-	-	8.19 (1H, d, J = 3)
H ⁵	7.48 (2H, s)	-	-	7.94 (1H, d, J = 3)
H ²	7.94 (2H, dd, J = 12, 6)	8.22 (2H, dd, J = 12, 6)	-	-
H ³	7.60 (2H, m)	7.79 (2H, m)	7.62 (2H, m)	8.31(1H, ddd, J = 9, 6, 3)
H ^{4'}	7.60 (2H, m)	8.01 (2H, td, J = 12, 6)	7.62 (2H, m)	8.87 (1H, m)
H ^{5'}	7.60 (2H, m)	7.79 (2H, m)	8.04 (2H, d, J = 6)	8.87 (1H, m)
H ^{6'}	7.94 (2H, dd, J = 12, 6)	8.22 (2H, dd, J = 12, 6)	-	9.64 (1H, d, J = 9)

^a J in Hz

Table 5.15 ^{13}C - $\{^1\text{H}\}$ and ^{15}N NMR data of complexes **19a**, **20a**, **21a** and **22a** in d-acetone

Complex	^{13}C NMR	^{15}N NMR	Chemical Structure
19a	33.7	-	
20a	26.6 163.7 65.0 82.7 121.9 130.8 130.9 135.8 130.9 130.8	-	
21a	26.9 146.5 66.7 78.0	Not observed	
22a	149.9 125.5 126.2	-	
^{13}C NMR	NMe CMe ₂ C ² C ⁴ C ⁵ C ^{1'} C ^{2'} C ^{3'} C ^{4'} C ^{5'} C ^{6'}	N ³	38.2 - 149.9 125.5 126.2 - 146.1 126.8 128.4 136.5 147.2
^{15}N NMR	-	-	-

2. Mass spectrometry

The FAB mass spectral data of complexes **19a** and **20a**, **21a**, and **22a** are summarised in Tables 5.16 and 5.17.

The molecular ions were not observed in the individual mass spectra, but peaks for the respective cationic fragments are visible at m/z 584, 619, 630 and 428.

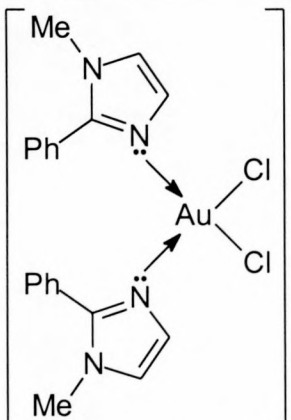
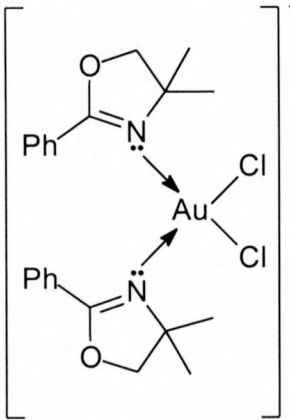
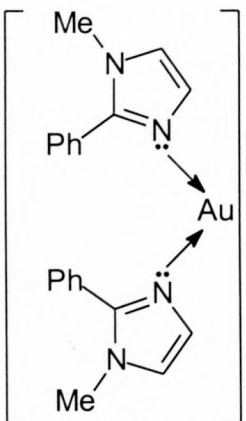
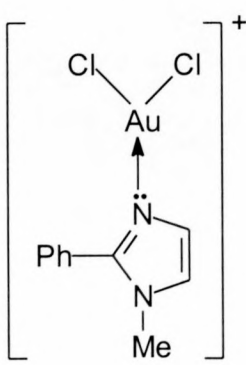
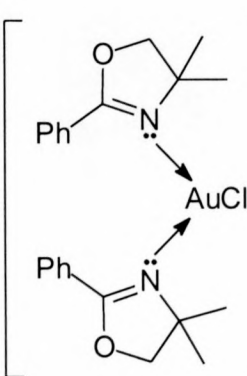
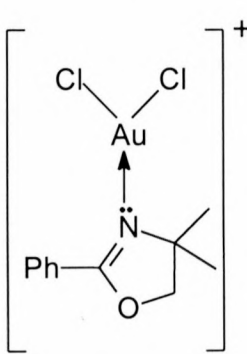
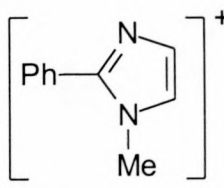
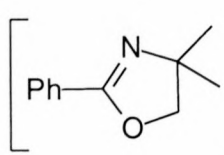
Two parallel fragmentation patterns were established for complex **19a**: (a) the loss of two chlorine atoms, to give $[\text{Au}\{\text{N}=\text{C}(\text{Ph})\text{NMeCH}=\text{CH}\}_2]^+$ with m/z 514; or (b) the expulsion of one azole ligand to form $[\text{Cl}_2\text{Au}\{\text{N}=\text{C}(\text{Ph})\text{NMeCH}=\text{CH}\}]^+$ with m/z 425.

Complex **20a** exhibits similar fragmentation patterns and the two daughter ions are present at m/z 584 and 444.

Complex **21a** loses the chlorine atoms sequentially and then gold to give the ions for $[\text{ClAu}\{\text{N}=\text{C}(\text{CSCH}=\text{CHCH})\text{OCH}_2\text{CMe}_2\}_2]^+$ and $[\text{Au}\{\text{N}=\text{C}(\text{CSCH}=\text{CHCH})\text{OCH}_2\text{CMe}_2\}_2]^+$ at m/z 595 and 560.

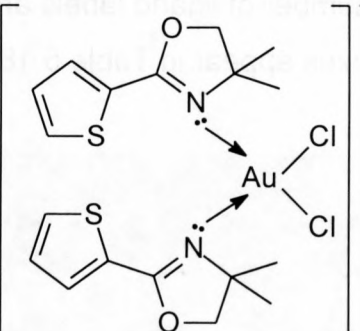
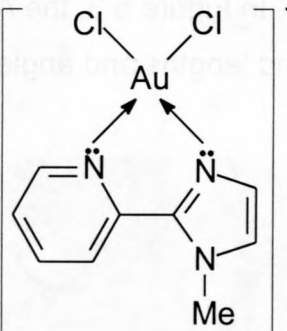
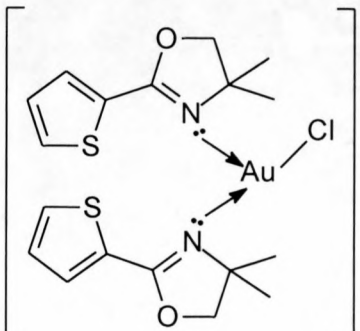
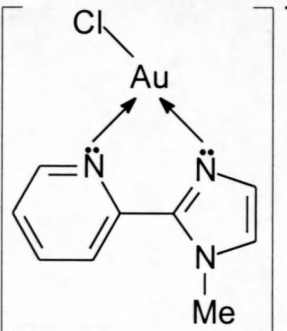
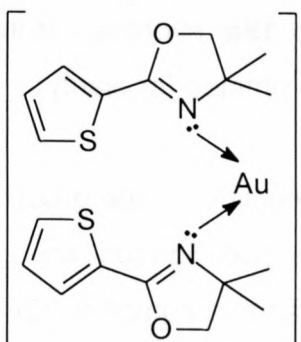
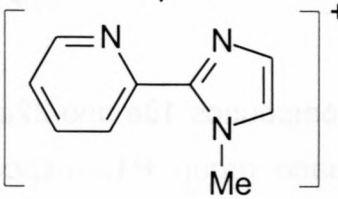
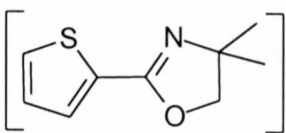
Ejection of chlorine and then AuCl to give the free ligand at m/z 159 is indicated by the mass spectrum of complex **22a**.

Table 5.16 Mass spectral data for complexes **19a**, and **20a**^a

Complex 19a	Complex 20a
 <p style="text-align: center;">m/z 584 (24)</p>	 <p style="text-align: center;">m/z 619 (20)</p>
<div style="display: flex; justify-content: space-around;"> <div data-bbox="96 873 341 1294">  <p style="text-align: center;">m/z 514 (7)</p> </div> <div data-bbox="452 873 697 1238">  <p style="text-align: center;">m/z 425 (18)</p> </div> </div>	<div style="display: flex; justify-content: space-around;"> <div data-bbox="764 873 1009 1249">  <p style="text-align: center;">m/z 584 (4)</p> </div> <div data-bbox="1135 873 1380 1227">  <p style="text-align: center;">m/z 444 (13)</p> </div> </div>
<div style="text-align: center;">  <p style="text-align: center;">m/z 158 (73)</p> </div>	<div style="text-align: center;">  <p style="text-align: center;">m/z 175 (90)</p> </div>

^a Relative intensities in parentheses

Table 5.17 Mass spectral data for complexes **21a** and **22a**^a

Complex 21a	Complex 22a
 <p style="text-align: center;">m/z 630 (55)</p>	 <p style="text-align: center;">m/z 428 (46)</p>
 <p style="text-align: center;">m/z 595 (5)</p>	 <p style="text-align: center;">m/z 392 (4)</p>
 <p style="text-align: center;">m/z 560 (8)</p>	 <p style="text-align: center;">m/z 159 (88)</p>
 <p style="text-align: center;">m/z 180 (79)</p>	

^a Relative intensities in parentheses

C Crystal and molecular structure of complexes **19a** and **22a**

The molecular structures of complexes **19a** and **22a** are shown in Figures 5.3 and 5.4 respectively. In Figure 5.3, the AuCl_4^- counterion and a number of ligand labels are omitted. Selected bond lengths and angles for the cationic complexes appear in Table 5.18.

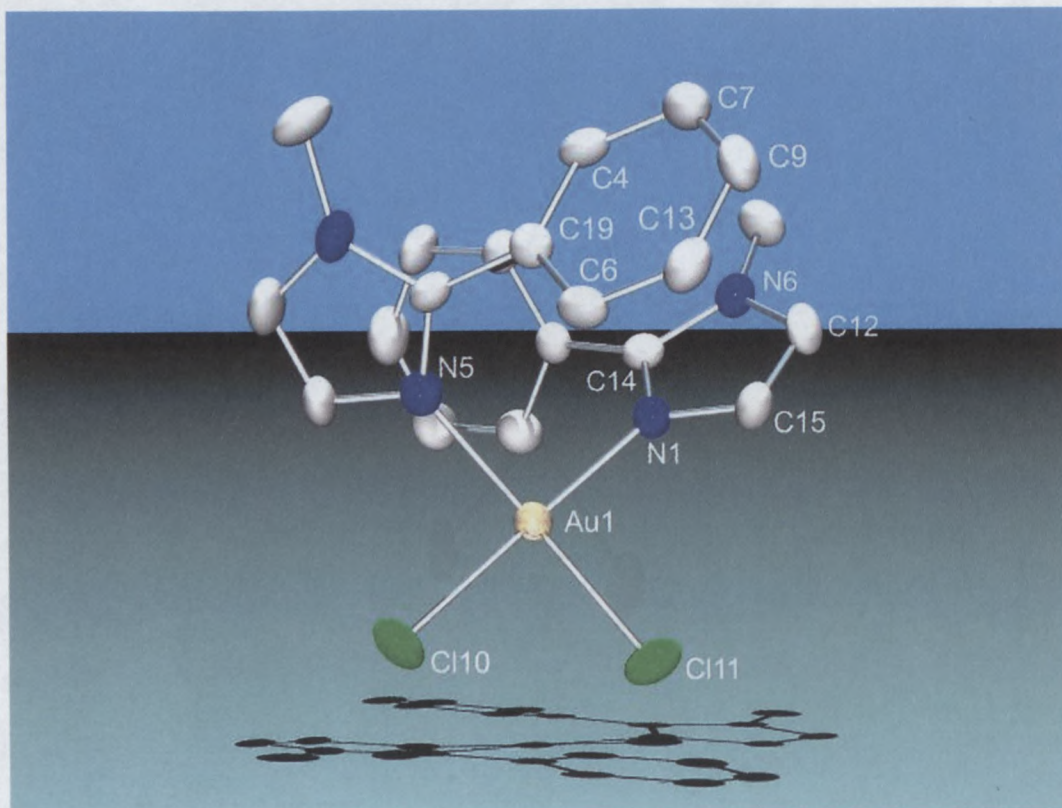


Figure 5.3 Molecular structure of the cation in complex **19a** (hydrogen atoms, AuCl_4^- and selected ligand atom labels omitted for clarity).

The two compounds **19a** and **22a** crystallised in the monoclinic space group $P2_1/n$ and the triclinic space group $P\bar{1}$, respectively. Whereas the two ligands are monodentately coordinated in the square planar complex **19a**, the ligand in complex **22a** is bidentately bonded to gold. The mean deviation from the least squares plane is 0.041 Å for complex **19a** (Au1-N1-N5-Cl10-Cl11) and 0.198 Å for complex **22a** (Au2-N1-N2-Cl5-Cl6). The Au-N bond lengths in the former and latter cations Au2-N1, 2.052(18) Å and Au2-N2, 2.045(18) Å and Au1-N1, 2.043(7) Å and Au1-N5, 2.016(6) Å are normal for Au-N (sp^2) bonds.^[16] The Au-Cl bond lengths are also typical for gold(III) compounds.^[17]

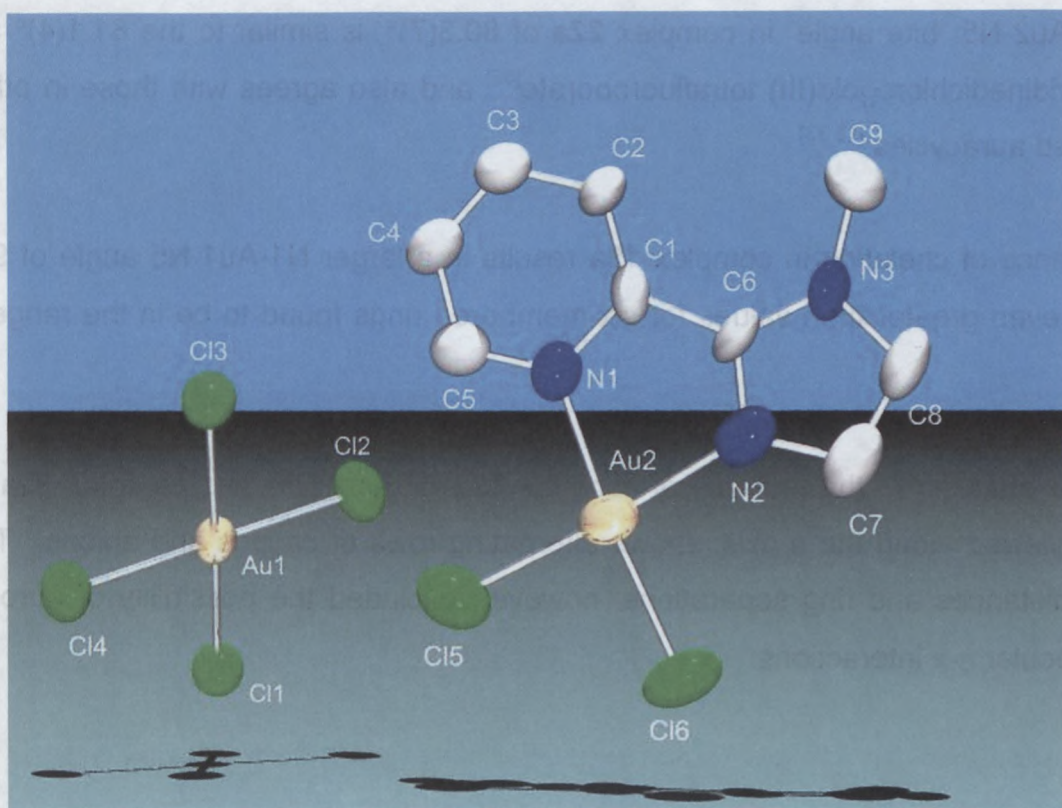


Figure 5.4 Molecular structure of complex **22a** (hydrogen atoms omitted for clarity).

A search of the Cambridge Structural Database^[30] revealed that a number of neutral and cationic gold(III) complexes in which monodentate C or N σ -donor ligands are situated *trans* have been structurally characterised, but that complex **19a** is only the second example exhibiting a *cis* arrangement of the ligands. The previously described complex, however, is a gold(III) complex containing two (diamino)carbene ligands,^[31] making complex **19a** the first example with two *cis* nitrogen donor ligands.

A possible explanation for the *cis* arrangement of the bulky bicyclic ligands could be that favourable π - π interactions occur between the individual ligands. A centroid distance of 3.786 Å was found between the imidazole ring plane through N2-C18-C20-N5-C8 (mean deviation from the best plane, 0.0032 Å) and the phenyl plane through C16-C5-C22-C21-C23-C10 (mean deviation from the best plane, 0.0053 Å). A shorter 3.559 Å separation exists between the other unlabelled imidazole-phenyl ring pair in Figure 5.3. These separations are significantly less than the 3.9 Å found between alternate 5-(thienyl)oxazole ligand rings in complex **21** (compare paragraph 5.2.3).

The N1-Au2-N5 “bite angle” in complex **22a** of $80.3(7)^\circ$, is similar to the $81.1(4)^\circ$ angle in 2,2'-bipyridinedichlorogold(III) tetrafluoroborate^[32] and also agrees with those in other five-membered auracycles.^[15,33]

The absence of chelation in complex **19a** results in a larger N1-Au1-N5 angle of $91.9(2)^\circ$, which is even greater than values for six-membered rings found to be in the range $85.2 - 88.3^\circ$ ^[18].

Molecular stacking in the unit cell of complex **19a** (Figure 5.5) and complex **22a** (Figure 5.6), as viewed along the *a*-axis, shows alternating rows of cations and anions. The long Au...Au distances and ring separations, however, excluded the possibility of aurophilic or intermolecular π - π interactions.

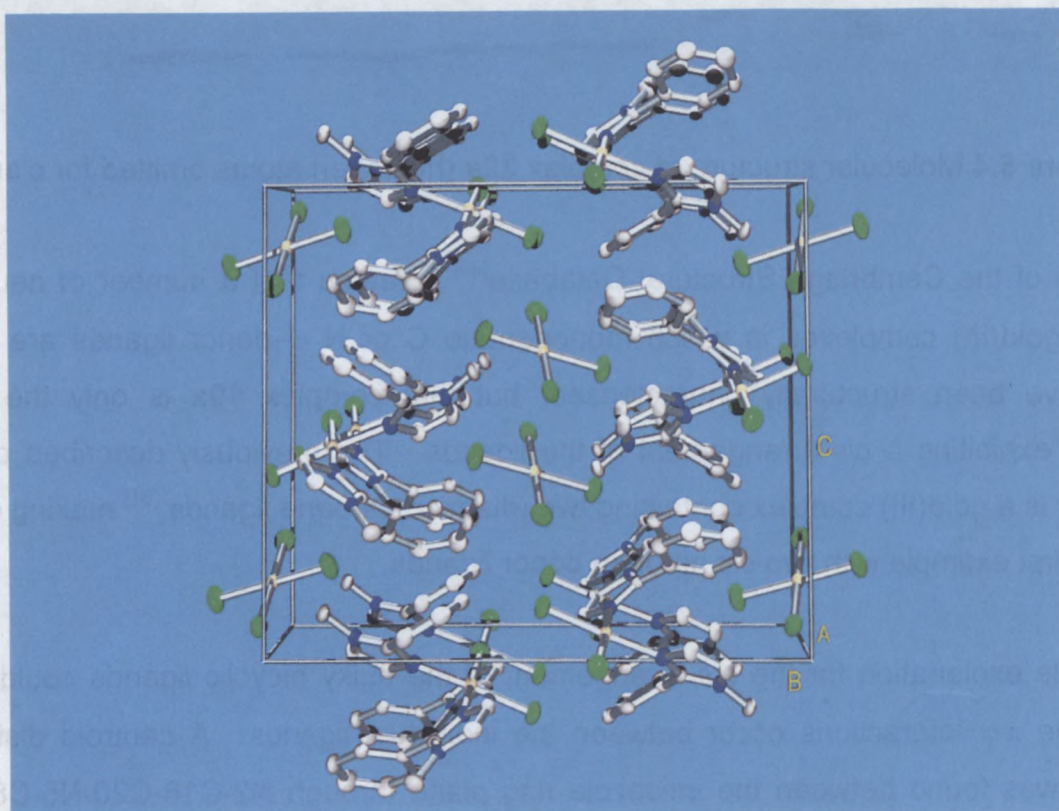


Figure 5.5 Unit cell packing of complex **19a**, viewed along the *a*-axis, showing rows of cations and anions (hydrogen atoms omitted)

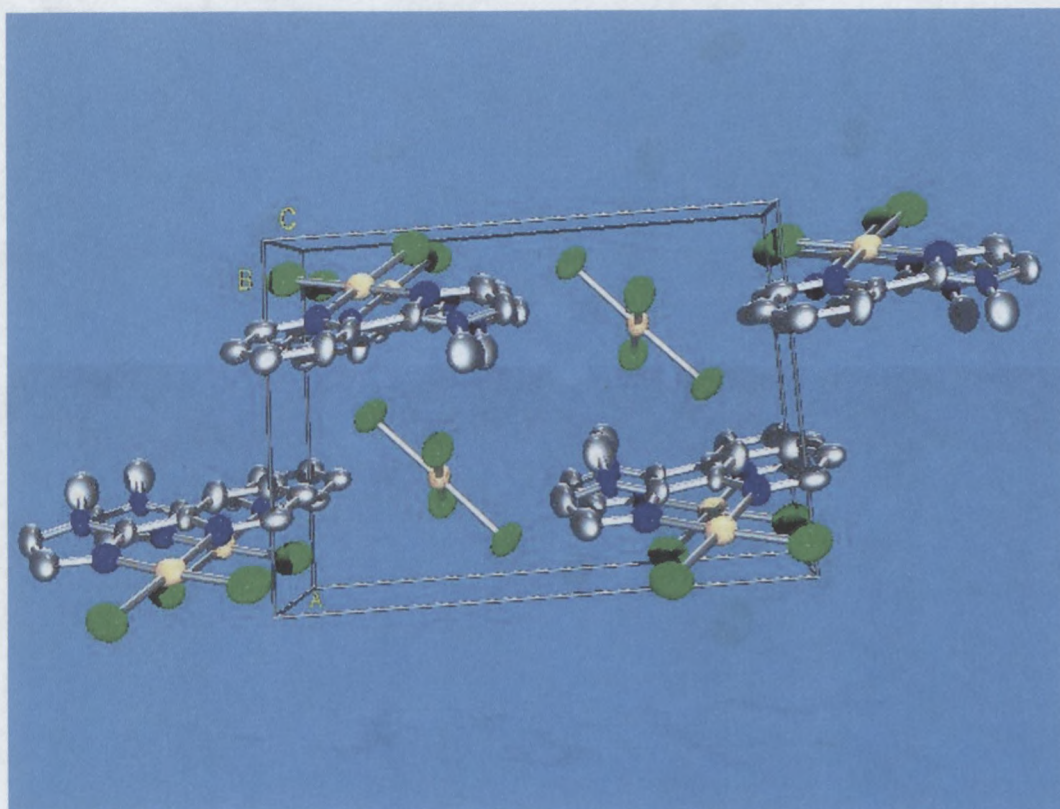


Figure 5.6 Unit cell packing of complex **12a**, viewed along the *a*-axis, showing rows of cations and anions (hydrogen atoms omitted).

The packing of complexes **19a** and **22a** in the crystals revealed the presence of weak H...Cl interactions between NMe protons of the cation and chlorine atoms of adjacent anions.

In complex **19a**, only three of the six NMe protons, H11a, H11b and H17c, are in contact with chlorine atoms in the neighbouring anions (Figure 5.7). H11a and H17c exhibit such interactions with chlorine atoms in the same anion *viz.* H17c-Cl8, 2.61 Å and H11b-Cl2, 2.85 Å. The H11a proton is 2.83 Å away from the Cl3 atom in a different counterion.

In complex **22a**, all three of the NMe protons have medium H...Cl contacts with neighbouring chlorine atoms (Figure 5.8). Two of the NMe protons are separated by 2.96 Å from Cl1 and Cl3 in adjacent anions, whereas the third proton is only 2.71 Å from Cl6, a chlorine present as a ligand in the neighbouring complex cation.

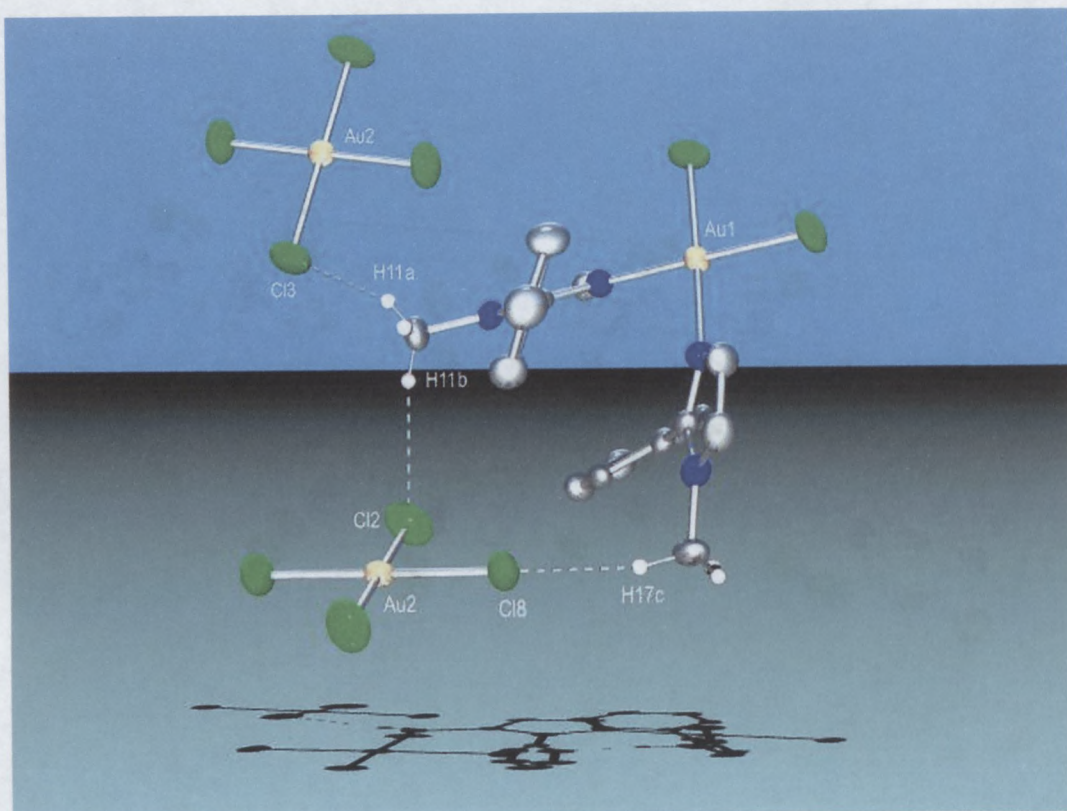


Figure 5.7 Packing in the unit cell of complex **19a**, as viewed along the *b*-axis, showing weak H...Cl interactions between one complex cation and two adjacent anions.

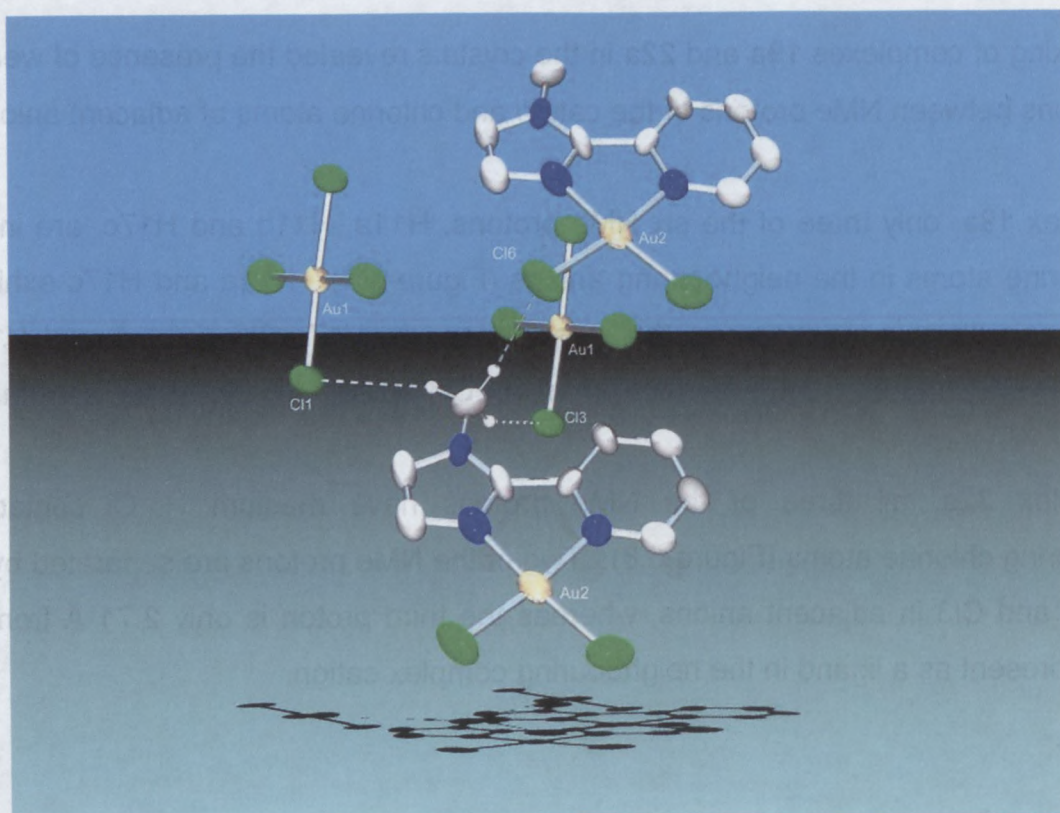


Figure 5.8 Packing diagram of complex **22a**, as viewed along the *b*-axis showing NMe proton interactions with two adjacent AuCl₄ anions and a neighbouring complex cation.

Table 5.18 Selected bond lengths (Å) and angles(°) for complexes **19a^a** and **22a^a**

Complex 19a			
Au1 – N1	2.016(6)	Au2 – Cl3	2.277(2)
Au1 – N5	2.043(7)	Au2 – Cl8	2.281(2)
Au1 – Cl11	2.257(2)	N1 – C14	1.330(9)
Au1 – Cl10	2.263(2)	N1 – C15	1.373(10)
Au2 – Cl2	2.269(2)	C8 – N5	1.328(10)
Au2 – Cl1	2.273(2)	C20 – N5	1.381(10)
N1 – Au1 – N5	91.9(2)	Cl2 – Au2 – Cl1	90.50(10)
N1 – Au1 – Cl11	88.09(19)	Cl2 – Au2 – Cl3	178.70(11)
N5 – Au1 – Cl11	177.0(2)	Cl1 – Au2 – Cl3	90.37(10)
N1 – Au1 – Cl10	177.93(19)	Cl2 – Au2 – Cl8	89.27(10)
N5 – Au1 – Cl10	89.06(19)	Cl1 – Au2 – Cl8	179.44(9)
Cl11 – Au1 – Cl10	91.08(9)	Cl3 – Au2 – Cl8	89.86(9)
Complex 22a			
Au1 – Cl1	2.278(5)	Au2 – N1	2.052(18)
Au1 – Cl2	2.293(5)	Au2 – N2	2.045(18)
Au1 – Cl3	2.274(5)	Au2 – Cl5	2.265(7)
Au1 – Cl4	2.275(5)	Au2 – Cl6	2.252(6)
N1 – C5	1.340(3)	N2 – C6	1.310(2)
N1 – C1	1.380(2)	N2 – C7	1.390(3)
N3 – C6	1.310(2)	C1 – C6	1.490(2)
N3 – C9	1.490(2)		
Cl3 – Au1 – Cl4	89.3(2)	N1 – Au2 – N2	80.3(7)
Cl3 – Au1 – Cl1	178.0(2)	N1 – Au2 – Cl6	173.9(5)
Cl4 – Au1 – Cl1	90.7(19)	N2 – Au2 – Cl6	94.0(19)
Cl3 – Au1 – Cl2	90.6(2)	N1 – Au2 – Cl5	95.3(5)
Cl4 – Au1 – Cl2	178.4(2)	N2 – Au2 – Cl5	175.7(5)
Cl1 – Au1 – Cl2	89.5(19)	Cl6 – Au2 – Cl5	90.3(3)
C5 – N1 – Au2	124.4(14)	C6 – N2 – Au2	114.3(14)
C1 – N1 – Au2	114.3(13)	C7 – N2 – Au2	136.8(17)

^a e.s.d.s. in parentheses

5.5 SUMMARY

The theme of this thesis is coordination chemistry involving N-containing heterocyclic compounds. Up to now, relatively few Au(I) and Au(III) complexes with such imine donor groups have been reported.

In this chapter it is shown that thioether ligands are readily displaced from gold(I) precursor complexes by imine donor groups, which is contrary to SHAB expectation and rules. In addition, the synthesis of neutral gold(III) adducts by reaction of NaAuCl_4 with bicyclic, imine compounds is described. The single crystal structure of one such compound showed that gold(III) is coordinate to the ligand through the nitrogen, even though a softer sulphur atom is readily available for the class (b) metal. By employing ^{15}N NMR measurements, diagnostic proof for the monodentate coordination of gold(III) to the imine donor in other bicyclic compounds was obtained. Moreover, these investigations showed that gold(III) preferentially bonds to nitrogen in a five-membered heterocyclic azolyl rather than to the pyridine nitrogen in an attached ring.

It has now also been established that whereas reaction of bicyclic imines with NaAuCl_4 affords neutral AuCl_3 adducts, similar preparations with HAuCl_4 furnish disubstituted, cationic complexes. In the literature, the former preparations are reported to produce only the protonated imine salt. Few crystal structure studies of gold imine complexes have been undertaken. We have now examined the first *cis*-diazole compound of gold(III). In some of our new compounds indications of chlorine-proton interactions were found in the solid state.

5.4 EXPERIMENTAL

5.4.1 Materials

The compounds 4,4-dimethyl-2-(2'-thienyl)oxazole,^[20] 4,4-dimethyl-2-(phenyl)oxazole,^[20] 1-methyl-2-(2-pyridinyl)imidazole,^[21] 1-methyl-2-(phenyl)imidazole,^[21] $[\text{Au}(\text{Cl})\text{Me}_2\text{S}]^{34}$ $[\text{Au}(\text{Cl})\text{tht}]$, HAuCl_4 and NaAuCl_4 ^[35] were prepared according to literature procedures.

Tetrahydrofuran, hexane and diethyl ether were distilled under nitrogen from sodium diphenylketyl and dichloromethane from CaH_2 . Acetonitrile was purified by distillation and stored over 3 Å molecular sieves. N-methylimidazole, bromobenzene and 2-bromobenzene were purchased from Fluka.

5.4.2 Physical Methods

The same experimental conditions apply as in Section 2.4.2, Section 3.4.2 and Section 4.3.2. ^{15}N NMR spectra were recorded on an Inova 600 FT apparatus with nitromethane as external standard.

5.4.3 Preparations

5.4.3.1 Preparation of $[\text{ClAu}\{\text{N}=\text{C}(\text{Ph})\text{NMeCH}=\text{CH}\}]$, **15**, $[\text{ClAu}\{\text{N}=\text{C}(\text{Ph})\text{OCH}_2\text{CMe}_2\}]$, **16**, $[\text{ClAu}\{\text{N}=\text{C}(\text{CSCH}=\text{CHCH})\text{OCH}_2\text{CMe}_2\}]$, **17**, $[\text{ClAu}\{\text{N}=\text{C}(\text{py})\text{NMeCH}=\text{CH}\}]$, **18** and $[\text{Cl}_2\text{Au}_2\{\text{N}=\text{C}(\text{py})\text{NMeCH}=\text{CH}\}]$, **18a**

A diethyl ether solution (5 cm³) of 4,4-dimethyl-2-(2'-thienyl)oxazole (181 mg, 1 mmol), 4,4-dimethyl-2-(phenyl)oxazole (158 mg, 1 mmol), 1-methyl-2-(2-pyridinyl)imidazole (159 mg, 1 mmol) or 1-methyl-2-(phenyl)imidazole (175 mg, 1 mmol) was added to a diethyl ether suspension (5 cm³) of $\text{AuCl}(\text{SMe}_2)$ (295 mg, 1 mmol) or $\text{AuCl}(\text{tht})$ (292 mg, 1 mmol) at -20°C and stirred for an hour. The reaction mixture was allowed to reach room temperature, filtered through anhydrous magnesium sulphate and the solvent evaporated. The residue was washed with pentane or hexane (3 x 5 cm³), dried *in vacuo* and stored under an Argon atmosphere at low temperature (ca. -25°C).

5.4.3.2 Preparation of $[\text{Cl}_3\text{Au}\{\text{N}=\text{C}(\text{Ph})\text{NMeCH}=\text{CH}\}]$, **19**,
 $[\text{Cl}_3\text{Au}\{\text{N}=\text{C}(\text{Ph})\text{OCH}_2\text{CMe}_2\}]$, **20**, $[\text{Cl}_3\text{Au}\{\text{N}=\text{C}(\text{CSCH}=\text{CHCH})\text{OCH}_2\text{CMe}_2\}]$, **21**
 and $[\text{Cl}_3\text{Au}\{\text{N}=\text{C}(\text{py})\text{NMeCH}=\text{CH}\}]$, **22**

The neutral gold(III) coordination complexes were prepared by modification of an existing literature procedure.^[36] An acetonitrile solution (4 cm³) of 4,4-dimethyl-2-(2'-thienyl)oxazole (181 mg, 1 mmol), 4,4-dimethyl-2-(phenyl)oxazole (158 mg, 1 mmol), 1-methyl-2-(2-pyridinyl)imidazole (159 mg, 1 mmol) or 1-methyl-2-(phenyl)imidazole (175 mg, 1 mmol) was added to an aqueous solution (4 cm³) of NaAuCl₄•4H₂O (434 mg, 1 mmol) at room temperature and stirred for an hour. The water-phase was extracted with dichloromethane (5 x 5 cm³) and the organic phase subsequently filtered through anhydrous magnesium sulphate. The dichloromethane volume was reduced to 5 cm³ and cooled to -20°C, whereafter the recrystallised products were removed by filtration.

5.4.3.3 Preparation of $[\text{Cl}_2\text{Au}\{\text{N}=\text{C}(\text{Ph})\text{NMeCH}=\text{CH}\}]_2[\text{AuCl}_4]$, **19a**,
 $[\text{Cl}_2\text{Au}\{\text{N}=\text{C}(\text{Ph})\text{OCH}_2\text{CMe}_2\}]_2[\text{AuCl}_4]$, **20a**,
 $[\text{Cl}_2\text{Au}\{\text{N}=\text{C}(\text{CSCH}=\text{CHCH})\text{OCH}_2\text{CMe}_2\}]_2[\text{AuCl}_4]$, **21a** and
 $[\text{Cl}_2\text{Au}\{\text{N}=\text{C}(\text{py})\text{NMeCH}=\text{CH}\}][\text{AuCl}_4]$, **22a**

The preparation was performed as in paragraph 5.4.3.2 but with HAuCl₄•4H₂O (411 mg, 1 mmol) instead of NaAuCl₄•4H₂O. The pure products were stored in a desiccator containing anhydrous CaCl₂ and silica gel crystals.

5.4.3.4 Crystallography for complexes **19a** and **21**

M. W. Esterhuysen solved the crystal and molecular structure of complexes **19a** and **21**. The crystal data as well as collection and refinement details for complexes **19a** and **21** are respectively given in Table 5.19 and Table 5.20. All other crystallographic information is available from M. W. Esterhuysen, Chemistry Department, Private Bag X1, Matieland, 7602, RSA.

X-ray diffraction data were collected on an Enraf-Nonius Kappa CCD diffractometer at 150(2)K using graphite monochromated Mo-K_α radiation ($\lambda = 0.71073\text{Å}$)^[37] and corrected for Lorenz and absorption effects using the Scalepack package.^[38] Structure solution and refinement was carried out using the program SHELX-97.^[39] ORTEP-3 for Windows was

used to generate the figures at 50% probability level.^[40] The structure was solved by interpretation of a Patterson synthesis that yielded the position of the gold atoms. The remaining non-hydrogen atoms were found by difference Fourier, refined by full-matrix least squares against F^2 and were allowed anisotropic thermal motion.

5.4.3.5 Crystallography for complex **22a**

D. G. Billing solved the crystal and molecular structure of complex **22a**. The crystal data as well as collection and refinement details for complex **22a** are given in Table 5.21. All other crystallographic information is available from D. G. Billing, Chemistry and Biochemistry Department, Rand Afrikaans University.

X-ray diffraction data were collected on a Phillips PW1100 diffractometer at 293(2)K using graphite monochromated Mo- K_α radiation ($\lambda = 0.71073\text{\AA}$) and corrected for Lorentz and absorption effects using the Scalepack package.^[38] Structure solution and refinement was carried out using the program SHELX-97.^[39] ORTEP-3 for Windows was used to generate the figures at 50% probability level.^[40] The structure was solved by interpretation of a Patterson synthesis that yielded the position of the gold atoms. The remaining non-hydrogen atoms were found by difference Fourier, refined by full-matrix least squares against F^2 and were allowed anisotropic thermal motion.

The relatively large residual density within 1 \AA of the Au atoms is probably due to series termination errors that were introduced when data collection was restricted to $\theta < 25^\circ$ due to crystal instability. Another possible explanation is errors introduced by crystal absorption, although these were corrected for during data reduction and should no longer be a factor.

Table 5.19 Crystal data, collection and refinement details for complex **19a**

Formula	C ₉ H ₁₁ AuCl ₃ NOS
Formula weight	484.56
Crystal system, space group	Monoclinic, P2 ₁ /n
Radiation, T/ °C	Mo-K α (0.71073Å), 175(2)
a, b, c/ Å	7.522(10), 12.905(2), 14.165(2)
α , β , γ / °	90, 100.480(10), 90
Z	4
U/ Å ³	1352.1(3)
Crystal size	0.30 x 0.25 x 0.20 mm ³
Calculated density D _c /g cm ⁻³	2.380
Absorption coefficient (μ)	11.605 mm ⁻¹
Absorption correction method	Empirical (Scalepack)
T _{min}	0.1284
T _{max}	0.2049
F(000)	704
Diffractometer	Enraf Nonius KappaCCD
Scan type	ϕ and ω to fill an Ewald sphere
Scan range, θ /°	2.15 \leq θ \leq 25.99
<i>hkl</i> ranges	-9 \leq <i>h</i> \leq 9, -14 \leq <i>k</i> \leq 14, -17 \leq <i>l</i> \leq 17
Reflections collected/ unique	2547 / 2372 [R(int) = 0.043]
Data / restraints / parameters	2547/ 0 / 146
Refinement method	Full-matrix least-squares on F ²
Final R indices [<i>l</i> > 2 σ (<i>l</i>)]	R ₁ = 0.0307, wR ₂ = 0.0776
R indices (all data)	R ₁ = 0.0408, wR ₂ = 0.0812
Weighting scheme	Calculated w = 1/[σ^2 (F _o ²) + [(0.0447P) ² + 3.5456P] where P = (F _o ² + 2F _c ²)/3
Goodness of fit on F ²	1.095
Largest peak, deepest hole	1.037 e ⁻ / Å ³ (0.535Å from C ⁵), -2.744 e ⁻ / Å ³ (1 Å ³ from Au)
Maximum shift/esd	0.004

Table 5.20 Crystal data, collection and refinement details for complex **21**

Formula	C ₂₀ H ₂₀ AuCl ₆ N ₄
Formula weight	923.064
Crystal system, space group	Monoclinic, P2 ₁ /c
Radiation, T/ °C	Mo-K α (0.71073Å), 293(2)
a, b, c/ Å	9.375(19), 18.160(4), 15.808(3)
α , β , γ / °	90, 98.58(3), 90
Z	4
U/ Å ³	2661.2(9)
Calculated density D _c /g cm ⁻³	2.304
Absorption coefficient (μ)	11.632 mm ⁻¹
Absorption correction method	Empirical (Scalepack)
F(000)	1712
Diffractometer	Enraf Nonius KappaCCD
Scan type	ϕ and ω to fill an Ewald sphere
Scan range, θ /°	1.72 \leq θ \leq 25.50
<i>hkl</i> ranges	-11 \leq <i>h</i> \leq 11, -15 \leq <i>k</i> \leq 20, -19 \leq <i>l</i> \leq 19
Reflections collected/ unique	4849 / 4046 [R(int) = 0.061]
Data / restraints / parameters	4849/ 0 / 291
Refinement method	Full-matrix least-squares on F ²
Final R indices [<i>I</i> > 2 σ (<i>I</i>)]	R ₁ = 0.0425, wR ₂ = 0.1078
R indices (all data)	R ₁ = 0.0558, wR ₂ = 0.1145
Weighting scheme	Calculated w = 1/[σ^2 (F _o ²) + [(0.0703) ² + 0.5680P] where P = (F _o ² + 2F _c ²)/3
Goodness of fit on F ²	1.042
Largest peak, deepest hole	1.04 e ⁻ / Å ³ (0.43Å from H5), -2.74 e ⁻ / Å ³ (1.00Å from Au)
Maximum shift/esd	0.011

Table 5.21 Crystal data, collection and refinement details for complex **22a**

Formula	C ₉ H ₉ Au ₂ Cl ₆ N ₃
Formula weight	765.83
Crystal system, space group	P $\bar{1}$, Triclinic
Radiation, T/ °C	Mo-K α (0.71073Å), 293(2)
a, b, c/ Å	8.1432(6), 9.5263(8), 12.3669(9)
α , β , γ / °	89.869(8), 88.139(8), 65.062(12)
Z	2
U/ Å ³	959.357(9)
Calculated density D _c /g cm ⁻³	2.925
Absorption coefficient (μ)	17.768 mm ⁻¹
Absorption correction method	Empirical (North)
F(000)	688
Diffractometer	Philips PW1100
Scan type	ω - 2 θ
Scan range, θ /°	2.76 \leq θ \leq 25.00
<i>hkl</i> ranges	-9 \leq <i>h</i> \leq 9, -11 \leq <i>k</i> \leq 11, -2 \leq <i>l</i> \leq 14
Reflections collected/ unique	3055 / 2802 [R(int) = 0.047]
Data / restraints / parameters	3055 / 0 / 183
Refinement method	Full-matrix least-squares on F ²
Final R indices [<i>l</i> > 2 σ (<i>l</i>)]	R ₁ = 0.0867, wR ₂ = 0.1820
R indices (all data)	R ₁ = 0.0763, wR ₂ = 0.1697
Weighting scheme	Calculated w = 1/[σ^2 (F _o ²) + [(0.1042P) ² + 2.7165P] where P = (F _o ² + 2F _c ²)/3
Goodness of fit on F ²	1.174
Largest peak, deepest hole	2.59e ⁻¹ Å ³ (0.97Å from Au1), -3.12e ⁻¹ Å ³ (0.89Å from Au1ni)
Maximum shift/esd	0.011

REFERENCES

- [1] R. G. Pearson, *Chemical Hardness*, Wiley-VCH, New York, 1997.
- [2] L. H. Skibsted and J. Bjerrum, *Acta Chem. Scand., Ser. A*, 1977, **31**, 155.
- [3] L. H. Skibsted, *Adv. Inorg. and Bioinorg. Mech.*, 1986, **4**, 137.
- [4] R. J. Puddephatt, *The Chemistry of Gold*, Elsevier, Amsterdam, 1978.
- [5] R. J. Puddephatt in, *Comprehensive Coordination Chemistry*, (eds. G. Wilkinson, R. D. Gillard and J. A. McCleverty) Pergamon, Oxford, 1987, p. 862.
- [6] J. Strähle, in *Gold: Progress in Chemistry, Biochemistry and Technology*, (ed. H. Schmidbaur), John Wiley and Sons, New York, 1999, p. 311.
- [7] G. Banditelli, A. L. Bandini, G. Minghetti and F. Bonati, *Canad. J. Chem.*, 1981, **59**, 1241.
- [8] J. Vicente, M. T. Chicote, R. Guerrero, I. M. Saura-Llama, P. G. Jones and M.C. Ramirez de Arellano, *Chem. Eur. J.*, 2001, **7**, 638.
- [9] M. Desmet, H. G. Raubenheimer and G. J. Kruger, *Organometallics*, 1997, **16**, 3324.
- [10] C. S. Gibson and W. M. Colles, *J. Chem. Soc.*, 1931, 2407.
- [11] M. L. Tobe, in *Comprehensive Coordination Chemistry*, (eds. G. Wilkinson, R. D. Gillard and J. A. McCleverty) Pergamon, Oxford, 1987, p. 310.
- [12] G. R. Newcome, W. E. Puckett, V. K. Gupta and G. E. Kiefer, *Chem. Rev.*, 1990, **90**, 403.
- [13] M. Pfeffer, *Pure Appl. Chem.*, 1992, **64**, 335.
- [14] K-H. Wong, K-K. Cheung, M. C-W. Chan and C-M. Che, *Organometallics*, 1998, **17**, 3505.
- [15] J. Vicente, M. T. Chicote and M. D. Bermúdez, *J. Organomet. Chem.*, 1984, **268**, 191.
- [16] M. A. Cinellu, A. Zucca, S. Stoccoro, G. Minghetti, M. Manassero and M. Sansoni, *J. Chem. Soc., Dalton Trans.*, 1995, 2865.
- [17] E. C. Constable, R. P. G. Henney, P. R. Raithby and L. R. Sousa, *J. Chem. Soc., Dalton Trans.*, 1992, 2251.
- [18] V. H-N. Adams and J. Strähle, *Z. Anorg. Allg. Chem.*, 1982, **485**, 65.
- [19] E. C. Constable and T. A. Leese, *J. Organomet. Chem.*, 1989, **363**, 419.
- [20] A. I. Meyer, D. L. Temple, R. L. Nolen and E. D. Mihelich, *J. Org. Chem.*, 1974, **39**, 2778.
- [21] A. S. Bell, D. A. Roberts and K. S. Ruddock, *Tetrahedron Lett.*, 1988, **29**, 5013.
- [22] N. S. Narasimhan and R. S. Mali, *Synthesis*, 1983, 957.

- [23] P. Beak and A. Brown, *J. Org. Chem.*, 1979, **44**, 4464.
- [24] A. Iggo, *NMR Spectroscopy in Inorganic Chemistry*, Oxford University Press, Oxford, 1999.
- [25] P. K. Byers and A. J. Canty, *Organometallics*, 1990, **9**, 210.
- [26] S. Cronje, University of Stellenbosch, unpublished results.
- [27] J. Strähle, in *Gold: Progress in Chemistry, Biochemistry and Technology*, (ed. H. Schmidbaur), John Wiley and Sons, New York, 1999, p. 311.
- [28] A. Grohmann and H. Schmidbaur in, *Comprehensive Organometallic Chemistry II*, (eds. E. W. Abel, F. G. A. Stone and G. Wilkinson), Pergamon, Oxford, 1995.
- [29] C. A. Hunter and J. K. M. Sanders, *J. Am. Chem. Soc.*, 1990, **112**, 5525.
- [30] F. H. Allen and O. Kennard, *Chem. Des. Autom. News*, 1993, **8**, 31.
- [31] L. Manojlovic-Muir, *J. Organomet. Chem.*, 1974, **73**, C45.
- [32] E. J. L. McInnes, A. J. Welch and L. J. Yellowlees, *Acta Crystallogr. A*, 1995, **C51**, 2023.
- [33] J. Vicente, M. D. Bermúdez, M. P. Carrillo and P. G. Jones, *J. Chem. Soc., Dalton Trans.*, 1992, 1975.
- [34] P. C. Rây and D. C. Chen, *J. Indian Chem. Soc.*, 1930, 67.
- [35] G. Brauer, *Handbuch der Präparativen Anorganischen Chemie*, 3rd ed., Verlag, Stuttgart, 1978, p. 1014.
- [36] E. C. Constable and T. A. Leese, *J. Organomet. Chem.*, 1989, **363**, 419.
- [37] Nonius, COLLECT, Nonius BV, Delft, The Netherlands, 1999.
- [38] Z. Otwinowski, W. Minor, *Methods Enzymol.*, 1997, **276**, 307.
- [39] G.M. Sheldrick, *SHELX-97 – Program for Crystal Structure Analysis*, Institut für Anorganische Chemie der Universität Göttingen, Tammanstrasse 4, D-3400, Germany, 1998.
- [40] L.J. Farrugia, *J. Appl. Cryst.*, 1997, **30**, 565.